Msander Reference Manual

Msander ("modern sander") is an updated version of *sander*, the basic energy minimizer and molecular dynamics program in the *AmberTools suite.* This program relaxes the structure by iteratively moving the atoms down the energy gradient until a sufficiently low average gradient is obtained. The molecular dynamics portion generates configurations of the system by integrating Newtonian equations of motion. MD will sample more configurational space than minimization, and will allow the structure to cross over small potential energy barriers. Configurations may be saved at regular intervals during the simulation for later analysis, and basic free energy calculations using thermodynamic integration may be performed. More elaborate conformational searching and modeling MD studies can also be carried out using the *sander* module. This allows a variety of constraints to be added to the basic force field, and has been designed especially for the types of calculations involved in NMR, Xray or cryo-EM structure refinement.

This collection also contains versions of a number of the "classic" (and most-used) parts of `AmberTools`: *tleap, antechamber*, *sqm,* and *paramfit*. With these tools, many systems can be set up for simulation in *msander*. Documentation for these programs are in Chapters 10 through 12, below. The tutorials at https://ambermd/org/tutorials illustrate the use of these programs. (Analysis of trajectories is most commonly carried out via *cpptraj*, which is distributed separately, at https://githbu.com/Amber-MD.) If you need more capabilities than these classic, stripped-down versions provide, consider installing the full `AmberTools` and `Amber` suites, available at https://ambermd.org.

One goal of this collection is to make compiling and installation as simple as possible. There is a pretty simple `configure` script, and minimal dependencies on external packages. If you have problems or questions, creating an issue at `github.com` is the recommended path, but you can also send email to dacase1@gmail.com.

Principal contributors to the current codes:

David A. Case (Rutgers)

Carlos Simmerling (Stony Brook)

Adrian Roitberg (Florida)

Tom Darden (OpenEye)

Celeste Sagui (NCSU)

Feng Pan (FSU)

Jason Swails (Entos)

David Cerutti (Rutgers)

Tyler Luchko (CSU Northridge)

Vinícius Wilian D. Cruzeiro (UC San Diego)

Nikolai R. Skrynnikov (Purdue, SPbU)

Oleg Mikhailovskii (Purdue, SPbU)

Yi Xue (Tsinghua)

Sergei A. Izmailov (SPbU)

Alexey Onufriev (Virginia Tech)

Saeed Izadi (Virginia Tech, Genentech)

Xiongwu Wu (NIH)

George Giambasu (Rutgers)

Jian Liu (Peking Univ.)

Andriy Kovalenko (NINT)

Contents

CONTENTS

1 msander

1.1 Introduction

This is a guide to *msander*, an Amber module which carries out energy minimization, molecular dynamics, and NMR refinements. The acronym stands for **S**imulated **A**nnealing with **N**MR-**D**erived **E**nergy **R**estraints, but this module is used for a variety of simulations that have nothing to do with NMR refinement. Some general features are outlined in the following paragraphs:

1. *msander* provides direct support for several force fields for proteins and nucleic acids, and for several water models and other organic solvents. The basic force field implemented here has the following form, which is about the simplest functional form that preserves the essential nature of molecules in condensed phases:

$$V(\mathbf{r}) \quad = \quad \sum_{bonds} K_b(b-b_0)^2 + \sum_{angles} K_\theta(\theta - \theta_o)^2$$
$$+ \sum_{dihedrals} (V_n/2)(1+\cos[n\phi - \delta]$$
$$+ \sum_{nonbij} (A_{ij}/r_{ij}^{12}) - (B_{ij}/r_{ij}^6) + (q_i q_j/r_{ij})$$

   In addition, charges that are not centered on atoms, but are off-center (as for lone-pairs or "extra points") can be included in the force field.

2. The particle-mesh Ewald (PME) procedure is used to handle long-range electrostatic interactions. Long-range van der Waals interactions are estimated by a continuum model. Biomolecular simulations in the NVE ensemble (*i.e.* with Newtonian dynamics) conserve energy well over multi-nanosecond runs without modification of the equations of motion.

3. Translational periodic (P1) symmetry is supported, but no other space-group symmetry is. The size of the unit cell can be coupled to a given external pressure, and velocities can be coupled to a given external temperature by several schemes. The external conditions and coupling constants can be varied over time, so various simulated annealing protocols can be specified in a simple and flexible manner.

4. It is also possible to carry out non-periodic simulations in which aqueous solvation effects are represented *implicitly* by a generalized Born/ surface area model by adding the following two terms to the "vacuum" potential function:

$$\Delta G_{sol} = \sum_{ij} (1 - \frac{1}{\varepsilon})(q_i q_j/f_{GB}(r_{ij}) + A\sum_i \sigma_i$$

   The first term accounts for the polar part of solvation (free) energy, designed to provide an approximation for the reaction field potential, and the second represents the non-polar contribution which is taken to be proportional to the surface area of the molecule.

5. Users can define internal restraints on bonds, valence angles, and torsions, and the force constants and target values for the restraints can vary during the simulation. The relative weights of various terms in the force field can be varied over time, allowing one to implement a variety of simulated annealing protocols in a single run.

6. Internal restraints can be defined to be "time-averaged", that is, restraint forces are applied based on the averaged value of an internal coordinate over the course of the dynamics trajectory, not only on its current value. Alternatively, restraints can be "ensemble-averaged" using the locally-enhanced-sampling (LES) option.

7. Restraints can be directly defined in terms of NOESY intensities (calculated with a relaxation matrix technique), residual dipolar couplings, scalar coupling constants and proton chemical shifts. There are provisions for handling overlapping peaks or ambiguous assignments. In conjunction with distance and angle constraints, this provides a powerful and flexible approach to NMR structural refinements.

8. Xray and cryoEM refinements can be carried out in reciprocal space, with GPU-accelerated structure factor calculations. Real-space electron density maps can also be used as restraints for refinement.

9. Replica exchange calculations can allow simultaneous sampling at a variety of conditions (such as temperature), and allow the user to construct Boltzmann samples in ways that converge more quickly than standard MD simulations. Other variants of biased MD simulations can also be used to improve sampling.

10. Restraints can also be defined in terms of the root-mean-square coordinate distance from some reference structure. This allows one to bias trajectories either towards or away from some target. Free energies can be estimated from non-equilibrium simulations based on targetting restraints.

11. Free energy calculations, using thermodynamic integration (TI) with a linear or non-linear mixing of the "unperturbed" and "perturbed" Hamiltonian, can be carried out. Alternatively, potentials of mean force can be computed using umbrella sampling.

1.2 Main changes from the *sander* code in AmberTools

1. Some pieces are missing from the sander program in AmberTools:

   a) Things that should be easy to re-introduce later: emil, sebomd, pbsa, APBS, the charge-relocation option.

   b) Things are are problably gone for good, but which don't represent the best current practice: Path-integral methods, thermostats that don't follow the "middle" scheme, Berendsen barostat

   c) Things that might be useful, but really complicate the code: EVB potentials, QM/MM, nudged elastic band, constant pH and constant redox potential simulations. The API interface to Fortran, C and Python codes has also been removed.

   d) Non-periodic 3D-RISM has been removed for now, in an attempt to get the simplest possible RISM code, perhaps as a basis for future GPU work.

2. Key pieces of code that are still there, and being emphasized:

   a) Periodic and non-periodic simulations, with all of Amber's GB models

   b) 3D-RISM in periodic boundary conditions

   c) NMR, cryoEM and Xray restraints (including quite a bit of new code; Xray restraints include NVIDIA GPU-enabled capabilities)

   d) Thermodynamic integration and non-equilibrium sampling methods

   e) Sampling and minimization using the lmod and xmin approaches; these can now be used in conjunction with SHAKE and SETTLE.

   f) Replica exchange capabilities, except for constant pH and redox potential simulations

1.3 Installation

```
./configure --help    # then choose options
make install
make test              # optional--more info is below
```

The test suite also serves as a source of example input files. Look especially in the *rism*, *xray* and *cryoem* folders to see sample inputs for these sorts of calculation.

1.4 File usage

```
msander [-help] [-O] [-A] -i mdin -o mdout -p prmtop -c inpcrd -r restrt
-ref refc -mtmd mtmd -x mdcrd -y inptraj -v mdvel -frc mdfrc -e mden
-inf mdinfo
-O  Overwrite output files if they exist.
-A  Append output files if they exist (used mainly for replica exchange).
```

Here is a brief description of the files referred to above; the first five files are used for every run, whereas the remainder are only used when certain options are chosen.

mdin *input* control data for the min/md run

mdout *output* user readable state info and diagnostics -o stdout will send output to stdout (to the terminal) instead of to a file.

mdinfo *output* latest mdout-format energy info

prmtop *input* molecular topology, force field, periodic box type, atom and residue names

inpcrd *input* initial coordinates and (optionally) velocities and periodic box size

refc *input* (optional) reference coords for position restraints; also used for targeted MD

mtmd *input* (optional) containing list of files and parameters for targeted MD to multiple targets

mdcrd *output* coordinate sets saved over trajectory

inptraj *input* coordinate sets in trajectory format, when imin=5

mdvel *output* velocity sets saved over trajectory

mdfrc *output* force sets saved over trajectory

mden *output* extensive energy data over trajectory (not synchronized with mdcrd or mdvel)

restrt *output* final coordinates, velocity, and box dimensions if any - for restarting run

suffix *output* this string will be added to all unspecified output files that are printed (for *multisander* runs, it will append this suffix to all output files)

1.5 Example input files

Here are a couple of sample files, just to establish a basic syntax and appearance. There are more examples of NMR-related files later in this chapter.

1. Simple restrained minimization

```
Minimization with Cartesian restraints
&cntrl
imin=1, maxcyc=200, (invoke minimization)
ntpr=5, (print frequency)
ntr=1, (turn on Cartesian restraints)
restraint_wt=1.0, (force constant for restraint)
restraintmask=':1-58', (atoms in residues 1-58 restrained)
/
```

2. "Plain" molecular dynamics run

```
molecular dynamics run
&cntrl
imin=0, irest=1, ntx=5, (restart MD)
ntt=3, temp0=300.0, gamma_ln=5.0, (temperature control)
ntp=1, taup=2.0, (pressure control)
ntb=2, ntc=2, ntf=2, (SHAKE, periodic bc.)
nstlim=500000, (run for 0.5 nsec)
ntwx=1000, ntpr=200, (output frequency)
```

1.6 Namelist Input Syntax

Namelist provides list-directed input, and convenient specification of default values, and is a part of the Fortran 90 standard, Namelist input groups take the form:

```
&name
var1=value, var2=value, var3(sub)=value,
var4(sub,sub,sub)=value,value,
var5=repeat*value,value,
/
```

The variables must be names in the Namelist variable list. The order of the variables in the input list is of no significance, except that if a variable is specified more than once, later assignments may overwrite earlier ones. Blanks may occur anywhere in the input, except embedded in constants (other than string constants, where they count as ordinary characters).

It is common in older inputs for the ending "/" to be replaced by "&end"; this is non-standard-conforming.

Letter case is ignored in all character comparisons, but case is preserved in string constants. String constants must be enclosed by single quotes ('). If the text string itself contains single quotes, indicate them by two consecutive single quotes, e.g. C1' becomes 'C1''' as a character string constant.

Array variables may be subscripted or unsubscripted. An unsubscripted array variable is the same as if the subscript (1) had been specified. If a subscript list is given, it must have either one constant, or exactly as many as the number in the declared dimension of the array. Bounds checking is performed for ALL subscript positions, although if only one is given for a multi-dimension array, the check is against the entire array size, not against the first dimension. If more than one constant appears after an array assignment, the values go into successive locations of the array. It is NOT necessary to input all elements of an array.

Any constant may optionally be preceded by a positive (1,2,3,..) integer repeat factor, so that, for example, 25*3.1415 is equivalent to twenty-five successive values 3.1415. The repeat count separator, *, may be preceded

and followed by 0 or more blanks. Valid LOGICAL constants are 0, F, .F., .FALSE., 1, T, .T., and .TRUE.; lower case versions of these also work.

1.7 Overview of the information in the input file

General minimization and dynamics input One or more title lines, followed by the (required) &cntrl and (optional) &pb, &ewald, &qmmm, &amoeba or &debugf namelist blocks. Described in Sections 1.8 and 1.9.

Varying conditions Parameters for changing temperature, restraint weights, etc., during the MD run. Each parameter is specified by a separate &wt namelist block, ending with &wt type="END", /. Described in Section 1.10.

File redirection TYPE=*filename* lines. Section ends with the first non-blank line which does not correspond to a recognized redirection. Described in Section 1.11.

Group information Read if *ntr*, *ibelly* or *idecomp* are set to nonzero values, and if some other conditions are satisfied; see sections on these variables, below. Described in Appendix 5.2.

1.8 General minimization and dynamics parameters

Each of the variables listed below is input in a namelist statement with the namelist identifier &cntrl.cmmu can enter the parameters in any order, using keyword identifiers. Variables that are not given in the namelist input retain their default values. Support for namelist input is included in almost all current Fortran compilers, and is a standard feature of Fortran 90. A detailed description of the namelist convention is given in Appendix A.

In general, namelist input consists of an arbitrary number of comment cards, followed by a record whose first seven characters after a " &" (e.g. " &cntrl ") name a group of variables that can be set by name.cmsys is followed by statements of the form " maxcyc=500, diel=2.0, ... ", and is concluded by an " / " token. The first line of input contains a title, which is then followed by the &cntrl namelist. Note that the first character on each line of a namelist block must be a blank.

Some of the options and variables are much more important, and commonlycmrdified, than are others. We have denoted the "common" options by printing them in **boldface** below. In general, you can skip reading about the non-bold options on a first pass, and you should change these from their defaults only if you think you know what you are doing.

1.8.1 General flags describing the calculation

imin   Flag to run minimization.

= 0 (default) Run molecular dynamics without any minimization.

= 1 Perform an energy minimization.

= 5 Read in a trajectory for analysis.

Although sander will write energy information in the output files (using *ntpr*), it is often desirable to calculate the energies of a set of structures at a later point. In particular, one may wish to post-process a set of structures using a different energy function than was used to generate the structures. An example of this is MM-PBSA analysis, where the explicit water is removed and replaced with a continuum model.

If *imin* is set to 5, sander will read a trajectory file (the "inptraj" argument, specified using −y on the command line), and will perform the functions described in the mdin file (e.g., an energy minimization) for each of the structures in this file. The final structure from each minimization will be written out to the normal mdcrd file. If you wish to read in a binary (i.e., NetCDF format) trajectory, be sure to set *ioutfm* to 1 (see below). Note that this will result in the output trajectory having NetCDF format as well.

For example, when *imin* = 5 and *maxcyc* = 1000, sander will minimize each structure in the trajectory for 1000 steps and write a minimized coordinate set for each frame to the mdcrd file. If *maxcyc* = 1, the output file can be used to extract the energies of each of the coordinate sets in the inptraj file.

Trajectories containing box coordinates can be post-processed. In order to read trajectories with box coordinates, *ntb* should be greater than 0.

IMPORTANT CAVEAT: The initial coordinates input file used (−c <inpcrd>) should be the same as the initial coordinates input file used to generate the original trajectory. This is because sander sets up parameters for PME from the box coordinates in the initial coordinates input file.

nmropt **= 0** (default) No nmr-type analysis will be done.

= 1 NMR restraints and weight changes will be read.

= 2 NMR restraints, weight changes, NOESY volumes, chemical shifts and residual dipolar restraints will be read.

1.8.2 Nature and format of the input

ntx Option to read the initial coordinates, velocities, and box size from the inpcrd file. Option 1 must be used when one is starting from minimized or model-built coordinates. If an MD restrt file is specified for inpcrd then option 5 is generally used (unless you explicitly wish to ignore the velocities that are present).

= 1 (default) Coordinates, but no velocities, will be read; either formatted (ASCII) files or NetCDF files can be used, as the input file type will be auto-detected.

= 5 Coordinates and velocities will be read from either a NetCDF or a formatted (ASCII) coordinate file. Box information will be read if *ntb* > 0. The velocity information will only be used if *irest* = 1 (see below).

irest Flag to restart a simulation.

= 0 (default) Do not restart the simulation; instead, run as a new simulation. Velocities in the input coordinate file, if any, will be ignored, and the time step count will be set to 0 (unless overridden by *t*; see below).

= 1 Restart the simulation, reading coordinates and velocities from a previously saved restart file. The velocity information is necessary when restarting, so *ntx* (see above) must be 5 (for Amber versions much older than 20, ntx must be greater than or equal to 4), if *irest* = 1.

1.8.3 Nature and format of the output

ntxo Format of the final coordinates, velocities, and box size (if a constant volume or pressure run) written to file "restrt".

= 1 Formatted (ASCII)

= 2 (default) NetCDF file (recommended, unless you have a workflow that requires the formatted form.)

ntpr Every *ntpr* steps, energy information will be printed in human-readable form to files "mdout" and "mdinfo". "mdinfo" is closed and reopened each time, so it always contains the most recent energy and temperature. Default 50.

ntwr Every *ntwr* steps during dynamics, the "restrt" file will be written, ensuring that recovery from a crash will not be so painful. No matter what the value of *ntwr*, a restrt file will be written at the end of the run, i.e., after *nstlim* steps (for dynamics) or *maxcyc* steps (for minimization). If *ntwr*

< 0, a unique copy of the file, "restrt_<nstep>", is written every abs(*ntwr*) steps. This option is useful if for example one wants to run free energy perturbations from multiple starting points or save a series of restrt files for minimization. Default = nstlim.

ntwx   Every *ntwx* steps, the coordinates will be written to the mdcrd file. If *ntwx* = 0, no coordinate trajectory file will be written. Default = 0.

ntwv   Every *ntwv* steps, the velocities will be written to the mdvel file. If *ntwv* = 0, no velocity trajectory file will be written. If *ntwv* = -1, velocities will be written to mdcrd, which then becomes a combined coordinate/velocity trajectory file, at the interval defined by *ntwx*. This option is available only for binary NetCDF output (*ioutfm* = 1). Most users will have no need for a velocity trajectory file and so can safely leave *ntwv* at the default. Default = 0. Note that dumping velocities frequently, like forces or coordinates, will introduce potentially significant I/O and communication overhead, hurting both performance and parallel scaling.

ionstepvelocities   Controls whether to print the half-step-ahead velocities (0, default) or on-step velocities (1). The half-step-ahead velocities can potentially be used to restart calculations, but the on-step velocities correspond to calculated kinetic energy/temperature.

ntwf   Every *ntwf* steps, the forces will be written to the mdfrc file. If *ntwf* = 0, no force trajectory file will be written. If *ntwf* = -1, forces will be written to the mdcrd, which then becomes a combind coordinate/force trajectory file, at the interval defined by *ntwx*. This option is available only for binary NetCDF output (*ioutfm* = 1). Most users will have no need for a force trajectory file and so can safely leave *ntwf* at the default. Default = 0. Note that dumping forces frequently, like velocities or coordinates, will introduce potentially significant I/O and communication overhead, hurting both performance and parallel scaling.

ntwe   Every *ntwe* steps, the energies and temperatures will be written to file "mden" in a compact form. If *ntwe* = 0 then no mden file will be written. Note that energies in the mden file are not synchronized with coordinates or velocities in the mdcrd or mdvel file(s). Assuming identical *ntwe* and *ntwx* values the energies are one time step before the coordinates (as well as the velocities which are synchronized with the coordinates). Consequently, an mden file is rarely written. Default = 0.

ioutfm   The format of coordinate and velocity trajectory files (mdcrd, mdvel and inptraj). As of Amber 9, the binary format used in previous versions is no longer supported; binary output is now in NetCDF trajectory format. Binary trajectory files have many advantages: they are smaller, higher precision, much faster to read and write, and able to accept a wider range of coordinate (or velocity) values than formatted trajectory files.

   = 0 Formatted ASCII trajectory

   = 1 (default) Binary NetCDF trajectory

ntwprt   The number of atoms to include in trajectory files (mdcrd and mdvel). This flag can be used to decrease the size of the these files, by including only the first part of the system, which is usually of greater interest (for instance, one might include only the solute and not the solvent). If *ntwprt* = 0, all atoms will be included.

   = 0 (default) Include all atoms of the system when writing trajectories.

   > 0 Include only atoms 1 to *ntwprt* when writing trajectories.

1.8.4 Frozen or restrained atoms

ibelly   Flag for belly type dynamics. If set to 1, a subset of the atoms in the system will be allowed to move, and the coordinates of the rest will be frozen. The *moving* atoms are specified with *bellymask*. This option is not available when *igb>0*. When belly type dynamics is in use, bonded energy terms, vdW interactions, and direct space electrostatic interactions are *not calculated* for pairs of frozen atoms. Note that this does *not* provide any significant speed advantage. Freezing

atoms can be useful for some applications but is maintained primarily for backwards compatibility with older versions of Amber. Most applications should use the *ntr* variable instead to restrain parts of the system to stay close to some initial configuration. Default = 0.

ntr   Flag for restraining specified atoms in Cartesian space using a harmonic potential, if ntr > 0. The restrained atoms are determined by the *restraintmask* string. The force constant is given by *restraint_wt*. The coordinates are read in "restrt" format from the "refc" file. Default = 0.

restraint_wt   The weight (kcal $\cdot$ mol$^{-1} \cdot$ Å^{-2}) for the positional restraints. The restraint is of the form $k(\Delta x)^2$, where k is the value given by this variable, and Δx is the difference between one of the Cartesian coordinates of a restrained atom and its reference position. There is a term like this for each Cartesian coordinate of each restrained atom.

restraintmask   String that specifies the *restrained* atoms when *ntr=1*.

bellymask   String that specifies the *moving* atoms when *ibelly=1*.

The syntax for both *restraintmask* and *bellymask* is given in Section 5.1.1. Note that these mask strings are limited to a maximum of 256 characters.

1.8.5 Energy minimization

maxcyc   The maximum number of cycles of minimization. Default = 1.

ntmin   Flag for the method of minimization.

= 3 The XMIN method is used, see Section 6.4.1. (default)

= 4 The LMOD method is used, see Section 6.4.2.

dx0   The initial step length. If the initial step length is too big then will give a huge energy; however the minimizer is smart enough to adjust itself. Default 0.01.

drms   The convergence criterion for the energy Derivative: minimization will halt when the Root-Mean-Square of the Cartesian elements of the gradient of the energy is less than this. Default is 10^{-4} kcal $\cdot$ mol$^{-1} \cdot$ Å^{-1}.

1.8.6 Molecular dynamics

The "middle" scheme offers a unified framework to develop efficient thermostatting algorithms for configurational sampling for the canonical ensemble, as described in Refs. [1–5]. It is the only MD scheme implemented in *msander*. It can be implemented for performing molecular dynamics (MD) or path integral molecular dynamics (PIMD), either with or without holonomic constraints. The "middle" scheme allows the use of much larger time intervals (i.e., time stepsizes) Δt to maintain the same accuracy, which significantly improves the configurational sampling efficiency. That is, it is efficient for calculating structural properties and thermodynamic observables that depend on coordinate variables. Most thermostats control the temperature by updating momenta of the system. Some prevailing thermostats include stochastic ones (such as the Andersen thermostat and Langevin dynamics) and deterministic ones (such as the Nosé-Hoover thermostat and Nosé-Hoover chain). In the "middle" scheme, immediately after the coordinate-updating step for half a time interval, the thermostat process for a full time interval takes place, which is then followed by the coordinate-updating step for another half time interval[1, 5].

nstlim   Number of MD-steps to be performed. Default 1.

nscm   Flag for the removal of translational and rotational center-of-mass (COM) motion at regular intervals (default is 1000). For non-periodic simulations, after every NSCM steps, translational and rotational motion will be removed. For periodic systems, just the translational center-of-mass motion will be removed. This flag is ignored for belly simulations.

For Langevin dynamics, the *position* of the center-of-mass of the molecule is reset to zero every NSCM steps, but the velocities are not affected. Hence there is no change to either the translation or rotational components of the momenta. (Doing anything else would destroy the way in which temperature is regulated in a Langevin dynamics system.) The only reason to even reset the coordinates is to prevent the molecule from diffusing so far away from the origin that its coordinates overflow the format used in restart or trajectory files.

t   The time at the start (psec) this is for your own reference and is not critical. Start time is taken from the coordinate input file if IREST=1. Default 0.0.

dt   The time step (psec). Recommended MAXIMUM is .002 if SHAKE is used, or .001 if it isn't. Note that for temperatures above 300K, the step size should be reduced since greater temperatures mean increased velocities and longer distance traveled between each force evaluation, which can lead to anomalously high energies and system blowup. Default 0.001.
The use of Hydrogen Mass Repartitioning (HMR) (see [6] and references therein for more information), together with SHAKE, allows the time step to be increased in a stable fashion by about a factor of two (up to .004) by slowing down the high frequency hydrogen motion in the system. To use HMR, the masses in the topology file need to be altered before starting the simulation. ParmEd can do this automatically with the HMassRepartition option; see Section **??** .

nrespa   This variable allows the user to evaluate slowly-varying terms in the force field less frequently. For PME, "slowly-varying" (now) means the reciprocal sum. For generalized Born runs, the "slowly-varying" forces are those involving derivatives with respect to the effective radii, and pair interactions whose distances are greater than the "inner" cutoff, currently hard-wired at 8 Å. If NRESPA>1 these slowly-varying forces are evaluated every *nrespa* steps. The forces are adjusted appropriately, leading to an impulse at that step. If *nrespa*dt* is less than or equal to 4 fs then the energy conservation is not seriously compromised. However if *nrespa*dt* > 4 fs then the simulation becomes less stable. Note that energies and related quantities are only accessible every *nrespa* steps, since the values at other times are meaningless.

1.8.7 Temperature regulation

   Note: Flag "ntt" is used for the temperature regulation in the default thermostat scheme as shown below. The "middle" thermostat scheme [Section **??**] is much more efficient than the default scheme to accurately sample the configuration/conformation space in the molecular dynamics simulation for the NVT ensemble. Please read Section **??** for more details.

ntt   Switch for temperature scaling. Note that setting *ntt*=0 corresponds to the microcanonical (NVE) ensemble (which should approach the canonical one for large numbers of degrees of freedom). Some aspects of the "weak-coupling ensemble" (*ntt*=1) have been examined, and roughly interpolate between the microcanonical and canonical ensembles.[7, 8] The *ntt*=2 and 3 options correspond to the canonical (constant T) ensemble.

   = 0 Constant total energy classical dynamics (assuming that *ntb*<2, as should probably always be the case when *ntt*=0).

   = 3 Use Langevin dynamics with the collision frequency γ given by *gamma_ln*, discussed below. Note that when γ has its default value of zero, this is the same as setting *ntt* = 0. Since Langevin simulations are highly susceptible to "synchronization" artifacts,[9, 10] you should explicitly set the *ig* variable (described below) to a different value at each restart of a given simulation. (Setting $ig = -1$ will randomize this starting seed, based on the system clock.)

   = 10 Stochastic Isokinetic Nose-Hoover RESPA integrator [11]. A novel isokinetic integrator developed by Tuckerman and co-workers that invokes an isokinetic constraint on the particle velocities combined with *nkija* (see below) auxiliary thermostat velocities *v1* and *v2*. The integrator includes a stochastic component in the equations of motion, which introduces white

noise into the system, for the purpose of minimizing resonance instabilities in the velocities, ultimately allowing for larger RESPA steps. The isokinetic constraint has the form $mv^2 + \frac{L}{L+1}\sum_{i=1}^{L} Q_1 v_{1i}^2 = Lk_BT$. Here L is the number of additional thermostat degrees of freedom, defined in AMBER as *nkija* (see below), and Q_1 is the thermostat mass, determined from *sinrtau* (below), v is the particle velocity and v_1 is one of two auxiliary velocities (e.g. thermostat velocities), and m, k_B, and T, are the particle mass, Boltzmann constant, and system temperature (*temp0*), respectively. In using this integrator, the system is placed in the isokinetic ensemble, as such the velocities are NOT canonical and no thermodynamic observables can be derived from them. This will lead to anomalous temperature readings throughout the simulation - for 1 thermostat degree of freedom ($L = nkija = 1$) the temperature will appear about one-half the specified temperature (*temp0*), and with additional thermostat DOF, the temperature will approach, but never exceed, the desired temperature, *temp0*. However, the particle coordinates ARE canonical and it can be said the configurations obtained from a simulation were sampled from a Boltzmann distribution at the specified temperature (*temp0*).

temp0   Reference temperature at which the system is to be kept, if $ntt > 0$. Note that for temperatures above 300K, the step size should be reduced since increased distance traveled between evaluations can lead to SHAKE and other problems. Default 300.

tempi   Initial temperature. For the initial dynamics run, (*ntx* = 1 or for Amber versions much older than 20, ntx < 3) the velocities are assigned from a Maxwellian distribution at *tempi* K. If *tempi* = 0.0, the velocities will be calculated from the forces instead. *tempi* has no effect if *ntx* = 5 (for Amber versions much older than 20, if ntx > 3). Default 0.0.

ig   The seed for the pseudo-random number generator. The MD starting velocity is dependent on the random number generator seed if *tempi* is nonzero and *ntx* = 1 (for Amber versions much older than 20, if ntx < 3). The value of this seed also affects the set of pseudo-random values used for Langevin dynamics or Andersen-like coupling, and hence should be set to a different value on each restart if *ntt* = 2 or 3. If *ig* = −1 (the default) then the random seed will be based on the current date and time, and hence will be different for every run. Unless you specifically desire reproducibility, it is recommended that you set *ig* = −1 for all runs involving *ntt* = 2 or 3.

gamma_ln   The collision frequency γ, in ps^{-1}, when *ntt* = 3. Default is 0. A. See Section **??** for details. Note that it is not necessary that γ approximate the physical collision frequency, which is about 50 ps^{-1} for liquid water. In fact, it is often advantageous, in terms of sampling[12, 13] or stability of integration[14], to use much smaller values, around 2 to 5 ps^{-1}.[12, 14] For implicit solvent (GB), even much lower values may be useful: for example, setting gamma_ln to 0.01 ps^{-1} can lead to significant, up to 100-fold in some cases, speedup of conformational sampling.[15]

The recommended value for *gamma_ln* is related to the characteristic frequency ($\tilde{\omega}$) of the specific system. The characteristic time of the potential energy autocorrelation function is

$$\tau_{UU} = \int_0^\infty \frac{\langle U(0)U(t)\rangle - \langle U\rangle^2}{\langle U^2\rangle - \langle U\rangle^2}\,\mathrm{d}t \tag{1.1}$$

The optimal value of the thermostat parameter that produces the minimum correlation time of the potential is $\xi^{opt} \approx \tilde{\omega}$ for Langevin dynamics and $\xi^{opt} \approx \sqrt{2}\tilde{\omega}$ for the Andersen thermostat, as the time interval Δt approaches zero. E.g. for a HO molecule, the frequency of the O-H stretch is around 3600 cm^{-1}(680 ps^{-1}), so one can choose 680 ps^{-1} as the value of *therm_par* when Langevin dynamics is used, or 960 ps^{-1} when the Andersen thermostat is employed. When the time interval Δt is finite in the two thermostatting methods, while the characteristic correlation time goes to infinity as the thermostat parameter approaches zero, the characteristic correlation time gradually reaches a plateau as the thermostat parameter increases. (Please see Refs. [3–5] for more discussion.) When condensed phase systems are simulated, it is not straightforward to estimate the optimal thermostat parameter(s) that could be related to the mixing of frequencies (or

time scales) of the system [16]. Some numerical tests are necessary for obtaining the reasonable region for the thermostat parameter such that the characteristic time divided by the time interval is relatively small. (This is true not only for the "middle" scheme but for all thermostat algorithms.) For a liquid water system (216 water molecules in a cell with periodic boundary conditions) with no holonomic constraints, the thermostat parameter is usually chosen to be $2 - 50$ ps^{-1}.

vlimit   If not equal to 0.0, then any component of the velocity that is greater than abs(VLIMIT) will be reduced to VLIMIT (preserving the sign). This can be used to avoid occasional instabilities in molecular dynamics runs. VLIMIT should generally be set to a value like 20 (the default), which is well above the most probable velocity in a Maxwell-Boltzmann distribution at room temperature. A warning message will be printed whenever the velocities are modified. Runs that have more than a few such warnings should be carefully examined.

nkija   For use with *ntt=10*. This specifies the number of additional auxiliary velocity variables *v1* and *v2*, which will total nkija×*v1* +nkija×*v2* *[11]*. Default is 1.

sinrtau   For the SINR (Stochastic Isokinetic Nose-Hoover RESPA) integrator (*ntt=10*), this specifies the time scale for determining the masses associated with the two auxiliary velocity variables *v1* and *v2* (e.g. thermostat velocities) and hence the magnitude of the coupling of the physical velocities with the auxiliary velocities. Generally this should be related to the time scale of the system. See [11] for more explanation. Default is 1.0.

1.8.8 Pressure regulation

In "constant pressure" dynamics, the volume of the unit cell is adjusted (by small amounts on each step) to make the computed pressure approach the target pressure, *pres0*. Equilibration with *ntp > 0* is generally necessary to adjust the density of the system to appropriate values. Pressure regulation only applies when Constant Pressure periodic boundary conditions are used (*ntp > 0*). The Monte Carlo barostat samples rigorously from the isobaric-isothermal ensemble and does not necessitate computing the virial. Please note: in general you will need to equilibrate the temperature to something like the final temperature using constant volume (*ntp=0*) *before* switching on constant pressure simulations to adjust the system to the correct density. If you fail to do this, the program will try to adjust the density too quickly, and bad things (such as SHAKE failures) are likely to happen.

ntp   Flag for constant pressure dynamics. This option should be set to 1 or 2 when Constant Pressure periodic boundary conditions are used.

    = 0 No pressure scaling (Default)

    = 1 md with isotropic position scaling

barostat   Flag used to control which barostat to use in order to control the pressure.

    = 2 Monte Carlo barostat

mcbarint   Number of steps between volume change attempts performed as part of the Monte Carlo barostat. Default is 100.

pres0   Reference pressure (in units of bars, where 1 bar $\approx$ 0.987 atm) at which the system is maintained (when NTP > 0). Default 1.0.

Surface tension regulation

Constant surface tension is used in statistical ensembles for simulating liquid interfaces. This is primarily intended for lipid membrane simulations with two or more interfaces. Constant surface tension is only available for simulations with anisotropic pressure or semiisotropic scaling. This algorithm is an extension to the Berendsen pressure scaling algorithm that adjusts the tangential pressure evaluation in order to maintain a "constant" surface tension.[17] Since the surface tension is a function of the pressure tensor, fluctuations of the surface tension will be large.

In order to use constant surface tension, periodic boundary conditions (ntb = 2), anisotropic or semiisotropic pressure scaling (ntp = 2 or ntp =3), and an orthogonal box must be used.

csurften Flag for constant surface tension dynamics.

   = 0 No constant surface tension (default)

   = 1 Constant surface tension with interfaces in the yz plane

   = 2 Constant surface tension with interfaces in the xz plane

   = 3 Constant surface tension with interfaces in the xy plane

gamma_ten Surface tension value in units of dyne/cm. Default value is 0.0 dyne/cm.

ninterface Number of interfaces in the periodic box. There must be at least two interfaces in the periodic box. Two interfaces is appropriate for a lipid bilayer system and is the default value.

1.8.9 SHAKE bond length constraints

ntc Flag for SHAKE to perform bond length constraints.[18] (See also NTF in the **Potential function** section. In particular, typically NTF = NTC.) The SHAKE option should be used for most MD calculations. The size of the MD timestep is determined by the fastest motions in the system. SHAKE removes the bond stretching freedom, which is the fastest motion, and consequently allows a larger timestep to be used. For water models, a special "three-point" algorithm is used.[19] Consequently, to employ TIP3P set NTF = NTC = 2.

   Since SHAKE is an algorithm based on dynamics, the minimizer is not aware of what SHAKE is doing; for this reason, minimizations generally should be carried out without SHAKE. One exception is short minimizations whose purpose is to remove bad contacts before dynamics can begin.

   For parallel versions of *sander* only intramolecular atoms can be constrained. Thus, such atoms must be in the same chain of the originating PDB file.

   = 1 SHAKE is not performed (default)

   = 2 bonds involving hydrogen are constrained

   = 3 all bonds are constrained (not available for parallel or qmmm runs in *sander*)

tol Relative geometrical tolerance for coordinate resetting in shake. Recommended maximum: <0.00005 Angstrom Default 0.00001.

jfastw Fast water definition flag. By default, the system is searched for water residues, and special routines are used to SHAKE these systems.[19]

   = 0 Normal operation. Waters are identified by the default names (given below), unless they are redefined, as described below.

   = 4 Do not use the fast SHAKE routines for waters.

   The following variables allow redefinition of the default residue and atom names used by the program to determine which residues are waters.

   WATNAM The residue name the program expects for water. Default 'WAT '.

   OWTNM The atom name the program expects for the oxygen of water. Default 'O '.

   HWTNM1 The atom name the program expects for the 1st H of water. Default 'H1 '.

   HWTNM2 The atom name the program expects for the 2nd H of water. Default 'H2 '.

`noshakemask` String that specifies atoms that are not to be shaken (assuming that ntc>1). Any bond that would otherwise be shaken by virtue of the *ntc* flag, but which involves an atom flagged here, will *not* be shaken. The syntax for this string is given in Chap. 13.5. Default is an empty string, which matches nothing. A typical use would be to remove SHAKE constraints from all or part of a solute, while still shaking rigid water models like TIPnP or SPC/E. Another use would be to turn off SHAKE constraints for the parts of the system that are being changed with thermodynamic integration, or which are the EVB or quantum regions of the system.

If this option is invoked, then all parts of the potential must be evaluated, that is, *ntf* must be one. The code enforces this by setting *ntf* to 1 when a *noshakemask* string is present in the input.

If you want the *noshakemask* to apply to all or part of the water molecules, you must also set *jfastw=4*, to turn off the special code for water SHAKE. (If you are not shaking waters, you presumably also want to issue the "set default FlexibleWater on" command in LEaP; see that chapter for more information.)

1.8.10 NMR refinement options

(Users to should consult the section NMR refinement to see the context of how the following parameters would be used.)

`iscale` Number of additional variables to optimize beyond the 3N structural parameters. (Default = 0). At present, this is only used with residual dipolar coupling and CSA or pseudo-CSA restraints.

`noeskp` The NOESY volumes will only be evaluated if mod(nstep, noeskp) = 0; otherwise the last computed values for intensities and derivatives will be used. (default = 1, i.e. evaluate volumes at every step)

`ipnlty` This parameter determines the the functional form of the penalty function for NOESY volume and chemical shift restraints.

> **= 1** the program will minimize the sum of the absolute values of the errors; this is akin to minimizing the crystallographic R-factor (default).

> **= 2** the program will optimize the sum of the squares of the errors.

> **= 3** For NOESY intensities, the penalty will be of the form $awt[I_c^{1/6} - I_o^{1/6}]^2$. Chemical shift penalties will be as for *ipnlty=1*.

`mxsub` Maximum number of submolecules that will be used. This is used to determine how much space to allocate for the NOESY calculations. Default 1.

`scalm` "Mass" for the additional scaling parameters. Right now they are restricted to all have the same value. The larger this value, the slower these extra variables will respond to their environment. Default 100 amu.

`pencut` In the summaries of the constraint deviations, entries will only be made if the penalty for that term is greater than PENCUT. Default 0.1.

`tausw` For noesy volume calculations (*NMROPT = 2*), intensities with mixing times less that TAUSW (in seconds) will be computed using perturbation theory, whereas those greater than TAUSW will use a more exact theory. See the theory section (below) for details. To always use the "exact" intensities and derivatives, set TAUSW = 0.0; to always use perturbation theory, set TAUSW to a value larger than the largest mixing time in the input. Default is TAUSW of 0.1 second, which should work pretty well for most systems.

1.8.11 EMAP restraints

EMAP restraints are used to perform targeted conformational search (TCS)[20]. EMAP uses maps to define restraints to maintain conformations and/or to induce simulation systems to the target conformations. The restraint map can be either obtained from electron microscopy experiments or derived from known protein structures, or defined from initial simulation coordinates. EMAP can be used to do rigid docking of molecules into maps and to do flexible fitting to obtain conformations defined by experimental maps. EMAP can also be used to maintain conformations of protein domains when studying large scale conformational change. Users should consult the section 9.1 to see how to define EMAP restraints.

iemap Turn on EMAP restrained simulation when *iemap*>0. (Default = 0). EMAP restraint information must be input from *&emap* namelists in the input file.

gammamap Friction constant for the EMAP restraint maps when allowed to move. (Default=1/ps). (See Section 9.1)

1.9 Potential function parameters

The parameters in this section generally control what sort of force field (or potential function) is used for the simulation.

1.9.1 Generic parameters

ntf Force evaluation. Note: If SHAKE is used (see NTC), it is not necessary to calculate forces for the constrained bonds.

  = 1 complete interaction is calculated (default)

  = 2 bond interactions involving H-atoms omitted (use with NTC=2)

  = 3 all the bond interactions are omitted (use with NTC=3)

  = 4 angle involving H-atoms and all bonds are omitted

  = 5 all bond and angle interactions are omitted

  = 6 dihedrals involving H-atoms and all bonds and all angle interactions are omitted

  = 7 all bond, angle and dihedral interactions are omitted

  = 8 all bond, angle, dihedral and non-bonded interactions are omitted

ntb This variable controls whether or not periodic boundaries are imposed on the system during the calculation of non-bonded interactions. Bonds spanning periodic boundaries are not yet supported. There is no longer any need to set this variable, since it can be determined from igb and ntp parameters. The "proper" default for ntb is chosen (ntb=0 when igb > 0, ntb=2 when ntp > 0, and ntb=1 otherwise). This behavior can be overridden by supplying an explicit value, although this is discouraged to prevent errors. The allowed values for NTB are

  = 0 no periodicity is applied and PME is off (default when igb > 0)

  = 1 constant volume (default when igb and ntp are both 0, which are their defaults)

  = 2 constant pressure (default when ntp > 0)

  If NTB is nonzero then there must be a periodic boundary in the topology file. Constant pressure is not used in minimization (IMIN=1, above).

  For a periodic system, constant pressure is the only way to equilibrate density if the starting state is not correct. For example, the solvent packing scheme used in LEaP can result in a net void when solvent molecules are subtracted which can aggregate into "vacuum bubbles" in a constant volume run. Another potential problem are small gaps at the edges of the box. The upshot is

that almost every system needs to be equilibrated at constant pressure (*ntb=2, ntp>0*) to get to a proper density. But be sure to equilibrate first (at constant volume) to something close to the final temperature, before turning on constant pressure.

dielc   Dielectric multiplicative constant for the electrostatic interactions. Default is 1.0. Please note this is NOT related to dielectric constants for generalized Born or Poisson-Boltzmann calculations. It should only be used for quasi-vacuum simulations.

cut   This is used to specify the nonbonded cutoff, in Angstroms. For PME, the cutoff is used to limit direct space sum, and 8.0 is usually a good value. When *igb>0*, the cutoff is used to truncate nonbonded pairs (on an atom-by-atom basis); here a larger value than the default is generally required. A separate parameter (**RGBMAX**) controls the maximum distance between atom pairs that will be considered in carrying out the pairwise summation involved in calculating the effective Born radii, see the generalized Born section below.
When *igb > 0*, the default is 9999.0 (effectively infinite)
When *igb==0*, the default is 8.0.

fswitch   When off, *fswitch<=0* , uses a truncation cutoff. When on *fswitch>0*, sets a force switching region where the force cutoff smoothly approaches 0 between the region of the fswitch value to the cut value. Force values below the fswitch value follow the standard Lennard-Jones force. Default is -1. This option is not supported for use with GB (i.e., only *igb=0* and *ntb>0*), nor is it compatible with the 12-6-4 Lennard-Jones model (*lj1264=1*). Due to performance regressions (about 20%) with running with the force switching on, it is recommended that simulations run with fswitch off unless using a force field that requires or recommends using the force switch.

nsnb   Determines the frequency of nonbonded list updates when *igb=0* and *nbflag=0*; see the description of *nbflag* for more information. Default is 25.

igb   Flag for using the generalized Born implicit solvent models. See Chapter 2 for information about using this option. Default is 0.

irism   Flag for 3D-reference interaction site model (RISM) molecular solvation method. See Section3.3for information about this option. Default is 0.

lj1264   In general, you should rarely have to set this variable. When the Lennard-Jones C-coefficient is found in your prmtop file, the default value is set to 1 (meaning it is active). When this flag is *not* present in the prmtop file, the default value is set to 0 (meaning the 12-6-4 potential [21] is inactive). Setting this to 0 when the C-coefficient is present will forcibly turn off the 12-6-4 potential. Setting lj1264 to 1 when no C-coefficient is present will result in a fatal error. Therefore, this flag can be used to quickly disable the r^{-4} term. However, the remaining L-J parameters will still be optimized for the 12-6-4 potential, so this should only be done when testing!.

1.9.2 Particle Mesh Ewald

The Particle Mesh Ewald (PME) method is always "on", unless *ntb* = 0. PME is a fast implementation of the Ewald summation method for calculating the full electrostatic energy of a unit cell (periodic box) in a macroscopic lattice of repeating images. The PME method is fast since the reciprocal space Ewald sums are B-spline interpolated on a grid and since the convolutions necessary to evaluate the sums are calculated via fast Fourier transforms (FFTs). Note that the accuracy of the PME method is related to the density of the charge grid (NFFT1, NFFT2, and NFFT3), the spline interpolation order (ORDER), and the direct sum tolerance (DSUM_TOL); see the descriptions below for more information.

The PME method was implemented originally in Amber 3a by Tom Darden and has been developed in subsequent versions by many people, in particular by Tom Darden, Celeste Sagui, Tom Cheatham and Mike Crowley.[22–25] Generalizations of this method to systems with polarizable dipoles and electrostatic multipoles are described in Refs. [26, 27].

The &ewald namelist is read immediately after the &cntrl namelist. We have tried hard to make the defaults for these parameters appropriate for solvated simulations. *Please take care in changing any values from their defaults.* The &ewald namelist has the following variables:

nfft1, nfft2, nfft3 These give the size of the charge grid (upon which the reciprocal sums are interpolated) in each dimension. Higher values lead to higher accuracy (when the DSUM_TOL is also lowered) but considerably slow the calculation. Generally it has been found that reasonable results are obtained when NFFT1, NFFT2 and NFFT3 are approximately equal to A, B and C, respectively, leading to a grid spacing (A/NFFT1, etc.) of 1.0 Å. Significant performance enhancement in the calculation of the fast Fourier transform is obtained by having each of the integer NFFT1, NFFT2 and NFFT3 values be a *product of powers* of 2, 3, and/or 5. If the values are not given, the program will chose values to meet these criteria.

order The order of the B-spline interpolation. The higher the order, the better the accuracy (unless the charge grid is too coarse). The minimum order is 3. An order of 4 (the default) implies a cubic spline approximation which is a good standard value. Note that the cost of the PME goes as roughly the order to the third power.

verbose Standard use is to have VERBOSE = 0. Setting VERBOSE to higher values (up to a maximum of 3) leads to voluminous output of information about the PME run.

dsum_tol This relates to the width of the direct sum part of the Ewald sum, requiring that the value of the direct sum at the Lennard-Jones cutoff value (specified in CUT as during standard dynamics) be less than DSUM_TOL. In practice it has been found that the relative error in the Ewald forces (RMS) due to cutting off the direct sum at CUT is between 10.0 and 50.0 times DSUM_TOL. Standard values for DSUM_TOL are in the range of 10^{-6} to 10^{-5}, leading to estimated RMS deviation force errors of 0.00001 to 0.0005. Default is 10^{-5}.

rsum_tol This serves as a way to generate the number of reciprocal vectors used in an Ewald sum. Typically the relative RMS reciprocal sum error is about 5-10 times RSUM_TOL. Default is 5 x 10^{-5}.

mlimit(1,2,3) This allows the user to explicitly set the number of reciprocal vectors used in a regular Ewald run. Note that the sum goes from -MLIMIT(2) to MLIMIT(2) and -MLIMIT(3) to MLIMIT(3) with symmetry being used in first dimension. Note also the sum is truncated outside an automatically chosen sphere.

ew_coeff Ewald coefficient, in Å^{-1}. Default is determined by *dsum_tol* and *cutoff*. If it is explicitly inputed then that value is used, and *dsum_tol* is computed from *ew_coeff* and *cutoff*.

nbflag If *nbflag = 0*, construct the direct sum nonbonded list in the "old" way, *i.e.* update the list every *nsnb* steps. If *nbflag = 1* (the default when *imin = 0* or *ntb > 0*), *nsnb* is ignored, and the list is updated whenever any atom has moved more than 1/2 *skinnb* since the last list update.

skinnb Width of the nonbonded "skin". The direct sum nonbonded list is extended to *cut + skinnb*, and the van der Waals and direct electrostatic interactions are truncated at *cut*. Default is 2.0 Å. Use of this parameter is required for energy conservation, and recommended for all PME runs.

netfrc The basic "smooth" PME implementation used here does not necessarily conserve momentum. If *netfrc = 1*, (the default) the total force on the system is artificially removed at every step. This parameter is set to 0 if minimization is requested, which implies that the gradient is an accurate derivative of the energy. You should only change this parameter if you really know what you are doing.

vdwmeth Determines the method used for van der Waals interactions beyond those included in the direct sum. A value of 0 includes no correction; the default value of 1 uses a continuum model correction for energy and pressure.

eedmeth   Determines how the switch function for the direct sum Coulomb interaction is evaluated. The default value of 1 uses a cubic spline. A value of 2 implies a linear table lookup. A value of three implies use of an "exact" subroutine call.

eedtbdns   Density of spline or linear lookup table, if *eedmeth* is 1 or 2. Default is 500 points per unit.

column_fft 1 or 0 flag to turn on or off, respectively, column-mode fft for parallel runs. The default mode is slab mode which is efficient for low processor counts. The column method can be faster for larger processor counts since there can be more columns than slabs and the communications pattern is less congested. This flag has no effect on non-parallel runs. Users should test the efficiency of the method in comparison to the default method before performing long calculations. Default is 0 (off).

1.9.3 Extra point options

   Several parameters deal with "extra-points" (sometimes called lone-pairs), which are force centers that are not at atomic positions. These are currently defined as atoms with "EP" in their names. These input variables are really only for the convenience of force-field developers; *do not change the defaults unless you know what you are doing, and have read the code.* These variables are set in the &ewald namelist.

frameon   If *frameon* is set to 1, (default) the bonds, angles and dihedral interactions involving the lone pairs/extra points are removed except for constraints added during parm. The lone pairs are kept in ideal geometry relative to local atoms, and resulting torques are transferred to these atoms. To treat extra points as regular atoms, set frameon=0.

chngmask   If *chngmask*=1 (default), new 1-1, 1-2, 1-3 and 1-4 interactions are calculated. An extra point belonging to an atom has a 1-1 interaction with it, and participates in any 1-2, 1-3 or 1-4 interaction that atom has. For example, suppose (excusing the geometry) C1,C2,C3,C4 form a dihedral and each has 1 extra point attached as below

```
        C1------C2------C3------C4
         |       |       |       |
        Ep1     Ep2     Ep3     Ep4
```
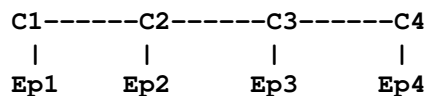
The 1-4 interactions include C1-C4, Ep1-C4, C1-Ep4, and Ep1-Ep4. (To see a printout of all 1-1, 1-2, 1-3 and 1-4 interactions set verbose=1.) These interactions are masked out of nonbonds. Thus the amber mask list is rebuilt from these 1-1, 1-2, 1-3 and 1-4 pairs. A separate list of 1-4 nonbonds is then compiled. This list does not agree in general with the above 1-4, since a 1-4 could also be a 1-3 if its in a ring. See the *ephi()* routine for the precise algorithm involved here. The list of 1-4 nonbonds is printed if *verbose=1*.

1.9.4 Detailed MPI Timings

profile_mpi Adjusts whether detailed per thread timings should be written to a file called profile_mpi when running sander in parallel. By default only average timings are printed to the output file. This is done for performance reasons, especially when running *multisander* runs. However for development it is useful to know the individual timings for each mpi thread. When running in serial the value of profile_mpi is ignored.

   = 0 No detailed MPI timings will be written (default).

   = 1 A detailed breakdown of the timings for each MPI thread will be written to the file: profile_mpi.

1.10 Varying conditions

This section of information is read (*if NMROPT > 0*) as a series of namelist specifications, with name "&wt". This namelist is read repeatedly until a namelist &wt statement is found with TYPE=END.

TYPE   Defines quantity being varied; valid options are listed below.

ISTEP1,ISTEP2   This change is applied over steps/iterations ISTEP1 through ISTEP2. If ISTEP2 = 0, this change will remain in effect from step ISTEP1 to the end of the run at a value of VALUE1 (VALUE2 is ignored in this case). *(default= both 0)*

VALUE1,VALUE2   Values of the change corresponding to ISTEP1 and ISTEP2, respectively. If ISTEP2=0, the change is fixed at VALUE1 for the remainder of the run, once step ISTEP1 is reached.

IINC   If IINC > 0, then the change is applied as a step function, with IINC steps/iterations between each change in the target VALUE (ignored if ISTEP2=0). If IINC =0, the change is done continuously. *(default=0)*

IMULT   If IMULT=0, then the change will be linearly interpolated from VALUE1 to VALUE2 as the step number increases from ISTEP1 to ISTEP2. *(default)* If IMULT=1, then the change will be effected by a series of multiplicative scalings, using a single factor, R, for all scalings. i.e.

$$VALUE2 = (R**INCREMENTS) * VALUE1.$$

INCREMENTS is the number of times the target value changes, which is determined by ISTEP1, ISTEP2, and IINC.

The remainder of this section describes the options for the TYPE parameter. For a few types of cards, the meanings of the other variables differ from that described above; such differences are noted below. Valid Options for TYPE (you must use uppercase) are:

BOND   Varies the relative weighting of bond energy terms.

ANGLE   Varies the relative weighting of valence angle energy terms.

TORSION   Varies the relative weighting of torsion (and J-coupling) energy terms. Note that any restraints defined in the input to the PARM program are included in the above. Improper torsions are handled separately (IMPROP).

IMPROP   Varies the relative weighting of the "improper" torsional terms. These are not included in TORSION.

VDW   Varies the relative weighting of van der Waals energy terms. This is equivalent to changing the well depth (epsilon) by the given factor.

HB   Varies the relative weighting of hydrogen-bonding energy terms.

ELEC   Varies the relative weighting of electrostatic energy terms.

NB   Varies the relative weights of the non-bonded (VDW, HB, and ELEC) terms.

ATTRACT   Varies the relative weights of the attractive parts of the van der waals and h-bond terms.

REPULSE   Varies the relative weights of the repulsive parts of the van der waals and h-bond terms.

RSTAR   Varies the effective van der Waals radii for the van der Waals (VDW) interactions by the given factor. Note that this is done by changing the relative attractive and repulsive coefficients, so ATTRACT/REPULSE should not be used over the same step range as RSTAR.

INTERN   Varies the relative weights of the BOND, ANGLE and TORSION terms. "Improper" torsions (IMPROP) must be varied separately.

ALL   Varies the relative weights of all the energy terms above (BOND, ANGLE, TORSION, VDW, HB, and ELEC; does not affect RSTAR or IMPROP).

REST   Varies the relative weights of *all* the NMR restraint energy terms.

RESTS   Varies the weights of the "short-range" NMR restraints. Short- range restraints are defined by the SHORT instruction (see below).

RESTL   Varies the weights of any NMR restraints which are not defined as "short range" by the SHORT instruction (see below). When no SHORT instruction is given, RESTL is equivalent to REST.

NOESY   Varies the overall weight for NOESY volume restraints. Note that this value multiplies the individual weights read into the "awt" array. (Only if NMROPT=2; see Section 4 below).

SHIFTS   Varies the overall weight for chemical shift restraints. Note that this value multiplies the individual weights read into the "wt" array. (Only if NMROPT=2; see section 4 below).

XRAY   Varies the xray_weight restraint weight.

SHORT   Defines the short-range restraints. For this instruction, ISTEP1, ISTEP2, VALUE1, and VALUE2 have different meanings. A short-range restraint can be defined in two ways.

              (1) If the residues containing each pair of bonded atoms comprising the restraint are close enough in the primary sequence:

$$ISTEP1 \leq ABS(delta\_residue) \leq ISTEP2,$$

              where delta_residue is the difference in the numbers of the residues containing the pair of bonded atoms.

              (2) If the distances between each pair of bonded atoms in the restraint fall within a prescribed range:

$$VALUE1 \leq distance \leq VALUE2.$$

              Only one SHORT command can be issued, and the values of ISTEP1, ISTEP2, VALUE1, and VALUE2 remain fixed throughout the run. However, if IINC>0, then the short-range interaction list will be re-evaluated every IINC steps.

TGTRMSD   Varies the RMSD target value for targeted MD.

TEMP0   Varies the target temperature TEMP0.

TEMP0LES   Varies the LES target temperature TEMP0LES.

TAUTP   Varies the coupling parameter, TAUTP, used in temperature scaling when temperature coupling options NTT=1 is used.

CUT   Varies the non-bonded cutoff distance.

NSTEP0   If present, this instruction will reset the initial value of the step counter (against which ISTEP1/ISTEP2 and NSTEP1/NSTEP2 are compared) to the value ISTEP1. This only affects the way in which NMR weight restraints are calculated. It does not affect the value of NSTEP that is printed as part of the dynamics output. An NSTEP0 instruction only has an effect at the beginning of a run. For this card (only) ISTEP2, VALUE1, VALUE2 and IINC are ignored. If this card is omitted, NSTEP0 = 0. This card can be useful for simulation restarts, where NSTEP0 is set to the final step on the previous run.

STPMLT If present, the NMR step counter will be changed in increments of STPMLT for each actual dynamics step. For this card, only VALUE1 is read. ISTEP1, ISTEP2, VALUE2, IINC, and IMULT are ignored. Default = 1.0.

DISAVE, ANGAVE, TORAVE If present, then by default time-averaged values (rather than instantaneous values) for the appropriate set of restraints will be used. DISAVE controls distance data, ANGAVE controls angle data, TORAVE controls torsion data. See below for the functional form used in generating time-averaged data.

For these cards: VALUE1 = τ (characteristic time for exponential decay) VALUE2 = POWER (power used in averaging; the nearest integer of value2 is used) Note that the range (ISTEP1→ISTEP2) applies only to TAU; The value of POWER is not changed by subsequent cards with the same ITYPE field, and time-averaging will always be turned on for the entire run if one of these cards appears.

Note also that, due to the way that the time averaged internals are calculated, changing τ at any time after the start of the run will only affect the relative weighting of steps occurring after the change in τ. Separate values for τ and POWER are used for bond, angle, and torsion averaging.

The default value of τ (if it is 0.0 here) is 1.0D+6, which results in no exponential decay weighting. Any value of $\tau \geq 1.D+6$ will result in no exponential decay.

If DISAVE,ANGAVE, or TORAVE is chosen, one can still force use of an instantaneous value for specific restraints of the particular type (bond, angle, or torsion) by setting the IFNTYP field to "1" when the restraint is defined (IFNTYP is defined in the DISANG file).

If time-averaging for a particular class of restraints is being performed, all restraints of that class that are being averaged (that is, all restraints of that class except those for which IFNTYP=1) *must* have the same values of NSTEP1 and NSTEP2 (NSTEP1 and NSTEP2 are defined below). (For these cards, IINC and IMULT are ignored) See the discussion of time-averaged restraints following the input descriptions.

DISAVI, ANGAVI, TORAVI **ISTEP1:** Ignored.

ISTEP2: Sets IDMPAV. If IDMPAV > 0, *and* a dump file has been specified (DUMPAVE is set in the file redirection section below), then the time-averaged values of the restraints will be written every IDMPAV steps. Only one value of IDMPAV can be set (corresponding to the first DISAVI/ANGAVI/TORAVI card with ISTEP2 > 0), and *all* restraints (even those with IFNTYP=1) will be "dumped" to this file every IDMPAV steps. The values reported reflect the current value of τ.

VALUE1: The integral which gives the time-averaged values is undefined for the first step. By default, for each time-averaged internal, the integral is assigned the current value of the internal on the first step. If VALUE1≠0, this initial value of internal r is reset as follows:

> **−1000. < VALUE1 < 1000.: Initial value = r_initial + VALUE**
> **VALUE1 <= −1000.: Initial value = r_target + 1000.**
> **1000. <= VALUE1 : Initial value = r_target − 1000.**

r_target is the target value of the internal, given by R2+R3 (or just R3, if R2 is 0). VALUE1 is in angstroms for bonds, in degrees for angles.

VALUE2: This field can be used to set the value of τ used in calculating the time-averaged values of the internal restraints reported at the end of a simulation (if LISTOUT is specified in the redirection section below). By default, no exponential decay weighting is used in calculating the final reported values, regardless of what value of τ was used during the simulation. If VALUE2>0, then τ = VALUE2 will be used in calculating these final reported averages. Note that the value of VALUE2 = τ specified here only affects the reported averaged values in at the end of a simulation. It does not affect the time-averaged values used during the

simulation (those are changed by the VALUE1 field of DISAVE, ANGAVE and TORAVE instructions).

IINC: If IINC = 0, then forces for the class of time-averaged restraints will be calculated exactly as (dE/dr_ave) (dr_ave/dx). If IINC = 1, then then forces for the class of time-averaged restraints will be calculated as (dE/dr_ave) (dr(t)/dx). Note that this latter method results in a non-conservative force, and does not integrate to a standard form. But this latter formulation helps avoid the large forces due to the $(1+i)$ term in the exact derivative calculation–and may avert instabilities in the molecular dynamics trajectory for some systems. See the discussion of time-averaged restraints following the input description. Note that the DISAVI, ANGAVI, and TORAVI instructions will have no affect unless the corresponding time average request card (DISAVE, ANGAVE or TORAVE, respectively) is also present.

DUMPFREQ   Istep1 is the only parameter read, and it sets the frequency at which the coordinates in the distance or angle restraints are dumped to the file specified by the DUMPAVE command in the I/O redirection section. (For these cards, ISTEP1 and IMULT are ignored).

END   END of this section.

NOTES:

1. All weights are relative to a default of 1.0 in the standard force field.

2. Weights are not cumulative.

3. For any range where the weight of a term is not modified by the above, the weight reverts to 1.0. For any range where TEMP0, SOFTR or CUTOFF is not specified, the value of the relevant constant is set to that specified in the input file.

4. If a weight is set to 0.0, it is set internally to 1.0D-7. This can be overridden by setting the weight to a negative number. In this case, a weight of exactly 0.0 will be used. *However,* if any weight is set to exactly 0.0, it cannot be changed again during this run of the program.

5. If two (or more) cards change a particular weight over the same range, the weight given on the last applicable card will be the one used.

6. Once any weight change for which NSTEP2=0 becomes active (i.e. one which will be effective for the remainder of the run), the weight of this term cannot be further modified by other instructions.

7. Changes to RSTAR result in exponential weighting changes to the attractive and repulsive terms (proportional to the scale factor**6 and **12, respectively). For this reason, scaling RSTAR to a very small value (e.g. ≤ 0.1) may result in a zeroing-out of the vdw term.

1.11 File redirection commands

Input/output redirection information can be read as described here. Redirection cards must follow the end of the weight change information. Redirection card input is terminated by the first non-blank line which does not start with a recognized redirection TYPE (e.g. LISTIN, LISTOUT, etc.).

The format of the redirection cards is

TYPE = filename

where TYPE is any valid redirection keyword (see below), and filename is any character string. The equals sign ("=") is required, and TYPE must be given in *uppercase* letters.

Valid redirection keywords are:

LISTIN   An output listing of the restraints which have been read, and their deviations from the target distances *before* the simulation has been run. By default, this listing is not printed. cedureIf POUT is used for the filename, these deviations will be printed in the normal output file.

LISTOUT   An output listing of the restraints which have been read, and their deviations from the target distances *_after* the simulation has finished. By default, this listing is not printed. If POUT is used for the filename, these deviations will be printed in the normal output file.

DISANG   The file from which the distance and angle restraint information described below (Section 8.1) will be read.

NOESY   File from which NOESY volume information (Section 8.2) will be read.

SHIFTS   File from which chemical shift information (Section 8.3) will be read.

PCSHIFT   File from which paramagnetic shift information (Section 8.3) will be read.

DIPOLE   File from which residual dipolar couplings (Section 8.5) will be read.

CSA   File from which CSA or pseduo-CSA restraints (Section 8.6) will be read.

DUMPAVE   File to which the time-averaged values of all restraints will be written. If DISAVI / ANGAVI / TORAVI has been used to set IDMPAV$\neq$0, then averaged values will be output. If the DUMPFREQ command has been used, the instantaneous values will be output.

1.12 Getting debugging information

The debug options in *sander* are there principally to help developers test new options or to test results between two machines or versions of code, but can also be useful to users who want to test the effect of parameters on the accuracy of their ewald or pme calculations. If the debug options are set, *sander* will exit after performing the debug tasks set by the user.

To access the debug options, include a &debugf namelist. Input parameters are:

do_debugf   Flag to perform this module. Possible values are zero or one. Default is zero. Set to one to turn on debug options.

One set of options is to test that the atomic forces agree with numerical differentiation of energy.

atomn   Array of atom numbers to test atomic forces on. Up to 25 atom numbers can be specified, separated by commas.

nranatm   number of random atoms to test atomic forces on. Atom numbers are generated via a random number generator.

ranseed   seed of random number generator used in generating atom numbers default is 71277

neglgdel   negative log of delta used in numerical differentiating; e.g. 4 means delta is 10^{-4} Angstroms. Default is 5. *Note*: In general it does no good to set nelgdel larger than about 6. This is because the relative force error is at best the square root of the numerical error in the energy, which ranges from 10^{-15} up to 10^{-12} for energies involving a large number of terms.

chkvir   Flag to test the atomic and molecular virials numerically. Default is zero. Set to one to test virials.

dumpfrc   Flag to dump energies, forces and virials, as well as components of forces (bond, angle forces etc.) to the file "forcedump.dat" This produces an ascii file. Default is zero. Set to one to dump forces.

rmsfrc   Flag to compare energies forces and virials as well as components of forces (bond, angle forces etc.) to those in the file "forcedump.dat". Default is zero. Set to one to compare forces.

Several other options are also possible to modify the calculated forces.

`zerochg`   Flag to zero all charges before calculating forces. Default zero. Set to one to remove charges.

`zerovdw`   Flag to remove all van der Waals interactions before calculating forces. Default zero. Set to one to remove van der Waals.

`zerodip`   Flag to remove all atomic dipoles before calculating forces. Only relevant when polarizability is invoked.

`do_dir, do_rec, do_adj, do_self, do_bond, do_cbond, do_angle, do_ephi, do_xconst, do_cap`
These are flags which turn on or off the subroutines they refer to. The defaults are one. Set to zero to prevent a subroutine from running. For example, set do_dir=0 to turn off the direct sum interactions (van der Waals as well as electrostatic). These options, as well as the zerochg, zerovdw, zerodip flags, can be used to fine tune a test of forces, accuracy, etc.

EXAMPLES:
This input list tests the reciprocal sum forces on atom 14 numerically, using a delta of 10^{-4}.

```
&debugf
neglgdel=4, nranatm = 0, atomn = 14,
do_debugf = 1,do_dir = 0,do_adj = 0,do_rec = 1, do_self = 0,
do_bond = 1,do_angle = 0,do_ephi = 0, zerovdw = 0, zerochg = 0,
chkvir = 0,
dumpfrc = 0,
rmsfrc = 0,
/
```

This input list causes a dump of force components to "forcedump.dat". The bond, angle and dihedral forces are not calculated, and van der Waals interactions are removed, so the total force is the Ewald electrostatic force, and the only nonzero force components calculated are electrostatic.

```
&debugf
neglgdel=4, nranatm = 0, atomn = 0,
do_debugf = 1,do_dir = 1,do_adj = 1,do_rec = 1, do_self = 1,
do_bond = 0,do_angle = 0,do_ephi = 0, zerovdw = 1, zerochg = 0,
chkvir = 0,
dumpfrc = 1,
rmsfrc = 0,
/
```

In this case the same force components as above are calculated, and compared to those in "forcedump.dat". Typically this is used to get an RMS force error for the Ewald method in use. To do this, when doing the force dump use ewald or pme parameters to get high accuracy, and then normal parameters for the force compare:

```
&debugf
neglgdel=4, nranatm = 0, atomn = 0,
do_debugf = 1,do_dir = 1,do_adj = 1,do_rec = 1, do_self = 1,
do_bond = 0,do_angle = 0,do_ephi = 0, zerovdw = 1, zerochg = 0,
chkvir = 0,
dumpfrc = 0,
rmsfrc = 1,
/
```

For example, if you have a 40x40x40 unit cell and want to see the error for default pme options (cubic spline, 40x40x40 grid), run 2 jobs—— (assume box params on last line of inpcrd file)
Sample input for 1st job:

```
    &cntrl
    dielc =1.0,
    cut = 11.0, nsnb = 5, ibelly = 0,
    ntx = 5, irest = 1,
    ntf = 2, ntc = 2, tol = 0.0000005,
    ntb = 1, ntp = 0, temp0 = 300.0, tautp = 1.0,
    nstlim = 1, dt = 0.002, maxcyc = 5, imin = 0, ntmin = 2,
    ntpr = 1, ntwx = 0, ntt = 0, ntr = 0,
    jfastw = 0, nmrmax=0, ntave = 25,
    /
    &debugf
    do_debugf = 1,do_dir = 1,do_adj = 1,do_rec = 1, do_self = 1,
    do_bond = 0,do_angle = 0,do_ephi = 0, zerovdw = 1, zerochg = 0,
    chkvir = 0,
    dumpfrc = 1,
    rmsfrc = 0,
    /
    &ewald
    nfft1=60,nfft2=60,nfft3=60,order=6, ew_coeff=0.35,
    /
```

Sample input for 2nd job:

```
    &cntrl
    dielc =1.0,
    cut = 8.0, nsnb = 5, ibelly = 0,
    ntx = 5, irest = 1,
    ntf = 2, ntc = 2, tol = 0.0000005,
    ntb = 1, ntp = 0, temp0 = 300.0, tautp = 1.0,
    nstlim = 1, dt = 0.002, maxcyc = 5, imin = 0, ntmin = 2,
    ntpr = 1, ntwx = 0, ntt = 0, ntr = 0,
    jfastw = 0, nmrmax=0, ntave = 25,
    /
    &debugf
    do_debugf = 1,do_dir = 1,do_adj = 1,do_rec = 1, do_self = 1,
    do_bond = 0,do_angle = 0,do_ephi = 0, zerovdw = 1, zerochg = 0,
    chkvir = 0,
    dumpfrc = 0,
    rmsfrc = 1,
    /
    &ewald
    ew_coeff=0.35,
    /
```

Note that an Ewald coefficient of 0.35 is close to the default error for an 8 Angstrom cutoff. However, the first job used an 11 Angstrom cutoff. The direct sum forces calculated in the 2nd job are compared to these, giving the RMS error due to an 8 Angstrom cutoff, with this value of ew_coeff. The reciprocal sum error calculated in the 2nd job is with respect to the pme reciprocal forces in the 1st job considered as "exact".

Note further that if in these two jobs you had not specified "ew_coeff" *sander* would have calculated ew_coeff according to the cutoff and the direct sum tolerance, defaulted to 10^{-5}. This would give two different ewald coefficients. Under these circumstances the direct, reciprocal and adjust energies and forces would not agree well between the two jobs. However the total energy and forces should agree reasonrespanably, (forces to within about $5x10^{-4}$ relative RMS force error) Since the totals are invariant to the coefficient.

Finally, note that if other force components are calculated, such as van der Waals, bond, angle, etc., then the total force will include these, and the relative RMS force errors will be with respect to this total force in the denominator.

1.13 multisander

The *multisander* functionality is available in the parallel versions of the programs (i.e., *sander.MPI*). This mode allows multiple independent simulations, or replicas, to be run in the same program instance. It is particularly useful for computer clusters in which priority is given to large CPU-count jobs. In this case, the command-line usage of sander and pmemd is slightly altered, as shown below:

mpirun –np <#proc> sander.MPI –ng <#groups> –groupfile groupfile

In this case, `#proc` processors will be evenly divided among `#groups` individual simulations (`#proc` must be a multiple of `#group`!). The groupfile consists of a number of lines which is the command-line for each of the `#groups` simulations you wish to run. Comment lines (i.e., those with # in the first column) are ignored, after which the first `#groups` lines are read as the command-line flags of the Nth simulation.

The multisander and multipmemd mechanisms are also utilized for methods requiring multiple simulations to communicate with one another, such as thermodynamic integration in sander and replica exchange molecular dynamics (both described later). An example groupfile and program call are shown below.

Groupfile:

```
# Comment lines must start with a pound sign
# and there can be as many comment lines as you
# want, wherever you want them.
-O -p prmtop1 -c inpcrd1 -i replica1.mdin -suffix replica1
-O -p prmtop2 -c inpcrd2 -i replica2.mdin -suffix replica2
-O -p prmtop3 -c inpcrd3 -i replica3.mdin -suffix replica3
-O -p prmtop4 -c inpcrd4 -i replica4.mdin -suffix replica4
```

The `-suffix` flag behaves slightly differently than it does for classical use. In standard simulations (*i.e.*, without *multisander* or *multipmemd*), the provided suffix will be applied only to output files that are printed but were not given names on the command-line. With multisander, however, each thread has to produce different output files so that different replicas do not try to write to the same file. As a result, a default suffix of 000, 001, 002, etc. is given to the replicas and is added to every unspecified output file. If a `-suffix` is specified in the groupfile, as shown above, every output file—including those given an explicit name for that replica—are given the additional suffix.

The four simulations shown in the groupfile above can be run on 8 processors each with the following command (note, running *sander.MPI* may differ on your system).

mpirun –np 32 sander.MPI –ng 4 –groupfile groupfile

The *multisander* and *multipmemd* concepts are implemented via the use of MPI communicators. Each replica is assigned a replica-wide communicator along which all communications required for standard MD simulations are performed (called `commsander` and `pmemd_comm` in *sander* and *pmemd*, respectively). Each replica communicator has a master thread (rank 0 in that communicator), and the master thread of each replica are joined in another MPI communicator of replica masters (called `commmaster` and `pmemd_master_comm` in *sander* and *pmemd*, respectively). All inter-replica communication is performed via `commmaster` or `pmemd_master_comm`.

By default, all N threads are allocated to each of the M groups by dividing the threads sequentially. That is, the first N/M threads are assigned to replica 0, the second group of N/M threads are assigned to replica 1, etc. The `-ng-nonsequential` flag will stripe the thread assignments. Replica 0 will receive threads 0, $N-1$, $2N-1$, etc., while replica 1 receives threads 1, N, $2N$, etc.

2 The Generalized Born/Surface Area Model

Implicit solvent methods can speed up atomistic simulations by approximating the discrete solvent as a continuum, thus drastically reducing the number of particles in the system. An additional effective speedup often comes from much faster sampling of the conformational space afforded by these methods.[15, 28–31] The generalized Born (GB) solvation model is the most commonly used implicit solvent model for atomistic MD simulation; it has been most widely tested on ff99SB and ff14SBonlysc, but in principle could be used with other non-polarizable force fields, such as ff03. A recent (2019) review gives a good overview.[32] To estimate the total solvation free energy of a molecule, ΔG_{solv}, one typically assumes that it can be decomposed into the "electrostatic" and "non-electrostatic" parts:

$$\Delta G_{solv} = \Delta G_{el} + \Delta G_{nonel} \tag{2.1}$$

where ΔG_{nonel} is the free energy of solvating a molecule from which all charges have been removed (i.e. partial charges of every atom are set to zero), and ΔG_{el} is the free energy of first removing all charges in the vacuum, and then adding them back in the presence of a continuum solvent environment. Generally speaking, ΔG_{nonel} comes from the combined effect of two types of interaction: the favorable van der Waals attraction between the solute and solvent molecules, and the unfavorable cost of breaking the structure of the solvent (water) around the solute. In the current Amber codes, this is taken to be proportional to the total solvent accessible surface area (SA) of the molecule, with a proportionality constant derived from experimental solvation energies of small non-polar molecules, and uses a fast LCPO algorithm [33] to compute an analytical approximation to the solvent accessible area of the molecule.

The Poisson-Boltzmann approach described in the next section has traditionally been used in calculating ΔG_{el}. However, in molecular dynamics applications, the associated computational costs are often very high, as the Poisson-Boltzmann equation needs to be solved every time the conformation of the molecule changes. Amber developers have pursued an alternative approach, the analytic generalized Born (GB) method, to obtain a reasonable, computationally efficient estimate to be used in molecular dynamics simulations. The methodology has become popular,[34–41] especially in molecular dynamics applications,[42–45] due to its relative simplicity and computational efficiency, compared to the more standard numerical solution of the Poisson-Boltzmann equation. Within Amber GB models, each atom in a molecule is represented as a sphere of radius R_i with a charge q_i at its center; the interior of the atom is assumed to be filled uniformly with a material of dielectric constant 1. The molecule is surrounded by a solvent of a high dielectric ε (80 for water at 300 K). The GB model approximates ΔG_{el} by an analytical formula,[34, 46]

$$\Delta G_{el} \approx -\frac{1}{2} \sum_{ij} \frac{q_i q_j}{f_{GB}(r_{ij}, R_i, R_j)} \left(1 - \frac{\exp[-\kappa f_{GB}]}{\varepsilon} \right) \tag{2.2}$$

where r_{ij} is the distance between atoms i and j, the R_i are the so-called *effective Born radii*, and $f_{GB}()$ is a certain smooth function of its arguments. The electrostatic screening effects of (monovalent) salt are incorporated [46] via the Debye-Huckel screening parameter κ.

A common choice [34] of f_{GB} is

$$f_{GB} = \left[r_{ij}^2 + R_i R_j \exp(-r_{ij}^2/4R_i R_j) \right]^{1/2} \tag{2.3}$$

although other expressions have been tried.[37, 47] The effective Born radius of an atom reflects the degree of its burial inside the molecule: for an isolated ion, it is equal to its van der Waals (VDW) radius ρ_i. Then one obtains the particularly simple form:

$$\Delta G_{el} = -\frac{q_i^2}{2\rho_i}\left(1 - \frac{1}{\varepsilon}\right) \tag{2.4}$$

where we assumed $\kappa = 0$ (pure water). This is the famous expression due to Born for the solvation energy of a single ion. The function $f_{GB}()$ is designed to interpolate, in a clever manner, between the limit $r_{ij} \to 0$, when atomic spheres merge into one, and the opposite extreme $r_{ij} \to \infty$, when the ions can be treated as point charges obeying the Coulomb's law.[40] For deeply buried atoms, the effective radii are large, $R_i \gg \rho_i$, and for such atoms one can use a rough estimate $R_i \approx L_i$, where L_i is the distance from the atom to the molecular surface. Closer to the surface, the effective radii become smaller, and for a completely solvent exposed side-chain one can expect R_i to approach ρ_i.

The effective radii depend on the molecule's conformation, and so have to be re-computed every time the conformation changes. This makes the computational efficiency a critical issue, and various approximations are normally made that facilitate an effective estimate of R_i. With the exception of GBNSR6 (see Section **??**), the so-called *Coulomb field approximation*, or *CFA*, is used for Amber GB models, which replaces the true electric displacement around the atom by the Coulomb field. Within this assumption, the following expression can be derived:[40]

$$R_i^{-1} = \rho_i^{-1} - \frac{1}{4\pi}\int \theta(|\mathbf{r}| - \rho_i)r^{-4}d^3\mathbf{r} \tag{2.5}$$

where the integral is over the solute volume surrounding atom i. For a realistic molecule, the solute boundary (molecular surface) is anything but trivial, and so further approximations are made to obtain a closed-form analytical expression for the above equation, *e.g.* the so-called pairwise de-screening approach of Hawkins, Cramer and Truhlar,[48] which leads to a GB model implemented in Amber with *igb=1*. The 3D integral used in the estimation of the effective radii is performed over the van der Waals (VDW) spheres of solute atoms, which implies a definition of the solute volume in terms of a set of spheres, rather than the complex molecular surface,[49] commonly used in the PB calculations. For macromolecules, this approach tends to underestimate the effective radii for buried atoms,[40] arguably because the standard integration procedure treats the small vacuum–filled crevices between the van der Waals (VDW) spheres of protein atoms as being filled with water, even for structures with large interior.[47] This error is expected to be greatest for deeply buried atoms characterized by large effective radii, while for the surface atoms it is largely canceled by the opposing error arising from the Coulomb approximation, which tends [35, 39, 50] to overestimate R_i.

The deficiency of the model described above can, to some extent, be corrected by noticing that even the optimal packing of hard spheres, which is a reasonable assumption for biomolecules, still occupies only about three quarters of the space, and so "scaling-up" of the integral by a factor of four thirds should effectively increase the underestimated radii by about the right amount, without any loss of computational efficiency. This idea was developed and applied in the context of pH titration,[40] where it was shown to improve the performance of the GB approximation in calculating pKa values of protein sidechains. However, the one-parameter correction introduced in Ref. [40] was not optimal in keeping the model's established performance on small molecules. It was therefore proposed [45] to re-scale the effective radii with the re-scaling parameters being proportional to the degree of the atom's burial, as quantified by the value I_i of the 3D integral. The latter is large for the deeply buried atoms and small for exposed ones. Consequently, one seeks a well-behaved re-scaling function, such that $R_i \approx (\rho_i^{-1} - I_i)^{-1}$ for small I_i, and $R_i > (\rho_i^{-1} - I_i)^{-1}$ when I_i becomes large. The following simple, infinitely differentiable re-scaling function was chosen to replace the model's original expression for the effective radii:

$$R_i^{-1} = \tilde{\rho}_i^{-1} - \rho_i^{-1}\tanh(\alpha\Psi - \beta\Psi^2 + \gamma\Psi^3) \tag{2.6}$$

where $\Psi = I_i\tilde{\rho}_i$, and α, β, γ are treated as adjustable dimensionless parameters which were optimized using the guidelines mentioned earlier (primarily agreement with the PB). Currently, Amber supports two GB models (termed OBC) based on this idea. These differ by the values of α, β, γ, and are invoked by setting igb to either igb=2 or igb=5. The details of the optimization procedure and the performance of the OBC model relative to the PB treatment and in MD simulations on proteins is described in Ref. [45]; an independent comparison to the PB in calculating the electrostatic part of solvation free energy on a large data set of proteins can be found in Ref. [51].

Our experience with generalized Born simulations is mainly with *ff99SB, ff14SBonlysc* or *ff03*; the current GB models are not compatible with polarizable force fields. Replacing explicit water with a GB model is equivalent to

1	2	5	7	8
mbondi	*mbondi2*	*mbondi2*	*bondi*	*mbondi3*

Table 2.1: *Recommended radii sets for various GB models. For values of igb given in the top row, the string in the second row should be entered in LEaP as "set default PBRadii xxx".*

specifying a different force field, and users should be aware that none of the GB options (in Amber or elsewhere) is as mature as simulations with explicit solvent; user discretion is advised. For example, it was shown that salt bridges are too strong in some of these models [52, 53] and some of them provide secondary structure distributions that differ significantly from those obtained using the same protein parameters in explicit solvent, with GB having too much α-helix present.[54, 55] The combination of the *ff14SBonlysc* force field with igb=8 gives the best results for proteins [56][57], nucleic acids and protein-nucleic acid complexes. [58]

Despite these limitations, implicit treatment of solvent is widely used in molecular simulations for two main reasons: algorithmic/computational speed and conformational sampling. [15, 59] Implicit solvent methods can be algorithmically/computationally faster, as measured by simulation time steps per processor (CPU) time, because the vast number of individual interactions between the atoms of individual solvent molecules do not need to be explicitly computed. Implicit-solvent simulations can also sample conformational space faster in the low viscosity regime afforded by the implicit solvent model.[15, 28–31] To some extent, the interest in implicit-solvent-based simulations is motivated by the need to sample very large conformational spaces for problems such as protein folding, binding-affinity calculations, or large-scale fluctuations of nucleosomal DNA fragments. The speedup of conformational change can vary considerably, depending on the details of the transition, and can range from no speedup at all to almost a 100-fold speedup. [15] In general, the larger the conformational change, the higher the speedup one may expect, but this tendency is not universal or uniform. These speedup values are also expected to vary by the specific flavour of GB model used, a detailed analysis for igb5 can be found in Ref. [15].

The generalized Born models used here are based on the "pairwise" model introduced by Hawkins, Cramer and Truhlar,[48, 60] which in turn is based on earlier ideas by Still and others.[34, 39, 50, 61] The so-called overlap parameters for most models are taken from the Tinker molecular modeling package (http://tinker.wustl.edu). The effects of added monovalent salt are included at a level that approximates the solutions of the linearized Poisson-Boltzmann equation.[46] The original implementation was by David Case, who thanks Charlie Brooks for inspiration. Details of our implementation of generalized Born models can be found in Refs. [62, 63].

2.1 GB/SA input parameters

As outlined above, there are several "flavors" of GB available, depending upon the value of *igb*. The version that has been most extensively tested corresponds to *igb*=1; the "OBC" models (*igb*=2 and 5) are newer, but appear to give significant improvements and are recommended for most projects (certainly for peptides or proteins). The newest, most advanced, and least extensively tested model, *GBn* (*igb*=7), yields results in considerably better agreement with molecular surface Poisson-Boltzmann and explicit solvent results than the "OBC" models under many circumstances.[55] The *GBn* model was parameterized for peptide and protein systems and is not recommended for use with nucleic acids. A modification on the GBn model (igb=8) further improves agreement between Poisson-Boltzmann and explicit solvent data compared to the original formulation (igb=7).[56] Users should understand that all (current) GB models have limitations and should proceed with caution. Generalized Born simulations can only be run for non-periodic systems, *i.e.* where *ntb*=0. Unlike its use in explicit solvent PME simulations, short nonbonded cutoff values have much stronger impact on accuracy of the GB calculations. Essentially, any cutoff values other than *cut > structure size* can lead to artifacts. Current GPU implementation of the GB can not use cutoffs. An alternative that retains most of the speed of the GB with a cutoff, but without most of its artifacts, is GB-HCP described in Section **??**. If the nonbonded cutoff is used in GB calculations, it should be greater than that for PME calculations, perhaps cut=16. The slowly-varying forces generally do not have to be evaluated at every step for GB, either nrespa=2 or 4, although that option may lead to some artifacts as well.

igb   **= 0** No generalized Born term is used. (Default)

= 1 The Hawkins, Cramer, Truhlar[48, 60] pairwise generalized Born model is used, with parameters described by Tsui and Case.[62] This model uses the default radii set up by LEaP. It is slightly different from the GB model that was included in Amber6. If you want to compare to Amber 6, or need to continue an ongoing simulation, you should use the command "set default PBradii amber6" in LEaP, and set *igb*=1 in *sander*. For reference, the Amber6 values are those used by an earlier Tsui and Case paper.[43] Note that most nucleic acid simulations have used this model, so you take care when using other values. Also note that Tsui and Case used an offset (see below) of 0.13 Å, which is different from its default value.

= 2 Use a modified GB model developed by A. Onufriev, D. Bashford and D.A. Case; the main idea was published earlier,[40] but the actual implementation here[45] is an elaboration of this initial idea. Within this model, the effective Born radii are re-scaled to account for the interstitial spaces between atom spheres missed by the GB^{HCT} approximation. In that sense, GB^{OBC} is intended to be a closer approximation to true molecular volume, albeit in an average sense. With *igb*=2, the inverse of the effective Born radius is given

by:cedure

$$R_i^{-1} = \overline{\rho}_i^{-1} - \tanh\left(\alpha\Psi - \beta\Psi^2 + \gamma\Psi^3\right)/\rho_i$$

where $\overline{\rho}_i = \rho_i - offset$, and $\Psi = I\rho_i$, with I given in our earlier paper. The parameters α, β, and γ were determined by empirical fits, and have the values 0.8, 0.0, and 2.909125. This corresponds to model I in Ref [45]. With this option, you should use the LEaP command "set default PBradii mbondi2" to prepare the *prmtop* file.

= 3 or 4 These values are unused; they were used in Amber 7 for parameter sets that are no longer supported.

= 5 Same as *igb=2*, except that now α, β, γ are 1.0, 0.8, and 4.85. This corresponds to model II in Ref [45]. With this option, you should use the command "set default PBradii mbondi2" in setting up the *prmtop* file, although "set default PBradii bondi" is also OK. When tested in MD simulations of several proteins,[45] both of the above parameterizations of the "OBC" model showed equal performance, although further tests [51] on an extensive set of protein structures revealed that the *igb=5* variant agrees better with the Poisson-Boltzmann treatment in calculating the electrostatic part of the solvation free energy.

= 6 With this option, there is no continuum solvent model used at all; this corresponds to a non-periodic, "vacuum", model where the non-bonded interactions are just Lennard-Jones and Coulomb interactions.

= 7 The *GBn* model described by Mongan, Simmerling, McCammon, Case and Onufriev[64] is employed. This model uses a pairwise correction term to GB^{HCT} to approximate a molecular surface dielectric boundary; that is to eliminate interstitial regions of high dielectric smaller than a solvent molecule. This correction affects all atoms and is geometry-specific, going beyond the geometry-free, "average" re-scaling approach of GB^{OBC}, which mostly affects buried atoms. With this method, you should use the bondi radii set. The overlap or screening parameters in the *prmtop* file are ignored, and the model-specific *GBn* optimized values are substituted. The model carries little additional computational overhead relative to the other GB models described above.[64] This method is not recommended fcedureor systems involving nucleic acids.

= 8 Same GB functional form as the GBn model (igb=7), but with different parameters. The offset, overlap screening parameters, and gbneckscale are changed. In addition, individual α, β, and γ parameters can be specified for each of the elements H, C, N, O, S, P. Parameters for other elements have not been optimized, and the default values used are the ones from igb=5, which were not element-dependent. Default values were optimized for H, C, N, O and S atoms in protein systems.[56] Although the parameters for P in proteins can be specified, the default values were not optimized and are the igb=5 values. Nucleic acids have separate

parameters from those used for proteins, and default values were optimized for H, C, N, O and P atoms in nucleic acid systems.[58]

The following are the default parameters sander uses with *igb=8*:

```
Sh=1.425952, Sc=1.058554, Sn=0.733599,
So=1.061039, Ss=-0.703469, Sp=0.5,
offset=0.195141, gbneckscale=0.826836,
gbalphaH=0.788440, gbbetaH=0.798699, gbgammaH=0.437334,
gbalphaC=0.733756, gbbetaC=0.506378, gbgammaC=0.205844,
gbalphaN=0.503364, gbbetaN=0.316828, gbgammaN=0.192915,
gbalphaOS=0.867814, gbbetaOS=0.876635, gbgammaOS=0.387882,
gbalphaP=1.0, gbbetaP=0.8, gbgammaP=4.85
screen_hnu=1.69654, screen_cnu=1.26890,
screen_nnu=1.425974, screen_onu=0.18401, screen_pnu=1.54506,
gb_alpha_hnu=0.53705, gb_beta_hnu=0.36286, gb_gamma_hnu=0.11670,
gb_alpha_cnu=0.33167, gb_beta_cnu=0.19684, gb_gamma_cnu=0.09342,
gb_alpha_nnu=0.68631, gb_beta_nnu=0.46319, gb_gamma_nnu=0.13872,
gb_alpha_onu=0.60634, gb_beta_onu=0.46301, gb_gamma_onu=0.14226,
gb_alpha_pnu=0.41836, gb_beta_pnu=0.29005, gb_gamma_pnu=0.10642
```

Parameters for proteins and for nucleic acids were optimized separately and can be independently specified. Protein parameters: Sh, Sc, Sn, So, Ss and Sp are scaling parameters, gbalphaX, gbbetaX, gbgammaX are the α, β, γ set for element X. gbalphaOS, gbbetaOS, gbgammaOS is the α, β, γ set applied to both O and S. The phosphorus parameters (in proteins) were not optimized and are simply taken as the parameters used in the OBC-2 model (igb=5). Nucleic acid parameters (end with "nu"): screen_Xnu (X=h, c, n, o, p) are scaling parameters, gb_alpha_Xnu (X=h, c, n, o, p) are the α, β, γ set for element X.

Since parameters are assigned for each atom based on its residue name (hard-coded in "sander/egb.F90" (subroutine isnucat)), users need to update the residue table in the sander source code if nucleic acids with different names are simulated using this GB model.

The default values for offset=0.195141, gbneckscale=0.826836 are recommended for both proteins and nucleic acids.

mbondi3 radii are recommended with igb=8 and can be employed with the LEaP command "set default PBradii mbondi3". The mbondi3 radii were adjusted based on protein simulations, and optimization of these radii for nucleic acids is currently underway.

=10 Calculate the reaction field and nonbonded interactions using a numerical Poisson-Boltzmann solver. This option is described in the Chapter **??**. Note that this is *not* a generalized Born simulation, in spite of its use of *igb*; it is rather an alternative continuum solvent model.

intdiel   Sets the interior dielectric constant of the molecule of interest. Default is 1.0. Other values have not been extensively tested.

extdiel   Sets the exterior or solvent dielectric constant. Default is 78.5.

saltcon   Sets the concentration (M) of 1-1 mobile counterions in solution, using a modified generalized Born theory based on the Debye-Hückel limiting law for ion screening of interactions.[46] Default is 0.0 M (*i.e.* no Debye-Hückel screening.) Setting *saltcon* to a nonzero value does result in some increase in computation time.

rgbmax   This parameter controls the maximum distance between atom pairs that will be considered in carrying out the pairwise summation involved in calculating the effective Born radii. Atoms whose associated spheres are farther way than *rgbmax* from given atom will not contribute to that atom's effective Born radius. This is implemented in a "smooth" fashion (thanks mainly to W.A. Svrcek-Seiler), so that when part of an atom's atomic sphere lies inside *rgbmax* cutoff, that part contributes

to the low-dielectric region that determines the effective Born radius. The default is 25 Å, which is usually plenty for single-domain proteins of a few hundred residues. Even smaller values (of 10-15 Å) are reasonable, changing the functional form of the generalized Born theory a little bit, in exchange for a considerable speed-up in efficiency, and without introducing the usual cut-off artifacts such as drifts in the total energy.

The *rgbmax* parameter affects only the effective Born radii (and the derivatives of these values with respect to atomic coordinates). The *cut* parameter, on the other hand, determines the maximum distance for the electrostatic, van der Waals and "off-diagonal" terms of the generalized Born interaction. The value of *rgbmax* might be either greater or smaller than that of *cut*: these two parameters are independent of each other. However, values of *cut* that are too small are more likely to lead to artifacts than are small values of *rgbmax*; therefore one typically sets *rgbmax <= cut*.

rbornstat   If *rbornstat = 1*, the statistics of the effective Born radii for each atom of the molecule throughout the molecular dynamics simulation are reported in the output file. Default is 0.

offset   The dielectric radii for generalized Born calculations are decreased by a uniform value "offset" to give the "intrinsic radii" used to obtain effective Born radii. Default is 0.09 Å.

gbsa   Option to carry out GB/SA (generalized Born/surface area) simulations. For the default value of 0, surface area will not be computed and will not be included in the solvation term. If *gbsa = 1*, surface area will be computed using the LCPO model.[33] If *gbsa = 2*, surface area will be computed by recursively approximating a sphere around an atom, starting from an icosahedra. Note that no forces are generated in this case, hence, *gbsa = 2* only works for a single point energy calculation and is mainly intended for energy decomposition in the realm of MM-GBSA. If *gbsa = 3,* surface area will be computed using a fast pairwise approximation [65] suitable for GPU computing in pmemd.cuda program; the acceleration in pmemd.cuda compared with *gbsa = 2* is ~30 times faster [65]. Note that *gbsa = 3* is currently not supported in sander, MM-GBSA, QM/MM or libsff. Although *gbsa = 3* is supported in pmemd, the general usage is not recommended as the speed gain is trivial, given that the algorithm was particularly designed for fast approximation of surface area in GPU-accelerated GB simulations. Therefore, we recommend users to use gbsa=3 with pmemd.cuda.

surften   Surface tension used to calculate the nonpolar contribution to the free energy of solvation (when *gbsa = 1*), as Enp = surften*SA. The default is 0.005 kcal/mol/A^2.[66] For *gbsa = 3*, suften works comparably with *gbsa = 1* given the same value. [65]

rdt   This parameter is only used for GB simulations with LES (Locally Enhanced Sampling). In GB+LES simulations, non-LES atoms require multiple effective Born radii due to alternate de-screening effects of different LES copies. When the multiple radii for a non-LES atom differ by less than RDT, only a single radius will be used for that atom. See Chapter **??** for more details. Default is 0.0 Å.

3 Reference Interaction Site Model

In addition to explicit and continuum implicit solvation models, Amber also has a third type of solvation model for molecular mechanics simulations, the reference interaction site model (RISM) of molecular solvation[67–80]. In AmberTools, 1D-RISM is available as rism1d. 3D-RISM is available as an option in NAB, MMPBSA.py and sander. rism3d.snglpnt is a simplified, standalone interface, ideal for calculating solvation thermodynamics on individual structures and trajectories. Details specific to using sander and sander.MPI can be found in Chapter 1.

3.1 Introduction

RISM is an inherently microscopic approach, calculating the equilibrium distribution of the solvent, from which all thermodynamic properties are then determined. Specifically, RISM is an approximate solution to the Ornstein-Zernike (OZ) equation[68, 77, 78, 81, 82]

$$h(r_{12}, \Omega_1, \Omega_2) = c(r_{12}, \Omega_1, \Omega_2) + \rho \int d\mathbf{r}_3 \, d\Omega_3 \, c(r_{13}, \Omega_1, \Omega_3) \, h(r_{32}, \Omega_3, \Omega_2), \tag{3.1}$$

where r_{12} is the separation between particles 1 and 2 while Ω_1 and Ω_2 are their orientations relative to the vector $\mathbf{r}_{12}$. The two functions in this relation are h, the total correlation function, and c, the direct correlation function. The total correlation function is defined as

$$h_{ab}(r_{ab}, \Omega_a, \Omega_b) \equiv g_{ab}(r_{ab}, \Omega_a, \Omega_b) - 1,$$

where g_{ab} is the pair-distribution function, which gives the conditional density distribution of species b about a. In cases where only radial separation is considered, for example by orientational averaging over site α of species a and site γ of species b, gives the familiar one dimensional site-site radial distribution function, $g_{\alpha\gamma}(r_{\alpha\gamma})$.

For real mixtures, it is often convenient to speak in terms of a solvent, V, of high concentration and a solute, U, of low concentration. A generic case of solvation is infinite dilution of the solute, i.e., $\rho^U \to 0$. We can rewrite Equation (3.1), in the limit of infinite dilution, as a set of three equations:

$$h^{VV}(r_{12}, \Omega_1, \Omega_2) = c^{VV}(r_{12}, \Omega_1, \Omega_2) + \rho^V \int d\mathbf{r}_3 \, d\Omega_3 \, c^{VV}(r_{13}, \Omega_1, \Omega_3) \, h^{VV}(r_{32}, \Omega_3, \Omega_2), \tag{3.2}$$

$$h^{UV}(r_{12}, \Omega_1, \Omega_2) = c^{UV}(r_{12}, \Omega_1, \Omega_2) + \rho^V \int d\mathbf{r}_3 \, d\Omega_3 \, c^{UV}(r_{13}, \Omega_1, \Omega_3) \, h^{VV}(r_{32}, \Omega_3, \Omega_2), \tag{3.3}$$

$$h^{UU}(r_{12}, \Omega_1, \Omega_2) = c^{UU}(r_{12}, \Omega_1, \Omega_2) + \rho^V \int d\mathbf{r}_3 \, d\Omega_3 \, c^{UV}(r_{13}, \Omega_1, \Omega_3) \, h^{VU}(r_{32}, \Omega_3, \Omega_2). \tag{3.4}$$

Equation (3.3) is directly relevant for biomolecular simulations where we are often interested in the properties of a single, arbitrarily complex solute in the solution phase. Solutions to Equation (3.3) can be obtained using 3D-RISM. However, a solution to Equation (3.2) for pure solvent is a necessary prerequisite and is readily obtained from 1D-RISM.

To obtain a solution to the OZ equations it is necessary to have a second equation that relates h and c or uniquely defines one of these functions. The general closure relation is[81]

$$g(r_{12}, \Omega_1, \Omega_2) = \exp\left[-\beta u(r_{12}, \Omega_1, \Omega_2) + h(r_{12}, \Omega_1, \Omega_2) - c(r_{12}, \Omega_1, \Omega_2) + b(r_{12}, \Omega_1, \Omega_2)\right] \tag{3.5}$$

u is the potential energy function for the two particles and b is known as the bridge function (a non-local functional, representable as infinite diagrammatic series in terms of h [81]). It should be noted that u is the only point at which the interaction potential enters the equations. Depending on the method used to solve the OZ equations, u is

generally an explicit potential. In principle, it should now be possible to solve our two equations. For example, we may wish to use SPC/E as a water model. Inputting the relevant aspects of the SPC/E model into u, 1D-RISM can be used to calculate the equilibrium properties of the SPC/E model. A different explicit water model will yield different properties.

A fundamental problem for all OZ-like integral equation theories is the bridge function, which contains multiple integrals that are readily solved only in special circumstances. In practice, an approximate closure relation must be used. While many closures have been developed, at this time only three are implemented in 3D-RISM: hypernetted-chain approximation (HNC), Kovalenko-Hirata (KH) and the partial series expansion of order-n (PSE-n).

For HNC, we set $b = 0$, giving[81]

$$
\begin{aligned}
g^{\mathrm{HNC}}(r_{12},\Omega_1,\Omega_2) &= \exp\left(-\beta u(r_{12},\Omega_1,\Omega_2) + h(r_{12},\Omega_1,\Omega_2) - c(r_{12},\Omega_1,\Omega_2)\right) \\
&= \exp\left(t^*(r_{12},\Omega_1,\Omega_2)\right)
\end{aligned}
\tag{3.6}
$$

where t^* is the renormalize-indirect correlation function. HNC works well in many situations, including charged particles, but has difficulties when the size ratios of particles in the system are highly varied and may not always converge on a solution when one should exist. Also, as the bridge term is generally repulsive, HNC allows particles to approach too closely, overestimating non-Coulombic interactions[78].

KH is a combination of HNC and the mean spherical approximation (MSA), the former being applied to the spatial regions of solvent density depletion ($g < 1$), including the repulsive core, and the latter to those of solvent density enrichment ($g > 1$), such as association peaks[77, 78]

$$
g^{\mathrm{KH}}(r_{12},\Omega_1,\Omega_2) = \begin{cases} \exp\left(t^*(r_{12},\Omega_1,\Omega_2)\right) & \text{for } g(r_{12},\Omega_1,\Omega_2) \le 1 \\ 1 + t^*(r_{12},\Omega_1,\Omega_2) & \text{for } g(r_{12},\Omega_1,\Omega_2) > 1 \end{cases}.
\tag{3.7}
$$

Like HNC, KH handles Coulombic systems well but overestimates non-Coulombic interactions. Unlike HNC, it does not have difficulties with highly asymmetric particle sizes and readily converges to stable solutions for almost all systems of practical interest. The reliability of the KH closure makes it particularly suitable for molecular mechanics calculations.

PSE-n offers the ability to interpolate between KH and HNC. Here, the exponential regions of solvent density enrichment are treated as a Taylor expansion,

$$
g^{\mathrm{PSE\text{-}n}}(r_{12},\Omega_1,\Omega_2) = \begin{cases} \exp\left(t^*(r_{12},\Omega_1,\Omega_2)\right) & \text{for } g(r_{12},\Omega_1,\Omega_2) \le 1 \\ \sum_{i=0}^{n} (t^*(r_{12},\Omega_1,\Omega_2))^i / i! & \text{for } g(r_{12},\Omega_1,\Omega_2) > 1 \end{cases}.
\tag{3.8}
$$

In the case of $n = 1$, the KH closure is obtained, while in the limit of $n \to \infty$ HNC is recovered. This allows a balance between the numerical stability of KH and the often better accuracy of HNC.

3.1.1 3D-RISM

With the results from 1D-RISM, a 3D-RISM calculation for a specific solute can be carried out. For 3D-RISM calculations, only the solvent orientational degrees of freedom are averaged over and Equation (3.3) becomes[76, 77]

$$
h_\gamma^{\mathrm{UV}}(\mathbf{r}) = \sum_\alpha \int d\mathbf{r}' c_\alpha^{\mathrm{UV}}(\mathbf{r} - \mathbf{r}') \chi_{\alpha\gamma}^{\mathrm{VV}}(r'),
\tag{3.9}
$$

where $\chi_{\alpha\gamma}^{\mathrm{VV}}(r)$ is the site-site susceptibility of the solvent, obtained from 1D-RISM and given by

$$
\chi_{\alpha\gamma}^{\mathrm{VV}}(r) = \omega_{\alpha\gamma}^{\mathrm{VV}}(r) + \rho_\alpha h_{\alpha\gamma}^{\mathrm{VV}}(r).
$$

3D-RISM supports HNC, KH and PSE-n closures (see Sections **??**, **??** and **??**). As with the 1D-RISM closures, these are constructed by analogy from Eqs. 3.6-3.8. For example, HNC becomes

$$
g_\gamma^{\mathrm{HNC,UV}}(\mathbf{r}) = \exp\left(-\beta u_\gamma^{\mathrm{UV}}(\mathbf{r}) + h_\gamma^{\mathrm{UV}}(\mathbf{r}) - c_\gamma^{\mathrm{UV}}(\mathbf{r})\right).
\tag{3.10}
$$

As with 1D-RISM, correlation functions are represented on (3D) grids, convolution integrals are performed in reciprocal space and a self-consistent solution is iteratively converged upon using the MDIIS accelerated solver. There is one 3D grid for each solvent type for each correlation function. For example, for a solute in SPC/E water there will be both $g_{\mathrm{H}}^{\mathrm{UV}}(\mathbf{r})$ and $g_{\mathrm{O}}^{\mathrm{UV}}(\mathbf{r})$ grids. Each point on the $g_{\mathrm{H}}^{\mathrm{UV}}(\mathbf{r})$ will give the fractional density of water hydrogen a that location of real-space.

To properly treat electrostatic forces in electrolyte solution with polar molecular solvent and ionic species, the electrostatic asymptotics of all the correlation functions (both the 3D and radial ones) are treated analytically [78, 79, 83]. The non-periodic electrostatic asymptotics are separated out in the direct and reciprocal space and the remaining short-range terms of the correlation functions are discretized on a 3D grid in a non-periodic box large enough to ensure decay of the short-range terms at the box boundaries [83]. The convolution of the short-range terms in the integral equation (3.9) is calculated using 3D fast Fourier transform [84, 85]. Accordingly, the electrostatic asymptotics terms in the thermodynamics integral (3.12) below are handled analytically and reduced to one-dimensional integrals easy to compute [83].

With a converged 3D-RISM solution for h^{UV} and c^{UV}, it is straightforward to calculate solvation thermodynamics. From the perspective of molecular simulations, the most important thermodynamic values are the excess chemical potential of solvation (solvation free energy), μ^{ex} and the mean solvation force, $\mathbf{f}_i^{\mathrm{UV}}(\mathbf{R}_i)$, on each solute atom, i. μ^{ex} can be obtained through analytical thermodynamic integration for HNC,

$$\mu^{\mathrm{ex,HNC}} = k_{\mathrm{B}}T \sum_\alpha \rho_\alpha^{\mathrm{V}} \int d\mathbf{r} \left[\frac{1}{2} \left(h_\alpha^{\mathrm{UV}}(\mathbf{r}) \right)^2 - c_\alpha^{\mathrm{UV}}(\mathbf{r}) - \frac{1}{2} h_\alpha^{\mathrm{UV}}(\mathbf{r}) c_\alpha^{\mathrm{UV}}(\mathbf{r}) \right], \tag{3.11}$$

KH ,

$$\mu^{\mathrm{ex,KH}} = k_{\mathrm{B}}T \sum_\alpha \rho_\alpha^{\mathrm{V}} \int d\mathbf{r} \left[\frac{1}{2} \left(h_\alpha^{\mathrm{UV}}(\mathbf{r}) \right)^2 \Theta\left(-h_\alpha^{\mathrm{UV}}(\mathbf{r}) \right) - c_\alpha^{\mathrm{UV}}(\mathbf{r}) - \frac{1}{2} h_\alpha^{\mathrm{UV}}(\mathbf{r}) c_\alpha^{\mathrm{UV}}(\mathbf{r}) \right], \tag{3.12}$$

and PSE-n,

$$\mu^{\mathrm{ex,PSE}\text{-}n} = k_{\mathrm{B}}T \sum_\alpha \rho_\alpha^{\mathrm{V}} \int d\mathbf{r} \left[\frac{1}{2} \left(h_\alpha^{\mathrm{UV}}(\mathbf{r}) \right)^2 - c_\alpha^{\mathrm{UV}}(\mathbf{r}) - \frac{1}{2} h_\alpha^{\mathrm{UV}}(\mathbf{r}) c_\alpha^{\mathrm{UV}}(\mathbf{r}) \right.$$
$$\left. - \frac{\left(t^*(\mathbf{r}) \right)^{n+1}}{(n+1)!} \Theta\left(h_\alpha^{\mathrm{UV}}(\mathbf{r}) \right) \right], \quad (3.13)$$

where Θ is the Heaviside function.

Analogous versions of Eqns. 3.6, 3.12 and 3.13 are used in 1D-RISM. While these are used for DRISM they are have been derived for XRISM. Furthermore, these equations have been derived a number of different ways with slightly different functional forms of the $-\frac{1}{2}hc$ term [77, 86–89]. These different functional forms are equivalent in XRISM but not in DRISM. The form introduced by Pettitt and Rossky [87] is the most popular in the literature and the default selection in `rism1d`. It is possible to have `rism1d` evaluate and output all three functional forms (see **??**) but, for DRISM, none of these expressions are strictly correct.

The force equation

$$\mathbf{f}_i^{\mathrm{UV}}(\mathbf{R}_i) = -\frac{\partial \mu^{\mathrm{ex}}}{\partial \mathbf{R}_i} = -\sum_\alpha \rho_\alpha \int d\mathbf{r} g_\alpha^{\mathrm{UV}}(\mathbf{r}) \frac{\partial u_\alpha^{\mathrm{UV}}(\mathbf{r} - \mathbf{R}_i)}{\partial \mathbf{R}_i}$$

is valid for all closures with a path independent expression for the excess chemical potential, such as HNC, KH and PSE-n closures implemented in 3D-RISM [67, 90–92].

In addition to closure specific expressions for the solvation free energy, other approximations also exist. The Gaussian fluctuation (GF) approximation[93, 94] is given as

$$\mu^{\mathrm{ex,GF}} = k_{\mathrm{B}}T \sum_\alpha \rho_\alpha^{\mathrm{V}} \int d\mathbf{r} \left[-c_\alpha^{\mathrm{UV}}(\mathbf{r}) - \frac{1}{2} h_\alpha^{\mathrm{UV}}(\mathbf{r}) c_\alpha^{\mathrm{UV}}(\mathbf{r}) \right] \tag{3.14}$$

and has been shown to yield improved absolute solvation free energies for both polar and non-polar solutes[94, 95] but not necessarily for relative free energies[96]. It is not associated with a particular closure but is typically used in place of the expression for a given closure.

Eqs. (3.11)-(3.13) give the total solvation free energy, ΔG_{sol}, but it is often useful to decompose this into electrostatic (solvent polarization), ΔG_{pol}, and non-electrostatic (dispersion and cavity formation), $(\Delta G_{\text{dis}} + \Delta G_{\text{cav}})$, terms. Conceptually, we can divide the path of the thermodynamic integration into two steps: first the solute without partial charges is inserted into the solvent (dispersion and cavity formation) and then partial charges are introduced, which polarize the solvent,

$$\mu^{\text{ex}} = \Delta G_{\text{sol}} = \Delta G_{\text{pol}} + \Delta G_{\text{dis}} + \Delta G_{\text{cav}}.$$

ΔG_{sol} is produced by a 3D-RISM calculation on the charged solute. ΔG_{pol} is then the difference of the two calculations. As a point of reference, generalized-Born and Poisson-Boltzmann methods calculate only ΔG_{pol} and, typically, use a calculation involving solvent accessible surface area to predict $\Delta G_{\text{dis}} + \Delta G_{\text{cav}}$.

3.2 Practical Considerations

3.2.1 Computational Requirements and Parallel Scaling

Calculating a 3D-RISM solution for a single solute conformation typically requires about 100 times more computer time than the same calculation with explicit solvent or PB. While there are other factors to consider, such as sampling confined solvent or overall efficiency of sampling in the whole statistical ensemble at once, this can be prohibitive for many applications. Memory is also an issue as the 3D correlation grids require anywhere from a few megabytes for the smallest solutes to gigabytes for large complexes. A lower bound and very good estimate for the total memory required is

$$\text{Total memory} \geq 8\,\text{bytes} \times \left[N_{\text{box}}\, N^{\text{V}} \left(\underbrace{2N_{\text{MDIIS}}}_{c,\text{residual}} + \underbrace{1}_{u} + \underbrace{N_{\text{decomp}}}_{\text{polar decomp}} \underbrace{N_{\text{propagate}}}_{\text{past solutions}} \right) \right.$$
$$\left. (N_{\text{box}} + 2N_y N_z) \left\{ \underbrace{4}_{\text{asymptotics}} + \underbrace{1}_{\text{FFT scratch}} + \underbrace{2}_{g,h} N^{\text{V}} \right\} \right]$$

where $N_{\text{box}} = N_x \times N_y \times N_z$ is the total number of grid points, N^{V} is the number of solvent atom species and N_{MDIIS} is the number of MDIIS vectors used to accelerate convergence. u^{UV}, c^{UV} and the residual of c^{UV} are stored in real-space only and require a full grid for each solvent. c^{UV} and its residual also require N_{MDIIS} grids for the MDIIS routine (see the mdiis_nvec keyword) and $N_{\text{propagate}}$ grids to make use of solutions from previous solute configurations to improve the initial guess (see the npropagate keyword). If a polar/non-polar decomposition is requested (see the polardecomp keyword) an additional set of grids for past solutions with no solute charges is kept ($N_{\text{decomp}} = 2$); by default this is turned off ($N_{\text{decomp}} = 1$). The full real space grid plus an additional $2N_y N_x$ grid points are needed (due to the FFT) for g and h for each solvent species and for the four grids required to compute the long range asymptotics. Memory, therefore, scales linearly with N_{box} while computation time scales as $O(N_{\text{box}} \log(N_{\text{box}}))$ due to the requirements of calculating the 3D fast Fourier transform (3D-FFT). To overcome these requirements, two options are available beyond optimizations already in place, multiple time steps and parallelization. Multiple time step methods are available only in sander (Chapter 1) and are applicable to molecular dynamics calculations only. Parallelization is available for all calculations but is limited by system size and computational resources.

Both sander and NAB have MPI implementations of 3D-RISM (see Section **??** for NAB compiling instructions) that distribute both memory requirements and computational load. As memory is distributed, the aggregate memory of many computers can be used to perform calculations on very large systems. Memory distribution is handled by the FFTW 3.3 library so decomposition is done along the z-axis. If a variable solvation box size is used, the only consideration is to avoid specifying a large, prime number of processes (≥ 7). For fixed box sizes, the number of grids points in each dimension must be divisible by two (a general requirement) and the number of grid points in the z-axis must be divisible by the number of processes. sander.MPI also has the additional consideration that the number of processes cannot be larger than the number of solute residues; NAB does not suffer

from this limitation.

3.2.2 Output

g^{UV}, h^{UV} and c^{UV} files can be output for 3D-RISM calculations and are useful for visualization and calculation of thermodynamic quantities. As all file formats save only one density per file (see https://ambermd.org/FileFormats.php), there is one file for each solvent atom type for each requested frame. For the default MRC format, each file is $(256 + N_{\mathrm{box}} \times 4)$ bytes, which can quickly fill disk space. Note that these file format use single precision floating point numbers.

3.2.3 Numerical Accuracy

Numerical accuracy depends on the residual tolerance specified for the numerical solution at runtime and the solvation box physical size and grid spacing. In most cases, you will need to test these parameters to ensure you have the accuracy required. As a rough guide, the numerical error in the solvation free energy is related to the tolerance by

$$\varepsilon_{\Delta G_{\mathrm{solv}}} \approx 10 \times \text{tolerance}. \tag{3.15}$$

Molecular dynamics [67], minimization and trajectory post-processing [96] have different requirements for the maximum residual tolerance. Molecular dynamics does well with a tolerance of 10^{-5} and `npropagate=5`. Minimization requires tolerances of 10^{-11} or lower and is typically limited to `drms` $\geq 10^{-4}$. Trajectory post-processing for MM/RISM should use enough digits to obtain the necessary accuracy when differences in solvation free energy are computed. For example, if a error $< 0.2 \, \mathrm{kcal/mol}$ is required for $\Delta\Delta G_{\mathrm{solv}}$, then ΔG_{solv} should be computed with an absolute error of $0.1 \, \mathrm{kcal/mol}$. The relative error required to achieve this depends on the magnitude of ΔG_{solv}.

Almost all applications should use a grid spacing of 0.3 to 0.5 Å or smaller. A larger grid spacing quickly leads to severe errors in thermodynamic quantities. Smaller grid spacing may be necessary for some applications (e.g., mapping potentials of mean force).

3.2.4 Solution Convergence

The default parameters for 3D-RISM are selected to provide the best performance for the majority of systems. In cases where a convergence is not achieved, the strategies below may be useful.

3.2.4.1 Closure Bootstrap

When a PSE-*n* or HNC closure is desired, the most effective method to overcome convergence issues is to use a low order closure solution as a starting guess. The KH closure should be the starting point as it is numerically robust and, typically, converges easily in the vast majority of case. After this, higher orders of PSE-*n* can be used until the desired closure is reached. The procedure for 1D-RISM and 3D-RISM differs slightly in practice.

3D-RISM All 3D-RISM interfaces have closure bootstrapping builtin via the *closure* and *tolerance* keywords. Closures should be specified as an ordered list with last closure being the highest order closure. The solutions of the intermediate closures can have a high tolerance. The default tolerance for intermediate closures is 1 and there is no observed benefit to tolerances less than 1e-2.

3.2.4.2 MDIIS Settings

MDIIS default setting are appropriate for most cases. Should your residual diverge or the solver get stuck on a particular value, you can try modest adjustments.

Decrease *mdiis_del* *mdiis_del* controls the step size of MDIIS. A smaller step size can help convergence but if this is set too small it can cause convergence problems. For `rism1d`, this should be no lower than 0.1 or 0.2. For 3D-RISM, it should be 0.5 at the lowest.

Increase *mdiis_nvec* This is the number of trial solutions that are saved for predicting a new solution. The optimal number for rapid convergence is typically 10 for 3D-RISM and 20 for 1D-RISM. However, for 3D-RISM, the default choice of 5 requires much less memory and is computationally faster even though more iterations are required. Increasing the *mdiis_nvec* may help for 3D-RISM but is unlikely to help for 1D-RISM.

Increase *mdiis_restart* Occasionally, the MDIIS routine goes in the wrong direction and the residual increases significantly. If it increases more than *mdiis_restart* then the MDIIS routine selects the solution with the lowest residual and purges the other trial solutions. The default value of 10 can be too aggressive and cause the solver to cycle. Increasing the value to 100 or 1000 sometimes allows the solver to recover from a misstep.

3.2.4.3 Parameter Annealing

Chargeless, hot gases are the easiest systems to converge. For 1D-RISM, this can be used to bootstrap a solution in a similar manner to closure bootstrapping. By slowly turning on charges, lowering the temperature or increasing the density, a converged solution may be reached. This only works for 1D-RISM because it requires restarting from a previous solution. As with closure bootstrapping, files should be carefully renamed during the procedure. There is no general protocol but the parameter increment should be reduced as the target value is approached. E.g., turning on charges in a linear fashion usually isn't helpful.

3.2.4.4 Forcefield selection

The forcefield may affect convergence due to the number of solvent sites involved or the particular parameters of the forcefield.

Number of Sites Molecules with more sites are more difficult to converge. Six or more sites is already difficult to converge and more that 10 may not be possible under any circumstances. One solution is to use a united atom or coarse grained forcefields to reduce the number of sites.

Alternate Parameterization Some parameter sets simply yield a stiffer set of equations to solve. Choosing an alternate parameter set may allow convergence with only small differences in the numerical results. For example, the cSPC/E water model with SPC/E Joung/Cheatham ions is easier to converge at higher ion concentrations in 1D-RISM than cTIP3P water with TIP3P Joung/Cheatham ions. Both models give nearly identical results in RISM at lower concentrations but NaCl in cTIP3P water will not converge above 0.5 M for the PSE-3 closure despite using all of the above methods.

3.3 3D-RISM in sander

3D-RISM functionality is available in *sander* and is built as part of the standard install procedure. MPI functionality for 3D-RISM in sander requires some additional information at compile time, described in Section **??**. Some features specific to *sander* are discussed here.

3.3.1 3D-RISM in `sander`

Full 3D-RISM functionality is available in `sander` as part of the standard install procedure. However, some methods available in `sander` are not compatible with 3D-RISM, such as QM/MM simulations. At this time, only standard molecular dynamics, minimization and trajectory post-processing with non-polarizable force fields are supported. With the exception of multiple time step features, 3D-RISM keywords in `sander` are identical to those in NAB, rism3d.snglpnt and MMPBSA.py.

3D-RISM specific command line options for `sander` are

```
sander [standard options] -xvv xvvfile -guv guvroot -huv huvroot
```

```
-cuv cuvroot -uuv uuvroot -asymp asympfile
-quv quvroot -chgdist chgdistroot
-exchem exchemroot -solvene solveneroot -entropy entropyroot -potUV potUVroot
```

xvvfile *input* description of bulk solvent properties, required for 3D-RISM calculations. Produced by `rism1d`.

guvroot *output* root name for solute-solvent 3D pair distribution function, $G^{UV}(\mathbf{R})$. This will produce one file for each solvent atom type for each frame requested.

huvroot *output* root name for solute-solvent 3D total correlation function, $H^{UV}(\mathbf{R})$. This will produce one file for each solvent atom type for each frame requested.

cuvroot *output* root name for solute-solvent 3D total correlation function, $C^{UV}(\mathbf{R})$. This will produce one file for each solvent atom type for each frame requested.

uuvroot *output* root name for solute-solvent 3D potential energy function, $U^{UV}(\mathbf{R})$, in units of kT. This will produce one file for each solvent atom type for each frame requested.

asympfile *output* root name for solute-solvent 3D long-range real-space asymptotics for *C* and *H*. This will produce one file for each of *C* and *H* for each frame requested and does not include the solvent site charge. Multiply the distribution by the solvent site charge to obtain the long-range asymptotics for that site.

quvroot *output* root name for solute-solvent 3D charge density distribution [*e/*Å]. This will produce one file that combines contributions from all solvent atom types for each frame requested.

chgdistroot *output* root name for solute-solvent 3D charge distribution [*e*]. This will produce one file that combines contributions from all solvent atom types for each frame requested.

exchemroot *output* root name for 3D excess chemical potential distribution files.

solveneroot *output* root name for 3D solvation energy distribution files.

entropyroot *output* root name for 3D solvation entropy distribution files.

potUVroot *output* root name for 3D solute-solvent potential energy distribution files.

Generated output files can be large and numerous. For each type of correlation, a separate file is produced for each solvent atom type. The frequency that files are produced is controlled by the `ntwrism` parameter. Every time step that output is produced, a new set of files is written with the time step number in the file name. For example, a molecular dynamics calculation using an SPC/E water model with `ntwrism=2` and `-guv guv` on the command line will produce two files on time step ten: `guv.O.10.mrc` and `guv.H1.10.mrc`.

3.3.1.1 Keywords

With the exception of irism, which is found in the &cntrl name list, all 3D-RISM options are specified in the &rism name list.

irism [0] Use 3D-RISM. Found in `&cntrl` name list.

      = 0 Off.

      = 1 On.

Closure Approximation

closure   [KH] Comma separate list of closure approximations. If more than one closure is provided, the 3D-RISM solver will use the closures in order to obtain a solution for the last closure in the list when no previous solutions are available. The solution for the last closure in the list is used for all output.

         = KH   Kovalenko-Hirata (KH).

         = HNC   Hyper-netted chain equation (HNC).

         =PSE*n*   Partial series expansion of order-*n* (PSE-*n*), where "*n*" is a positive integer.

Solvation Free Energy Corrections

gfCorrection [0] Compute the Gaussian fluctuation excess chemical potential functional (see §3.1.1).

         = 0   Off.

         = 1   On.

pcpluscorrection [0] Compute the PC+/3D-RISM excess chemical potential functional (see §**??**).

         = 0   Off.

         = 1   On.

uccoeff   [0,0,0,0] Compute the UC excess chemical potential functional with the provided coefficients (see §**??**). *a* and *b* are the coefficients for the original UC functional, though using the closure excess chemical potential functional. *a1* and *b1* are optional and provide temperature dependence to the correction (UCT in [97]).

Fixed Box Size

ng3   [] Sets the number of grid points for a fixed size solvation box. This is only used if buffer< 0.

     nx,ny,nz   Points for *x*, *y* and *z* dimensions.

solvbox   [] Sets the size in Å of the fixed size solvation box. This is only used if buffer< 0. See §3.2.3 for details on how this affects numerical accuracy and how this interacts with ljTolerance, and tolerance.

     lx,ly,lz   Box length in *x*, *y* and *z* dimensions.

Solution Convergence

tolerance   [1e-5] A list of maximum residual values for solution convergence. When used in combination with a list of closures it is possible to define different tolerances for each of the closures. This can be useful for difficult to converge calculations (see Subsection **??** for details). For the sake of efficiency, it is best to use as high a tolerance as possible for all but the last closure. For minimization a tolerance of 1e-11 or lower is recommended. See §3.2.3 for details on how this affects numerical accuracy and how this interacts with ljTolerance, buffer, and solvbox. Three formats of list are possible.

     one tolerance   All closures but the last use a tolerance of 1. The last tolerance in the list is used by the last closure. In practice this, is the most efficient.

     two tolerances   All closures but the last use the first tolerance in the list. The last tolerance in the list is used by the last closure.

     n tolerances   Tolerances from the list are assigned to the closure list in order.

ljTolerance [-1] Determines the Lennard-Jones cutoff distance based on the desired accuracy of the calculation. See §3.2.3 for details on how this affects numerical accuracy and how this interacts with tolerance, buffer, and solvbox.

asympKSpaceTolerance [-1] Determines the reciprocal space long range asymptotics cutoff distance based on the desired accuracy of the calculation. See §3.2.3 for details on how this affects numerical accuracy. Possible values are

< 0	asympKSpaceTolerance=tolerance/10,
0	no cutoff, and
> 0	given value determines the maximum error in the reciprocal-space long range asymptotics calculations.

mdiis_del [0.7] "Step size" in MDIIS.

mdiis_nvec [5] Number of vectors used by the MDIIS method. Higher values for this parameter can greatly increase memory requirements but may also accelerate convergence.

mdiis_restart [10] If the current residual is mdiis_restart times larger than the smallest residual in memory, then the MDIIS procedure is restarted using the lowest residual solution stored in memory. Increasing this number can sometimes help convergence.

mdiis_method [2] Specify implementation of the MDIIS routine.

= 0 Original. For small systems (e.g. $< 64^3$ grid points) this implementation may be faster than the BLAS optimized version.

= 1 BLAS optimized.

= 2 BLAS and memory optimized.

maxstep [10000] Maximum number of iterations allowed to converge on a solution.nrespa

npropagate [5] Number of previous solutions propagated forward to create an initial guess for this solute atom configuration.

= 0 Do not use any previous solutions

= 1..5 Values greater than 0 but less than 4 or 5 will use less system memory but may introduce artifacts to the solution (e.g., energy drift).

Minimization and Molecular Dynamics

zerofrc [1] Redistribute solvent forces across the solute such that the net solvation force on the solute is zero.

= 0 Unmodified forces.

= 1 Zero net force.

Trajectory Post-Processing

apply_rism_force [1] Calculate and use solvation forces from 3D-RISM. Not calculating these forces can save computation time and is useful for trajectory post-processing.

= 0 Do not calculate forces.

= 1 Calculate forces.

Output

ntwrism [0] Indicates that solvent density grid should be written to file every `ntwrism` iterations.

> **= 0** No files written.
>
> **>= 1** Output every `ntwrism` time steps.

`molReconstruction` [0] For any thermodynamic distributions requested, also out the molecular reconstruction (see section **??**).

`volfmt` ['mrc'] Format of volumetric data files. May be mrc, ccp4, dx or xyzv (see section **??**).

`verbose` [0] Indicates level of diagnostic detail about the calculation written to the log file.

> **= 0** No output.
>
> **= 1** Print the number of iterations used to converge.
>
> **= 2** Print details for each iteration and information about what FCE is doing every `progress` iterations.

write_thermo [1] Print solvation thermodynamics in addition to standard sander output. The format is the same as that found in NAB and rism3d.snglpnt.

polarDecomp [0] Decomposes solvation free energy into polar and non-polar components. Note that this typically requires 80% more computation time.

> **= 0** No polar/non-polar decomposition.
>
> **= 1** Polar/non-polar decomposition.

`progress` [1] Display progress of the 3D-RISM solution every `kshow` iterations. 0 indicates this information will not be displayed. Must be used with `verbose` > 1.

3.3.1.2 Example

Molecular Dynamics (`imin=0`)

```
molecular dynamics with 3D-RISM and impulse MTS
&cntrl
    ntx=1, ntpr=100, ntwx=1000,ntwr=10000,
    nstlim=10000,dt=0.001,                  !No shake or r-RESPA
    ntt=3, temp0=300, gamma_ln=20,          !Langevin dynamics
    ntb=0,                                  !Non-periodic
    cut=999.,                               !Calculate all
                                            !solute-solute
                                            !interactions
    irism=1,
/
&rism
    rismnrespa=5,                           !r-RESPA MTS
    fcenbasis=10,fcestride=2,fcecrd=2       !FCE MTS
/
```

Minimization (`imin=1`)

```
Default XMIN minimization with 3D-RISM
&cntrl
    imin=1, maxcyc=200,
    drms=1e-3,            !RMS force. Can be as low as 1e-4
    ntmin=3,              !XMIN
    ntpr=5,
    ntb=0,               !Non-periodic
    cut=999.,            !Calculate all
                         !solute-solute interactions
    irism=1
/
&rism
    tolerance=1e-11,      !Low tolerance
    solvcut=9999,         !No cut-off for
                          !solute-solvent interactions
    centering=2           !Solvation box centering
                          !using center-of-geometry
/
```

Trajectory Post-Processing (`imin=5`)

```
Trajectory post-processing with 3D-RISM
&cntrl
    ntx=1, ntpr=1, ntwx=1,
    imin=5,maxcyc=1,        !Single-point energy calculation
                            !on each frame
    ntb=0,                 !Non-periodic
    cut=9999.,             !Calculate all
                           !solute-solute interactions
    irism=1
/
&rism
    tolerance=1e-4,         !Saves some time compared to 1e-5
    apply_rism_force=0,     !Saves some time. Forces are not used.
    npropagate=1            !Saves some time and 4*8*Nbox bytes
                            !of memory compared to npropagate=5.
/
```

4 sqm: Semi-empirical quantum chemistry

AmberTools contains its own quantum chemistry program, called *sqm*. This is code extracted from the QM/MM portions of *sander*, but is limited to "pure QM" calculations. A principal current use is as a replacement for MOPAC for deriving AM1-bcc charges, but the code is much more general than that. Presently, it is limited to single point calculations and energy minimizations (geometry optimizations) for closed-shell systems. It supports a wide variety of semi-empirical Hamiltonians, including many recent ones. An external electric field generated by a set of point charges can be included for single point calculations. Our plan is to add capabilities to subsequent versions. The major contributors are as follows:

- The original semi-empirical support was written by Ross Walker, Mike Crowley, and Dave Case,[98] based on public-domain MOPAC codes of Various SCF convergence schemes were added by Tim Giese and Darrin York.

- The PM6 Hamiltonian was added by Andreas Goetz and dispersion and hydrogen bond corrections were added by Andreas Goetz and Kyoyeon Park.

- The extension for MNDO type Hamiltonians to support d orbitals was written by Tai-Sung Lee, Darrin York and Andreas Goetz.

- The charge-dependent exchange-dispersion corrections of vdW interactions[99] was contributed by Tai-Sung Lee, Tim Giese, and Darrin York.

- Support for reading user-defined parameters for NDDO methods was added by Tai-Sung Lee and Darrin York.

4.1 Available Hamiltonians

Available MNDO-type semi-empirical Hamiltonians are PM3,[100] AM1,[101] RM1,[102] MNDO,[103] PDDG/PM3,[104] PDDG/MNDO,[104] PM3CARB1,[105], PM3-MAIS[106, 107], MNDO/d[108–110], AM1/d (Mg from AM1/d[111] and H, O, and P from AM1/d-PhoT[112]) and PM6[113].

Also available is the density functional theory-based tight-binding (DFTB) Hamiltonian[114–116] and its self-consistent-charge version with Taylor expansion up to second order (SCC-DFTB or DFTB2)[117] and third-order (DFTB3)[118]. If you use the mio-1-1 parameters for DFTB2, you can add an empirical correction for dispersion effects[119] and calculate CM3 charges[120] (both only for elements H, C, N, O, S, P). Diagonal third-order corrections are available for DFTB2[121] with mio-1-1 parameters but it is recommended to perform full DFTB3 simulations instead. Neither dispersion corrections nor halogen corrections are implemented for DFTB3.

The elements supported by each QM method are:

- MNDO: H, Li, Be, B, C, N, O, F, Al, Si, P, S, Cl, Zn, Ge, Br, Cd, Sn, I, Hg, Pb

- MNDO/d: H, Li, Be, B, C, N, O, F, Na, Mg, Al, Si, P, S, Cl, Zn, Ge, Br, Sn, I, Hg, Pb

- AM1: H, C, N, O, F, Al, Si, P, S, Cl, Zn, Ge, Br, I, Hg

- AM1/d: H, C, N, O, F, Mg, Al, Si, P, S, Cl, Zn, Ge, Br, I, Hg

- PM3: H, Be, C, N, O, F, Mg, Al, Si, P, S, Cl, Zn, Ga, Ge, As, Se, Br, Cd, In, Sn, Sb, Te, I, Hg, Tl, Pb, Bi

- PDDG/PM3: H, C, N, O, F, Si, P, S, Cl, Br, I

- PDDG/MNDO: H, C, N, O, F, Cl, Br, I

- RM1: H, C, N, O, P, S, F, Cl, Br, I

- PM3CARB1: H, C, O

- PM3-MAIS: H, O, Cl

- PM6: H, He, Li, Be, B, C, N, O, F, Ne, Na, Mg, Al, Si, P, S, Cl, Ar, K, Ca, Sc, Ti, V, Cr, Mn, Fe, Co, Ni, Cu, Zn, Ga, Ge, As, Se, Br, Kr, Rb, Sr, Y, Zr, Nb, Mo, Tc, Ru, Rh, Pd, Ag, Cd, In, Sn, Sb, Te, I, Xe, Cs, Ba, La, Lu, Hf, Ta, W, Re, Os, Ir, Pt, Au, Hg, Tl, Pb, Bi

The PM6 implementation has not been extensively tested for all available elements. Please check your results carefully, possibly by comparison to other codes that implement PM6, if transition metal elements are present. SCF convergence may be more difficult to achieve for transition metal elements with partially filled valence shells.

If the PM6 Hamiltonian is used in a QM/MM simulation with *sander* using electrostatic embedding (see Section **??**) or if an electric field of external point charges is used, then the electrostatic interactions between QM and MM atoms are modeled using the MNDO type core repulsion function for interactions between QM and MM atoms. Parameters for the exponents α of the QM atoms are taken from PM3 (a default value of five is used for the exponents α of the MM atoms as is the case for MNDO, AM1 and PM3). Since PM3 does not have parameters for all elements that are supported by PM6, the missing exponents were defined in an ad hoc manner (see the source code in \$AMBERHOME/AmberToosl/src/sqm/qm2_parameters.F90, variable alp_pm6). The magnitude of the coefficients α is probably not critical for the accuracy of QM/MM calculations but this should be tested on a case by case basis. This does not affect QM calculations with *sqm*.

4.2 Dispersion and hydrogen bond correction

An empirical dispersion and hydrogen bonding correction is implemented for the MNDO type Hamiltonians AM1 and PM6[122]. The empirical dispersion correction follows the formalism for DFT-D[123] and consists of a physically sound r^{-6} term that is damped at short distances to avoid the short-range repulsion which can be written as

$$E_{dis} = -s_6 \sum_{ij} f_{damp}(r_{ij}, R_{ij}^0) C_{6,ij} r_{ij}^{-6}, \tag{4.1}$$

where r_{ij} is the distance between two atoms i and j, R_{ij}^0 is the equilibrium van der Waals (vdW) separation derived from the atomic vdW radii, $C_{6,ij}$ the dispersion coefficient, and s_6 a general scaling factor. The damping function is given as

$$f_{damp}(r_{ij}, R_{ij}^0) = \left[1 + \exp\left(-\alpha \frac{r_{ij}}{s_R R_{ij}^0} - 1 \right) \right]^{-1}. \tag{4.2}$$

Bondi vdW radii[124] are used and for a pair of unlike atoms we have

$$R_{ij}^0 = \frac{R_{ii}^{0\,3} + R_{jj}^{0\,3}}{R_{ii}^{0\,2} + R_{jj}^{0\,2}}. \tag{4.3}$$

For the C_6 coefficients the following equation is used,

$$C_{6,ij} = 2 \frac{(C_{6,ii}^2 C_{6,jj}^2 N_{eff,i} N_{eff,j})^{1/3}}{(C_{6,ii} N_{eff,j}^2)^{1/3} + (C_{6,jj} N_{eff,i}^2)^{1/3}}, \tag{4.4}$$

where the Slater-Kirkwood effective number of electrons $N_{eff,i}$ and the C_6 coefficients can easily be found in the literature[123].

An empirical hydrogen bonding correction[122] that is transferable among different semiempirical Hamiltonians and has been parametrized for use with the dispersion correction described above is also available. This correction does not make the assumption of a specific acceptor/hydrogen/donor binding situation. Instead it considers the hydrogen bond as a charge-independent atom- atom term between two atoms capable of serving an acceptor

or donor (for example, O, N) and weights this by a function that accounts for the steric arrangement of the two atoms and the favorable positioning of a hydrogen atom inbetween. A damping function corrects for long- and short-range behavior,

$$E_{\text{H}-bond} = \frac{C_{AB}}{r_{AB}^2} f_{geom} f_{damp},$$ (4.5)

$$f_{geom} = \cos(\theta_A)^2 \cos(\phi_A)^2 \cos(\psi_A)^2 \cos(\phi_B)^2 \cos(\phi_B)^2 \cos(\psi_B)^2 f_{bond},$$ (4.6)

$$f_{bond} = 1 - \frac{1}{1 + \exp[-60(r_{XH}/1.2 - 1)]},$$ (4.7)

$$f_{damp} = \left(\frac{1}{1 + \exp[-100(r_{AB}/2.4 - 1)]} \right) \left(1 - \frac{1}{1 + \exp[-10(r_{AB}/7.0 - 1)]} \right),$$ (4.8)

$$C_{AB} = \frac{C_A + C_B}{2}.$$ (4.9)

Here, C_A and C_B are the atomic hydrogen bonding correction parameters and the (torsion) angles in the function f_{geom} are defined similarly to an earlier hydrogen bond correction[125].

The hydrogen bond correction can be used both for single point energy calculations or geometry optimizations with SQM and for molecular dynamics simulations with SANDER. However, we do not recommend the use for molecular dynamics at present since cutoffs needed to be implemented for the calculation of f_{geom} of equation (4.6). This and some other conditional evaluations give rise to discontinuities in the potential energy surface and thus make this method unattractive for MD simulations.

4.3 Usage

The *sqm* program uses the following simple command line:

sqm [-O] -i <input-file> -o <output-file>

mdin is the default input-file name, and *mdout* is the default output-file name.As in other Amber programs, the "-O" flag allows the program to over-write the output file.

An example input file for running a simple minimization is shown here:

```
Run semi-empirical minimization
 &qmmm
 qm_theory='AM1',   qmcharge=0,
 /
    6    CG        -1.9590        0.1020        0.7950
    6    CD1       -1.2490        0.6020       -0.3030
    6    CD2       -2.0710        0.8650        1.9630
    6    CE1       -0.6460        1.8630       -0.2340
    6    C6        -1.4720        2.1290        2.0310
    6    CZ        -0.7590        2.6270        0.9340
    1    HE2       -1.5580        2.7190        2.9310
   16    S15       -2.7820        0.3650        3.0600
    1    H19       -3.5410        0.9790        3.2740
    1    H29       -0.7870       -0.0430       -0.9380
    1    H30        0.3730        2.0450       -0.7840
    1    H31       -0.0920        3.5780        0.7810
    1    H32       -2.3790       -0.9160        0.9010
```

The *&qmmm* namelist contains variables that allow you to control the options used. Following that is one line per atom, giving the atomic number, atom name, and Cartesian coordinates (free format). The variables in the *&qmmm* namelist are these:

qm_theory   Level of theory to use for the QM region of the simulation (Hamiltonian). Default is to use the semi-empirical Hamiltonian PM3. Options are AM1, RM1, MNDO, PM3-PDDG, MNDO-PDDG,

PM3-CARB1, MNDO/d (same as MNDOD), AM1/d (same as AM1D), PM6, DFTB2 (same as DFTB), and DFTB3. The dispersion correction can be switched on for AM1 and PM6 by choosing AM1-D* and PM6-D, respectively. The dispersion and hydrogen bond correction will be applied for AM1-DH+ and PM6-DH+.

qmcharge   Charge on the QM system in electron units (must be an integer). (Default = 0)

spin   Multiplicity of the QM system. Currently only singlet calculations are possible and so the default value of 1 is the only available option. Note that this option is ignored by DFTB/SCC-DFTB, which allows only ground state calculations. In this case, the spin state will be calculated from the number of electrons and orbital occupancy.

qmqmdx   Flag for whether to use analytical or numerical derivatives of the semiempirical electron repulsion integrals. The default (and recommended) option is to use ANALYTICAL QM-QM derivatives.

= 1 (default) - Use analytical derivatives for QM-QM forces.

= 2 Use numerical derivatives for QM-QM forces. Note: the numerical derivative code has not been optimised as aggressively as the analytical code and as such is significantly slower. Numerical derivatives are intended mainly for testing purposes.

verbosity   Controls the verbosity of QM/MM related output. *Warning:* Values of 2 or higher will produce a *lot* of output.

= 0 (default) - only minimal information is printed - Initial QM geometry and link atom positions as well as the SCF energy at every ntpr steps.

= 1 Print SCF energy at every step to many more significant figures than usual. Also print the number of SCF cycles needed on each step.

= 2 As 1 and also print info about memory reallocations, number of pairs per QM atom, QM core - QM core energy, QM core - MM atom energy, and total energy.

= 3 As 2 and also print SCF convergence information at every step.

= 4 As 3 and also print forces on the QM atoms due to the SCF calculation and the coordinates of the link atoms at every step.

= 5 As 4 and also print all of the info in kJ/mol as well as kcal/mol.

tight_p_conv   Controls the tightness of the convergence criteria on the density matrix in the SCF.

=0 (default) - loose convergence on the density matrix (or Mulliken charges, in case of a SCC-DFTB calculation). SCF will converge if the energy is converged to within scfconv and the largest change in the density matrix is within 0.05*sqrt(scfconv).

= 1 Tight convergence on density(or Mulliken charges, in case of a SCC-DFTB calculation). Use same convergence (scfconv) for both energy and density (charges) in SCF. Note: in the SCC-DFTB case, this option can lead to instabilities.

scfconv   Controls the convergence criteria for the SCF calculation, in kcal/mol. In order to conserve energy in a dynamics simulation with no thermostat it is often necessary to use a convergence criterion of 1.0d-9 or tighter. Note, the tighter the convergence the longer the calculation will take. Values tighter than 1.0d-11 are not recommended as these can lead to oscillations in the SCF, due to limitations in machine precision, that can lead to convergence failures. Default is 1.0d-8 kcal/mol. Minimum usable value is 1.0d-14.

pseudo_diag   Controls the use of 'fast' pseudo diagonalisations in the SCF routine. By default the code will attempt to do pseudo diagonalisations whenever possible. However, if you experience convergence problems then turning this option off may help. Not available for DFTB/SCC-DFTB.

= 0 Always do full diagonalisation.

= 1 Do pseudo diagonalisations when possible (default).

`pseudo_diag_criteria` Float controlling criteria used to determine if a pseudo diagonalisation can be done. If the difference in the largest density matrix element between two SCF iterations is less than this criteria then a pseudo diagonalisation can be done. This is really a tuning parameter designed for expert use only. Most users should have no cause to adjust this parameter. (Not applicable to DFTB/SCC-DFTB calculations.) Default = 0.05

`diag_routine` Controls which diagonalization routine will be used during the SCF procedure. This is an advanced option to fine-tune performance which has negligible effect on energies (and generally little effect on geometries in the case of SQM energy minimizations). The speed of each diagonalizer is a function of the number and type of QM atoms as well as the LAPACK library that the program was linked to. As such there is not always an obvious choice to obtain the best performance. The simplest option is to set diag_routine = 0 in which case the program will test each diagonalizer in turn, including the pseudo diagonalizer, and select the one that gives optimum performance. As of AmberTools 15 diag_routine = 0 is the default for both SQM and QMMM in Sander. Not available for DFTB/SCC-DFTB.

= 0 Automatically select the fastest routine (default).

= 1 Use internal diagonalization routine.

= 2 Use lapack dspev.

= 3 Use lapack dspevd.

= 4 Use lapack dspevx.

= 5 Use lapack dsyev.

= 6 Use lapack dsyevd.

= 7 Use lapack dsyevr.

`printcharges` **= 0** Don't print any info about QM atom charges to the output file (default)

= 1 Print Mulliken QM atom charges to output file every *ntpr* steps.

`print_eigenvalues` Controls printing of MO eigenvalues.

= 0 Do not print MO eigenvalues

= 1 Print MO eigenvalues at the end of a single point calculation or geometry optimization (default)

= 2 Print MO eigenvalues at the end of every SCF cycle (only NDDO methods, not DFTB)

= 3 Print MO eigenvalues during each step of the SCF cycle (only NDDO methods, not DFTB)

`qxd` Flag to turn on (=.true.) or off (=.false., default) the charge-dependent exchange-dispersion corrections of vdW interactions[99].

`parameter_file` **=** 'PARAM.FILE' Read user-defined parameters from the file 'PARAM.FILE'. The first three space-separated entries (case insensitive) of each line will be interpreted as a user-modified parameter in the sequence of *parameter name, element name,* and *value*. For example, a line contains "USS Cl -111.6139480D0 " will cause the USS parameter of the Cl element changed to -111.6139480. A line beginning with "END" will stop the reading. This function currently only works for MNDO, AM1, PM3, MNDO/d, and AM1/d. Also, when new nuclear core-core parameters (FN, in PM3, AM1, and AM1/d) are re-defined, the number of FNN parameter sets (NUM_FN) also needs to be defined. For example, if FNn3 (n = 1, 2, or 3) is defined, then NUM_FN needs to be set to 3 or 4.

`peptide_corr` **= 0** Don't apply MM correction to peptide linkages. (default)

     = 1 Apply a MM correction to peptide linkages. This correction is of the form $E_{scf} = E_{scf} + h_{type}(i_{type})\sin^2 \phi$, where ϕ is the dihedral angle of the H-N-C-O linkage and h_{type} is a constant dependent on the Hamiltonian used. (Recommended, except for DFTB/SCC-DFTB.)

itrmax   Integer specifying the maximum number of SCF iterations to perform before assuming that convergence has failed. Default is 1000. Typically higher values will not do much good since if the SCF hasn't converged after 1000 steps it is unlikely to. If the convergence criteria have not been met after itrmax steps the SCF will stop and the minimisation will proceed with the gradient at itrmax. Hence if you have a system which does not converge well you can set itrmax smaller so less time is wasted before assuming the system won't converge. In this way you may be able to get out of a bad geometry quite quickly. Once in a better geometry SCF convergence should improve.

maxcyc   Maximum number of minimization cycles to allow, using the *xmin* minimizer (see Section **??**) with the TNCG method. Default is 9999. Single point calculations can be done with *maxcyc* = 0.

ntpr   Print the progress of the minimization every *ntpr* steps; default is 10.

grms_tol   Terminate minimization when the gradient falls below this value; default is 0.02

ndiis_attempts   Controls the number of iterations that DIIS (direct inversion of the iterative subspace) extrapolations will be attempted. Not available for DFTB/SCC-DFTB. The SCF does not even begin to exhaust its attempts at using DIIS extrapolations until the end of iteration 100. Therefore, for example, if ndiis_attempts=50, then DIIS extrapolations would be performed at end of iterations 100 to 150. The purpose of not performing DIIS extrapolations before iteration 100 is because the existing code base performs quite well for most molecules; however, if convergence is not met after 100 iterations, then it is presumed that further iterations will not yield SCF convergence without doing something different, i.e., DIIS. Thus, the implementation of DIIS in SQM is a mechanism to try and force SCF convergence for molecules that are otherwise difficult to converge. Default 0. Maximum 1000. Minimum 0. Note that DIIS will automatically turn itself on for 100 attempts at the end of iteration 800 even if you did not explicitly set ndiis_attempts to a nonzero value. This is done as a final effort to achieve convergence.

ndiis_matrices   Controls the number of matrices used in the DIIS extrapolation. Including only one matrix is the same as not performing an extrapolation. Including an excessive number of matrices may require a large amount of memory. Not available for DFTB/SCC-DFTB. Default 6. Minimum 1. Maximum 20.

vshift   Controls level shifting (only NDDO methods, not DFTB). Virtual orbitals can be shifted up by vshift (in eV) to improve SCF convergence in cases with small HOMO/LUMO gap. Default 0.0 (no level shift).

errconv   SCF tolerance on the maximum absolute value of the error matrix, i.e., the commutator of the Fock matrix with the density matrix. The value has units of hartree. The default value of errconv is sufficiently large to effectively remove this tolerance from the SCF convergence criteria. Not available for DFTB/SCC-DFTB. Default 1.d-1. Minimum 1.d-16. Maximum 1.d0.

qmmm_int   When running QM calculations in the sqm program, an electric field of external point charges can be added. In this way, the electrostatic effect outside of the QM region can be modeled, making the calculation a simplified QM/MM calculation without QM/MM vdW's contribution. Like QM/MM calculations (see Section **??**), the method to couple QM and MM electrostatic interactions for external charges and semiempirical Hamiltonians can be specified via the *qmmm_int* namelist variable.

      The current implementation limits use of external charges to only single point energy calculations. To run such a calculation, an additional field, which begins with #EXCHARGES and ends with #END, is required to specify the external point charges in the input. Each external point charge must include atomic number, atom name, X, Y, Z coordinates and the charge in units of the electron charge. An example input looks like:

```
single point energy calculation (adenine), with external charges (thymine)
&qmmm
 qm_theory = 'PM3',
 qmcharge = 0,
 maxcyc = 0,
 qmmm_int = 1,
/
7  N    1.0716177  -0.0765366   1.9391390
1  H    0.0586915  -0.0423765   2.0039181
1  H    1.6443796  -0.0347395   2.7619159
6  C    1.6739638  -0.0357766   0.7424316
7  N    0.9350155  -0.0279801  -0.3788916
6  C    1.5490760   0.0012569  -1.5808009
1  H    0.8794435   0.0050260  -2.4315709
7  N    2.8531510   0.0258031  -1.8409596
6  C    3.5646109   0.0195446  -0.7059872
6  C    3.0747955  -0.0094480   0.5994562
7  N    4.0885824  -0.0054429   1.5289786
6  C    5.1829921   0.0253971   0.7872176
1  H    6.1882591   0.0375542   1.1738824
7  N    4.9294871   0.0412404  -0.5567274
1  H    5.6035368   0.0648755  -1.3036811
#EXCHARGESwill be
6  C   -4.7106131   0.0413373   2.1738637  -0.03140
1  H   -4.4267056   0.9186178   2.7530256   0.06002
1  H   -4.4439282  -0.8302573   2.7695655   0.05964
1  H   -5.7883971   0.0505530   2.0247280   0.03694
6  C   -3.9917387   0.0219348   0.8663338  -0.25383
6  C   -4.6136833   0.0169051  -0.3336520   0.03789
1  H   -5.6909220   0.0269347  -0.4227183   0.16330
7  N   -3.9211729  -0.0009646  -1.5163659  -0.47122
1  H   -4.4017172  -0.0036078  -2.4004924   0.35466
6  C   -2.5395897  -0.0149474  -1.5962357   0.80253
8  O   -1.9416783  -0.0291878  -2.6573783  -0.63850
7  N   -1.9256484  -0.0110593  -0.3638948  -0.58423
1  H   -0.8838255  -0.0216168  -0.3784269   0.35404
6  C   -2.5361367   0.0074651   0.8766724   0.71625
8  O   -1.8674730   0.0112093   1.9120833  -0.60609
#END
```

5 Atom and Residue Selections

There are three ways to select atoms and residues in AMBER-related routines: the **AMBER "mask"** notation, used by most programs, the **NAB "atom expressions"**, which work only with NAB-compiled applications, and an older "GROUP" specification used in *sander* and *pmemd*. Information about these is collected in this chapter.

5.1 Amber Masks

A "mask" is a notation which selects atoms or residues for special treatment. A frequent usage is fixing or tethering selected atoms or residues during minimization or molecular dynamics.

The following lines are partially copied from the original AMBER documentation. For more details, refer to the entire section of that documentation describing the *ambmask* utility.

The "mask" selection expression is composed of "elementary selections". These start with "**:**" to select by residues, or "@" to select by atoms. Residues can be selected by numbers (given as numbers separated by commas, or as ranges separated by a dash) or by names (given as a list of residue names separated by commas). The same holds true for atom selections by atom numbers or atom names. In addition, atoms can be selected by AMBER atom type, in which case "@" must be immediately followed by "%". The notation ":*" means all residues and "@*" means all atoms. The following examples show the usage of this syntax.

Residue Number List Examples

```
:1-10     = "residues 1 to 10"
:1,3,5    = "residues 1, 3, and 5"
:1-3,5,7-9 = "residues 1 to 3 and residue 5 and residues 7 to 9"
```

Residue Name List Examples

```
:LYS         = "all lysine residues"
:ARG,ALA,GLY = "all arginine and alanine and glycine residues"
```

Atom Number List Examples

Note that these masks use the **actual sequential numbers of atoms** in the file. This is tricky and a serious source of error. You must know these numbers correctly. Using the atom numbers of a PDB file written out by an AMBER tool is an appropriate way to avoid pitfalls. **Do not use the original atom numbers from the raw PDB file you started with.**

```
@12,17      = "atoms 12 and 17"
@54-85      = "all atoms from 54 to 85"
@12,54-85,90 = "atom 12 and all atoms from 54 to 85 and atom 90"
```

Atom Name List Examples

```
@CA          = all atoms with the name CA (i.e., all C-alpha atoms)
@CA,C,O,N,H = all atoms with names CA or C or O or N or H
                (i.e., the entire protein backbone)
```

Atom Type List Examples

This last mask type is only used by specialists and mentioned here for completeness. It allows the selection of AMBER atom types and requires detailed knowledge of AMBER force fields.

```
@%CT         = all atoms with the force field type CT
                (the standard sp3 aliphatic carbon)
@%N*,N3      = all atoms with the force field type N* or N3
                (N* is a special sp2 nitrogen, N3 is an sp3 nitrogen)
```

Note that in the above example, N* is actually an atom type. The * is **not** a wild card meaning "all N-something types"!

Logical Combinations

The selections above can be combined by various logical operators, including selections like "all atoms within a certain distance from...". The use of such combinations goes beyond this introductory script. Interested users should refer to the next section for details.

5.1.1 ambmask

NAME

ambmask - test group input FIND mask (or mask string given in the &cntrl section) and dump the resulting atom selection in a given format

SYNOPSIS

ambmask -p prmtop -c inpcrd -prnlev [0-3] -out [short| pdb| amber] -find [maskstr]

DESCRIPTION

ambmask acts as a filter that inputs an Amber topology file and an Amber coordinate file and applies the "maskstr" selection string to select specific atoms or residues. (The "maskstr" selection string is similar syntactically to UCSF Chimera/Midas.) Residues can be selected by their numbers or names. Atoms can be selected by numbers, names, or Amber (forcefield) type. Selections are case insensitive. The selected atoms are printed to **stdout** (by default, in Amber-style PDB format). Atom and residue names and numbers are taken from the Amber topology. Beware that the selection string works on those names and not the ones from the original PDB file. If you are not sure how atoms or residues are named or numbered in the Amber topology, use **ambmask** with a selection string ":*" (which is the default) to dump the whole PDB file with corresponding Amber atom/residue names and numbers.

The "maskstr" selection expression is composed of "elementary selections". These start with ":" to select by residues, or "@" to select by atoms. Residues can be selected by numbers (given as numbers separated by commas, or as ranges separated by a dash) or by names (given as a list of residue names separated by commas). The same holds true for atom selections by atom numbers or atom names. In addition, atoms can be selected by Amber atom type, in which case "@" must be immediately followed by "%". ":*" means all residues and "@*" means all atoms. The following examples show the usage of this syntax. Square brackets should not be used in actual expressions, they are only used below to denote individual selection string examples:

```
:{residue numlist} [:1-10] [:1,3,5] [:1-3,5,7-9]
:{residue namelist} [:LYS] [:ARG,ALA,GLY]
@{atom numlist} [@12,17] [@54-85] [@12,54-85,90]
@{atom namelist} [@CA] [@CA,C,O,N,H]
@%{atom typelist} [@%CT] [@%N*,N3]
```

These "elementary selections" can be combined into more complex selections using binary operators "&" (and) and "|" (or), unary operator "!" (negation), distance binary operators "<:", ">:", "<@", ">@", and parentheses. Spaces around operators are irrelevant. Parentheses have the highest priority, followed by distance operators ("<:", ">:", "<@", ">@"), "!" (negation), "&" (and) and "|" (or) in order of descending priority. A wildcard "=" in an atom or residue name matches any name starting with a given character (or characters). For example, [:AS=] would match all aspartic acid residues (ASP), and asparagines (ASN); [@H=] would match all atom names starting with H (which are effectively all hydrogens). It cannot be used to match the end part of names (such as [:=A]). Some examples of more complex selections follow:

```
[@C= & !@CA,C]
```

.. all carbons except backbone alpha and carbonyl carbon

```
[(:1-3@CA | :5-7@CB)]
```

.. alpha carbons in residues 1-3 and beta carbons in residues 5-7

```
[:CYS,ARG & !(:1-10 | @CA,CB)]
```

.. all CYS and ARG atoms except those which are in residues 1-10 and which are CA or CB

```
[:* & !@H=] or [!@H=]
```

.. all heavy atoms (i.e. except hydrogens)

```
[:5 <@4.5]
```

.. all atoms within 4.5A from residue 5

```
[(:1-55 <:3.0) & :WAT]
```

.. all water molecules within 3A from residues 1-55

Compound expressions of the following type are also allowed:

```
:{residue numlist|namelist}@{atom numlist|namelist|typelist}
[:1-10@CA] is equivalent to [:1-10 & @CA]
[:LYS@H=] is equivalent to [:LYS & @H=]
```

OPTIONS

The program needs an Amber topology file and coordinates (restrt format). The filename specified with the *-p* option is Amber topology, while the filename given with the *-c* option is a coordinate file. If *-p* or *-c* options are not given, the program expects that files "prmtop" and/or "inpcrd" exist in the current directory, which will be taken as topology and coordinate files correspondingly. If no command line options are given, the program prints the usage statement.

The option *-prnlev* specifies how much (debugging) information is printed to **stdout**. If it is 0, only selected atoms are printed. More verbose output (which might be useful for debugging purposes) is achieved with higher values: 1 prints original "maskstr" in its tokenized (with operands enclosed in square brackets) and postfix (or Reverse Polish Notation) forms; number of atoms and residues in the topology file and number of selected atoms are also printed to **stdout**. 2 prints the resulting mask array, which is an array of integer values, with '1' representing a selected atom, and '0' an unselected one. Value of 3, in addition, prints mask arrays as they are pushed or popped from the stack (this is really only useful for tracing the problems occurring during stack operations). The *-prnlev* values of 0 or 1 should suffice for most uses.

The option *-out* specifies the format of printed atoms. "short" means a condensed output using residue (:) and atom (@) designators followed by residue ranges and atom names. "pdb" (default) prints atoms in Amber-style PDB format with the original "maskstr" printed as a REMARK at the top of the PDB file, and "amber" prints atom/residue ranges in the format suitable for copying into group input section of Amber input file.

The option *-find* is followed by "maskstr" expression. This is a string where some characters have a special meaning and thus express what parts (atoms/residues) of the molecule will get selected. The syntax of this string is explained in the section above (DESCRIPTION). If this option is left out, it defaults to ":*", which selects all atoms in the given topology file. The length of "maskstr" is limited to 80 characters. If the "maskstr" contains spaces or special characters (which would be expanded by the shell), it should be protected by single or double quotes (depending on the shell). In addition, for C-shells even a quoted exclamation character may be expanded for history substitution. Thus, it is recommended that the operand of the negation operator always be enclosed in parentheses so that "!" is always followed by a "(" to produce "!(" which disables the special history interpretation. For example, [@C= & !(@CA,C)] selects all carbons except backbone alpha and carbonyl carbon; the parentheses are redundant but shell safe. The man page indicates further ways to disable history substitution.

FILES

Assumes that *prmtop* and *inpcrd* files exists in the current directory if they are not specified with *-p* and *-c* options. Resulting (i.e. selected) atoms are written to **stdout**.

BUGS

Because all atom names are left justified in Amber topology and the selections are case insensitive, there is no way to distinguish some atom names: alpha carbon CA and a calcium ion Ca are a notorious example of that.

5.2 GROUP Specification

This section describes the format used to define groups of atoms in various Amber programs. In *sander*, a group can be specified as a movable "belly" while the other atoms are fixed absolutely in space (aside from scaling caused by constant pressure simulation), and/or a group of movable atoms can independently restrained (held by a potential) at their positions. In *anal*, groups can be defined for energy analysis. In sander and pmemd, GROUP input comes at the end of the mdin input file, as discussed in Section 1.7.

Except in the analysis module where different groups of atoms are considered with different group numbers for energy decomposition, in all other places the groups of atoms defined are considered as marked atoms to be included for certain types of calculations. In the case of constrained minimization or dynamics, the atoms to be constrained are read as groups with a different weight for each group.

Reading of groups is performed by the routine RGROUP, and you are advised to consult it if there is still some ambiguity in the documentation.

Input description:

```
- 1 - Title format(20a4)
ITITL Group title for identification.
Setting ITITL = 'END' ends group input.
----------------------------------------------------------------------
- 1A - Weight format(f)
This line is only provided/read when using GROUP input to
define restrained atoms.
WT The harmonic force constants in kcal/mol-A**2 for the group
of atoms for restraining to a reference position.
----------------------------------------------------------------------
- 1B - Control to define the group
KTYPG , (IGRP(I) , JGRP(I) , I = 1,7) format(a,14i)
KTYPG Type of atom selection performed. A molecule can be
defined by using only 'ATOM' or 'RES', or part of the
molecule can be defined by 'ATOM' and part by 'RES'.
```

'ATOM' The group is defined in terms of atom numbers. The atom
number list is given in igrp and jgrp.
'RES' The group is defined in terms of residue numbers. The
residue number list is given in igrp and jgrp.
'FIND' This control is used to make additional conditions
(apart from the 'ATOM' and 'RES' controls) which a given
atom must satisfy to be included in the current group.
The conditions are read in the next section (1C) and are
terminated by a SEARCH card.
Note that the conditions defined by FIND filter any set(s) of atoms
defined by the following ATOM/RES instructions. For example,
-- group input: select main chain atoms --
FIND
* * M *
SEARCH
RES 1 999
END
END
'END' End input for the current group. Followed by either another
group definition (starting again with line 1 above), or by a second
'END' "card", which terminates all group input.
IGRP(I) , JGRP(I)
The atom or residue pointers. If ktypg .eq. 'ATOM' all
atoms numbered from igrp(i) to jgrp(i) will be put into
the current group. If ktypg .eq. 'RES' all atoms in the
residues numbered from igrp(i) to jgrp(i) will be put
into the current group. If igrp(i) = 0 the next control
card is read.
It is not necessary to fill groups according to the
numerical order of the residues. In other words, Group 1
could contain residues 40-95 of a protein, Group 2 could
contain residues 1-40 and Group 3 could contain residues
96-105.
If ktypg .eq. 'RES', then associating a minus sign with
igrp(i) will cause all residues igrp(i) through jgrp(i)
to be placed in separate groups.
In the analysis modules, all atoms not explicitly defined
as members of a group will be combined as a unit in the
(n + 1) group, where the (n) group in the last defined
group.

- 1C - Section to read atom characteristics
***** Read only if KTYPG = 'FIND' *****
JGRAPH(I) , JSYMBL(I) , JTREE(I) , JRESNM(I) *format(4a)*
A series of filter specifications are read. Each filter consists
of four fields (JGRAPH,JSYMBL,JTREE,JRESNM), and each filter is placed
on a separate line. Filter specification is terminated by a line with
JGRAPH = 'SEARCH'. A maximum of 10 filters may be specified for a
single 'FIND' command.
The union of the filter specifications is applied to the atoms defined
by the following ATOM/RES cards. I.e. if an atom satisfies any of the
filters, it will be included in the current group. Otherwise, it is not
included. For example, to select all non main chain atoms from residues
1 through 999:
-- group input: select non main chain atoms --
FIND
* * S *

```
* * B *
* * 3 *
* * E *
SEARCH
RES 1 999
END
END
'END' End input for the current group. Followed by either another
The four fields for each filter line are:
JGRAPH(I) The atom name of atom to be included. If this and the
following three characteristics are satisfied the atom is
included in the group. The wild card '*' may be used to
to indicate that any atom name will satisfy the search.
JSYMBL(I) Amber atom type of atom to be included. The wild card
'*' may be used to indicate that any atom type will
satisfy the search.
JTREE(I) The tree name (M, S, B, 3, E) of the atom to be included.
The wild card '*' may be used to indicate that any tree
name will satisfy the search.
JRESNM(I) The residue name to which the atom has to belong to be
included in the group. The wild card '*' may be used to
indicate that any residue name will satisfy the search.
----------------------------------------------------------------
```

Examples:

The molecule 18-crown-6 will be used to illustrate the group options. This molecule is composed of six repeating (-CH2-O-CH2-) units. Let us suppose that one created three residues in the PREP unit: CRA, CRB, CRC. Each of these is a (-CH2-O-CH2-) moiety and they differ by their dihedral angles. In order to construct 18-crown-6, the residues CRA, CRB, CRC, CRB, CRC, CRB are linked together during the LINK module with the ring closure being between CRA(residue 1) and CRB(residue 6).

Input 1:

```
Title one
RES 1 5
END
Title two
RES 6
END
END
```

Output 1: Group 1 will contain residues 1 through 5 (CRA, CRB, CRC, CRB, CRC) and Group 2 will contain residue 6 (CRB).

Input 2:

```
Title one
RES 1 5
END
Title two
ATOM 36 42
END
END
```

Output 2: Group 1 will contain residues 1 through 5 (CRA, CRB, CRC, CRB, CRC) and Group 2 will contain atoms 36 through 42. Coincidentally, atoms 36 through 42 are also all the atoms in residue 6.

Input 3:

```
Title one
```

```
RES -1 6
END
END
```

Output 3: Six groups will be created; Group 1: CRA, Group 2: CRB,..., Group 6: CRB.

Input 4:

```
Title one
FIND
O2 OS M CRA
SEARCH
RES 1 6
END
END
```

Output 4: Group 1 will contain those atoms with the atom name 'O2', atom type 'OS', tree name 'M' and residue name 'CRA'.

Input 5:

```
Title one
FIND
O2 OS * *
SEARCH
RES 1 6
END
END
```

Output 5: Group 1 will contain those atoms with the atom name 'O2', atom type 'OS', any tree name and any residue name.

Input 6:

```
Title one
RES 1 3 6 6
END
END
```

Output 6: One group is created containing residues 1 to 3 and 6. Up to seven ranges of contiguous residues can be specified per group. (In this case there are two ranges).

Input 7:

```
First restraint group
10.0
FIND
CA * * *
SEARCH
RES 1 17   25 36
END
Second restraint group, with a different restraint weight
1.0
FIND
CA * * *
SEARCH
RES 61 127
END
END
```

Output 7: CA atoms in residues 1-17 and 25-36 will be restrained to their initial positions with a strong weight of $10.0 \text{kcal} \cdot \text{mol}^{-1} \cdot \text{Å}^{-2}$; CA atoms in residues 61 to 127 will have a weaker restraint force constant.

6 Sampling configuration space

The "middle" scheme [Section **??**] offers an efficient approach to accurately sample configuration space in standard molecular dynamics simulations. There are many instances when standard molecular dynamics simulations get "stuck" near the starting configuration, and fail to adequately sample the available low-energy configurational space. This chapter describes a variety of techniques that can partially overcome such problems. The following chapter (on Free Energies) continues many of these ideas, adapting them to the calculation of alchemical or configurational free energy differences. There is no good distinction between these two chapters, because good sampling of the canonical distribution and estimation of free energies go hand-in-hand. But the present chapter covers methods that are *primarily* devoted to enhanced or accelerated sampling, whereas the following chapter considers methods that explicitly estimate free energy differences.

6.1 Self-Guided Langevin dynamics

Self-guided Langevin dynamics (SGLD) is designed to enhance conformational search efficiency in either a molecular dynamics (MD) simulation (when *gamma_ln=0*) or a Langevin dynamics (LD) simulation (when *gamma_ln>0*). This method accelerates low frequency motion to enhance conformational sampling. [126–130]

Overview: The input parameter, *tsgavg*, defines the lower limit period of the low frequency motion. Typically, *tsgavg*=0.2 ps is sutiable to define bond stretching and bending motions as high frequency motion and is recommended to enhance motions like phase separation, secondary structure folding, and ligand docking, while *tsgavg*=1.0 ps is suitable to include more local motions such as bond rotation and solvent relaxation and is recommended for protein domain motion, and protein-protein docking. The input parameter, *sgft* or *sgff*, defines the strength of the guiding effect. *sgft* between −1 and +1 sets the momentum guiding effect, with 0 for regular LD or MD simulations. A larger *sgft* will enhance low frequency motion to accelerate conformational search. *sgff* between −0.32 and +0.32 defines a force guiding factor to target energy barriers. A negative value will flatten energy barriers. Normally, *sgft* and *sgff* have opposite effects on conformational distribution and there exist balanced values to conserve the canonical ensemble. SGLD accelerates slow events to an affordable time scale while minimizing the perturbation to the conformational distribution. The guiding force can be applied to a part of a simulation system between atom *isgsta* and atom *isgend*.

The conformational distribution of SGLD can be reweighted to produce canonical ensemble averages[127, 130, 131]. The current implementation is mainly based on the most recent reformulation named the generallized self-guided molecular simulation method (SGMDg or SGLDg)[130]. The previous method[131, 132], SGLDfp is no longer available. As an alternative to Langevin dynamics (LD), self-guided Langevin dynamics via generalized Langevin equation (SGLD-GLE) [129] can exactly preserve canonical ensemble while avoiding the slow down by friction forces. SGLD-GLE method can be turned on by setting *sgfg* between −1 and +1. SGLD-GLE can be used with SGLDg by setting *sgft*, *sgff*, and *sgfg*.

isgld   SGLD algorithm index. Default *isgld*= 0, SGLD is diabled; *isgld*>0 will turn on SGLDg/SGMDg and/or SGLD-GLE method.

tsgavg   Local averaging time (*psec*) for the guiding force calculation. Default 0.2 *psec*. A larger value defines slower motion to be enhanced.

sgft   Momentum guiding factor. Defines the strength of the guiding effect. Default 0.0. Suggested value is 1.0 when *sgff=0*. Its value range is -1~1 with larger value leads to stronger low frequency motion. When *sgft* is set <-1 or >1, it is reset to the balanced value of *sgff* to preserve canonical ensemble.

sgff   Force guiding factor. *sgff* is used to scale down low frequency energy surface by a factor, (1+*sgff*). *sgff* is suggested to take values between -0.32 and 0.32, with default value of 0. Suggested value is -0.3 when *sgft=0*. When sgff is set <-1 or >1, it is reset to the balanced value of *sgft* to preserv canonical ensemble.

sgfg   momentum guiding factor for SGLD-GLE. Degault is 0. Its value range is -1~1 with larger value resulting in faster low frequency motion. Suggested value is 1 when *sgft=0 and sgff=0*.

isgsta   The first atom index of SGLD region. Default is 1.

isgend   The last atom index of SGLD region. Default is *natom*.

nsgsize   size of the bonded substructure for each atom used to calculate average guiding forces. 1 for no bonded structure is considered; 2 for all atoms connected through bonds or angles ; 3 for all atoms connected through bonds, angles, and dihedral angles. Default is 1.

The output of SGMD/SGLD simulations contains the following properties related to the enhancement in conformational search and reweighting of conformational distribution:
    METHOD: GAMM TEMPLF TEMPHF EPOTLF EPOTHF EPOTLLF SGWT

These quantities are instantaneous values defined as below:

    METHOD: SGLD when *gamma_ln>0* or SGMD when *gamma_ln=0*
    GAMM: Average atomic friction constant based on atom interactions.
    TEMPLF: low frequency temperature
    TEMPHF: high frequency temperature. Apparent temperature=TEMPLF+TEMPHF
    EPOTLF: low frequency potential energy
    EPOTHF: high frequency potential energy, EPOT=EPOTLF+EPOTHF
    EPOTLLF: Average of low frequency potential energy. It is needed for reweighting.
    SGWT: Weighting number. exp(SGWT) is the weighting factor of current frame.

The weight of a conformation is calculated by

```
Weight=exp(SGWT) =exp(((p(sgft)-sgff)*(EPOTLF-EPOTLLF)/(KBOLTZ*Temp))
where: sgft=(1+p(sgft))^2-1/(1+p(sgft))
```

or:

$$w_i = \exp\left(\frac{\lambda_{FP} - \lambda_F}{kT}(E_{LF} - E_{LLF})\right)$$

    where p(sgft) or λ_{FP} is called the balanced force guiding factor of λ_P. The relation between sgft, λ_P, and p(sgft), λ_{FP}, is: $\lambda_P = (1 + \lambda_{FP})^2 - \frac{1}{1+\lambda_{FP}}$. Similarly, λ_{PF} is called the balanced momentum guiding factor of λ_F, where $\lambda_{PF} = (1 + \lambda_F)^2 - \frac{1}{1+\lambda_F}$. When both λ_P and λ_F are used in a SGMDg/SGLDg simulation, it is recommanded that $-1 \leq \lambda_p - \lambda_{PF} \leq 1$.

For convenience, two scripts, *sgldinfo.sh* and *sgldwt.sh*, are provided in the AMBERHOME/bin directory to extract SGLD properties and weighting factors from sander output files. For example, one can run:

sgldinfo.sh mdout

to examine the SGLD properties, and run:

sgldwt.sh mdout

to print weighting factors at each print time frame, averages and reweighted averages of the SGMD/SGLD properties. Ensemble average properties can be calculated through reweighting:

$$< P >= \frac{\sum_{i=N_0}^{N} w_i P_i}{\sum_{i=N_0}^{N} w_i}$$

Below are example input files to run SGMD/SGLD simulations.

1. a SGLD simulation with sgft only:

```
Sample SGLD simulation for enhanced conformational search
&cntrl
nstlim=1000, cut=99.0, igb=1, saltcon=0.1,
ntpr=100, ntwr=100000, ntt=3, gamma_ln=10.0,
ntx=5, irest=1,
ntc=2, ntf=2, tol=0.000001,
dt=0.002, ntb=0, tempi=300., temp0=300.,
isgld=1,tsgavg=0.2,sgft=1.0,
/
```

2. a SGLD simulation using bonded substructure(nsgsize=2) to estimate low frequency motion, which reduces noises due to bond stretching and bending.

```
Sample SGLD simulation using bonded substructures
&cntrl
nstlim=1000, cut=99.0, igb=1, saltcon=0.1,
ntpr=100, ntwr=100000, ntt=3, gamma_ln=10.0,
ntx=5, irest=1,
ntc=2, ntf=2, tol=0.000001,
dt=0.002, ntb=0, tempi=300., temp0=300.,
isgld=1,tsgavg=0.2,sgft=1.0, nsgsize=2,
/
```

3. a SGLDg simulation using both *sgft* and *sgff* factors. When both guiding factors are used, it is recommand that $-1 \leq \lambda_p - (1+\lambda_F)^2 + \frac{1}{1+\lambda_F} \leq 1$.

```
Sample SGLDg simulation using both sgft and sgff
&cntrl
nstlim=1000, cut=99.0, igb=1, saltcon=0.1,
ntpr=100, ntwr=100000, ntt=3, gamma_ln=10.0,
ntx=5, irest=1,
ntc=2, ntf=2, tol=0.000001,
dt=0.002, ntb=0, tempi=300., temp0=300.,
isgld=1,tsgavg=0.2,sgft=0.5,sgff=-0.1,
/
```

4. a SGMDg simulation when gamma_ln=0:

```
Sample SGMDg simulation using both sgft and sgff
&cntrl
nstlim=1000, cut=99.0, igb=1, saltcon=0.1,
ntpr=100, ntwr=100000, ntt=1, tautp=1.0,
ntx=5, irest=1,
ntc=2, ntf=2, tol=0.000001,
dt=0.002, ntb=0, tempi=300., temp0=300.,
isgld=1,tsgavg=0.2,sgft=0.5,sgff=-0.1,
/
```

5. a SGLD-GLE simulation using sgfg to achieve enhanced conformational search while conserve canonical ensemble exactly:

```
Sample SGLD-GLE simulation to conserve canonical ensemble
```

```
&cntrl
nstlim=1000, cut=99.0, igb=1, saltcon=0.1,
ntpr=100, ntwr=100000, ntt=3, gamma_ln=10.0,
ntx=5, irest=1,
ntc=2, ntf=2, tol=0.000001,
dt=0.002, ntb=0, tempi=300., temp0=300.,
isgld=1,tsgavg=0.2,sgfg=1.0,
/
```

6.2 Targeted MD

The targeted MD option adds an additional term to the energy function based on the mass-weighted root mean square deviation of a set of atoms in the current structure compared to a reference structure. The reference structure is specified using the *-ref* flag in the same manner as is used for Cartesian coordinate restraints (NTR=1). Targeted MD can be used with or without positional restraints. If positional restraints are not applied (ntr=0), *sander* performs a best-fit of the reference structure to the simulation structure based on selection in *tgtfitmask* and calculates the RMSD for the atoms selected by *tgtrmsmask*. The two masks can be identical or different. This way, fitting to one part of the structure but calculating the RMSD (and thus restraint force) for another part of the structure is possible. If targeted MD is used in conjunction with positional restraints (ntr=1), only *tgtrmsmask* should be given in the control input because the molecule is 'fitted' implicitly by applying positional restraints to atoms specified in *restraintmask*.
The energy term has the form:

$$E = 0.5 * TGTMDFRC * NATTGTRMS * (RMSD-TGTRMSD)**2$$

The energy will be added to the RESTRAINT term. Note that the energy is weighted by the number of atoms that were specified in the *tgtrmsmask* (NATTGTRMS). The RMSD is the root mean square deviation and is mass weighted. The force constant is defined using the *tgtmdfrc* variable (see below). This option can be used with molecular dynamics or minimization. When targeted MD is used, *sander* will print the current values for the actual and target RMSD to the energy summary in the output file.

itgtmd   **= 0** no targeted MD (default)

          = 1 use targeted MD

          = 2 use targeted MD to multiple targets (Multiply-targeted MD, or MTMD, see next section below)

tgtrmsd   Value of the target RMSD. The default value is 0. This value can be changed during the simulation by using the weight change option.

tgtmdfrc This is the force constant for targeted MD. The default value is 0, which will result in no penalty for structure deviations regardless of the RMSD value. Note that this value can be negative, which would force the coordinates AWAY from the reference structure.

tgtfitmask Define the atoms that will be used for the rms superposition between the current structure and the reference structure. Syntax is in Chapter 5.1.1.

tgtrmsmask Define the atoms that will be used for the rms difference calculation (and hence the restraint force), as outlined above. Syntax is in Chapter 5.1.1.

One can imagine many uses for this option, but a few things should be kept in mind. In this implementation of targeted MD, there is currently only one reference coordinate set, so there is no way to force the coordinates to any specific structure other than the one reference. To move a structure toward a reference coordinate set, one might use an initial *tgtrmsd* value corresponding to the actual RMSD between the input and reference (*inpcrd* and *refc*). Then the weight change option could be used to decrease this value to 0 during the simulation. To move a structure

away from the reference, one can increase *tgtrmsd* to values larger than zero. The minimum for this energy term will then be at structures with an RMSD value that matches *tgtrmsd*. Keep in mind that many different structures may have similar RMSD values to the reference, and therefore one cannot be sure that increasing *tgtrmsd* to a given value will result in a particular structure that has that RMSD value. In this case it is probably wiser to use the final structure, rather than the initial structure, as the reference coordinate set, and decrease *tgtrmsd* during the simulation. To address this, multiply-targeted MD is now available in Amber (*sander only*), and is described in the next section. As an additional note, a negative force constant *tgtmdfrc* can be used, but this can cause problems since the energy will continue to decrease as the RMSD to the reference increases.

Also keep in mind that phase space for molecular systems can be quite complex, and this method does not guarantee that a low energy path between initial and target structures will be followed. It is possible for the simulation to become unstable if the restraint energies become too large if a low-energy path between a simulated structure and the reference is not accessible.

Note also that the input and reference coordinates are expected to match the *prmtop* file and have atoms in the same sequence. No provision is made for symmetry; rotation of a methyl group by 120° would result in a nonzero RMSD value.

6.3 Multiply-Targeted MD (MTMD)

In Amber (*sander only*), the user may perform targeted MD calculations using multiple reference structures. Each reference may have its own associated target RMSD value and force constant, each of which can evolve independently in time. Additionally, the masks for each defined target may differ, and targeting to any given reference structure can be activated for some or part of the simulation. The energy term for MTMD is simply the sum of the energies that would be calculated for the molecule calculated relative to each target given the target RMSD and force constant for that target. The energy will then be added to the RESTRAINT term.

To use MTMD, the MTMD input file is specified using the *-mtmd* flag in the command line arguments for *sander*. The MTMD input file will contain one instance of the tgt namelist ("&tgt") for each reference structure used. The user may specify any number of reference structures.

6.3.1 Variables in the &tgt namelist:

refin   The file name of the reference structure used. The input and reference coordinates are expected to match the *prmtop* file and have atoms in the same sequence. *Default for refin is ", no reference structure given.*

mtmdform   If MTMDFORM > 0, then the reference coordinate file is formatted. Otherwise, the reference coordinate file is an unformatted (binary) file. *Default for MTMDFORM is the value assigned to MTMDFORM in the most recent namelist where MTMDFORM was specified. If MTMDFORM has not been specified in any namelist, it defaults to 1.*

mtmdstep1, mtmdstep2 Targeted MD for this structure is run for steps/iterations MTMDSTEP1 through MTMDSTEP2. If MTMDSTEP2 = 0, then TMD will be run through the end of the run, and the values of the target RMSD and the force constant will not change with time. Note that the first step/iteration is considered step 0. *Defaults for MTMDSTEP1 and MTMDSTEP2 are the values assigned to them in the most recent namelist where MTMDSTEP1 and MTMDSTEP2 were specified. If MTMDSTEP1 and MTMDSTEP2 have not been specified in any namelist, they default to 0.*

mtmdvari   If MTMDVARI > 0, then the force constant and target RMSD will vary with step number. Otherwise, they are constant throughout the run. If MTMDVARI >0, then the values MTMDSTEP2, MTMDRMSD2, and MTMDFORCE2 must be specified (see below). *Default for* MTMDVARI *is the value assigned to* MTMDVARI *in the most recent namelist where* MTMDVARI *was specified. If* MTMDVARI *has not been specified in any namelist, it defaults to 0.*

mtmdrmsd, mtmdrmsd2 The target RMSD for this reference. If MTMDVARI >0, then the value of MTMDRMSD will vary between MTMDSTEP1 and MTMDSTEP2, so that, e.g. MTMDRMSD(MTMDSTEP1) = MTMDRMSD and MTMDRMSD(MTMDSTEP2) = MTMDRMSD2. *Defaults for MTMDRMSD and MTMDRMSD2 are the values assigned to them in the most recent namelist where MTMDRMSD and MTMDRMSD2 were specified. If MTMDRMSD and MTMDRMSD2 have not been specified in any namelist, they default to 0.0.*

mtmdforce, mtmdforce2 The force constant for this reference. If MTMDVARI >0, then the value of MTMDFORCE will vary between MTMDSTEP1 and MTMDSTEP2, so that, e.g. MTMDFORCE(MTMDSTEP1) = MTMDFORCE and MTMDFORCE(MTMDSTEP2) = MTMDFORCE2. *Defaults for* MTMDFORCE *and* MTMDFORCE2 *are the values assigned to them in the most recent namelist where* MTMDFORCE *and* MTMDFORCE2 *were specified. If* MTMDFORCE *and* MTMDFORCE2 *have not been specified in any namelist, they default to 0.0.*

mtmdninc If MTMDVARI >0 and MTMDNINC > 0, then the changes in the values of of MTMDRMSD and MTMDFORCE are applied as a step function, with NINC steps/iterations between each change in the target values. If MTMDNINC = 0, the change is effected continuously (at every step). *Default for MTMDNINC is the value assigned to MTMDNINC in the most recent namelist where MTMDNINC was specified. If MTMDNINC has not been specified in any namelist, it defaults to 0.*

mtmdmult If MTMDMULT=0, and the values of MTMDFORCE changes with step number, then the changes in the force constant will be linearly interpolated from MTMDFORCE→MTMDFORCE2 as the step number changes. If MTMDMULT=1 and the force constant is changing with step number, then the changes in the force constant will be effected by a series of multiplicative scalings, using a single factor, R, for all scalings. *i.e.*

MTMDFORCE2 = R**INCREMENTS * MTMDFORCE

INCREMENTS is the number of times the target value changes, which is determined by MTMDSTEP1, MTMDSTEP2, and MTMDNINC. *Default for MTMDMULT is the value assigned to MTMDMULT in the most recent namelist where MTMDMULT was specified. If MTMDMULT has not been specified in any namelist, it defaults to 0.*

mtmdmask Define the atoms that will be used for both the rms superposition between the current structure and the reference structure and the rms difference calculation (and hence the restraint force), as outlined above. Syntax is in Chapter 5.1.1.*Default for MTMDMASK is the value assigned to MTMDMASK in the most recent namelist where MTMDMASK was specified. If MTMDMASK has not been specified in any namelist, it defaults to '*', use all atoms in the fit and force calculations.* \

Namelist &tgt is read for each reference structure. Input ends when a namelist statement with refin = " (or refin not specified) is found. Note that comments can precede or follow any namelist statement, allowing comments and reference definitions to be freely mixed.

6.4 Low-MODe (LMOD) methods

István Kolossváry's LMOD methods for minimization, conformational searching, and flexible docking[133–136] are fully implemented in Amber. The centerpiece of LMOD is a conformational search algorithm based on eigenvector following of low frequency vibrational modes. It has been applied to a spectrum of computational chemistry domains including protein loop optimization and flexible active site docking.

In the Amber 2020 release, the LMOD optimization code has been updated with major improvements and new features including more accurate flexible docking, the option to visualize normal modes, utilization of random mixtures of low-frequency modes, and the option to work with a range of modes anywhere in the spectrum and not just the lowest frequency modes. The latter is particularly useful for docking where the modes relevant to

binding a ligand molecule are usually not the lowest frequency modes. The interface of the new LMOD has not changed, everything works exactly the same way as in Amber18 and earlier versions, a few parameters simply have additional options as documented below. The new features are demonstrated with production quality examples.

Details of the LMOD procedure, and hints on getting good performance, are given Section **??**, which should be consulted before trying the procedures in *sander*. The only difference between the *sander* and *NAB* implementations is the input specification; the same LMOD code is linked into both. The sections below give input details for *sander*.

There are **four "real-life" examples** of performing LMOD searches and in *lmod_vib_anim* **three examples** of updates in Amber20 including generating LMOD-vibration visualization. These are available at *https://ambermd.org/Manuals.php*. Each directory in the tar file has a README file with more information.

6.4.1 XMIN

The XMIN methods for minimization are traditional and manifold in the field of unconstrained optimization: PRCG is a Polak-Ribiere nonlinear Conjugate Gradient algorithm,[137] LBFGS is a Limited-memory Broyden-Fletcher-Goldfarb-Shanno quasi-Newton algorithm,[138] and TNCG is a Truncated Newton linear Conjugate Gradient method with optional LBFGS preconditioning.[139]

Some of the &cntrl namelist variables that control Amber's other minimization facilities also control XMIN. Consequently, non-experts can employ the default XMIN method merely by specifying ntmin = 3.

maxcyc   The maximum number of cycles of minimization. Default is 1 to be consistent with Amber's other minimization facilities although it may be unrealistically short.

ntmin   The flag for the method of minimization.

   = 3 The XMIN method is used.

   = 4 The LMOD method is used. The LMOD procedure employs XMIN for energy relaxation and minimization.

drms   The convergence criterion for the energy gradient: minimization will halt when the root-mean-square of the Cartesian elements of the gradient is less than this. Default is 10^{-4}kcal·mol^{-1}·Å^{-1}. This is consistent with Amber's other minimization facilities. In Amber18 and earlier this default may have been unrealistically strict. In Amber20 this criterion refers to the minimization of the input structure for which the normal modes are computed, and to avoid unnatural vibrational modes it should be set to even stricter values, e.g., 10^{-8}. Compare with input parameter lmod_minimize_grms below.

Other options that control XMIN are in the scope of the &lmod namelist. These parameters enable expert control of XMIN.

lbfgs_memory_depth The depth of the LBFGS memory for LBFGS minimization, or LBFGS preconditioning in TNCG minimization. Default is 3. Suggested alternate value is 5. The value 0 turns off LBFGS preconditioning in TNCG minimization.

matrix_vector_product_method The finite difference Hv matrix-vector product method: "forward" = forward difference, "central" = central difference. Default is forward difference.

xmin_method The minimization method: "PRCG" = Polak-Ribiere Conjugate Gradient, "LBFGS" = Limited-memory Broyden-Fletcher-Goldfarb-Shanno, and "TNCG" = Optionally LBFGS-preconditioned Truncated Newton Conjugate Gradient. Default is LBFGS.

xmin_verbosity The verbosity of the internal status output from the XMIN package: 0 = none, 1 = minimization details, and 2 = minimization and line search details plus CG details in TNCG. Currently, the XMIN status output may be disordered with respect to Amber's output. Default is 0, no output of the XMIN package internal status. Note that XMIN is also available in AmberTools, in the NAB package. An annotated example output corresponding to XMIN_VERBOSITY=2 can be found in the NAB documentation.

6.4.2 **LMOD**

Some of the options that control LMOD have the same names as Amber's other minimization facilities. See the XMIN section immediately above. Other options that control LMOD are in the scope of the &lmod namelist. These parameters enable expert control of LMOD.

arnoldi_dimension The dimension of the ARPACK Arnoldi factorization. Zero specifies the whole space, that is, three times the number of atoms. Default is 0, the whole space. Basically, the ARPACK package used for the eigenvector calculations solves multiple "small" eigenvalue problems instead of a single "large" problem, which is the diagonalization of the three times the number of atoms by three times the number of atoms Hessian matrix. This parameter is the user specified dimension of the "small" problem. The allowed range is total_low_modes + 1 <= arnoldi_dimension <= three times the number of atoms. The default means that the "small" problem and the "large" problem are identical. This is the preferred, i.e., fastest, calculation for small to medium size systems, because ARPACK is guaranteed to converge in a single iteration. The ARPACK calculation scales with three times the number of atoms times the arnoldi_dimension squared and, therefore, for larger molecules there is an optimal arnoldi_dimension much less than three times the number of atoms that converges much faster in multiple iterations (possibly thousands or tens of thousands of iterations). The key to good performance is to select an arnoldi_dimension such that all the ARPACK storage fits in memory. For proteins, arnoldi_dimension=1000 is generally a good value, but often a very small 50-100 Arnoldi dimension provides the fastest net computational cost with very many iterations.

conflib_filename The user-given filename of the LMOD conformational library. The file format is Amber standard formatted trajectory output regardless of the value of &cntrl namelist variable ioutfm. The conformations are stored in energetic order (global minimum energy structure first), the number of conformations<= conflib_size. The default filename is *conflib*.

conflib_size The number of conformations to store in conflib. Default is 3.

energy_window The energy window for conformation storage; the energy of a stored structure will be in the interval [global_min, global_min + energy_window]. Default is 0, only storage of the global minimum structure.

explored_low_modes The number of low frequency vibrational modes used per LMOD iteration. Default is 3.

frequency_eigenvector_recalc The frequency, measured in LMOD iterations, of the recalculation of eigenvectors. Default is 3.

frequency_ligand_rotrans The frequency, measured in LMOD iterations, of the application of rigid-body rotational and translational motions to the ligand(s). At each frequency_ligand_rotrans-th LMOD iteration number_ligand_rotrans rotations and translations are applied to the ligand(s). Default is 1, ligand(s) are rotated and translated at every LMOD iteration.

lmod_job_title The user-given title for the job that goes in the first line of the conflib and lmod_trajectory files. The default job title is "job_title_goes_here".

lmod_minimize_grms In Amber18 and earlier the gradient root-mean-square convergence criterion of structure minimization. In Amber 20 this was specified to be the criterion to minimize low-energy conformations; such conformations do not require as strict a convergence criterion as does the first minimization whose convergence is now controlled with input parameter drms, see above. Default is 0.1.

lmod_relax_grms The gradient RMS convergence criterion of structure relaxation. Default is 1.0.

lmod_restart_frequency The frequency, in LMOD iterations, of conflib updating and LMOD restarting with a randomly chosen structure from the pool. Default is 5.

lmod_step_size_max The maximum length of a single LMOD ZIG move. Default is 5.0 Å.

lmod_step_size_min The minimum length of a single LMOD ZIG move. Default is 2.0 Å.

lmod_trajectory_filename The filename of the LMOD pseudo trajectory. The file format is standard Amber trajectory file. The conformations in this file show the progress of the LMOD search. The number of conformations = number_lmod_iterations + 1. The default filename is *lmod_trajectory*.

lmod_verbosity The verbosity of the internal status output from the LMOD package: 0 = none, 1 = some details, 2 = more details, 3 = everything including ARPACK information, 4 = ARPACK only, 5 = visualize normal modes. Currently, the LMOD status output may be disordered with respect to Amber's output. Default is 0, no output of the LMOD package internal status. Note that LMOD is also available in AmberTools, in the NAB package. An annotated example output corresponding to LMOD_VERBOSITY=2 can be found in the NAB documentation.

monte_carlo_method The Monte Carlo method: "Metropolis" = Metropolis Monte Carlo, "Total_Quench" = the LMOD trajectory always proceeds towards the lowest lying neighbor of a particular energy well found after exhaustive search along all of the low modes, and "Quick_Quench" = the LMOD trajectory proceeds towards the first neighbor found, which is lower in energy than the current point on the path, without exploring the remaining modes. Default is Metropolis Monte Carlo.

number_free_rotrans_modes In Amber18 and earlier this was solely the number of rotational and translational degrees of freedom (dof) which is related to the number of frozen or tethered atoms in the system: 0 atoms dof=6, 1 atom dof=3, 2 atoms dof=1, >=3 atoms dof=0. In Amber20 the input domain was extended to any non-negative integer, and it represents the number of modes for LMOD to skip. In this way LMOD can now explore a range of modes instead of simply modes starting with the lowest frequency. Note that it is recommended to set this to 0 once in order to examine the ro-translational modes. Default is 6.

number_ligand_rotrans The number of rigid-body rotational and translational motions applied to the ligand(s). Such applications occur at each frequency_ligand_rotrans-th LMOD iteration. Default is 0, no rigid-body motions applied to the ligand(s).

number_ligands The number of ligands for flexible docking. Default is 0, no ligand(s).

number_lmod_iterations The number of LMOD iterations. Default is 10. Note that setting number_lmod_iterations = 0 will result in a single energy minimization.

number_lmod_moves The number of LMOD ZIG-ZAG moves. Zero means that the number of ZIG-ZAG moves is not pre-defined, instead LMOD will attempt to cross the barrier in as many ZIG-ZAG moves as it is necessary. The criterion of crossing an energy barrier is stated above in the "LMOD Procedure" background section. number_lmod_moves > 0 means that multiple barriers may be crossed and LMOD can carry the molecule to a large distance on the potential energy surface without severely distorting the geometry. Default is 0, LMOD will determine automatically where to stop the ZIG-ZAG sequence.

random_seed The seed of the random number generator. Default is 314159.

restart_pool_size The size of the pool of lowest-energy structures to be used for restarting. Default is 3.

rtemperature The value of RT in Amber energy units. This is utilized in the Metropolis criterion. Default is 1.5.

total_low_modes The total number of low frequency vibrational modes to be used. Default is the minimum of 10 and three times the number of atoms minus the number of rotational and translational degrees of freedom (number_free_rotrans_modes).

The following commands are part of the &lmod namelist. These commands control the way LMOD applies explicit translations and rotations to one or more ligands and take effect only if number_ligands >= 1. All commands are lists in square brackets, separated by commas such as [1, 33, 198], however, the list is read by Sander as a string and, therefore, it should be enclosed in single quotes.

ligstart_list, ligend_list The serial number(s) of the first/last atom(s) of the ligand(s). Type integer. The number(s) should correspond to the numbering in the Amber input files prmtop and inpcrd/restart. For example, if there is only one ligand and it starts at atom 193, the command should be ligstart_list = '[193]'. If there are three ligands, the command should be, e.g., '[193, 244, 1435]'. The same format holds for all of the following commands. Note that the ligand(s) can be anywhere in the atom list, however, a single ligand must have continuous numbering between the corresponding ligstart_list and ligend_list values. For example, ligstar_list = '[193, 244, 1435]' and ligend_list = '[217, 302, 1473]'.

ligcent_list The serial number(s) of the atom(s) of the ligand(s), which serves as the center of rotation. Type integer. The value zero means that the center of rotation will be the geometric center of gravity of the ligand.

rotmin_list, rotmax_list The range of random rotation of a particular ligand about the origin defined by the corresponding ligcent_list value is specified by the commands rotmin_list and rotmax_list. The angle is given in +/- degrees. Type float. For example, in case of a single ligand and ligcent_list = '[0]', rotmin_list = '[30.0]' and rotmax_list = '[180.0]' means that random rotations by an angle +/- 30-180 degrees about the center of gravity of the ligand, will be applied. Similarly, with number_ligands = 2, ligcent_list= 120.0]' means that the first ligand will be rotated like in the single ligand example in this paragraph, but a second ligand will be rotated about its atom number 201, by an angle +/- 60-120 degrees.

trmin_list, trmax_list The range of random translation(s) of ligand(s) is defined by the same way as rotation. For example, with number_ligand = 1, trmin_list = '[0.1]' and trmax_list = '[1.0]' means that a single ligand is translated in a random direction by a random distance between 0.1 and 1.0 Angstroms.

7 Free energies

7.1 Thermodynamic integration

In a free energy calculation, the system evolves according to a mixed potential (such as in Eqs. 7.3 or 7.4, below). The essence of free energy calculations is to record and analyze the fluctuations in the values of V_0 and V_1 (that is, what the energies *would have been* with the endpoint potentials) as the simulation progresses. For thermodynamic integration (which is a very straightforward form of analysis) the required averages can be computed "on-the-fly" (as the simulation progresses), and printed at the end of a run. For more complex analyses (such as the Bennett acceptance ratio scheme), one needs to write the history of the values of V_0 and V_1 to a file, and later post-process this file to obtain the final free energy estimates.

There is not room here to discuss the theory of free energy simulations, and there are many excellent discussions elsewhere.[140–142] There are also plenty of recent examples to consult.[143, 144] Such calculations are demanding, both in terms of computer time, and in a level of sophistication to avoid pitfalls that can lead to poor convergence. Since there is no one "best way" to estimate free energies, *sander* and *pmemd* primarily provide the tools to collect the statistics that are needed. Assembling these into a final answer, and assessing the accuracy and significance of the results, generally requires some calculations outside of what Amber provides, *per se*. The discussion here will assume a certain level of familiarity with the basis of free energy calculations.

Both *sander* and *pmemd* have the capability of doing simple thermodynamic free energy calculations, using either PME or generalized Born potentials. When *icfe* is set to 1, information useful for doing thermodynamic integration estimates of free energy changes will be computed. The implementation is different between *sander* and *pmemd*. For *sander*, you must use the *multisander* capability to create two groups, one corresponding to the starting state, and a second corresponding to the ending state (see Section 1.13 for information); you will need a *prmtop* file for each of these two endpoints. For *pmemd*, you use a single *prmtop* file which contains both the starting and ending states. For both *sander* and *pmemd* a mixing parameter λ is used to interpolate between the "unperturbed" and "perturbed" potential functions.

7.1.1 Thermodynamic integration using Sander

There are now two different ways to prepare a thermodynamic integration free energy calculation in Sander. The first is unchanged from previous versions of Amber: Here, the two prmtop files that you create must have the same number of atoms, and the atoms must appear *in the same order* in the two files. This is because there is only one set of coordinates that are propagated in the molecular dynamics algorithm. If there are more atoms in the initial state than in the final, "dummy" atoms must be introduced into the final state to make up the difference. Although there is quite a bit of flexibility in choosing the initial and final states, it is important in general that the system be able to morph "smoothly" from the initial to the final state. Alternatively, you can set up your system to use the softcore potential algorithm described below. This will remove the requirement to prepare "dummy" atoms and allows the two *prmtop* files to have different numbers of atoms.

The basics of the *multisander* functionality are given in Section 1.13, but the mechanics are really quite simple. You start a free energy calculation as follows:

```
mpirun -np 4 sander.MPI -ng 2 -groupfile <filename>
```

Since there are 4 total cpu's in this example, each of the two groups will run in parallel with 2 cpu's each. The number of processors must be a multiple of two. The *groups* file might look like this:

```
-O -i mdin -p prmtop.0 -c eq1.x -o md1.o -r md1.x -inf mdinfo
-O -i mdin -p prmtop.1 -c eq1.x -o md1b.o -r md1b.x -inf mdinfob
```

The input (*mdin*) and starting coordinate files must be the same for the two groups. Furthermore, the two *prmtop* files must have the same number number of atoms, in the same order (since one common set of coordinates will be used for both.) The simulation will use the masses found in the first *prmtop* file; in classical statistical mechanics, the Boltzmann distribution in coordinates is independent of the masses so this should not represent any real restriction.

On output, the two restart files should be identical, and the two output files should differ only in trivial ways such as timings; there should be no differences in any energy-related quantities, except if energy decomposition is turned on (*idecomp* > 0); then only the output file of the first group contains the per residue contributions to $\langle \partial V / \partial \lambda \rangle$. For our example, this means that one could delete the *md1b.o* and *md1b.x* files, since the information they contain is also in *md1.o* and *md1.x*. (It is a good practice, however, to check these file identities, to make sure that nothing has gone wrong.)

7.1.2 Basic inputs for thermodynamic integration

icfe   The basic flag for free energy calculations. The default value of 0 skips such calculations. Setting this flag to 1 turns them on, using the mixing rules in Eq. 7.3, below.

clambda   The value of λ for this run, as in Eqs. 7.3 and 7.4, below. Zero corresponds to the unperturbed Hamiltonian V_0. $\lambda=1$ corresponds to the perturbed Hamiltonian V_1.

klambda   The exponent in Eq. 7.4, below.

tishake   Flag that determines how SHAKE is handled:

   = 0 Coordinates are synchronized after SHAKE, no constraints removed (default).

   = 1 SHAKE is removed between bonds containing one common and one unique atom. This was the default in previous versions of *sander*. Note that disabling SHAKE requires the use of a 1 fs timestep.

7.1.2.1 Input flags specific to Sander

idecomp   Flag that turns on/off decomposition of $\langle \partial V / \partial \lambda \rangle$ on a per-residue level. The default value of 0 turns off energy decomposition. A value of 1 turns the decomposition on, and 1-4 nonbonded energies are added to internal energies (bond, angle, torsional). A value of 2 turns the decomposition on, and 1-4 nonbonded energies are added to EEL and VDW energies, respectively. The frequency by which values of $\langle \partial V / \partial \lambda \rangle$ are included into the decomposition is determined by the NTPR flag. This ensures that the sum of all contributions equals the average of all total $\langle \partial V / \partial \lambda \rangle$ values output every NTPR steps. All residues, including solvent molecules, have to be chosen by the RRES card to be considered for decomposition. The RES card determines which residue information is finally output. The output comes at the end of the *mdout* file. For each residue contributions of internal -, VdW-, and electrostatic energies to $\langle \partial V / \partial \lambda \rangle$ are given as an average over all (NSTLIM/NTPR) steps. In a first section total per residue values are output followed below by further decomposed values from backbone and sidechain atoms.

7.1.3 Background theory of thermodynamic integration

The *sander and pmemd* programs do not compute free energies; it is up to the user to combine the output of several runs (at different values of λ) and to numerically estimate the integral:

$$\Delta A = A(\lambda = 1) - A(\lambda = 0) = \int_0^1 \langle \partial V / \partial \lambda \rangle_\lambda \, d\lambda \tag{7.1}$$

If you understand how free energies work, this should not be at all difficult. However, since the actual values of λ that are needed, and the exact method of numerical integration, depend upon the problem and upon the precision desired, we have not tried to pre-code these into the program.

The simplest numerical integration is to evaluate the integrand at the midpoint:

$$\Delta A \simeq \langle \partial V / \partial \lambda \rangle_{1/2}$$

This might be a good first thing to do to get some picture of what is going on, but is only expected to be accurate for very smooth or small changes, such as changing just the charges on some atoms. Gaussian quadrature formulas of higher order are generally more useful:

$$\Delta A = \sum_i w_i \langle \partial V / \partial \lambda \rangle_i \tag{7.2}$$

Some weights and quadrature points are given in the accompanying table; other formulas are possible,[145] but the Gaussian ones listed there are probably the most useful. The formulas are always symmetrical about $\lambda = 0.5$, so that λ and $(1 - \lambda)$ both have the same weight. For example, if you wanted to use 5-point quadrature, you would need to run five jobs, setting λ to 0.04691, 0.23076, 0.5, 0.76923, and 0.95308 in turn. (Each value of λ should have an equilibration period as well as a sampling period; this can be achieved by setting the *ntave* parameter.) You would then multiply the values of $\langle \partial V / \partial \lambda \rangle_i$ by the weights listed in the Table, and compute the sum.

When *icfe=1* and *klambda* has its default value of 1, the simulation uses the mixed potential function:

$$V(\lambda) = (1 - \lambda) V_0 + \lambda V_1 \tag{7.3}$$

where V_0 is the potential with the original Hamiltonian, and V_1 is the potential with the perturbed Hamiltonian. The program also computes and prints $\langle \partial V / \partial \lambda \rangle$ and its averages; note that in this case, $\langle \partial V / \partial \lambda \rangle = V_1 - V_0$. This is referred to as linear mixing, and is often what you want unless you are making atoms appear or disappear. If some of the perturbed atoms are "dummy" atoms (with no van der Waals terms, so that you are making these atoms "disappear" in the perturbed state), the integrand in Eq. 7.1 diverges at $\lambda = 1$; this is a mild enough divergence that the overall integral remains finite, but it still requires special numerical integration techniques to obtain a good estimate of the integral.[141] *Sander and pmemd* implement one simple way of handling this problem: if you set *klambda* > 1, the mixing rules are

$$V(\lambda) = (1 - \lambda)^k V_0 + [1 - (1 - \lambda)^k] V_1 \tag{7.4}$$

where k is given by *klambda*. Note that this reduces to Eq. 7.3 when $k = 1$, which is the default. If $k \geq 4$, the integrand remains finite as $\lambda \to 1$.[141] We have found that setting $k = 6$ with disappearing groups as large as tryptophan works, but using the softcore option (*ifsc*>0) instead is generally preferred.[146] Note that the behavior of $\langle \partial V / \partial \lambda \rangle$ as a function of λ is not monotonic when *klambda* > 1. You may need a fairly fine quadrature to get converged results for the integral, and you may want to sample more carefully in regions where $\langle \partial V / \partial \lambda \rangle$ is changing rapidly.

Notes:

1. This is implemented in *sander* by calling the force() routine independently for each *multisander* group and then combining the forces on each step. For a fixed number of processors this increases the cost of the calculation compared with the *pmemd* code, which only calculates the differences between V_0 and V_1.

2. It is rather easy to make mistakes when running TI calculations. It is generally good to carry out a short run (say 50 steps) setting ntpr=1. Then check the following; if either test fails, be sure to fix the problem before proceeding.

   a) The restart files from V_0 and V_1 should be identical for *sander* (for *pmemd* there will only be a single restart file).

   b) If you diff the output files for *sander*, there should only be simple differences (for *pmemd* there will only be a single combined output file). All energies, temperatures, pressures, etc. should be the same in the two files. Simulations with *sander* using the QM/MM facility may show differences in the SCF energies, but be sure that the total energies, and all the MM components, are the same.

3. Eq. 7.4 is designed for having dummy atoms in the perturbed Hamiltonian, and "real" atoms in the regular Hamiltonian. You must ensure that this is the case when you set up the system in LEaP. (See the softcore

section, below, for a more general way to handle disappearing atoms, which does not require dummy atoms at all.)

4. One common application of this model is to pKa calculations, where the charges are mutated from the protonated to the deprotonated form. Since H atoms bonded to oxygen already have zero van der Waals radii (in the Amber force fields and in TIP3P water), once their charge is removed (in the deprotonated form) they are really then like dummy atoms. For this special situation, there is no need to use *klambda* > 1: since the van der Waals terms are missing from both the perturbed and unperturbed states, the proton's position can never lead to the large contributions to $\langle \partial V / \partial \lambda \rangle$ that can occur when one is changing from a zero van der Waals term to a finite one.

5. The implementation requires that the masses of all atoms be the same on all threads. To enforce this, the masses found for V_0 are used for V_1 as well. In classical statistical mechanics, the canonical distribution of configurations (and hence of potential energies) is unaffected by changes in the masses, so this should not pose a limitation. Since the masses for V_1 are ignored, they do not have to match those found for V_0.

6. Special care needs to be taken when using SHAKE for atoms whose force field parameters differ in the two end points. The same bonds must be SHAKEN in both cases, and the equilibrium bond lengths must also be the same. By default, the coordinates from V_0 are synchronized with those from V_1 after SHAKE. This will work for small perturbations, but if there is a significant change in bond length, it may be necessary to use the *noshakemask* input to remove SHAKE from the regions that are being perturbed. If this is done, be sure to set *tishake*=1 and to use a 1 fs timestep. Special care needs to be taken when water molecules are part of the region that is changing. You need to make sure that the "number of 3-point waters" is the same in both V_0 and V_1. This may require setting *jfastw* and/or building the structure so that *sander or pmemd* do not think that the water molecules involved are actually rigid waters. Also, just setting *noshakemask* might not be enough, since this flag does not affect the *settle* routine that handles rigid waters.

n	λ_i	$1 - \lambda_i$	w_i
1	0.5		1.0
2	0.21132	0.78867	0.5
3	0.1127	0.88729	0.27777
	0.5		0.44444
5	0.04691	0.95308	0.11846
	0.23076	0.76923	0.23931
	0.5		0.28444
7	0.02544	0.97455	0.06474
	0.12923	0.87076	0.13985
	0.29707	0.70292	0.19091
	0.5		0.20897
9	0.01592	0.98408	0.04064
	0.08198	0.91802	0.09032
	0.19331	0.80669	0.13031
	0.33787	0.66213	0.15617
	0.5		0.16512
12	0.00922	0.99078	0.02359
	0.04794	0.95206	0.05347
	0.11505	0.88495	0.08004
	0.20634	0.79366	0.10158
	0.31608	0.68392	0.11675
	0.43738	0.56262	0.12457

Table 7.1: *Abscissas and weights for Gaussian integration.*

7.1.4 Softcore Potentials in Thermodynamic Integration

Softcore potentials provide an additional way to perform thermodynamic integration calculations in Amber. The system setup has been simplified so that appearing and disappearing atoms can be present at the same time and no dummy atoms need to be introduced. For *sander*, two prmtop files, corresponding to the start and end states (V_0 and V_1) of the desired transformation need to be used. The common atoms that are present in both states need to appear in the same order in both prmtop files and must have identical starting positions. In addition to the common atoms, each process can have any number of unique soft core atoms, as specified by scmask. For *pmemd*, a single prmtop file is used, containing the unique atoms for both the start and end states. The soft core atoms are specified by scmask1 and scmask2 for V_0 and V_1 respectively.

A modified version of the vdW equation is used to smoothly switch off non-bonded interactions of these atoms with their common atom neighbors:

$$V_{V_0, disappearing} = 4\varepsilon(1-\lambda) \left[\frac{1}{\left[\alpha\lambda + \left(\frac{r_{ij}}{\sigma}\right)^6\right]^2} - \frac{1}{\alpha\lambda + \left(\frac{r_{ij}}{\sigma}\right)^6} \right] \tag{7.5}$$

$$V_{V_1, appearing} = 4\varepsilon\lambda \left[\frac{1}{\left[\alpha(1-\lambda) + \left(\frac{r_{ij}}{\sigma}\right)^6\right]^2} - \frac{1}{\alpha(1-\lambda) + \left(\frac{r_{ij}}{\sigma}\right)^6} \right] \tag{7.6}$$

Please refer to Ref [146] for a description of the implementation and performance testing when compared to the TI methods described above using *sander*. For similar information pertaining to pmemd please see Ref [147]. Note that the term "disappearing" is used here, but it would probably be better to say that atoms present in V_0 but not in V_1 are "decoupled" from their environment: the interactions among the "disappearing" atoms are not changed, and do not contribute to $\langle \partial V / \partial \lambda \rangle$. If the disappearing atoms are a separate molecule (say a non-covalently-bound ligand), this can be viewed as a transfer to the gas-phase.

Note that a slightly different setup is required for using soft core potentials compared to older TI-implementations. Specifically, the difference is that to add or remove atoms without soft core potentials, they are transformed into interactionless dummy particles, so both end state prmtop files have the same number of atoms. When using soft core potentials instead, no dummy atoms are needed and the end states should be built without them. Therefore prmtop files for non soft core simulations may have to be adapted to be used with soft core potentials and vice versa.

All bonded interactions of the unique atoms are recorded separately in the output file (see below). Any bond, angle, dihedral or 1-4 term that involves at least one appearing or disappearing atom is not scaled by λ and does not contribute to $\langle \partial V / \partial \lambda \rangle$. Therefore, output from both processes will not be identical when soft core potentials are used. Softcore transformations avoid the origin singularity effect and therefore linear mixing can (and should) always be used with them. Since the unique atoms become decoupled from their surroundings at high or low lambdas and energy exchange between them and surrounding solvent becomes inefficient, a Berendsen type thermostat should not be used for SC calculations. Unlike in previous versions, SHAKE constraints are not automatically removed from bonds between common and unique atoms. Instead, the coordinates corresponding to common atoms in $V_0$are synchronized with those of V_1. The original behavior can be restored using *tishake*. The icfe and klambda parameters should be set to 1 for a soft core run and the desired lambda value will be specified by clambda. When using softcore potentials with *sander*, λ values should be picked so that 0.01 < clambda < 0.99. The *pmemd* implementation allows lambda to be set to any value between 0.0 and 1.0, thus simulations at the endpoints are possible.

Additionally, the following parameters are available to control the TI calculation:

ifsc   Flag for soft core potentials

> **= 0** SC potentials are not used (default)

> **= 1** SC potentials are used. Be sure to use prmtop files that are suitable for this, i.e. not-containing dummy atoms (see above)

scalpha   The α parameter in 7.5 and 7.6, its default value is 0.5. Other values have not been extensively tested

logdvdl   If set to .ne. 0, a summary of all $\partial V/\partial \lambda$ values calculated during every step of the run will be printed out at the end of the simulation for postprocessing.

dvdl_norest   This option is now deprecated. Restraints involving soft core atoms are now decoupled from the rest of the system. The energy is listed separately and does not contribute to $\partial V/\partial \lambda$.

dynlmb   If set to a value .gt. zero, clambda is increased by dynlmb every ntave steps. This can be used to perform simulations with dynamically changing lambdas.

crgmask   Specifies a number of atoms (in ambmask format) that will have their atomic partial charges set to zero. This is mainly for convenience because it removes the need to build additional prmtop files with uncharged atoms for TI calculations involving the removal of partial charges.

7.1.4.1 Input flags specific to Sander

scmask   Specifies the unique (soft core) atoms for this process in ambmask format. This, along with crgmask, is the only parameter that will frequently be different in the two mdin files for V_0 and V_1. It is valid to set scmask to an empty string. A summary of the atoms in scmask is printed at the end of mdout.

7.1.4.2 One step transformations using soft core electrostatics

Alternatively to the two-step process of removing charges from atoms first and then changing the vdW parameters of chargeless atoms in a second TI calculation, *sander and pmemd* also have a soft core version of the Coulomb equation implemented for single step transformations under periodic boundary conditions. This is automatically applied to all atoms in scmask and their interactions with common atoms are given by:

$$V_{V_0,disappearing} = (1-\lambda)\frac{q_i q_j}{4\pi\varepsilon_o\sqrt{\beta\lambda + r_{ij}^2}} \tag{7.7}$$

for disappearing atoms. Replace λ by $(1-\lambda)$ and vice versa for the form for appearing atoms. This introduces a new parameter β which controls the 'softness' of the potential. This is set in the input file via:

scbeta   The parameter β in 7.7. Default value is 12A^2, other values have not been extensively tested.

With the use of soft core vdW and electrostatics interactions, arbitrary changes between systems are possible in single TI calculations. However, due to the unusual potential function forms introduced, it is not always clear that a single-step calculation will converge faster than one broken down into several steps. Ref. [148] contains detailed information on the performance of such single step TI calculations.

7.1.5 Collecting potential energy differences for FEP calculations

In addition to the Thermodynamic Integration capabilities described above, *sander* can also collect potential energy values during free energy simulation runs for postprocessing by e.g. the Bennett acceptance ratio scheme. This will make sander calculate at given points during the simulation the total potential energy of the system as it would be for different λ-values at this conformation. This functionality is controlled by:

ifmbar   If set to 1 (Default = 0), additional output is generated for later postprocessing.

mbar_states number of lambda windows considered.

mbar_lambda lambda windows simulated.

For   example, if you want to run mbar with 15 lambda windows at 0.00, 0.05, 0.10, 0.15, 0.20, 0.30, 0.40, 0.50, 0.60, 0.70, 0.80, 0.85, 0.90, 0.95, 1.00, you would use the following options:

```
ifmbar = 1,
mbar_states = 15,
mbar_lambda = 0.00, 0.05, 0.10, 0.15, 0.20, 0.30, 0.40, 0.50, 0.60, 0.70, 0.80, 0.85, 0.90, 0.95,
```

The   options below have been deprecated. They are here for anyone using AMBER 16 or older, but will not work in AMBER 18.

bar_intervall Compute potential energies every bar_intervall steps (Default = 100)

bar_l_min Minimum λ-value (Default = 0.1)

bar_l_max Maximum λ-value (Default = 0.9)

bar_l_incr The increment to increase λ by between the minimum and maximum (Default = 0.1)

Such energy collection will normally be part of a regular free energy calculation (using icfe=1 and ifsc=1) involving simulations at various λ-values. Activating this functionality will not have any influence on the simulation trajectory which will evolve according to the preset *clambda* value, it is merely a bookkeeping scheme that removes the necessity of postprocessing output files later.

7.2 Linear Interaction Energies

sander contains rudimentary facilities to compute binding free energies using the linear interaction energy model.

ilrt   if set to 1, turns on the computation of LIE contributions (default=0)

lrt_interval Computer LIE contributions every lrt_interval MD steps (default=50)

lrtmask   The 'solute'. Interaction Energies between the atoms in lrtmask and the remainder of the system are computed.

The LIE facilities work by computing the system energies several times using different charge and vdW-parameter sets. This results in reduced performance if lrt_interval is set to less than approx. 10. The LIE output at the end of the *mdout* file gives the electrostatic interaction energy between the solute and rest of the system *times 0.5*, i.e. in accordance with the original formulation of LIE theory. The solute SASA and vdW-interaction energy with its surroundings is calculated unscaled.

7.3 Adaptively Biased MD, Steered MD, Umbrella Sampling with REMD and String Method

7.3.1 Overview

The following describes a suite of modules useful for the calculation of the free energy associated with a reaction coordinate $\sigma(\mathbf{r}_1, \ldots, \mathbf{r}_N)$ (which is defined as a smooth function of the atomic positions $\mathbf{r}_1, \ldots, \mathbf{r}_N$):

$$f(\xi) = -k_B T \ln \left\langle \delta \left[\xi - \sigma(\mathbf{r}_1, \ldots, \mathbf{r}_N) \right] \right\rangle,$$

(the angular brackets denote an ensemble average, k_B is the Boltzmann constant and T is the temperature) that is also frequently referred to as the *potential of mean force*.

Specifically, new frameworks are provided for equilibrium umbrella sampling and steered molecular dynamics that enhance the functionality delivered by earlier implementations (described earlier in this manual), along with a new Adaptively Biased Molecular Dynamics (ABMD) method [149] that belongs to the general category of umbrella sampling methods with a time-dependent potential. Such methods were first introduced by Huber, Torda and van

Gunsteren (the Local Elevation Method [150]) in the molecular dynamics (MD) context, and by Wang and Landau in the context of Monte Carlo simulations [151]. More recent approaches include the metadynamics method [152, 153]. All these methods estimate the free energy of a reaction coordinate from an evolving ensemble of realizations, and use that estimate to bias the system dynamics to flatten an effective free energy surface. Collectively, these methods may all be considered to be umbrella sampling methods with an evolving potential. The algorithms discussed here were developed by the group of Prof. Celeste Sagui (sagui@ncsu.edu) and Prof. Christopher Roland (cmroland@ncsu.edu); the current version was implemented by Dr. Volodymyr Babin.

The ABMD method grew out of attempts to speed up and streamline the metadynamics method for free energy calculations with a *controllable* accuracy. It is characterized by a favorable scaling in time, and only a few (two) control parameters. It is formulated in terms of the following equations:

$$m_a \frac{\mathrm{d}^2 \mathbf{r}_a}{\mathrm{d}t^2} = \mathbf{F}_a + \frac{\partial}{\partial \mathbf{r}_a} U\big[t | \sigma(\mathbf{r}_1, \dots, \mathbf{r}_N)\big],$$

$$\frac{\partial U(t|\xi)}{\partial t} = \frac{k_B T}{\tau_F} G\big[\xi - \sigma(\mathbf{r}_1, \dots, \mathbf{r}_N)\big],$$

where the first equation represents Newton's law that governs ordinary MD (temperature and pressure regulation terms are not shown) augmented with an additional force coming from the time dependent biasing potential $U(t|\xi)$ [$U(t=0|\xi)=0$], whose time evolution is given by the second equation. $G(\xi)$ is a positive definite and symmetric kernel, which may be thought of as a smoothed Dirac delta function. For large enough τ_F (the flooding timescale) and small kernel width, the biasing potential $U(t|\xi)$ converges towards $-f(\xi)$ as $t \to \infty$.

Our numerical implementation of the ABMD method involves the use of a bi-weight kernel along with the use of cubic B-splines (or products thereof) to discretize the biasing potential $U(t|\xi)$ w.r.t. ξ, and an Euler-like scheme for time integration. ABMD admits two important extensions, which lead to a more uniform flattening of $U(t|\xi) + f(\xi)$ due to an improved sampling of the "evolving" canonical distribution. The first extension is identical in spirit to the *multiple walkers metadynamics* [154, 155]. It amounts to carrying out several different MD simulations biased by the same $U(t|\xi)$, which evolves via:

$$\frac{\partial U(t|\xi)}{\partial t} = \frac{k_B T}{\tau_F} \sum_\alpha G\big[\xi - \sigma(\mathbf{r}_1^\alpha, \dots, \mathbf{r}_N^\alpha)\big],$$

where α labels different MD trajectories. A second extension is to gather several different MD trajectories, each bearing its own biasing potential and, if desired, its own distinct collective variable, into a generalized ensemble for "replica exchange" with modified "exchange" rules [156–158]. Both extensions are advantageous and lead to a more uniform flattening of $U(t|\xi) + f(\xi)$.

In order to assess and improve the accuracy of the free energies, the ABMD accumulations may need to be followed up with equilibrium umbrella sampling runs, which make use of the biasing potential $U(t|\xi)$ as is. Such a procedure is very much in the spirit of adaptive umbrella sampling. With these runs, one calculates the biased probability density:

$$p^B(\xi) = \big\langle \delta[\xi - \sigma(\mathbf{r}_1, \dots, \mathbf{r}_N)] \big\rangle_B.$$

The idea here is that if, as a result of an ABMD run, $f(\xi) + U(t|\xi) = 0$ exactly, then the biased probability density $p^B(\xi)$ would be flat (constant). In practice, this is typically not the case, but one can use $p^B(\xi)$ to "correct" the free energy via:

$$f(\xi) = -U(\xi) - k_B T \ln p^B(\xi).$$

With the ABMD procedure, one can obtain accurate free energy curves and equilibrium properties. We note that to obtain ABMD free energies requires a (minor) amount of post-processing by means of the nfe-umbrella-slice utility freely available in AmberTools as described in Subsection 7.3.7. This methodology has been applied to a variety of biomolecular systems, including small peptides [149, 159, 160], sugar puckering [161], polyproline systems [162–164], guest-host systems [165, 166], polyglutamine systems [167, 168], and DNA systems [169–173]. In addition, SMD simulations (discussed below) have been used to examine transition pathways and mechanisms, to estimate free energy differences [163, 174], and to calculate transition rates [175–177].

While the above represents the basic ABMD implementation, AMBER20 introduced three additional algorithms

– the Well-Tempered (WT) ABMD, a selection mechanism for multiple walker ABMD and Driven ABMD (D-ABMD)[178] – all of which enhance the stability and convergence of an ABMD simulation. Also implemented is the Swarms-of-Trajectories String Method (STSM) [179], which gives a way of exploring the Minimum Free Energy Path (MFEP) on free energy lansdscape. Current version of these codes were inplemented by Dr. Mahmoud Moradi (moradi@uark.edu), Dr. Feng Pan (fpan3@ncsu.edu) and Ashkan Fakharzadeh (afakhar@ncsu.edu).

The Well-Tempered ABMD: An alternative to the follow-up equilibrium simulations for increased ABMD accuracy is provided by the WT-ABMD, which is implemented in the spirit of the WT-metadynamics [180]. In the original ABMD implementation, the history dependent biasing potential is built up at a fixed rate:

$$U(\xi,t) = U^0(\xi) + \int_0^t dt' \, \omega \, G(\xi - \xi^{t'}),$$

(7.8)

in which $U(\xi,t)$ is the biasing potential at time t, U^0 is an arbitrary function that typically represents the initial guess for the biasing potential (in the absence of a guess, this is assumed to be flat) and $\omega = k_B T / \tau_F$ is a constant, unbiased rate. As the simulation proceeds and reaches convergence, then $\langle U(\xi, t \to \infty) \rangle_a \approx U^s(\xi) + u(t)$, in which $\langle . \rangle_a$ is the ensemble-average over the adaptive trajectories, the stationary term is $U^s \approx -F(\xi)$, and $u(t)$ is an additive time-dependent constant [180]. Unfortunately, updating the biasing potential at the same rate throughout the simulation may lead to a poorly converged result, since the biasing potential ends up fluctuating around $-F(\xi)$ with an amplitude that depends on ω.

One way to resolve this problem is to update the kernel at a non-uniform rate by means of a "well-tempered" ω:

$$U(\xi,t) = U^0(\xi) + \int_0^t dt' \, \omega(\xi^{t'},t') \, G(\xi - \xi^{t'}),$$

(7.9)

in which $\omega(\xi,t)$ is a time-dependent, non-uniform rate chosen to be $\omega_0 e^{-\beta' U(\xi,t)}$ ($1/\beta' = k_B T'$ where T' is a pseudo-temperature) that reduces to a constant ω_0 in the $\beta' \to 0$ limit (*i.e.*, resulting in conventional ABMD). With this choice, one can show that $\langle U(\xi, t \to \infty) \rangle_a \approx U^s(\xi) + u(t)$, ($u(t)$ is an additive constant) in which $U^s(\xi)$ and $F(\xi)$ are related via $U^s(\xi) = -(1 + \frac{\beta'}{\beta})^{-1} F(\xi)$ or $F(\xi) = -(1 + \frac{T}{T'}) U^s(\xi)$. This way of updating the biasing potential leads to a considerably smoother convergence to the desired free energy and more stable ABMD simulations.

Multiple walker selection algorithm: The ABMD multiple walker algorithm can be improved by allowing for periodic interactions between the different walkers and "resampling" on-the-fly. The rationale behind this is that not all walkers are equally effective in sampling the configuration space. A situation that is all too common is that different walkers end up being "bunched up" or clustered together in some local metastable region, because of hidden barriers that are oriented along orthogonal degrees of freedom to the reaction coordinate. To improve this situation, one would like to facilitate walkers that are sampling the undersampled regions of phase space, and force the walkers in the oversampled regions to move away and explore regions not yet covered. Such an algorithm has previously been implemented via scripts in the NAMD code for the adaptive biasing force algorithm [181].

A resampling or selection algorithms for interacting multiple walkers requires a continual monitoring of the walkers by means of a periodic evaluation of a fitness function and a resampling of the walkers according to their fitness efficiency[181]. Efficient walkers that are wandering in the undersampled regions are enhanced by being cloned, while inefficient walkers found in the oversampled regions of phase space are correspondingly killed. This procedure is then repeated periodically during the simulation, thereby accelerating convergence to a more uniform distribution of walkers and flattening of the free energy landscape.

Our specific interacting/resampling/selection multiple-walker algorithm is implemented as follows. Each walker n is assigned a weight w_n, which is evaluated at the end of each resampling period of time τ. At the ith resampling period, i.e., from time $t_{(i-1)} = (i-1)\tau$ to $t_i = i\tau$, walker n moves through configuration space building up its own trajectory $(r_1^n, \ldots, r_N^n)$. The weights are then tested and updated every fixed time interval of length τ. Specifically, after the ith time interval, weights are estimated by:

$$w_n = K^{-1} \exp\left(\int_{t_{i-1}}^{t_i} S(\xi_n^t) dt \right),$$

where ξ_n^t represents the collective variable evaluated at time t for trajectory n, $K = \sum_{n=1}^{N_w} w_n$ is the normalization factor, and

$$S(\xi) = C\nabla^2(\rho(\xi))/\rho(\xi),$$

with $\rho(\xi)$ representing the density of microstates in the collective variable space and C a constant. The quantity $S(\xi)$ will be positive typically if the walker is found in the undersampled regions, which have a convex density function. Similarly, a negative $S(\xi)$ value indicates that the system is in the concave region of the density function, which typically is oversampled. In the context of ABMD implementation, the biasing potential is approximately proportional to the histogram of the collective variable by construction, and represents a good estimate for ρ. The implementation is therefore straightforward; the integral above is estimated for each trajectory independently by summing over $S(\xi_n^t)$ at every step from $t = t_{i-1}$ to $t = t_i$, in which Δt is the MD *timestep*. At the end of each period the walkers send their unnormalized weight estimates to the "master processor" to normalize them. A stochastic resampling method is then used to clone/kill the replicas based on their weight factors [181]. The number of copies present in the next period for walker n is determined by the integer number:

$$
\begin{aligned}
W_1 &= \lfloor \eta_1 + N_w w_1 \rfloor, \\
W_n &= \lfloor \eta_n + N_w \sum_{m=1}^{n} w_m \rfloor - \lfloor \eta_n + N_w \sum_{m=1}^{n-1} w_m \rfloor, \quad \text{for } n > 1.
\end{aligned}
$$

in which $0 < \eta_n < 1$ is drawn from a uniform distribution (using a random number generator). The atomic coordinates and velocities of the walkers with $N_n > 0$ are "sent" to N_n walkers. The resampling algorithm above guarantees $\sum_n W_n = N_w$.

In terms of an ABMD simulation, the selection algorithm is most beneficial during the initial and middle parts of the simulation when there are large variations in the biasing potential. In the latter parts, when the effective free energy is almost flat, the distribution of walkers should be roughly uniform. In that case, the selection mechanism is unnecessary and, if one wishes to continue the simulation, it is best to proceed with the non interacting multiple walker algorithm. It has been found that a convenient stopping mechanism may be based on the entropy of the weights. Defining $H = \sum_n w_n log(w_n)$, the selection mechanism will be stopped if $E_w = H - log(1/N_w)$ goes below $-\varepsilon log(1/N_w)$. Here, $log(1/N_w)$ represents the entropy of uniform weights, and the stopping parameter ε varies between $0 \le \varepsilon \le 1$. When $\varepsilon = 0$, the algorithm never stops, while $\varepsilon = 1$ forces a stop irrespective of the values of the weights.

In addition to ε, there are also two other user-defined variables in the selection algorithm, including the constant C and the interval time τ. While the physical interpretation of τ is straightforward, C represents a pseudo diffusion constant. One may think of the selection algorithm as an induced diffusion in the reaction coordinate space; The larger the value of C, the faster the system will diffuse along the reaction coordinate space. Therefore C determines the strength or aggressiveness of the resampling algorithm. The most efficient value for C is dependent on the nature of the collective variable and the shape of its density ρ. Since the best choice of C for a given problem is somewhat of an art, we refer the interested reader to the ABMD tutorials on the AMBER webpage for insight into choosing this variable. Finally, we also note that the multiple walker selection mechanism can be invoked as is or in conjunction with the WT-ABMD for enhanced stability and convergence.

Driven ABMD: ABMD and SMD schemes are both powerful nonequilibrium sampling methods; however, each comes with its own practical limitations. For instance, SMD is often associated with a very slow convergence if used for free energy calculations. However it can be used to explore the transition paths, at least qualitatively; an advantage over ABMD, in which the system starting from one end of the configuration space (the reactant) may take a long time to visit the other end (the product). SMD and ABMD schemes, however can be integrated into a novel driven adaptive-bias 3 scheme, termed driven ABMD (D-ABMD) that takes advantage of both its driven and adaptive-bias components and is advantageous over both components in isolation. D-ABMD has an advantage over conventional (or well-tempered) ABMD in that it ensures the exploration of the transition pathway (from one end to the other) in the early stages of the simulation and gradually improves the estimate of the free energies almost uniformly along the reaction coordinate. D-ABMD has also an advantage over the conventional SMD in that the effective free energy surface gradually becomes smooth and flat such that the system can move along the reaction coordinate with progressively less amount of work. The D-ABMD method is similar to D-MetaD method,

```
&colvar
   cv_type = STRING
   cv_ni = N, cv_nr = M
   cv_i = i1, i2, ..., iN
   cv_r = r1, r2, ..., rM
/
```

Figure 7.1: *Syntax of reaction coordinate definition:* `cv_type` *is a* `STRING`, `cv_i` *is a list of integer numbers and* `cv_r` *is a list of real numbers.*

which was recently introduced in Ref.[178] as an example of driven, adaptive-bias schemes.

In order to combine the two schemes described above, we have developed a driven adaptive-bias scheme that adds an adaptive $U_a(\xi, t)$ and a driving $U_d(\xi, t)$ potential to the Hamiltonian. We use an iterative approach in which an independent simulation is performed from time t = 0 to t = T in the nth iteration (n = 1, 2, . . .), biased by the potential $U_d(\xi, t) + U_a^n(\xi, t)$ in which $U_d(\xi, t) = \frac{k}{2}(\xi - \eta(t))^2$ for all n ($\eta(t)$ is moving center of the SMD harmonic potential in the ξ space), and:

$$U_a^n(\xi, t) = U^{n-1}(\xi) + \int_0^t dt' \omega(\xi^{t'}, t') K(\xi - \xi^{t'}) e^{-\beta \omega^{t'}}$$

in which ω^t is either defined as the accumulated work or the transferred work. The accumulated and transferred works are defined as $\omega_{ac}^t = \int_0^t dt' \frac{\partial}{\partial t'} U_d(\xi^{t'}, t')$ and $\omega_{tr}^t = \omega_{ac}^t - U_d(\xi^t, t)$. Theoretically the $e^{-\beta \omega_{tr}^{t'}}$ factor or "constant weight" is more accurate but for practical reasons the $e^{-\beta \omega_{ac}^{t'}}$ factor or "pulling wight" is preferred. Particularly, in our algorithm, the constant weight $e^{-\beta \omega_{tr}^{t'}} = e^{-\beta \omega_{ac}^{t'}} e^{\beta U_d(\xi^{t'}, t')}$ may become instable for large biasing potentials. To avoid the instability in either case a cutoff for ω^t is used (i.e., the algorithm will not be applied if ω^t is smaller than the cutoff). At the moment, Driven ABMD is only applicable to one-dimensional reaction coordinate.

If any of these modules prove to be useful, please consider quoting the following papers: V. Babin, C. Roland and C. Sagui, *"Adaptively biased molecular dynamics for free energy calculations"*, J. Chem. Phys. **128**, 134101 (2008); V. Babin, V. Karpusenka, M. Moradi, C. Roland and C. Sagui, *"Adaptively biased molecular dynamics: an umbrella sampling method with a time-dependent potential"*, Int. J. Quant. Chem. **109**, 3666 (2009).

From Amber16, we implement these modules from SANDER to PMEMD and the modules are GPU compatible. To keep the consistency in format, we do a series of changes and updates to the usage of these modules. One big change is that you must set *infe* = 1 in &cntrl to activate these modules. Also, the input format has been changed to namelist style and reaction coordinate variables will be read from separate files. For the details, please read Subsection **??**

`infe` This variable controls the usage of the non-equilibrium free energy method. When *infe=0*, the ABMD and related methods are turned off; when *infe=1*, they are turned on and the blocks &smd, &pmd, &abmd, &bbmd and &stsm will be recognized. The default value is 0. Note that use of these algorithms may require a (minor) amount of post-processing by means of the nfe-umbrella-slice utility freely available in AmberTools described in Subsection 7.3.7.

7.3.2 Reaction Coordinates

A reaction coordinate is defined in the `colvar` namelist in a separate file. (see Fig. 7.1). This section must contain a `cv_type` keyword along with a value of type `STRING` and a list of integers `cv_i` (the number of integers is defined by `cv_ni`). For some types of reaction coordinates the `colvar` section must also contain a list of real numbers, `cv_r`, whose length is defined by `cv_nr`.

The following reaction coordinates (specfied by `cv_type`) are currently implemented:

DISTANCE: distance (in Å) between two atoms whose indexes are read from the list `cv_i`.

COM_DISTANCE: distance between the center of mass of two atom groups. The `cv_i` list is interpreted as a list of indexes of participating atoms. Zeros separate the groups, the last zero is optional. eg: `cv_i = a1,...,aN,0,b1,...,bM,0`.

DF_COM_DISTANCE: difference of distances between the center of mass of first two atom groups and second two atom groups. The `cv_i` list is interpreted as a list of indexes of participating atoms. Zeros separate the groups, the last zero is optional. eg: `cv_i = a1,...,aN,0,b1,...bM,0,c1,...cL,0,d1,...,dK,0`, `DF_COM_DISTANCE` is `COM_DISTANCE(a1,...,aN,0,b1,...,bM)` − `COM_DISTANCE(c1,...cL,0,d1,...,dK)`.

LCOD: linear combination of distances (in Å) between pairs of atoms listed in `cv_i` with the coefficients read from `cv_r` list. For example, `i = 1,2,3,4` and `r = 1.0,-1.0` define the difference between 1-2 and 3-4 distances, *i.e.* LCOD = r1*distance(1, 2) + r2*distance(3,4).

ANGLE: angle (in radians) between the lines joining atoms with indexes `i1` and `i2` and atoms with indexes `i2` and `i3`.

COM_ANGLE: angle (in radians) formed by the center of mass of three atom groups. The `cv_i` list is interpreted as a list of indexes of participating atoms. Zeros separate the groups, the last zero is optional. eg: `cv_i = a1,...,aN,0,b1,...bM,0,c1,...,cK,0`.

TORSION: dihedral angle (in radians) formed by atoms with indexes `i1`, `i2`, `i3` and `i4`.

COM_TORSION: dihedral angle (in radians) formed by the center of mass of four atom groups. The `cv_i` list is interpreted as a list of indexes of participating atoms. Zeros separate the groups, the last zero is optional. eg: `cv_i = a1,...,aN,0,b1,...bM,0,c1,...,CK,0,d1,...,dL,0`.

COS_OF_DIHEDRAL: sum of cosines of dihedral angles formed by atoms with indexes in the list `cv_i`. The number of atoms must be a multiple of four.

SIN_OF_DIHEDRAL: sum of sines of dihedral angles formed by atoms with indexes in the list `cv_i`. The number of atoms must be a multiple of four.

PAIR_DIHEDRAL: sum of cosines of a list of angles each formed by summing two neighboring dihedral angles from a list formed by atoms with indices `cv_i`. The number of atoms must be a multiple of four. For a list of dihedral angles such as $\{\alpha_1, \ldots, \alpha_N\}$, PAIR_DIHEDRAL is $\sum_{i=1}^{N-1} cos(\alpha_i + \alpha_{i+1})$ which ranges between $-N+1$ and $N-1$.

PATTERN_DIHEDRAL: a particular pattern-recognizing function defined on a list of dihedral angles formed by atoms with indices `cv_i`. The number of atoms must be a multiple of four. The definition is particularly relevant for the dihedral angles with a binary-like behavior of being either around 0 or 180 (e.g., ω backbone dihedral angle). For a list of dihedral angles such as $\{\alpha_1, \ldots, \alpha_N\}$, PATTERN_DIHEDRAL is $\sum_{i=1}^{N} cos^2(\alpha_i/2)2^{i-1}$ which ranges between 0 and $2^N - 1$.

R_OF_GYRATION: radius of gyration (in Å) of atoms with indexes given in the `cv_i` list (mass weighted).

MULTI_RMSD: RMS (in Å, mass weighted) of RMSDs of several groups of atoms w.r.t. reference positions provided in the `cv_r` list. The `cv_i` list is interpreted as a list of indexes of participating atoms. Zeros separate the groups. An atom may enter several groups simultaneously. The `cv_r` array is expected to contain the reference positions (without zero sentinels). The implementation uses the method (and the code) introduced in Ref. [182]. An example of variable of this type is presented in Fig. 7.2. Two groups are defined here: one comprises the atoms with indexes 1, 2, 3, 4 (line 3 in Fig. 7.2, numbers prior to the first zero) and another one of atoms with indexes 3, 4, 5. The code will first compute the (mass weighted) RMSD (R_1) of atoms belonging to the first group w.r.t. reference coordinates provided in the `cv_r` array (first $12 = 4 \times 3$ real numbers of it; lines 4, 5, 6, 7 in Fig. 7.2). Next, the (mass weighted) RMSD (R_2) of atoms of the second

```
&colvar
   cv_type = 'MULTI_RMSD'
   cv_ni = 9, cv_nr = 21,
   cv_i = 1, 2, 3, 4, 0, 3, 4, 5, 0 ! the last zero is optional
   cv_r = 1.0, 1.0, 1.0, ! group #1, atom 1
        2.0, 2.0, 2.0, ! group #1, atom 2
        3.0, 3.0, 3.0, ! group #1, atom 3
        4.0, 4.0, 4.0, ! group #1, atom 4
       23.0, 23.0, 23.0, ! group #2, atom 3
          4.0, 4.0, 4.0, ! group #2, atom 4
          5.0, 5.0, 5.0 ! group #2, atom 5
/
```

Figure 7.2: *An example of* `MULTI_RMSD` *variable definition.*

group w.r.t. the corresponding reference coordinates (last $9 = 3 \times 3$ elements of the `cv_r` array in Fig. 7.2) will be computed. Finally, the code will compute the value of the variable as follows:

$$\text{value} = \sqrt{\frac{M_1}{M_1 + M_2} R_1^2 + \frac{M_2}{M_1 + M_2} R_2^2},$$

where M_1 and M_2 are the total masses of atoms in the corresponding groups.

N_OF_BONDS:

$$\text{value} = \sum_p \frac{1 - \left(r_p \big/ r_0\right)^6}{1 - \left(r_p \big/ r_0\right)^{12}},$$

where the sum runs over pairs of atoms p, r_p denotes distance between the atoms of pair p and r_0 is a parameter measured in Å. The `cv_r` array must contain exactly one element that is interpreted as r_0. The `cv_i` array is expected to contain pairs of indexes of participating atoms. For example, if 1 and 2 are the indexes of Oxygen atoms and 3, 4, 5 are the indexes of Hydrogen atoms and one intents to count all possible O-H bonds, the `cv_i` list must be (1, 3, 1, 4, 1, 5, 2, 3, 2, 4, 2, 5), that is, it must explicitly list all the pairs to be counted.

HANDEDNESS:

$$\text{value} = \sum_a \frac{\mathbf{u}_{a,3} \cdot [\mathbf{u}_{a,1} \times \mathbf{u}_{a,2}]}{|\mathbf{u}_{a,1}| \, |\mathbf{u}_{a,2}| \, |\mathbf{u}_{a,3}|},$$

where

$$\mathbf{u}_{a,1} = \mathbf{r}_{a+1} - \mathbf{r}_a$$
$$\mathbf{u}_{a,2} = \mathbf{r}_{a+3} - \mathbf{r}_{a+2}$$
$$\mathbf{u}_{a,3} = (1-w)(\mathbf{r}_{a+2} - \mathbf{r}_{a+1}) + w(\mathbf{r}_{a+3} - \mathbf{r}_a),$$

and $\mathbf{r}_a$ denote the positions of participating atoms. The `cv_i` array is supposed to contain indexes of the atoms and the `cv_r` array may provide the value of w ($0 \leq w \leq 1$, the default is zero).

N_OF_STRUCTURES:

$$\text{value} = \sum_g \frac{1 - \left(R_g \big/ R_{0,g}\right)^6}{1 - \left(R_g \big/ R_{0,g}\right)^{12}},$$

where the sum runs over groups of atoms, R_g denotes the `RMSD` of the group g w.r.t. some reference coordinates and $R_{0,g}$ are positive parameters measured in Å. The `cv_i` array is expected to contain indexes of

```
&colvar
   cv_type = 'N_OF_STRUCTURES'
   cv_ni = 9, cv_nr = 23,
   cv_i = 1, 2, 3, 4, 0, 3, 4, 5, 0 ! the last zero is optional
   cv_r = 1.0, 1.0, 1.0, ! group #1, atom 1
        2.0, 2.0, 2.0, ! group #1, atom 2
        3.0, 3.0, 3.0, ! group #1, atom 3
        4.0, 4.0, 4.0, ! group #1, atom 4
        1.0,           ! R0 for group #1
     23.0, 23.0, 23.0, ! group #2, atom 3
        4.0, 4.0, 4.0, ! group #2, atom 4
        5.0, 5.0, 5.0, ! group #2, atom 5
        2.0            ! R0 for group #2
/
```

Figure 7.3: *An example of* `N_OF_STRUCTURES` *variable.*

participating atoms with zeros separating different groups. The elements of the `cv_r` array are interpreted as the reference coordinates of the first group followed by their corresponding R_0; then followed by the reference coordinates of the atoms of the second group, followed by the second R_0, and so forth. To make the presentation clearer, let us consider the example presented in Fig. 7.3. The atomic groups and reference coordinates are the same as the ones shown in Fig. 7.2. Lines 7 and 11 in Fig. 7.3 contain additional entries that set the values of the threshold distances $R_{0,1}$ and $R_{0,2}$. To compute the variable, the code first computes the mass weighted `RMSD` values R_1 and R_2 for both groups –much like in the `MULTI_RMSD` case– and then combines those in a manner similar to that used in the `N_OF_BONDS` variable.

$$\text{value} = \frac{1 - \left(R_1 \middle/ R_{0,1}\right)^6}{1 - \left(R_1 \middle/ R_{0,1}\right)^{12}} + \frac{1 - \left(R_2 \middle/ R_{0,2}\right)^6}{1 - \left(R_2 \middle/ R_{0,2}\right)^{12}}.$$

In other words, the variable "counts" the number of structures that match (stay close in `RMSD` sense) with the reference structures.

QUATERNIONS: Describing large-scale atomistic conformational changes in biomolecular systems requires one to deal with orientational changes of atomistic domains with large numbers of atoms. While there are several ways of defining a collective variable that quantifies an orientation based conformational change, the orientation quaternion technique[183–186] has proven successful as a well-behaved, flexible method for defining system-specific CVs, specifically aimed at inducing interdomain orientational changes or restraining the orientation of certain domains. The CVs in the orientation quaternion class, are all derived from an 'optimal rotation' between a set of reference coordinates $\mathbf{X}_k$ ($1 \leq k \leq N$; where N is the number of atoms involved) and the set of target coordinates $\mathbf{Y}_k$. A 'quaternion' is introduced as a four-component vector that can be expressed as $q_0 + q_1\hat{i} + q_2\hat{j} + q_3\hat{k}$ where q_0 and $q_1\hat{i} + q_2\hat{j} + q_3\hat{k}$ are called scalar and vector parts respectively. The optimal rotation can be parametrized[1] by a unit quaternion, $\hat{q} = (q_0, q_1, q_2, q_3)$, that minimize $< ||\hat{q}\mathbf{X}_k\hat{q}^* - \mathbf{Y}_k||^2 >$ in which $< . >$ denotes an average over k,q^* is the conjugate of q and $||q||^2 = q^*q$ (see Ref.[183] for more details). The optimal rotation unit quaternion (or orientation quaternion)$\hat{q}$ can be written as $\left(cos(\theta/2), sin(\theta/2)\hat{u}\right)$, where θ is the optimal rotation angle and $\hat{u}$ is a unit vector associated with the optimal axis of rotation. To deal with large atomistic conformational changes, a set of quaternion-based CVs has implemented in AMBER20. For the details of usage, send emails to Ashkan Fakharzadeh (afakhar@ncsu.edu), Dr. Feng Pan (fpan3@ncsu.edu), and Prof. Mahmoud Moradi (moradi@uark.edu). The specific quaternion-based CVs implemented are: ORIENTATION_ANGLE, ORIENTATION_PROJ, TILT, SPINANGLE, QUATERNION0, QUATERNION1, QUATERNION2, and QUATERNION3.

---

[1]Assuming both sets have been already shifted to bring their barycenters to the origin (optimum translation).

```
&colvar
   cv_type = 'QUATERNION0'

   ! number of participating atoms
   cv_ni = ni

   ! index of participating atoms
   cv_i = a1, a2,..., aN

   ! AMBER coordinate/restart file to read reference coordinates
   refcrd_file = 'refcrd_file'

   ! number of references which must be 3*ni; Should not be set if
   ! refcrd_file is being used
   cv_nr = nr

   ! reference coordinates of participating atoms; Should not be set if
   ! refcrd_file is being used
   cv_r = a1x, a1y, a1z, a2x, a2y, a2z, a3x, a3y, a3z, ...

   ! an arbitrary integer between 1 to 100
   q_index = n
/
```

Figure 7.4: *Syntax of Quaternion reaction coordinates.*

Orientation (QUATERNION0,...,QUATERNION3): These define the orientation of several atoms with respect to a set of reference coordinates in terms of a unit quaternion vector $\hat{q} = (q_0, q_1, q_2, q_3)$ according to the method introduced in Ref.[183, 184]. These variables return the best-fit rotation, also used in best-fit RMSD calculation procedures, to superimpose the coordinates $\mathbf{X}$ onto a set of reference coordinates $\mathbf{X}_0$. The unit quaternion $\hat{q} = (q_0, q_1, q_2, q_3)$ can be written as $\left(cos(\theta/2), sin(\theta/2)\hat{u}\right)$, where θ is the rotation angle and $\hat{u}$ is a unit vector associated with the axis of rotation; for example, a rotation of $90°$ around the z axis $(0,0,1)$ is expressed as $(cos(90°/2), 0.0, 0.0, sin(90°/2)) = (\sqrt{2}/2, 0, 0, \sqrt{2}/2)$. The components of the unit quaternion (q_0, q_1, q_2, q_3) were implemented separately as QUATERNION0, QUATERNION1, QUATERNION2, and QUATERNION3 CVs. To find the orientation, all four CVs QUATERNION0,...,QUATERNION3 are being used. To calculate the quaternion CVs one needs to specify a list of participating atoms and also their reference coordinates. The reference coordinates may be passed to AMBER either via direct specification inside the CV call, or by passing the name of a reference coordinates file. It is recommended that if the set of participating atoms is small (say no larger than 15), then these are specified directly inside the CV call. Otherwise, the passing of information via filename is recommended since these lists may contain hundreds if not thousands of atoms. Relevant parameters pertaining to the input of this information are: *cv_ni* represents the number of participating atoms; *cv_i* represents the list of the indices of all participating atoms; *cv_r* represents the reference coordinates (when passed directly) and *refcrd_file* is the filename for the reference coordinates when they are to be read from file. The file *refcrd_file* should be an AMBER coordinates/restart file containing coordinates, velocities, etc. of all atoms. The list participating atoms, *cv_i*, and their reference coordinates (*cv_r* and or *refcrd_file*) must be the same for all QUATERNION0,...,QUATERNION3. The CVs are linked together using an attribute *'q_index'*. The *'q_index'* accepts an integer between $1,...,100$, where its default value is one. The Fig. 7.4 is an example of Quaternion CVs syntax. An example this type of CVs is presented in the Fig. 7.5. Two set of orientations are defined here: each set consists of QUATERNION0,.., QUATERNION3. The first set comprises 18 atoms with indexes $11, 41, 48, 74, 104, ...$ and another one of 24 atoms with indexes $12, 16, 46, 55, 75, ...$. A file, 'inpcrd' is used as an AMBER coordinate/restart file to read reference coordinates. There is no need to set *'q_index'* for the first four quaternions since the default value is one, but it is set to be 2 for all quaternion CVs in the second set

to link and normalize them. The returned value of each QUATERNION0,...,QUATERNION3 CVs is the corresponding component of the unit orientation vector $\hat{q} = (q_0, q_1, q_2, q_3)$.

ORIENTATION_ANGLE: The angle of rotation $\theta = 2cos^{-1}(q_0)$ between the current and the reference positions. This angle is between $0°$ to $180°$. The cv_i list is interpreted as a list of indexes of participating atoms.

$$\text{orientation angle: } \theta = 2cos^{-1}(q_0)$$

ORIENTATION_PROJ: The cosine of the angle of rotation θ between the current and the reference positions. While ORIENTATION_ANGLE diverges near $\theta = 0$, because of $\nabla_X \theta$, ORIENTATION_PROJ might be used instead to apply forces. The range of ORIENTATION_PROJ is $[-1, 1]$. The cv_i array is supposed to contain indexes of the atoms.

$$\text{orientation proj: } 2q_0^2 - 1$$

SPINANGLE: Angle of rotation ϕ around a given unit axis $\hat{\mathbf{e}}$. The axis $\hat{\mathbf{e}}$ is being used to decompose a complete orientation rotation in two sub-rotations, spin ϕ and tilt ω. An advantage of this decomposition is ϕ and ω have the same values, regardless of which one is applied first (in comparison to Euler angles methods). The participating atoms with indexes are given in the cv_i. The *'axis'* must provide three components of the axis[2]$\hat{\mathbf{e}}$ in $A°$. The default axis of rotation is $(0.0, 0.0, 1.0)$. The range of SPINANGLE is between$[-180 : 180]$ degrees. The reference coordinates are specified either via cv_r or *refcrd_file*.

$$\text{spin angle: } \phi = 2tan^{-1}(\mathbf{q}.\mathbf{e}/q_0)$$

where $\mathbf{q}$ is the vector part of quaternion, namely (q_1, q_2, q_3). An example of SPINANGLE cv is presented in Fig. 7.6. The same atoms as example one are used, but the axis of rotation is set to be 'x-axis'. The reference coordinates are given by cv_nr, cv_r options.

TILT: Cosine of the rotation orthogonal to an unit given axis. The tilt angle ω, shows a rotation away from the direction $\hat{\mathbf{e}}$. The tilt combined with the 'spin' sub-rotation provides the complete orientation rotation of a group of atoms. Similar to ORIENTATION_PROJ, to avoid the discontinuity around $0°$ and $180°$, the cosine of the tilt is implemented instead of the tilt angle itself, so that derivatives are continuous almost everywhere. The cv_i and *'axis'* are the participating atoms with indexes and the given axis, respectively. The reference coordinates are specified either via cv_r or *refcrd_file*. The value of TILT is between -1 to 1, where the value 1 represents an orientation fully parallel to $\hat{\mathbf{e}}$ ($\omega = 0°$), and the value -1 represents an anti-parallel orientation.

$$\text{tilt: } t = cos(\omega) = 2\Big(\frac{q_0}{cos(\frac{tan^{-1}\mathbf{q}.\mathbf{e}}{q_0})}\Big)^2 - 1$$

7.3.3 Steered Molecular Dynamics

The `&smd` namelist, if present in the `MDIN` file, activates the steered `MD` code (the method itself is extensively described in the literature: see for example Ref. [187] and references therein). The prefix NFE appears in several switches to do with steered MD: this stands for "Non-equilibrium Free Energy".

The following is recognized within the `&smd` namelist:

`output_file` sets the output file name. Default is 'nfe-smd.txt'.

`output_freq` sets the output frequency (in `MD` steps). Default is 50.

`cv_file` sets the collective variable file name. Default is 'nfe-smd-cv'.

There must be at least one reaction coordinate defined (that is, there must be at least one `&colvar` namelist in the cv_file). The steered `MD` code requires that additional entries be present in the `&colvar` namelist:

---

[2]The axis is from the origin$(0.0, 0.0, 0.0)$ to that point.

path   the steering path whose elements must be real numbers. The `path` must include at least two elements. The upper limit on the number of entries is 20000. The elements define Catmull-Rom spline used for steering.

npath   sets the number of elements in `path`. Default is 0.

path_mode The way steering paths are constructed. There are two modes available. In `SPLINE` mode (default) the path is approximated by a spline that passes through the given points; in `LINES` mode the path is represented by the line segments joining the control points.

harm   specifies the harmonic constant. If a single number is provided, e.g., `harm = 10.0`, then it is constant throughout the run. If two or more numbers are provided, e.g., `harm = 10.0, 20.0`, then the harmonic constant follows a Catmull-Rom spline built upon the provided values.

nharm   sets the number of elements in `harm`. Default is 0.

harm_mode The way harmonical paths are constructed, similar with `path_mode`.

An example of `MDIN` file and `CV.IN` file for steered `MD` is shown in Fig. 7.7. The reaction coordinate is defined in `cv.in`. The spring constant is set constant throughout the run and the steering path is configured from 5.0 to 3.0. The values of the reaction coordinate, harmonic constant and the work performed on the system are requested to be dumped to the `smd.txt` file every 50 MD steps.

7.3.4 Umbrella sampling

To activate the umbrella sampling code, the `&pmd` namlist must be present in the `MDIN` file. `&pmd` is currently available to both SANDER and PMEMD, and also can be fully applied in GPU accelerated PMEMD. The `output_file`, `output_freq` and `cv_file` entries are recognized just as in the steered `MD` case presented earlier. The `cv_file` must contain at least one `&colvar` namelist section. For umbrella sampling, the `&colvar` section(s) must contain two additional entries:

anchor_position: this consists of four real numbers $(r1, r2, r3, r4)$ that determine the rectangle of the umbrella (harmonic) potential. The default value is that all of the $r's$ is set to zero.

anchor_strength: two non-negative real numbers $(k1, k2)$ that set the harmonic constant for the umbrella (harmonic) potential. The default value is zero.

The umbrella (harmonic) potential U is determined by (supposing R is the value of reaction coordinate)

- $U = k1 * (r1 - r2) * R \quad (R \leqslant r1)$

- $U = 0.5 * k1 * (R - r2)^2 \quad (r1 < R \leqslant r2)$

- $U = 0 \qquad\qquad (r2 < R \leqslant r3)$

- $U = 0.5 * k2 * (R - r3)^2 \quad (r3 < R \leqslant r4)$

- $U = k2 * (r4 - r3) * R \quad (R > r4)$

A plot of the umbrella potential is shown below
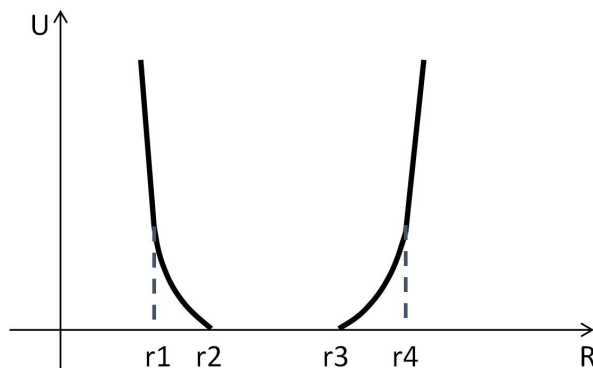
eg1: if $r2 = r3$, $r1 \ll r2$ and $r4 \gg r3$, then the generated U is simply the traditional harmonic potential.

eg2: if $r1$ is slightly less than $r2$ and $r4$ is slightly larger than $r3$, also with very large $k1$, $k2$, the reaction coordinate is restrained in the range $(r2, r3)$ with no potential added.

An example of an `MDIN` file and `CV.IN` file for an umbrella sampling simulation is shown in Fig. 7.8. The first reaction coordinate here is the angle formed by the lines joining the 5th with 9th and 9th with 15th atoms. It is to be harmonically restrained near 1.0 *rad* (`anchor_position` entry) using the spring of strength 10.0 $kcal/mol/rad^2$ (`anchor_strength` entry). The second reaction coordinate requested in Fig. 7.8 is a dihedral angle (`type = 'TORSION'`) formed by the 1st, 2nd, 3rd and 4th atoms (the `cv_i` array). It is to be restrained near zero with strength 23.8 $kcal/mol/rad^2$. The values of the reaction coordinate(s) are to be dumped every 50 MD steps to the `pmd.txt` file. Another example of restraining reaction coordinate in a specific range is shown in Fig. 7.9. The reaction coordinates here are φ and ψ angles of dialanine. φ is restrained between -2.0 *rad* and 2.0 *rad*, ψ is restrained between -1.8 *rad* and 1.8 *rad*.

The `NFE` implementation of umbrella sampling works correctly with the Amber standard replica-exchange MD described earlier in this manual (compatible with different types of REMD for different values of -rem flag in both SANDER and PMEMD). For example, the typical umbrella sampling with Hamiltonian Replica Exchange can be performed by setting -rem to 3. In this case, both `anchor_position` and `anchor_strength` may be different for different temperatures. Even the number and type of reaction coordinate(s) could vary for different replicas. The output files (set by the `output_file` keyword on a per-replica basis) are `MDIN`-bound, consistent with -rem.

7.3.5 Adaptively Biased Molecular Dynamics

The implementation has a very simple and intuitive interface: the code is activated if either an `&abmd` (both SANDER and PMEMD) or an `&bbmd` (both SANDER and PMEMD) namelist is present in the `MDIN` file (the difference between those "flavors" is purely technical and will become clear later). Unlike in the `&smd` and `&pmd` cases, the dimensionality of a reaction coordinate (the number of `&colvar` namelists in the `cv_file`) cannot exceed five (though three is already hardly useful due to statistical reasons).

As previously noted, in order to activate the ABMD and related algorithm, the variable ***infe*** in &cntrl must be set to unity (*i.e.* ***infe* = 1**; default value ***infe* = 0**).

In addition to the `cv_file` entry, the following entries are recognized within the `&abmd` (or `&bbmd`) namelist:

mode sets the execution mode. There are three modes available: `'ANALYSIS'` | `'UMBRELLA'` | `'FLOODING'`. In `ANALYSIS` mode the dynamics is not altered. The only effect of this mode is that the value(s) of the reaction coordinate(s) is(are) dumped every `monitor_freq` to `monitor_file`. In `UMBRELLA` mode, biasing potential from the `umbrella_file` is used to bias the simulation ($\tau_F = \infty$, biasing potential does not change). In `FLOODING` mode the adaptive biasing is enabled.

monitor_file sets the name of the file to which value(s) of reaction coordinate(s) (along with the magnitude of biasing potential in `FLOODING` mode) are dumped.

monitor_freq the frequency of the output to the monitor_file.

timescale τ_F, the flooding timescale in picoseconds (only required in FLOODING mode).

umbrella_file biasing potential file name (the file must exist for the UMBRELLA mode).

In FLOODING mode, the following two entries are optional:

snapshots_basename sets the name of the file to which the biasing potential is dumped during the simulation for snapshot.

snapshots_freq the frequency of dumping snapshot biasing potential (in MD steps). If snapshots_freq is not specified, the snapshot biasing potential will not be dumped.

and the &colvar namelist for &abmd method must also contain the following entries:

cv_min smallest desired value of the reaction coordinate (required, unless the reaction coordinate is limited from below).

cv_max largest desired value of the reaction coordinate (required, unless the reaction coordinate is limited from above).

resolution the "spatial" resolution for the reaction coordinate.

To access the biasing potential files created in the course of FLOODING simulations, the nfe-umbrella-slice utility is provided (it prints a short description of itself if invoked with --help option).

The multiple-walker selection algorithm can improve the simulation by resampling between different walkers. The well-tempered ABMD can lead to a smoother convergence to the desired free energy. These two algorithm are implemented to SANDER and PMEMD from Amber16 onwards.

The multiple-walker selection algorithm currently works with &abmd only. The algorithm should be used only within the multiple-walker scheme (*i.e.*, when command-line **-rem** flag is set to zero). The following entries are recognized regarding with the selection algorithm (selection algorithm can work with FLOODING and UMBRELLA mode):

selection_freq positive integer number that sets the frequency of the resampling algorithm (in MD steps). If selection_freq is not specified, the selection algorithm will not be used.

selection_constant positive real number that sets the parameter *C*. if selection_freq is specified, specifying selection_constant is required (no default value). Parameter *C* is to determine how strong the selection mechanism is. If *C* is too large, all the walkers will be replaced with the most dominant one. If *C* is too small, there will be no killing/duplicating of walkers.

selection_epsilon positive real number (typically less than unity) that sets the stopping criterion parameter ε . Parameter ε determines the threshold for stopping the selection algorithm. If selection_epsilon is not specified, there will be no stop to the algorithm. If selection_epsilon is equal or larger than one, the algorithm will be stopped after the first attempt.

The well-tempered flavor can be used within either &abmd or &bbmd namelist. There are two entries relevant to the well-tempered feature:

wt_temperature positive real number that sets the pseudo-temperature T'. If this flag is not specified, conventional ABMD will be used (*i.e.*, T' $\to \infty$ or $\beta' \to 0$). The smaller the T'; the smoother/slower the convergence.

wt_umbrella_file the file name of true biasing potential after modification by 1 + (T /T') in which T is the reference temperature of the system (temp0).

An example `MDIN` file and `CV.IN` file for the `&abmd` flavor of `ABMD` is shown in the Fig. 7.10.

In this example, the reaction coordinate is defined as the distance between the 5th and 9th atoms (more than one reaction coordinates might be requested by mere inclusion of additional `&colvar` subsections). The `mode` is set to `FLOODING` thus enabling the adaptive biasing with flooding timescale $\tau_F = 100ps$. The region of interest of the reaction coordinate is specified to be between -1 Å and 10 Å and the resolution is set to 0.5 Å. The lower bound (-1 Å) could have been omitted for `DISTANCE` variable: the default value of zero would be used in such case. The code will try to load the biasing potential from the `umbrella.nc` file and use it as the value of $U(t|\xi)$ at the beginning of the run. The biasing potential built in the course of simulation will be saved to the same file (`umbrella.nc`) every time the `RESTRT` file is written. The selection algorithm is used with the frequency of selection defined as 10000 MD steps and selection constant defined as 0.001. The well-tempered algorithm is also used, with the pseudo-temperature defined as 10000 K in and the true biasing potential will be dumped as `wt_umbrella.nc` file. The `nfe-umbrella-slice` utility can then be used to access its content. An `MDIN` file for the follow up biased run at equilibrium would look much like the one shown in the Fig. 7.10, but with `mode` changed from `FLOODING` to `UMBRELLA`.

Driven ABMD can be performed using &smd block (for the SMD part of the algorithm) along with &abmd block (for the ABMD part of the algorithm). There is no additional flag for the &smd block relevant to the algorithm; however, there are two additional flags to ABMD relevant to the "driven" feature.

driven_weight string that sets the weighting scheme. The default option (i.e., not using the flag) is NONE which indicates no reweighting is used (NOT RECOMMENDED if SMD is performed along ABMD). Other options include CONSTANT and PULLING for constant and pulling reweighting protocols.

driven_cutoff positive real number that sets a cutoff for work for applying the reweighting algorithm (default: 0.0). If the work (accumulated or transferred depending on the scheme) at any given time is lower than the cutoff, no reweighting is done at that particular time. If the cutoff is too small, it may result in instability of the algorithm.

For both SANDER and PMEMD since Amber18, the `&abmd` code works correctly with Amber replica-exchange similar with `&pmd` (that is, for `-rem` flag set to different values). If `-rem` is set to 3, ABMD with replica-exchange is carried out. In such case different replicas can have different temperatures, collective variables and even different `mode`. The monitor and umbrella files are `MDIN`-bound. If number of `sander` groups exceeds one (the flag `-ng` is greater than one) and `-rem` flag is set to zero, the code runs *multiple walkers* `ABMD`. In both cases the number and type(s) of variable(s) must be the same across all replicas.

Finally, the `&bbmd` flavor allows one to run replica-exchange (AB)MD with different reaction coordinates and different modes (`ANALYSIS`, `UMBRELLA` or `FLOODING`) in different replicas (along with different temperatures, if desired). This module is outdated since `&abmd` has been compatible with `-rem` equals 3. The only advantage of `&bbmd` is that the number of replicas can be odd numbers if desired by runs, while this cannot be achieved in any `-rem` types. To applying `&bbmd` module, the `-rem` flag must be set to zero and the `&bbmd` sections must be present in all `MDIN` files. The `MDIN` file for the replica of rank zero (first line in the group file) is expected to contain additional information as compared to `&abmd` case (an example of such `MDIN` file for replica zero is shown in Fig. 7.11). The `MDIN` files for all other replicas except zero do not need any additional information, and therefore take the same form as in the `&abmd` flavor (except that the namelist is changed from `&abmd` to `&bbmd`, thus activating a slightly different code path). Each `MDIN` file may define its own reaction coordinates, have different `mode` and temperature if desired.

Within the first replica `&bbmd` namelist the following additional entries are recognized:

exchange_freq number of `MD` steps between the exchange attempts.

exchange_log_file the name of the file to which exchange statistics is to be reported.

exchange_log_freq frequency of `exchange_log_file` updates.

mt19937_seed seed for the random generator (Mersenne twister [188]).

mt19937_file the name of the file to which the state of the Mersenne twister is dumped periodically (for restarts).

The MDOUT, MDCRD, RESTRT, umbrella_file and monitor_file files are MDIN-bound in course of the bbmd-enabled run. An example that uses this kind of replica exchange is presented in Ref.161.

7.3.6 Swarms-of-Trajectories String Method

ABMD is a robust method for calculating free energy landscapes as a function of a small number of collective variables. Since the required computer time grows enormously with the number of collective variables, ABMD is best for exploring one- or two-dimensional phase spaces. However, rather than calculating full n-dimensional free energy maps, it is often fruitful to focus on the so-called Minimum Free Energy Path (MFEP) which the system is likely to take when transitioning between two minima. Calculating a MFEP in a complicated phase space is often difficult, and so-called "string methods"[189][179] represent one of the best approaches for finding the MFEP. Since sampling in string methods is essentially limited to regions around the MFEP, the cost of the method scales linearly with the length of the string or path, but only weakly on the number of collective variables. This results in considerable computational savings since the full free energy landscape is not calculated.

The swarms-of-trajectories string method (STSM)[179] is one of the most popular versions of the string method and has been implemented here by Dr. Moradi (moradi@uark.edu). The module is available in both SANDER and PMEMD from Amber18 onwards. It is a path-finding algorithm that refines a putative transition pathway iteratively until the path is deemed to have been converged. The string is defined by a number of nodes or images parameterized in a high-dimensional space of collective variables, whose position is updated iteratively. The center of each image is first used as a restraining center to generate representative conformations at the current center before allowing of a small change in this center for the next iteration. The change in the center of each image is estimated by averaging over the drifts of a swarm of short unbiased trajectories all starting at the current image position (generated using the constrained simulations. Thus, each iteration consists of a series of restrained and free simulations. In the current serial version of the code, these simulations are performed independently. In parallel versions -- which are more efficient -- a very large number of replicas is required which are run in parallel; this method is particularly efficient on large supercomputers.

To invoke the swarms-of-trajectories string method, the &stsm must be invoked in the MDIN file. For a string consisting of N_s nodes each requiring M copies $N_s \times M$ replicas will be required. The parallel implemention of the STSM method is based on iterative restrained and free MD simulations followed by a reparametrization of the image centers defined in a multidimensional collective variable space ξ. For the ith iteration, first M copies of the nth image are generated around the old center ξ_n^{i-1} by MD equilibration lasting τ_E timesteps. The generated M copies of the nth image are expected to be close to ξ_n^{i-1} for time τ_E, assuming that the invoked harmonic constant k for the restraining potential is large enough. The parameters τ_E and k thus need to be appropriately chosen in order to ensure that all copies of each image will be close to the image center. The restraint is then released, and each copy (swarm) is allowed to drift for τ_R timesteps. The newly shifted center ξ_n^i for the nth image is then determined by averaging over all drifted copies $\xi_{n,m}^t$ at time $t = \tau_E + \tau_R$. The resulting string of images is then smoothed using a linear interpolation protocol. A smoothing parameter ε with $0 \leq \varepsilon \leq 1$ determines the smoothness of the curve; it is recommended that ε be of the order of $1/(N_s - 1)$. The last setep is a reparameterization, which gain follows a linear interpolation protocol in order to generate N_s equidistant centers along the string. The two key parameters of the method are M and τ_R. Generally, the large the M and the shorter τ_R, the smoother (but slower) the evolution of the MFEP will be. These variables must be optimized empirically, but typically 10 - 30 copies and 5 - 20 ps are reasonable values. It is often advantageous to set $\tau_E = \tau_R$.

An improved sequential repeat version of the algorithm has also been implemented, which avoids the large number of copies and does not require a large number of processors to run. Here a new variable N_R is introduced, as the number of repeat runs for each replica. Now for each copy, it will run around the old center ξ_n^{i-1} for N_R times sequentially. And each repeat run can be equally considered as a parallel run of a new copy around the old center. Namely, the new shifted center will be determined by averaging on $N_R \times M$ copies. So the number of processors needed will be reduced to $1/N_R$, while the running time will be multipled by N_R.

The following is recognized within the &stsm namelist:

image positive integer number that sets the image id (between 1 and N). Default is 0.

repeats   positive integer number that sets the number of repeat runs, should be the same for each image and each copy. Equal to parallel implementation when not set. Default is 1.

equilibration non-negative integer number that sets the number of MD steps specified for biased equlibration (restraining) at each iteration. Default is 0.

release   Number of MD steps specified for the release (drift) at each iteration. Note: the total number of iterations is determined by the total simulation time (`nstlim` flag in `mdin` file) divided by total time for each iteration given by `equilibration+release`.

smoothing   positive number that sets the smoothing parameter for reparametrization (between 0 and 1). Smoothing parameter should be, preferably, on the order of $1/(N_s - 1)$. If this flag is not used, no smoothing will be performed.

report_centers a string that determines if drifted and/or smoothed and/or reparametrized centers will be reported. The default value is `NONE` and other available options include `ALL`,`DRIFT`,`SMOOTHED`, `REPARAMETRIZED`, `NO_DRIFT`, `NO_SMOOTHED`, `NO_REPARAMETRIZED`.

The `output_file`, `output_freq` and `cv_file` entries are recognized just as `&smd` and `&pmd`, the information of reaction coordinates will be read from `cv_file`. The number of collective variables can not exceed five. (here be attention that the `anchor_postion` and `anchor_strength` will be defined using the traditional harmonical potential, different with `&pmd`!). An example of `MDIN` file and `CV.IN` file for STSM in parallel case is shown in Fig. 7.12. Here we run 8 images along the path, with `I` defining the image ID. We run 980 MD steps for equlibration and 20 MD steps release at each iteration, so there are totally 1000 MD steps for each iteration. With nstlim set to 10000, 10 iterations will be carried out. The smoothing parameter is set to 0.1 and all the centers will be reported. For each image, 16 copies will be run in parallel, with `J` defining the copy ID. The evolution of reaction coordinate will recorded in the file `stsm.00I.J.txt`. For this run, at least $128(8 \times 16)$ processors are needed. Another example of `MDIN` file of equivalent sampling level in sequential case is shown in Fig. 7.13. Here we still have 8 images to run. We set the number of repeats to be 16, namely 16 repeat runs for each image to get the new drifted center. Therefore, 16000 MD steps are needed for one iteration, and so we set nstlim to 160000 to complete 10 iterations. For this run, 8 processors are needed at least.

Part of sample `MDOUT` file is shown in Fig. 7.14. The restoring restraint part will be only in sequential run, since the restraint needs to be restored after each repeat. The values of reaction coordinates before reporting centers are the averaged value over repeats for this copy and the instantaneous value. All the centers will be reported only in the `MDOUT` file of first copy of first image. The drifted centers are the averaged value over copies, and also the smoothed ans reparametrized centers can be reported. Always the reparametrized centers will be extracted to draw the MFEP in the phase space.

7.3.7 Post-processing of biasing potential

When you get the biasing potential (`*.nc` file), you can always use the `nfe-umbrella-slice` utility to access its content and get a friendly-written ASCII file from which one can obtain the free energy map. The output is the free energy value, which is the opposite of the biasing potential ($f = -U$ (*units kcal/mol*)). The `nfe-umbrella-slice` utility has been included in AmberTools.

Usage: `nfe-umbrella-slice [options] bias_potential.nc`

Options:

-h,--help Print out a usage summary

-p,--pretend Only print out the basic properties of source without biasing potential data (off by default)

-g,--gradient Print out the gradients (off by default)

-r,--reset Set the value of minimum to zero (off by default)

-t,--translate Translate the numerical value of biasing potential by a real number (0 by default)

-d,--dimensions Set the way of slice in different dimensions. The format is "D1:D2:...:Dn", where n is the number of dimensions. Each D can only be set with one number or three numbers separated by commas. If only one number is set, the variable will be fixed at that value. If three numbers are set, the first two define the boundary of the slice and the last one defines the number of points.

Example:

- `nfe-umbrella-slice -r -d "-5.0,5.0,50" 1d-bias.nc > FE.dat`

This processes the 1-dimensional biasing potential file `1d-bias.nc` and prints out the results to `FE.dat`. The minimum of free energy will be set to zero. The variable will be taken from -5.0 to 5.0 using 50 points.

- `nfe-umbrella-slice -g -t 50.0 -d "1.0:-2.0,2.0,20" 2d-bias.nc > FE.dat`

This processes the 2-dimensional biasing potential file `2d-bias.nc` and prints out the results to `FE.dat`. All the free energy will be incremented by a constant 50.0. The gradients in both dimensions will be printed out. For the first dimension, the variable will be fixed at 1.0; for the second dimension, the variable will be taken from -2.0 to 2.0 using 20 points.

- `nfe-umbrella-slice wt_umbrella.nc > wt_FE.dat`

This processes the biasing potential after WT-ABMD and prints out the results to `wt_FE.dat`. The default dimensional information is obtained and used by the program from the biasing potential file.

```
&colvar
   cv_type = 'QUATERNION0'
   cv_ni = 18,
   cv_i = 11 , 41 , 48 , 74 , 104 , 111 , 137 , 167 , 174 , 199 , 229 , 236, 262 ,
          292 , 299 , 325 , 355 , 362 ,
   refcrd_file = 'inpcrd'
/
&colvar
   cv_type = 'QUATERNION1'
   cv_ni = 18,
   cv_i = 11 , 41 , 48 , 74 , 104 , 111 , 137 , 167 , 174 , 199 , 229 , 236, 262 ,
          292 , 299 , 325 , 355 , 362 ,
   refcrd_file = 'inpcrd'
/
&colvar
   cv_type = 'QUATERNION2'
   cv_ni = 18,
   cv_i = 11 , 41 , 48 , 74 , 104 , 111 , 137 , 167 , 174 , 199 , 229 , 236, 262 ,
          292 , 299 , 325 , 355 , 362 ,
   refcrd_file = 'inpcrd'
/
&colvar
   cv_type = 'QUATERNION3'
   cv_ni = 18,
   cv_i = 11 , 41 , 48 , 74 , 104 , 111 , 137 , 167 , 174 , 199 , 229 , 236, 262 ,
          292 , 299 , 325 , 355 , 362 ,
   refcrd_file = 'inpcrd'
/
&colvar
   cv_type = 'QUATERNION0'
   cv_ni = 24,
   cv_i = 12 , 16 , 46 , 55 , 75 , 79 , 109 , 118 , 138 , 142 , 172 , 181 , 200 ,
          204 , 234 , 243 , 263 , 267 , 297 , 306 , 326 , 330 , 360 , 369 ,
   refcrd_file = 'inpcrd',
   q_index = 2
/
&colvar
   cv_type = 'QUATERNION1'
   cv_ni = 24,
   cv_i = 12 , 16 , 46 , 55 , 75 , 79 , 109 , 118 , 138 , 142 , 172 , 181 , 200 ,
          204 , 234 , 243 , 263 , 267 , 297 , 306 , 326 , 330 , 360 , 369 ,
   refcrd_file = 'inpcrd',
   q_index = 2
/
&colvar
   cv_type = 'QUATERNION2'
   cv_ni = 24,
   cv_i = 12 , 16 , 46 , 55 , 75 , 79 , 109 , 118 , 138 , 142 , 172 , 181 , 200 ,
          204 , 234 , 243 , 263 , 267 , 297 , 306 , 326 , 330 , 360 , 369 ,
   refcrd_file = 'inpcrd',
   q_index = 2
/
&colvar
   cv_type = 'QUATERNION3'
   cv_ni = 24,
   cv_i = 12 , 16 , 46 , 55 , 75 , 79 , 109 , 118 , 138 , 142 , 172 , 181 , 200 ,
          204 , 234 , 243 , 263 , 267 , 297 , 306 , 326 , 330 , 360 , 369 ,
   refcrd_file = 'inpcrd',
   q_index = 2
/
```

Figure 7.5: *An example of* `Orientation` *variable.*

```
&colvar
   cv_type = 'SPINANGLE'
   cv_ni = 18, cv_nr = 54,
   cv_i = 11 , 41 , 48 , 74 , 104 , 111 , 137 , 167 , 174 , 199 , 229 ,
          236, 262 , 292 , 299 , 325 , 355 , 362 ,
   cv_r = 0.96 , -4.47 , -0.31 , 3.48 , -3.00 , 3.06 , 0.88 , 0.01 ,
          3.36 ,4.55 , -0.51 , 6.46 , 3.93 , 2.38 , 9.81 , 0.26 ,
          0.84 , 10.12 , 1.90 , 4.16 , 13.21 , -1.06 , 4.47 , 16.58 ,
          -0.71 , 0.52 , 16.88 , -0.96 , -4.47 , 17.21 , -3.48 ,
          -3.00 , 13.84 , -0.88 , 0.01 , 13.54 , -4.55 , -0.51 , 10.44 ,
          -3.93 , 2.38 , 7.09 , -0.26 , 0.84, 6.78 , -1.90 , 4.16 ,
          3.69 , 1.06 , 4.47 , 0.32 , 0.71 , 0.52 , 0.02 ,
   axis = 1.0, 0.0, 0.0
/
```

Figure 7.6: *An example of* SPINANGLE *variable.*

```
title line
&cntrl
..., infe = 1
/

&smd
   output_file = 'smd.txt'
   output_freq = 50
   cv_file = 'cv.in'
/
```

```
cv_file
&colvar
  cv_type = 'DISTANCE'
  cv_ni = 2
  cv_i = 5, 9
  npath = 2, path = 5.0, 3.0, path_mode = 'LINES',
  nharm = 1, harm = 10.0
/
```

Figure 7.7: *An example* MDIN *file and* CV.IN *file for steered* MD*. Only the relevant part is shown.*

```
title line
&cntrl
..., infe = 1
/

&pmd
   output_file = 'pmd.txt'
   output_freq = 50
   cv_file = 'cv.in'
/
```

```
cv_file
&colvar ! first
   cv_type = 'ANGLE'
   cv_ni = 3, cv_i = 5, 9, 15
   anchor_position = -10.0,1.0,1.0,10.0
   anchor_strength = 10.0,10.0
/
&colvar ! second
   cv_type = 'TORSION'
   cv_ni = 4, cv_i = 1, 2, 3, 4
   anchor_position = -10.0,0.0,0.0,10.0
   anchor_strength = 23.8,23.8
/
```

Figure 7.8: *An example* MDIN *file and* CV.IN *file for umbrella sampling (only relevant part is presented in full).*

```
cv_file
&colvar ! phi
   cv_type = 'TORSION'
   cv_ni = 4, cv_i = 5, 7, 9, 15
   anchor_position = -2.05,-2.0,2.0,2.05
   anchor_strength = 500.0,500.0
/
&colvar ! psi
   cv_type = 'TORSION'
   cv_ni = 4, cv_i = 7, 9, 15, 17
   anchor_position = -1.85,-1.8,1.8,1.85
   anchor_strength = 500.0,500.0
/
```

Figure 7.9: *An example* CV.IN *file to restrain the φ and ψ of dialanine.*

```
title line
&cntrl
..., infe = 1
/

&abmd
   mode = 'FLOODING'

   monitor_file = 'abmd.txt'
   monitor_freq = 33
   cv_file = 'cv.in'

   umbrella_file = 'umbrella.nc'

   timescale = 100.0 ! in ps

   selection_freq = 10000
   selection_constant = 0.001

   wt_temperature = 10000.0
   wt_umbrella_file = 'wt_umbrella.nc'
/
```

```
cv_file
&colvar
  cv_type = 'DISTANCE'
  cv_ni = 2, cv_i = 5, 9
  cv_min = -1.0, cv_max = 10.0 ! min is not needed for DISTANCE
  resolution = 0.5 ! required for mode = FLOODING
/
```

Figure 7.10: *An example* `MDIN` *file and* `CV.IN` *file for* ABMD *(only the relevant part is presented in full).*

```
title line
&cntrl
..., infe = 1
/

&bbmd

   ! 0th replica only

   exchange_freq = 100 ! try for exchange every 100 steps

   exchange_log_file = 'bbmd.log'
   exchange_log_freq = 25

   mt19937_seed = 123455 ! random generator seed
   mt19937_file = 'mt19937.nc' ! file to store/load the PRG

   ! not specific for 0th replica

   mode = 'ANALYSIS'

   monitorfile = 'bbmd.01.txt' ! it is wise to have different
                               ! names in different replicas
   monitor_freq = 123
   cv_file = 'cv.in'
/
```

```
cv_file
&colvar
  cv_type = 'DISTANCE'
  cv_ni = 2, cv_i = 5, 9
/
```

Figure 7.11: *An example* MDIN *file and* CV.IN *file for* &bbmd *flavor of* ABMD *(only the relevant part is presented in full).*

```
title line
&cntrl
..., nstlim = 10000
..., infe = 1
/

&stsm      ! parallel case, I from 1 to 8, J from 1 to 16
  image = I
  equilibration = 980
  release = 20
  smoothing = 0.1
  report_centers = 'ALL'

  output_file = 'stsm.00I.J.txt'
  output_freq = 10
  cv_file = 'cv.I'
/
```

```
cv_file
&colvar ! phi
   cv_type = 'TORSION'
   cv_ni = 4, cv_i = 5, 7, 9, 15
   anchor_position = -3.00
   anchor_strength = 20.0
/
&colvar ! psi
   cv_type = 'TORSION'
   cv_ni = 4, cv_i = 7, 9, 15, 17
   anchor_position = 3.00
   anchor_strength = 20.0
/
```

Figure 7.12: *An example* MDIN *file and* CV.IN *file for* &stsm *in parallel case (only the relevant part is presented in full)*

```
title line
&cntrl
..., nstlim = 160000
..., infe = 1
/

&stsm      ! sequential case, I from 1 to 8
  image = I
  repeats = 16
  equilibration = 980
  release = 20
  smoothing = 0.1
  report_centers = 'ALL'

  output_file = 'stsm.00I.txt'
  output_freq = 10
  cv_file = 'cv.I'
/
```

Figure 7.13: *An example* MDIN *file for* &stsm *in sequential case (only the relevant part is presented in full)*

```
NFE : #   restoring restraint:
NFE : #   << colvar(1) = -3.000000 >>
NFE : #   << colvar(2) = 3.000000 >>
NFE : #   equilibration begins...
......
NFE : #   << colvar(1) = -2.500688 -2.586429 >>
NFE : #   << colvar(2) = 2.782725 3.082205 >>
NFE : #  drifted center of image 1 :        8     -2.54041796      2.70644813
NFE : #  drifted center of image 2 :        8     -2.54963153      2.71715138
......
NFE : #  drifted center of image 8 :        8      1.02191205      0.16837852
NFE : #  smoothed center of image 1 :       8     -2.54041796      2.70644813
NFE : #  smoothed center of image 2 :       8     -2.60416697      2.75924174
......
NFE : #  smoothed center of image 8 :       8      1.02191205      0.16837852
NFE : #  reparametrized center of image 1 :        8       -2.54041796
2.70644813
NFE : #  reparametrized center of image 2 :        8       -2.06027108
2.47738701
......
NFE : #  reparametrized center of image 8 :        8        1.02191205
0.16837852
```

Figure 7.14: *An example of* MDOUT *file for STSM run (only part is presented, and some centers are also omitted)*

8 NMR refinement

We find the *sander* module to be a flexible way of incorporating a variety of restraints into a optimization procedure that includes energy minimization and dynamical simulated annealing. The "standard" sorts of NMR restraints, derived from NOE and J-coupling data, can be entered in a way very similar to that of programs like DISGEO, DIANA or X-PLOR; an aliasing syntax allows for definitions of pseudo-atoms, connections with peak numbers in spectra, and the use of "ambiguous" constraints from incompletely-assigned spectra. More "advanced" features include the use of time-averaged constraints, use of multiple copies (LES) in conjunction with NMR refinement, and direct refinement against NOESY intensities, paramagnetic and diamagnetic chemical shifts, or residual dipolar couplings. In addition, a key strength of the program is its ability to carry out the refinements (usually near the final stages) using an explicit-solvent representation that incorporates force fields and simulation protocols that are known to give pretty accurate results in many cases for unconstrained simulations; this ability should improve predictions in regions of low constraint density and should help reduce the number of places where the force field and the NMR constraints are in "competition" with one another.

Since there is no generally-accepted "recipe" for obtaining solution structures from NMR data, the comments below are intended to provide a guide to some commonly-used procedures. Generally speaking, the programs that need to be run to obtain NMR structures can be divided into three parts:

1. *front-end* modules, which interact with NMR databases that provide information about assignments, chemical shifts, coupling constants, NOESY intensities, and so on. We have tried to make the general format of the input straightforward enough so that it could be interfaced to a variety of programs. We generally use the FELIX and NMRView codes, but the principles should be similar for other ways of keeping track of a database of NMR spectral information. As the flow-chart in Section 8.7 indicates, there are only a few files that need to be created for NMR restraints; these are indicated by the solid rectangles. The primary distance and torsion angle files have a fairly simple format that is largely compatible with the DIANA programs; if one wishes to use information from ambiguous or overlapped peaks, there is an additional "MAP" file that makes a translation from peak identifiers to ambiguous (or partial) assignments. Finally, there are some specialized (but still pretty straightforward) file formats for chemical shift or residual dipolar coupling restraints.

   There are a variety of tools, besides the ones described below, that can assist in preparing input for structure refinement in Amber.

   - The SANE (Structure Assisted NOE Evaluation) package, *https://ambermd.org/sane.zip*, is widely used at The Scripps Research Institute.[190]

   - If you use Bruce Johnson's NmrView package, you might also want to look at the additions to that: *http://garbanzo.scripps.edu/nmrgrp/wisdom/pipe/tips_scripts.html*. In particular, the *xpkTOupl* and *starTOupl* scripts there convert NmrView peak lists into the "7-column" needed for input to makeDIST_RST.

   - Users of the MARDIGRAS programs from UCSF can use the *mardi2amber* program to do conversion to Amber format: *http://picasso.ucsf.edu/mardihome.html*

2. *restrained molecular dynamics,* which is at the heart of the conformational searching procedures. This is the part that *sander* itself handles.

3. *back-end* routines that do things like compare families of structures, generate statistics, simulate spectra, and the like. For many purposes, such as visualization, or the running of procheck-NMR, the "interface" to such programs is just the set of PDB files that contain the family of structures to be analyzed. These general-purpose structure analysis programs are available in many locations and are not discussed here. The

principal *sander*-specific tool is *sviol*, which prepares tables and statistics of energies, restraint violations, and the like.

8.1 Distance, angle and torsional restraints

Distance, angle, and other restraints are read from the DISANG file if *nmropt* > 0. Namelist rst ("&rst") contains the following variables; it is read repeatedly until a namelist &rst statement is found with IAT(1)=0, or until reaching the end of the DISANG file.

[In many cases, the user will not prepare this section of the input by hand, but will use the auxiliary programs *makeDIST_RST, makeANG_RST* and *makeCHIR_RST* to prepare input from simpler files. See also the programs *cyanarest_to_amberRST* and *nef_to_RST* if you have restraints in Cyana or NEF (NMR Exchange Format) formats.]

8.1.1 Variables in the &rst namelist:

`iat(1)`→`iat(8)`

- *If IRESID = 0 (normal operation):* The atoms defining the restraint. Type of restraint is determined (in order) by:

    1. If IAT(3) = 0, this is a distance restraint.

    2. If IAT(4) = 0, this is an angle restraint.

    3. If IAT(5) = 0, this is a torsional (or J-coupling, if desired) restraint or a genereralized distance restraint of 4 atoms, a type of restraint new as of Amber 10 (*sander* only, see below).

    4. If IAT(6) = 0, this is a plane-point angle restraint, a second restraint new as of Amber 10 (*sander* only). The angle is measured between the normal of a plane defined by IAT(1)..IAT(4) and the vector from the center of mass of atoms IAT(1)..IAT(4) to the position of IAT(5). The normal is defined by (r1 - r2) $\times$ (r3 - r4), where rn is the position of IAT(n).

    5. If IAT(7) = 0, this is a generalized distance restraint of 6 atoms (see below).

    6. Otherwise, if IAT(1)..IAT(8) are all nonzero, this is a plane- plane angle restraint, a third new restraint type as of Amber 10 (*sander* only, or a generalized distance restraint of 8 atoms (see below). For the plane-plane restraint, the angle is measured between the two normals of the two planes, which are defined by (r1 - r2) $\times$ (r3 - r4) and (r5 - r6) $\times$ (r7 - r8). In the case of either planar restraint, the plane may be defined using three atoms instead of four simply by using one atom twice.

    If any of IAT(n) are < 0, then a corresponding group of atoms is defined below, and the coordinate- averaged position of this group will be used in place of atom IAT(n). A new feature as of Amber 10, atom groups may be used not only in distance restraints, but also in angle, torsion, the new plane restraints, or the new generalized restraints. If this is a distance restraint, and IAT1 $<$0, then a group of atoms is defined below, and the coordinate-averaged position of this group will be used in place of the coordinates of atom 1 [IAT(1)]. Similarly, if IAT(2) < 0, a group of atoms will be defined below whose coordinate-averaged position will be used in place of the coordinates for atom 2 [IAT(2)].

- *If IRESID=1:* IAT(1)..IAT(8) point to the *residues* containing the atoms comprising the internal. Residue numbers are the absolute in the entire system. In this case, the variables ATNAM(1)..ATNAM(8) must be specified and give the character names of the atoms within the respective residues. If any of IAT(n) are less than zero, then group input will still be read in place of the corresponding atom, as described below.

- *Defaults for IAT(1)→IAT(8) are 0.*

`rstwt(1)`→`rstwt(4)` New as of Amber 10 (*sander* only), users may now define a single restraint that is a function of multiple distance restraints, called a "generalized distance coordinate" restraint. The energy of such a restraint has the following form:

$$U = k(w_1|\mathbf{r}_1 - \mathbf{r}_2| + w_2|\mathbf{r}_3 - \mathbf{r}_4| + w_3|\mathbf{r}_5 - \mathbf{r}_6| + w_4|\mathbf{r}_7 - \mathbf{r}_8| - r_0)^2$$

where the weights w_n are given in rstwt(1)..rstwt(4) and the positions $\mathbf{r}_n$ are the positions of the atoms in iat(1)..iat(8).

Generalized distance coordinate restraints must be defined with either 4, 6, or 8 atoms and 2, 3, or 4 corresponding nonzero weights in rstwt(1)..rstwt(4). Weights may be any positive or negative real number.

If all the weights in rstwt(1)..rstwt(4) are zero and four atoms are given in iat(1)..iat(4) for the restraint, the restraint is a torsional or J-coupling restraint. If eight atoms are given in iat(1)..iat(8) and all weights are zero, the restraint is a plane-plane angle restraint. However, if the weights are nonzero, the restraint will be a generalized distance coordinate restraint.

Default for rstwt(1)..rstwt(4) is 0.0

`restraint`   New as of Amber 10 (*sander* only), users may now use a "natural language" system to define restraints by using the RESTRAINT character variable. Valid restraints defined in this manner will begin with a "distance( )" "angle( )" "torsion( )" or "coordinate( )" keyword. Within the parentheses, the atoms that make up the restraint are specified. Atoms may be defined either with an explicit atom number or by using ambmask format, namely :(residue#)@(atom name). Atoms may be separated by commas, spaces, or parentheses. Additionally, negative integers may be used if atom groupings are defined in other variables in the namelist as described below. In addition to the principle distance, angle, torsion, and coordinate keywords, Some keywords may be used within the principle keywords to define more complicated restraints. The keyword "plane( )" may be used once or twice within the parentheses of the "angle( ) keyword to define a planar restraint. Defining one plane grouping plus one other atom in this manner will create a plane-point angle restraint as described above. Defining two plane groupings will create a plane-plane angle restraint. The keyword "plane( )" may only be used inside of "angle( )," and is necessary to define either a plane-point or plane-plane restraint.
Within the "coordinate( )" keyword, the user must use 2 to 4 "distance( )" keywords to define a generalized distance coordinate restraint. The "distance( )" keyword functions just like it does when used to define a traditional distance restraint. The user may specify any two atom numbers, masks, or negative numbers corresponding to atom groups defined outside of RESTRAINT. Additionally, following each "distance( )" keyword inside "coordinate( )" the user must specify a real-number weight to be applied to each distance making up the generalized coordinate.
The "com( )" keyword may be used within any other keyword to define a center of mass grouping of atoms. Within the parenthesis, the user will enter a list of atom numbers or masks. Negative numbers, which correspond to externally-defined groups, may not be used.
Any type of parenthetical character, i.e., ( ), [ ], or { }, may be used wherever parentheses have been used above.

The following are all examples of valid restraint definitions:

```
restraint = "distance( (45) (49) )"
= "angle (:21@C5' :21@C4' 108)"
= "torsion[-1,-1,-1, com(67, 68, 69)]"
= "angle( -1, plane(81, 85, 87, 90) )"
= "angle(plane(com(9,10),:5@CA,31,32),plane(14,15,15,16))"
= "coordinate(distance(:5@C3',:6@O5'),-1.0,distance(134,-1),1.0)"
```

There is a 256 character limit on RESTRAINT, so if a particularly large atom grouping is desired, it is necessary to specify a negative number instead of "com( )" and define the group as described below. RESTRAINT will only be parsed if IAT(1) = 0, otherwise the information in IAT(1) .. IAT(8) will define the restraint. *Default for restraint is ' '.*

atnam   If IRESID = 1, then the character names of the atoms defining the internal are contained in ATNAM(1)→ATNAM(8). Residue IAT(1) is searched for atom name ATNAM(1); residue IAT(2) is searched for atom name ATNAM(2); etc. *Defaults for ATNAM(1)→ATNAM(8) are ' '.*

iresid   Indicates whether IAT(I) points to an atom # or a residue #. See descriptions of IAT() and AT-NAM() above. If RESTRAINT is used to define the internal instead of IAT(), IRESID has no effect on how RESTRAINT is parsed. However, it will affect the behavior of atom group definitions as described below if negative numbers are specified within RESTRAINT. *Default = 0.*

nstep1, nstep2 This restraint is applied for steps/iterations NSTEP1 through NSTEP2. If NSTEP2 = 0, the restraint will be applied from NSTEP1 through the end of the run. Note that the first step/iteration is considered step zero (0). *Defaults for NSTEP1, NSTEP2 are both 0.*

irstyp   Normally, the restraint target values defined below (R1→R4) are used directly. If IRSTYP = 1, the values given for R1→R4 define relative displacements from the current value (value determined from the starting coordinates) of the restrained internal. For example, if IRSTYP=1, the current value of a restrained distance is 1.25, and R1 (below) is -0.20, then a value of R1=1.05 will be used. *Default is IRSTYP=0.*

ialtd   Determines what happens when a distance restraint gets very large. If IALTD=1, then the potential "flattens out", and there is no force for large violations; this allows for errors in constraint lists, but might tend to ignore constraints that *should* be included to pull a bad initial structure towards a more correct one. When IALTD=0 the penalty energy continues to rise for large violations. See below for the detailed functional forms that are used for distance restraints. Set IALTD=0 to recover the behavior of earlier versions of *sander*. Default value is 0, or the last value that was explicitly set in a previous restraint. This value is set to 1 if *makeDIST_RST* is called with the *-altdis* flag.

ifvari   If IFVARI > 0, then the force constants/positions of the restraint will vary with step number. Otherwise, they are constant throughout the run. If IFVARI >0, then the values R1A→R4A, RK2A, and RK3A must be specified (see below). *Default is IFVARI=0.*

ninc   If IFVARI > and NINC > 0, then the change in the target values of of R1→R4 and K2,K3 is applied as a step function, with NINC steps/ iterations between each change in the target values. If NINC = 0, the change is effected continuously (at every step). *Default for NINC is the value assigned to NINC in the most recent namelist where NINC was specified. If NINC has not been specified in any namelist, it defaults to 0.*

imult   If IMULT=0, and the values of force constants RK2 and RK3 are changing with step number, then the changes in the force constants will be linearly interpolated from rk2→rk2a and rk3→rk3a as the step number changes. If IMULT=1 and the force constants are changing with step number, then the changes in the force constants will be effected by a series of multiplicative scalings, using a single factor, R, for all scalings. *i.e.*

           rk2a = R**INCREMENTS * rk2
           rk3a = R**INCREMENTS * rk3.

      INCREMENTS is the number of times the target value changes, which is determined by NSTEP1, NSTEP2, and NINC. *Default for IMULT is the value assigned to IMULT in the most recent namelist where IMULT was specified. If IMULT has not been specified in any namelist, it defaults to 0.*

r1→r4, rk2, rk3, r1a→r4a, rk2a, rk3a If IALTD=0, the restraint is a well with a square bottom with parabolic sides out to a defined distance, and then linear sides beyond that. If R is the value of the restraint in question:

      • R < r1 Linear, with the slope of the "left-hand" parabola at the point R=r1.

- r1 <= R < r2 Parabolic, with restraint energy $k_2(R - r_2)^2$.

- r2 <= R < r3 E = 0.

- r3 <= R < r4 Parabolic, with restraint energy $k_3(R - r_3)^2$.

- r4 <= R Linear, with the slope of the "right-hand" parabola at the point R=r4.

For torsional restraints, the value of the torsion is translated by +-n*360, if necessary, so that it falls closest to the mean of r2 and r3. Specified distances are in Angstroms. Specified angles are in degrees. Force constants for distances are in kcal/mol-Å2 Force constants for angles are in kcal/mol-rad 2 . (Note that angle positions are specified in degrees, but force constants are in radians, consistent with typical reporting procedures in the literature).

If IALTD=1, distance restraints are interpreted in a slightly different fashion. Again, If R is the value of the restraint in question:

- R < r2 Parabolic, with restraint energy $k_2(R - r_2)^2$.

- r2 <= R < r3 E = 0.

- r3 <= R < r4 Parabolic, with restraint energy $k_3(R - r_3)^2$.

- r4 <= R Hyperbolic, with energy $k_3[b/(R - r_3) + a]$, where $a = 3(r_4 - r_3)^2$ and $b = -2(r_4 - r_3)^3$. This function matches smoothly to the parabola at $R = r_4$, and tends to an asymptote of ak_3 at large R. The functional form is adapted from that suggested by Michael Nilges, *Prot. Eng.* **2,** 27-38 (1988). Note that if *ialtd=1*, the value of r1 is ignored.

ifvari   **= 0** The values of r1→r4, rk2, and rk3 will remain constant throughout the run.

        > 0 The values r1a, r2a, r3a, r4a, r2ka and r3ka are also used. These variables are defined as for r1→r4 and rk2, rk3, but correspond to the values appropriate for NSTEP = NSTEP2: e.g., if IVARI >0, then the value of r1 will vary between NSTEP1 and NSTEP2, so that, e.g. r1(NSTEP1) = r1 and r1(NSTEP2) = r1a. Note that you *must* specify an explicit value for *nstep1* and *nstep2* if you use this option. *Defaults for r1→r4,rk2,rk3,r1a→r4a,rk2a and rk3a are the values assigned to them in the most recent namelist where they were specified. They should always be specified in the first* &rst *namelist.*

r0, k0, r0a, k0a New as of Amber 10 (*sander* only), the user may more easily specify a large parabolic well if desired by using R0 and K0, and then R0A and K0A if IFVARI > 0. The parabolic well will have its zero at R = R0 and a force constant of K0. These variables simply map the disired parabolic well into r1→r4, rk2, rk3, r1a→r4a, rk2a, and rk3a in the following manner:

- R1 = 0 for distance, angle, and planar restraints, R1 = R0 - 180 for torsion restraints

- R1A = 0 for distance, angle, and planar restraints, R1A = R0A - 180 for torsion restraints

- R2 = R0; R3 = R0

- R2A = R0A; R3A = R0A

- R4 = R0 + 500 for distance restraints, R4 = 180 for angle and planar restraints, R4 = R0 + 180 for torsion restraints

- RK2 = K0; RK3 = K0

- RK2A = K0A; RK3A = K0A

rjcoef(1)→rjcoef(3) By default, 4-atom sequences specify torsional restraints. It is also possible to impose restraints on the vicinal 3 J-coupling value related to the underlying torsion. J is related to the torsion τ by the approximate Karplus relationship: $J = A\cos^2(\tau) + B\cos(\tau) + C$. If you specify a nonzero value for either RJCOEF(1) or RJCOEF(2), then a J-coupling restraint, rather than a torsional restraint, will be imposed. At every MD step, J will be calculated from the Karplus relationship with A = RJCOEF(1), B = RJCOEF(2) and C = RJCOEF(3). In this case, the target values (R1->R4, R1A->R4A) and force constants (RK2, RK3, RK2A, RK3A) refer to J-values

for this restraint. RJCOEF(1)->RJCOEF(3) must be set individually for each torsion for which you wish to apply a J-coupling restraint, and RJCOEF(1)->RJCOEF(3) may be different for each J-coupling restraint. With respect to other options and reporting, J-coupling restraints are treated identically to torsional restraints. This means that if time-averaging is requested for torsional restraints, it will apply to J-coupling restraints as well. The J-coupling restraint contribution to the energy is included in the "torsional" total. And changes in the relative weights of the torsional force constants also change the relative weights of the J-coupling restraint terms. Setting RJCOEF has no effect for distance and angle restraints. *Defaults for RJCOEF(1)->RJCOEF(3) are 0.0.*

igr1(i),i=1→200, igr2(i),i=1→200, ... igr8(i),i..1=1→200 If IAT(n) < 0, then IGRn() gives the atoms defining the group whose coordinate averaged position is used to define "atom n" in a restraint. Alternatively, if RESTRAINT is used to define the internal, then if the nth atom specified is a number less than zero, IGRn() gives the atoms defining the group whose coordinate averaged position is used to define "atom n" in a restraint. If IRESID = 0, absolute atom numbers are specified by the elements of IGRn(). If IRESID = 1, then IGRn(I) specifies the number of the residue containing atom I, and the name of atom I must be specified using GRNAMn(I). A maximum of 200 atoms (N # of atoms if using pmemd) are allowed in any group. Only specify those atoms that are needed. Default value for any unspecified element of IGRn(i) is 0.

fxyz   If iat(3)=0 and igr1 and/or igr2 is defined then it is possible to weight the x, y, z components of the force in the restraint to 0 (no force) or 1 (full restraint force). Ex: fxyz=0, 0, 1. This sets no additional restraint force on the x component or y-component of the restraint force, and full z-component restraint force. Default fxyz=1,1,1. Note: When setting fxyz, the r1, r2, r3, r4 values should be set relative to a weighted distance $\sqrt{(w_x * d_x)^2 + (w_y * d_y)^2 + (w_z * d_z)^2}$, so if fxyz=0,0,1 then the only distance taken into account when comparing to r1,r2,r3,r4 is the z distance between the molecule and the center of mass. Note that the DUMPAVE value when outxyz=0 is also just the weighted distance.

outxyz   If iat(3)=0 and igr1 and/or igr2 is defined then it is possible to output the x, y, z components of the force in the restraint if outxyz is set to 1. Default outyz=0. When outxyz is set to 1, the components of the distance and total distance are outputed in DUMPAVE in the order of the x-component, y-component, z-component, total distance.

grnam1(i),i=1→200, grnam2(i),i=1→200, ... grnam8(i),i=1→200 If group input is being specified (IGRn(1) > 0), *and* IRESID = 1, then the character names of the atoms defining the group are contained in GRNAMn(i), as described above. In the case IAT(1) < 0, each residue IGR1(i) is searched for an atom name GRNAM1(i) and added to the first group list. In the case IAT(2) < 0, each residue IGR2(i) is searched for an atom name GRNAM2(i) and added to the second group list. *Defaults for GRNAMn(i) are ' '.*

ir6   If a group coordinate-averaged position is being used (see IGR1 and IGR2 above), the average position can be calculated in either of two manners: If IR6 = 0, center-of-mass averaging will be used. If IR6=1, the $\langle r^{-6} \rangle^{-1/6}$ average of all interaction distances to atoms of the group will be used. *Default for IR6 is the value assigned to IR6 in the most recent namelist where IR6 was specified. If IR6 has not been specified in any namelist, it defaults to 0.*

ifntyp   If time-averaged restraints have been requested (see DISAVE/ANGAVE/TORAVE above), they are, by default, applied to all restraints of the class specified. Time-averaging can be overridden for specific internals of that class by setting IFNTYP for that internal to 1. IFNTYP has no effect if time-averaged restraint are not being used. *Default value is IFNTYP=0.*

ixpk, nxpk These are user-defined integers than can be set for each constraint. They are typically the "peak number" and "spectrum number" associated with the cross-peak that led to this particular distance restraint. Nothing is ever done with them except to print them out in the "violation summaries", so that NMR people can more easily go from a constraint violation to the corresponding peak in their spectral database. Default values are zero.

iconstr   If *iconstr* > 0, (default is 0) a Lagrangian multiplier is also applied to the two-center internal co-ordinate defined by IAT(1) and IAT(2). The effect of this Lagrangian multiplier is to maintain the initial orientation of the internal coordinate. The rotation of the vector IAT(1)->IAT(2) is pro-hibited, though translation is allowed. For each defined two-center internal coordinate, a separate Lagrangian multiplier is used. Therefore, although one can use as many multipliers as needed, defining centers should NOT appear in more than one multiplier. This option is compatible with mass centers (i.e., negative IAT(1) or IAT(2)). ICONSTR can be used together with harmonic restraints. RK2 and RK3 should be set to 0.0 if the two-center internal coordinate is a simple Lagrangian multiplier. An example has been included in $AMBERHOME/example/lagmul.

Namelist &rst is read for each restraint. Restraint input ends when a namelist statement with iat(1) = 0 (or iat(1) not specified) is found. Note that comments can precede or follow any namelist statement, allowing comments and restraint definitions to be freely mixed.

8.2 NOESY volume restraints

After the previous section, NOESY volume restraints may be read. This data described in this section is only read if NMROPT = 2. The molecule may be broken in overlapping submolecules, in order to reduce time and space requirements. Input *for each submolecule* consists of namelist "&noeexp", followed *immediately* by standard Amber "group" cards defining the atoms in the submolecule. In addition to the submolecule input ("&noeexp"), you may also need to specify some additional variables in the cntrl namelist; see the "NMR variables" description in that section.

In many cases, the user will not prepare this section of the input by hand, but will use the auxiliary program *makeDIST_RST* to prepare input from simpler files.

Variables in the &noeexp namelist:

For each submolecule, the namelist "&noeexp" is read (either from *stdin* or from the NOESY redirection file) which contains the following variables. There are no effective defaults for *npeak, emix, ihp, jhp,* and *aexp*: you must specify these.

npeak*(imix)* Number of peaks for each of the "imix" mixing times; if the last mixing time is *mxmix*, set NPEAK(*mxmix+1*) = -1. End the input when NPEAK(1) < 0.

emix*(imix)* Mixing times (in seconds) for each mixing time.

ihp*(imix,ipeak)*, jhp*(imix,ipeak)* Atom numbers for the atoms involved in cross-peak "ipeak" at mixing time "imix"

aexp(imix,ipeak) Experimental target integrated intensity for this cross peak. If AEXP is negative, this cross peak is part of a set of overlapped peaks. The computed intensity is added to the peak that follows; the next time a peak with AEXP > 0 is encountered, the running sum for the calculated peaks will be compared to the value of AEXP for that last peak in the list. In other words, a set of overlapped peaks is represented by one or more peaks with AEXP < 0 followed by a peak with AEXP > 0. The computed total intensity for these peaks will be compared to the value of AEXP for the final peak.

arange*(imix,ipeak)* "Uncertainty" range for this peak: if the calculated value is within ±ARANGE of AEXP, then no penalty will be assessed. Default uncertainties are all zero.

awt*(imix,ipeak)* Relative weight for this cross peak. Note that this will be multiplied by the overall weight given by the NOESY weight change cards in the weight changes section (Section 1). Default values are 1.0, unless INVWT1,INVWT2 are set (see below), in which case the input values of AWT are ignored.

invwt1,invwt2 Lower and upper bounds on the weights for the peaks respectively, such that the relative weight for each peak is 1/intensity if 1/intensity lies between the lower and upper bounds. This is the intensity after being scaled by *oscale*. The inverse weighing scheme adopted by this option prevents placing too much influence on the strong peaks at the expense of weaker peaks and was previously invoked using the compilation flag "INVWGT". Default values are IN-VWT1=INVWT2=1.0, placing equal weights on all peaks.

omega   Spectrometer frequency, in Mhz. Default is 500. It is possible for different sub-molecules to have different frequencies, but omega will only change when it is explicitly re-set. Hence, if all of your data is at 600 Mhz, you need only set *omega* to 600. in the first submolecule.

taurot   Rotational tumbling time of the molecule, in nsec. Default is 1.0 nsec. Like *omega*, this value is "sticky", so that a value set in one submolecule will remain until it is explicitly reset.

taumet   Correlation time for methyl jump motion, in ns. This is only used in computing the intra-methyl contribution to the rate matrix. The ideas of Woessner are used, specifically as recommended by Kalk & Berendsen.[191] Default is 0.0001 ns, which is effectively the fast motion limit. The default is consistent with the way the rest of the rate matrix elements are determined (also in the fast motion limit,) but probably is not the best value to use, since methyl groups appear to have T1 values that are systematically shorter than other protons, and this is likely to arise from the fact that the methyl correlation time can be near to the inverse of the spectrometer frequency. A value of 0.02 - 0.05 ns is probably better than 0.0001, but this is still an active research area, and you are on your own here, and should consult the literature for further discussion.[192] As with *omega*, *taumet* can be different for different sub-molecules, but will only change when it is explicitly re-set.

id2o   Flag for determining if exchangeable protons are to be included in the spin-diffusion calculation. If ID2O=0 (default) then all protons are included. If ID2O=1, then all protons bonded to nitrogen or oxygen are assumed to not be present for the purposes of computing the relaxation matrix. No other options exist at present, but they could easily be added to the subroutine *indexn*. Alternatively, you can manually rename hydrogens in the *prmtop* file so that they do not begin with "H": such protons will not be included in the relaxation matrix. (*Note:* for technical reasons, the HOH proton of tyrosine must always be present, so setting ID2O=1 will not remove it; we hope that this limitation will be of minor importance to most users.) The *id2o* variable retains its value across namelist reads, *i.e.* its value will only change if it is explicitly reset.

oscale   overall scaling factor between experimental and computed volume units. The experimental intensities are multiplied by *oscale* before being compared to calculated intensities. This means that the weights WNOESY and AWT always refer to "theoretical" intensity scales rather than to the (arbitrary) experimental units. The *oscale* variable retains its value across namelist reads, *i.e.* its value will only change if it is explicitly reset. The initial (default) value is 1.0.

The atom numbers *ihp* and *jhp* are the absolute atom numbers. For methyl groups, use the number of the last proton of the group; for the delta and epsilon protons of aromatic rings, use the delta-2 or epsilon-2 atom numbers. Since this input requires you to know the absolute atom numbers assigned by Amber to each of the protons, you may wish to use the separate *makeDIST_RST* program which provides a facility for more turning human-readable input into the required file for *sander*.

Following the &noeexp namelist, give the Amber "group" cards that identify this submolecule. This combination of "&noeexp" and "group" cards can be repeated as often as needed for many submolecules, subject to the limits described in the *nmr.h* file. As mentioned above, this input section ends when NPEAK(1) < 0, or when and end-of-file is reached.

8.3 Chemical shift restraints

After reading NOESY restraints above (if any), read the chemical shift restraints in namelist *&shf*, or the pseudocontact restraints in namelist *&pcshift*. Reading this input is triggered by the presence of a SHIFTS line in the I/O redirection section. In many cases, the user will not prepare this section of the input by hand, but will use the auxiliary programs *shifts* or *fantasian* to prepare input from simpler files.

Variables in the &shf namelist.

(Defaults are only available for *shrang, wt*, *nter*, and *shcut*; you must specify the rest.)

nring   Number of rings in the system.

natr(*i*)   Number of atoms in the *i-th* ring.

iatr(*j*,*i*)   Absolute atom number for the *j-th* atom of the *i-th* ring.

namr(*i*)   Eight-character string that labels the *i-th* ring. The first three characters give the residue name (in caps); the next three characters contain the residue number (right justified); column 7 is blank; column 8 may optionally contain an extra letter to distinguish the two rings of trp, or the 5 or 8 rings of the heme group.

str(*i*)   Ring current intensity factor for the *i-th* ring. Older values are summarized by Cross and Wright;[193] more recent empirical parametrizations seem to give improved results.[194, 195]

nprot   Number of protons for which penalty functions are to be set up.

iprot(*i*)   Absolute atom number of the *i-th* proton whose shifts are to be evaluated. For equivalent protons, such as methyl groups or rapidly flipping phenylalanine rings, enter all two or three atom numbers in sequence; averaging will be controlled by the *wt* parameter, described below.

obs(*i*)   Observed secondary shift for the *i-th* proton. This is typically calculated as the observed value minus a random coil reference value.

shrang(*i*)   "Uncertainty" range for the observed shift: if the calculated shift is within ±SHRANG of the observed shift, then no penalty will be imposed. The default value is zero for all shifts.

wt(*i*)   Weight to be assigned to this penalty function. Note that this value will be multiplied by the overall weight (if any) given by the SHIFTS command in the assignment of weights (above). Default values are 1.0. For sets of equivalent protons, give a negative weight for all but the last proton in the group; the last proton gets a normal, positive value. The average computed shift of the group will be compared to *obs* entered for the last proton.

shcut   Values of calculated shifts will be printed only if the absolute error between calculated and observed shifts is greater than this value. *Default = 0.3 ppm.*

nter   Residue number of the N-terminus, for protein shift calculations; *default = 1.*

cter   Residue number of the C-terminus, for protein shift calculations. Believe it or not, the current code cannot figure this out for itself.

In typical usage, the *shifts* program (`http://casegroup.rutgers.edu/shifts.html`) would be used to create this file, with a typical command line:

```
shifts −readobs −sander '::H*' gcg10
```

Sample input and output files are in `$AMBERHOME/test/rdc`.

8.4 Pseudocontact shift restraints

The PCSHIFT module allows the inclusion of pseudocontact shifts as constraints in energy minimization and molecular dynamics calculations on paramagnetic molecules. The pseudocontact shift depends on the magnetic susceptibility anisotropy of the metal ion and on the location of the resonating nucleus with respect to the axes of the magnetic susceptibility tensor. For the nucleus i, it is given by:

$$\delta_{pc}^i = \sum_j \frac{1}{12\pi r_{ij}^3} \left[\Delta\chi_{ax}^j (3n_{ij}^2 - 1) + (3/2)\Delta\chi_{rh}^j (l_{ij}^2 - m_{ij}^2) \right]$$

where l_{ij}, m_{ij}, and n_{ij} are the direction cosines of the position vector of atom i with respect to the j-th magnetic susceptibility tensor coordinate system, r_{ij} is the distance between the j-th paramagnetic center and the proton i, $\Delta\chi_{ax}$ and $\Delta\chi_{rh}$ are the axial and the equatorial (rhombic) anisotropies of the magnetic susceptibility tensor of the j-th paramagnetic center. For a discussion, see Ref. [196].

The PCSHIFT module to be used needs a namelist file which includes information on the magnetic susceptibility tensor and on the paramagnetic center, and a line of information for each nucleus. This module allows to include more than one paramagnetic center in the calculations. To include pseudocontact shifts as constraints in energy minimization and molecular dynamics calculations the NMROPT flag should be set to 2, and a *PCSHIFT=filename* statement entered in the I/O redirection section.

To perform molecular dynamics calculations it is necessary to eliminate the rotational and translational degree of freedom about the center of mass (this because during molecular dynamics calculations the relative orientation between the external reference coordinate system and the magnetic anisotropy tensor coordinate system has to be fixed).This option can be obtained with the NSCM flag of *sander*.

Variables in the pcshift namelist

nprot   number of pseudocontact shift constraints.

nme   number of paramagnetic centers.

nmpmc   name of the paramagnetic atom

optphi(n), opttet(n), optomg(n), opta1(n), opta2(n) the five parameters of the magnetic anisotropy tensor for each paramagnetic center.

optkon   force constant for the pseudocontact shift constraints

Following this, there is a line for each nucleus for which the pseudocontact shift information is given has to be added. Each line contains :

iprot(i)   atom number of the i-th proton whose shift is to be used as constraint.

obs(i)   observed pseudocontact shift value, in ppm

wt(i)   relative weight

tolpro(i)   relative tolerance ix mltpro

mltpro(i)   multiplicity of the NMR signal (for example the protons of a methyl group have mltprot(i)=3)

Example

Here is a &pcshf namelist example: a molecule with three paramagnetic centers and 205 pseudocontact shift constraints.

```
&pcshf
nprot=205,
nme=3,
nmpmc='FE ',
optphi(1)=-0.315416,
opttet(1)=0.407499,
optomg(1)=0.0251676,
opta1(1)=-71.233,
opta2(1)=1214.511,
optphi(2)=0.567127,
opttet(2)=-0.750526,
optomg(2)=0.355576,
opta1(2)=-60.390,
opta2(2)=377.459,
optphi(3)=0.451203,
opttet(3)=-0.0113097,
optomg(3)=0.334824,
opta1(3)=-8.657,
opta2(3)=704.786,
optkon=30,
iprot(1)=26, obs(1)=1.140, wt(1)=1.000, tolpro(1)=1.00, mltpro(1)=1,
iprot(2)=28, obs(2)=2.740, wt(2)=1.000, tolpro(2)=.500, mltpro(2)=1,
iprot(3)=30, obs(3)=1.170, wt(3)=1.000, tolpro(3)=.500, mltpro(3)=1,
iprot(4)=32, obs(4)=1.060, wt(4)=1.000, tolpro(4)=.500, mltpro(4)=3,
iprot(5)=33, obs(5)=1.060, wt(5)=1.000, tolpro(5)=.500, mltpro(5)=3,
iprot(6)=34, obs(6)=1.060, wt(6)=1.000, tolpro(6)=.500, mltpro(6)=3,
...
...
iprot(205)=1215, obs(205)=.730, wt(205)=1.000, tolpro(205)=.500,
mltpro(205)=1,
/
```

An *mdin* file that might go along with this, to perform a maximum of 5000 minimization cycles, starting with 500 cycles of steepest descent. PCSHIFT=./pcs.in redirects the input from the namelist "pcs.in" which contains the pseudocontact shift information.

```
Example of minimization including pseudocontact shift constraints
&cntrl
ibelly=0,imin=1,ntpr=100,
ntr=0,maxcyc=500,
ncyc=50,ntmin=1,dx0=0.0001,
drms=.1,cut=10.,
nmropt=2,pencut=0.1, ipnlty=2,
/
&wt type='REST', istep1=0,istep2=1,value1=0.,
value2=1.0, /
&wt type='END' /
DISANG=./noe.in
PCSHIFT=./pcs.in
LISTOUT=POUT
```

8.5 Direct dipolar coupling restraints

Energy restraints based on direct dipolar coupling constants are entered in this section. All variables are in the namelist &align; reading of this section is triggered by the presence of a DIPOLE line in the I/O redirection

section.

When dipolar coupling restraints are turned on, the five unique elements of the alignment tensor are treated as additional variables, and are optimized along with the structural parameters. Their effective masses are determined by the *scalm* parameter entered in the &cntrl namelist. Unlike some other programs, the variables used are the Cartesian components of the alignment tensor in the axis system defined by the molecule itself: *e.g.* $S_{mn} \equiv \langle (3\cos\theta_m \cos\theta_n - \delta_{mn})/2 \rangle$, where $m, n = x, y, z$, and θ_x is the angle between the x axis and the spectrometer field.[197] The factor of 10^5 is just to make the values commensurate with atomic coordinates, since both the coordinates and the alignment tensor values will be updated during the refinement. The calculated dipolar splitting is then

$$D_{calc} = - \left(\frac{10^{-5}\gamma_i\gamma_j h}{2\pi^2 r_{ij}^3} \right) \sum_{m,n=xyz} \cos\phi_m \cdot S_{mn} \cdot \cos\phi_n$$

where ϕ_x is the angle between the internuclear vector and the x axis. Geometrically, the splitting is proportional to the transformation of the alignment tensor onto the internuclear axis. This is just Eqs. (5) and (13) of the above reference, with any internal motion corrections (which might be a part of S_{system}) set to unity. If there is an internal motion correction which is the same for all observations, this can be assimilated into the alignment tensor. The current code does not allow for variable corrections for internal motion. See Ref. [198] for a fuller discussion of these issues.

At the end of the calculation, the alignment tensor is diagonalized to obtain information about its principal components. This allows the alignment tensor to be written in terms of the "axial" and "rhombic" components that are often used to describe alignment.

Variables in the &align namelist.

ndip   Number of observed dipolar couplings to be used as restraints.

id,jd   Atom numbers of the two atoms involved in the dipolar coupling.

dobsl, dobsu Limiting values for the observed dipolar splitting, in Hz. If the calculated coupling is less than *dobsl*, the energy penalty is proportional to $(D_{calc} - D_{obs,l})^2$; if it is larger than *dobsu*, the penalty is proportional to $(D_{calc} - D_{obs,lu})^2$. Calculated values between *dobsl* and *dobsu* are not penalized. Note that *dobsl* must be less than *dobsu*; for example, if the observed coupling is -6 Hz, and a 1 Hz "buffer" is desired, you could set *dobsl* to -7 and *dobsu* to -5.

dwt   The relative weight of each observed value. Default is 1.0. The penalty function is thus:

$$E_{align}^i = D_{wt}^i (D_{calc}^i - D_{obs(u,l)}^i)^2$$

where D_{wt} may vary from one observed value to the next. Note that the default value is arbitrary, and a smaller value may be required to avoid overfitting the dipolar coupling data.[198]

dataset   Each dipolar peak can be associated with a "dataset", and a separate alignment tensor will be computed for each dataset. This is generally used if there are several sets of experiments, each with a different sample or temperature, etc., that would imply a different value for the alignment tensor. By default, there is one dataset to which each observed value is assigned.

num_datasets The number of datasets in the constraint list. Default is 1.

s11,s12,s13,s22,s23 Initial values for the Cartesian components of the alignment tensor. The tensor is traceless, so S33 is calculated as -(S11+S22). In order to have the order of magnitude of the S values be roughly commensurate with coordinates in Angstroms, the alignment tensor values must be multiplied by 10^5.

gigj   Product of the nuclear "g" factors for this dipolar coupling restraint. These are related to the nuclear gyromagnetic rations by $\gamma_N = g_N \beta_N /$. Common values are ^{1}H = 5.5856, ^{13}C = 1.4048, ^{15}N = -0.5663, ^{31}P = 2.2632.

dij   The internuclear distance for observed dipolar coupling. If a nonzero value is given, the distance is considered to be fixed at the given value. If a *dij* value is zero, its value is computed from the structure, and it is assumed to be a variable distance. For one-bond couplings, it is usually best to treat the bond distance as "fixed" to an effective zero-point vibration value.[199]

dcut   Controls printing of calculated and observed dipolar couplings. Only values where abs(dobs(u,l) - dcalc) is greater than *dcut* will be printed. Default is 0.1 Hz. Set to a negative value to print all dipolar restraint information.

freezemol   If this is set to *.true.*, the molecular coordinates are not allowed to vary during dynamics or minimization: only the elements of the alignment tensor will change. This is useful to fit just an alignment tensor to a given structure. Default is *.false.*.

8.6 Residual CSA or pseudo-CSA restraints

Resonance positions in partially aligned media will be shifted from their positions in isotropic media, and this can provide information that is very similar to residual dipolar coupling constraints. This section shows how to input these sorts of restraints. The entry of the alignment tensor is done as in Section 8.5, so you must have a DIPOLE file (with an &align namelist) even if you don't have any RDC restraints. Then, if there is a CSA line in I/O redirection section, that file will be read with the following inputs:

Variables in the &csa namelist.

ncsa   Number of observed residual CSA peaks to be used as restraints.

icsa,jcsa,kcsa Atom numbers for the csa of interest: *jcsa* is the atom whose $\Delta\sigma$ value has been measured; *icsa* and *kcsa* are two atoms bonded to it, used to define the local axis frame for the CSA tensor. See *amber12/test/pcsa/RST.csa* for examples of how to set these.

cobsl, cobsu Limiting values for the observed residual CSA, in Hz (not ppm or ppb!). If the calculated value of $\Delta\sigma$ is less than *cobsl*, the energy penalty is proportional to $(\Delta\sigma_{calc} - \Delta\sigma_{obs,l})^2$; if it is larger than *cobsu*, the penalty is proportional to $(\Delta\sigma_{calc} - \Delta\sigma_{obs,u})^2$. Calculated values between *cobsl* and *cobsu* are not penalized. Note that *cobsl* must be less than *cobsu*.

cwt   The relative weight of each observed value. Default is 1.0. The penalty function is thus:

$$E_{csa}^i = C_{wt}^i (\Delta\sigma_{calc}^i - \Delta\sigma_{obs(u,l)}^i)^2$$

where C_{wt} may vary from one observed value to the next. Note that the default value is arbitrary, and a smaller value may be required to avoid overfitting the data.

datasetc Each residual CSA can be associated with a "dataset", and a separate alignment tensor will be computed for each dataset. This is generally used if there are several sets of experiments, each with a different sample or temperature, etc., that would imply a different value for the alignment tensor. By default, there is one dataset to which each observed value is assigned. The tensors themselves are entered for each dataset in the DIPOLE file.

field   Magnetic field (in MHz) for the residual CSA being considered here. This is indexed from 1 to *ncsa*, and is nucleus dependent. For example, if the proton frequency is 600 MHz, then *field* for ^{13}C would be 150, and that for ^{15}N would be 60.

sigma11, sigma22, sigma12, sigma13, sigma23 Values of the CSA tensor (in ppm) for atom *icsa*, in the local coordinate frame defined by atoms *icsa*, *jcsa* and *kcsa*. See *$AMBERHOME/test/pcsa/RST.csa* for examples of how to set these.

ccut   Controls printing of calculated and observed residual CSAs. Only values where abs(cobs(u,l) - ccalc) is greater than *ccut* will be printed. Default is 0.1 Hz. Set to a negative value to print all information.

The residual CSA facility is new as of Amber 10, and has not been used as much as other parts of the NMR refinement package. You should study the example files listed above to see how things work. The residual CSA values should closely match those found by the RAMAH package (*http://www-personal.umich.edu/~hashimi/Software.html*), and testing this should be a first step in making sure you have entered the data correctly.

8.7 Preparing restraint files for Sander

Fig. 8.1 shows the general information flow for auxiliary programs that help prepare the restraint files. Once the restraint files are made, Fig. 8.2 shows a flow-chart of the general way in which *sander* refinements are carried out.

The basic ideas of this scheme owe a lot to the general experience of the NMR community over the past decade. Several papers outline procedures in the Scripps group, from which a lot of the NMR parts of *sander* are derived.[190, 200–204] They are by no means the only way to proceed. We hope that the flexibility incorporated into *sander* will encourage folks to experiment with refinement protocols.

8.7.1 Preparing distance restraints: makeDIST_RST

The *makeDIST_RST* program converts a simplified description of distance bounds into a detailed input for *sander*. A variety of input and output filenames may be specified on the command line:

input:

```
-upb <filename> 7-col file of upper distance bounds, OR
-ual <filename> 8-col file of upper and lower bounds, OR
-vol <filename> 7-col file of NOESY volumes
-pdb <filename> Brookhaven format file
-map <filename> MAP file (default:map.DG-AMBER)
-les <filename> LES atom mappings, made by addles
```

output:

```
-dgm <filename> DGEOM95 restraint format
-rst <filename> SANDER restraint format
-svf <filename> Sander Volume Format, for NOESY refinement
```

other options:

```
-help (gives you this explanation, overrides other parameters)
-report (gives you short runtime diagnostic output)
-nocorr (do not correct upper bound for r**-6 averaging)
-altdis (use alternative form for the distance restraints)
```

The *7/8 column distance bound* file is essentially that used by the DIANA or DISGEO programs. It consists of one-line per restraint, which would typically look like the following:

```
23 ALA HA 52 VAL H 3.8 # comments go here
```

The first three columns identify the first proton, the next three the second proton, and the seventh column gives the upper bound. Only the first three letters of the residue name are used, so that DIANA files that contain residues like "ASP-" will be correctly interpreted. An alternate, 8-column, format has both upper and lower bounds as the seventh and eighth columns, respectively. A typical line might in an "8-col" file might look like this:
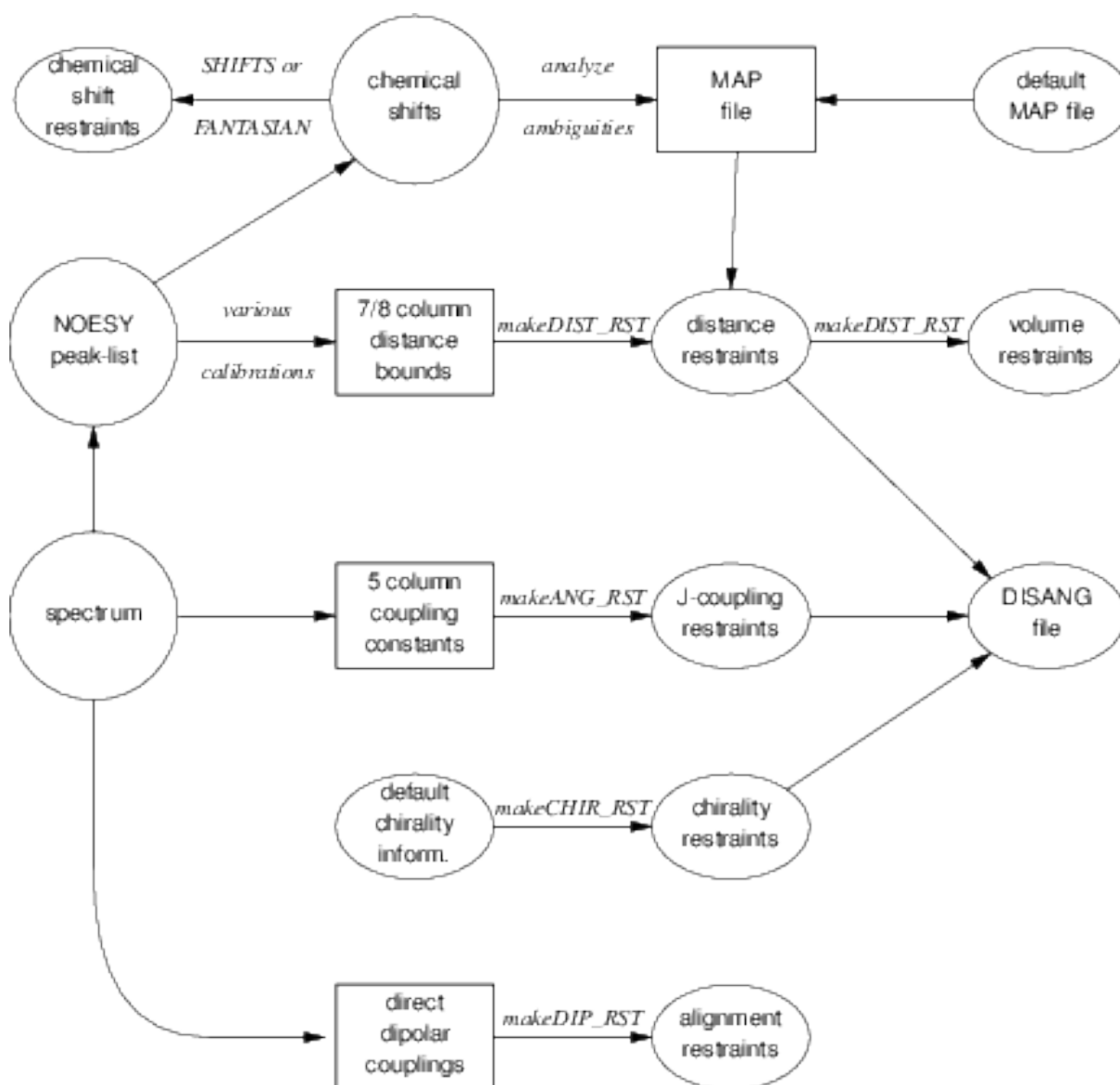
Figure 8.1: *Notation:* circles *represent logical information, whose format might differ from one project to the next;* solid rectangles *are in a specific format (largely compatible with DIANA and other programs), and are intended to be read and edited by the user;* ellipses *are specific to* sander, *and are generally not intended to be read or edited manually. The conversion of NOESY volumes to distance bounds can be carried out by a variety of programs such as* mardigras *or* xpk2bound *that are not included with Amber. Similarly, the analysis and partial assignment of ambiguous or overlapped peaks is a separate task; at TSRI, these are typically carried out using the programs* xpkasgn *and* filter.pl
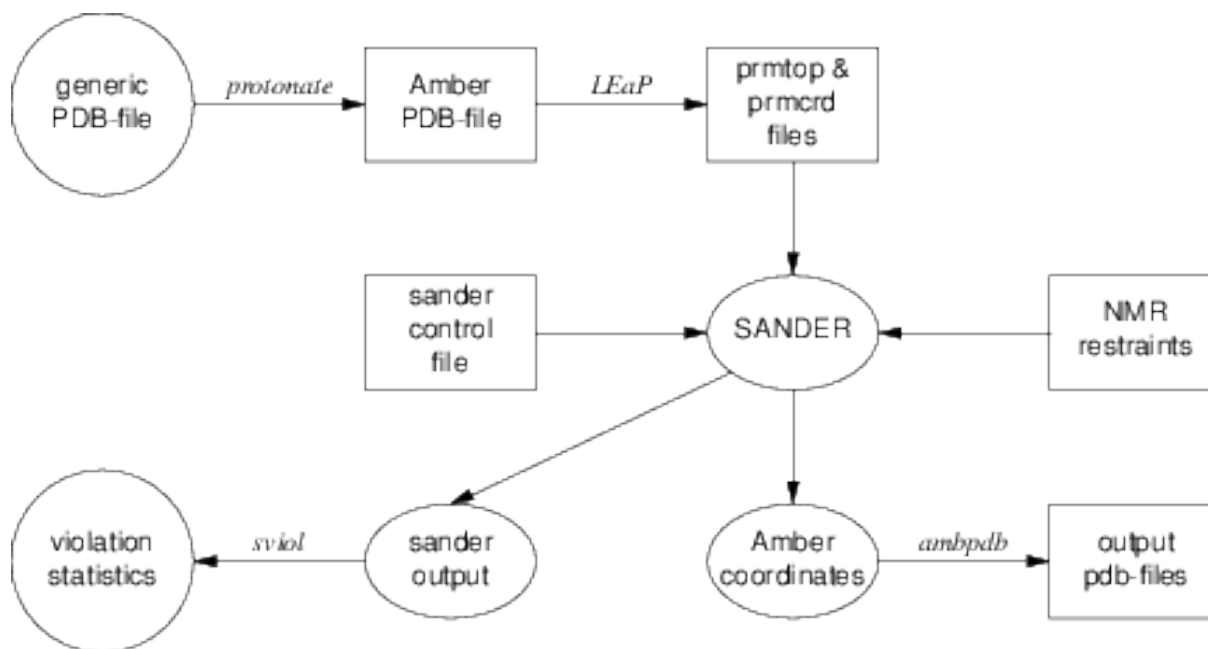
Figure 8.2: *General organization of NMR refinement calculations.*

```
23 ALA HA 52 VAL H 3.2 3.8 # comments go here
```

Here the lower bound is 3.2 Åand the upper bound is 3.8 Å. Comments typically identify the spectrum and peak-number or other identification that allow cross-referencing back to the appropriate spectrum. If the comment contains the pattern "<integer>:<integer>", then the first integer is treated as a peak-identifier, and the second as a spectrum-identifier. These identifiers go into the *ixpk* and *nxpk* variables, and will later be printed out in *sander*, to facilitate going back to the original spectra to track down violations, etc.

The format for the *-vol* option is the same as for the *-upb* option except that the seventh column holds a peak intensity (volume) value, rather than a distance upper bound.

The input PDB file must exactly match the Amber *prmtop* file that will be used; use the ambpdb -aatm command to create this.

If all peaks involved just single protons, and were fully assigned, this is all that one would need. In general, though, some peaks (especially methyl groups or fast-rotating aromatic rings) represent contributions from more than one proton, and many other peaks may not be fully assigned. *Sander* handles both of these situations in the same way, through the notion of an "ambiguous" peak, that may correspond to several assignments. These peaks are given two types of special names in the 7/8-column format file:

1. Commonly-occurring ambiguities, like the lack of stereospecific assignments to two methylene protons, are given names defined in the default MAP file. These names, also more-or-less consistent with DIANA, are like the names of "pseudo-atoms" that have long been used to identify such partially assigned peaks, e.g. "QB" refers to the (HB2,HB3) combination in most residues, and "MG1" in valine refers collectively to the three methyl protons at position CG1, etc.

2. There are generally also molecule-specific ambiguities, arising from potential overlap in a NOESY spectrum. Here, the user assigns a unique name to each such ambiguity or overlap, and prepares a list of the potential assignments. The names are arbitrary, but might be constructed, for example, from the chemical shifts that identify the peak, e.g. "p_2.52" might identify the set of protons that could contribute to a peak at 2.52 ppm. The chemical shift list can be used to prepare a list of potential assignments, and these lists can often be pruned by comparison to approximate or initial structures.

The default and molecule-specific MAP files are combined into a single file, which is used, along with the 7-column restraint file, the the program *makeDIST_RST* to construct the actual *sander* input files. You should

consult the help file for makeDIST_RST for more information. For example, here are some lines added to the MAP file for a recent TSRI refinement:

```
AMBIG n2:68 = HE 86 HZ 86
AMBIG n2:72 = HE 24 HD 24 HZ 24
AMBIG n2:73 = HN 81 HZ 13 HE 13 HD 13 HZ 24
AMBIG n2:78 = HN 76 HZ 13 HE 13 HZ 24
AMBIG n2:83 = HN 96 HN 97 HD 97 HD 91
AMBIG n2:86 = HD1 66 HZ2 66
AMBIG n2:87 = HN 71 HH2 66 HZ3 66 HD1 66
```

Here the spectrum name and peak number were used to construct a label for each ambiguous peak. Then, an entry in the restraint file might look like this:

```
123 GLY HN 0 AMB n2:68 5.5
```

indicating a 5.5 åupper bound between the amide proton of Gly 123 and a second proton, which might be either the HE or HZ protons of residue 86. (The "zero" residue number just serves as a placeholder, so that there will be the same number of columns as for non-ambiguous restraints.) If it is possible that the ambiguous list might not be exhaustive (e.g. if some protons have not been assigned), it is safest to set *ialtd*=1, which will allow "mistakes" to be present in the constraint list. On the other hand, if you want to be sure that every violation is "active", set *ialtd*=0.

If the *-les* flag is set, the program will prepare distance restraints for multiple copies (LES) simulations. In this case, the input PDB file is one *without* LES copies, i.e. with just a single copy of the molecule. The "lesfile" specified by this flag is created by the *addles* program, and contains a mapping from original atom numbers into the copy numbers used in the multiple-copies simulation.

The *-rst* and *-svf* flags specify outputs for *sander*, for distance restraints and NOESY restraints, respectively. In each case, you may need to hand-edit the outputs to add additional parameters. You should make it a habit to compare the outputs with the descriptions given earlier in this chapter to make sure that the restraints are what you want them to be.

It is common to run makeDIST_RST several times, with different inputs that correspond to different spectra, different mixing times, etc. It is then expected that you will manually edit the various output files to combine them into the single file required by *sander*.

8.7.2 Preparing torsion angle restraints: makeANG_RST

There are fewer "standards" for representing coupling constant information. We have followed the DIANA convention in the program *makeANG_RST*. This program takes as input a five-column torsion angle constraint file along with an Amber PDB file of the molecule. It creates as output (to standard out) a list of constraints in RST format that is readable by Amber.

```
Usage: makeANG_RST -help
makeANG_RST -pdb ambpdb_file [-con constraint] [-lib libfile]
[-les lesfile ]
```

The input torsion angle constraint file can be read from standard in or from a file specified by the -con option on the command line. The input constraint file should look something like this:

```
1 GUA PPA 111.5 144.0
2 CYT EPSILN 20.9 100.0
2 CYT PPA 115.9 134.2
3 THY ALPHA 20.4 35.6
4 ADE GAMMA 54.7 78.8
5 GLY PHI 30.5 60.3
6 ALA CHI 20.0 50.0
....
```

Lines beginning with "#" are ignored. The first column is the residue number; the second is the residue name (three letter code, or as defined in your personal torsion library file). Only the first three letters of the residue name are used, so that DIANA files that contain residues like "ASP-" will be correctly interpreted. Third is the angle name (taken from the torsion library described below).The fourth column contains the lower bound, and the fifth column specifies the upper bound. Additional material on the line is (presently) ignored.

Note: It is assumed that the lower bound and the upper bound define a region of allowed conformation on the unit circle that is swept out in a clockwise direction from $lb \to ub$. If the number in the lb column is greater than the the number in the ub column, 360°will successively be subtracted from the lb until $lb < ub$. This preserves the clockwise definition of the allowed conformation space, while also making the number that specifies the lower bound less than the number that specifies the upper bound, as is required by Amber. If this occurs, a warning message will be printed to *stderr* to notify the user that the data has been modified.

The angles that one can constrain in this manner are defined in the library file that can be optionally specified on the command line with the -lib flag, or the default library "tordef.lib" (written by Garry P. Gippert) will be used. If you wish to specify your own nomenclature, or add angles that are not already defined in the default file, you should make a copy of this file and modify it to suit your needs. The general format for an entry in the library is:

```
LEU PSI N CA C N+
```

where the first column is the residue name, the second column is the angle name that will appear in the input file when specifying this angle, and the last four columns are the atom names that define the torsion angle. When a torsion angle contains atom(s) from a preceding or succeeding residue in the structure, a "-" or "+" is appended to those atom names in the library, thereby specifying that this is the case. In the example above, the atoms that define PSI for LEU residues are the N, CA, and C atoms of that same LEU and the N atom of the residue after that LEU in the primary structure. Note that the order of atoms in the definition is important and should reflect that the torsion angle rotates about the two central atoms as well as the fact that the four atoms are bonded in the order that is specified in the definition.

If the first letter of the second field is "J", this torsion is assumed to be a J-coupling constraint. In that case, three additional floats are read at the end of the line, giving the A,B and C coefficients for the Karplus relation for this torsion. For example:

```
ALA JHNA H N CA HA 9.5 -1.4 0.3
```

will set up a J-coupling restraint for the HN-HA 3-bond coupling, assuming a Karplus relation with A,B, C as 9.5, -1.4 and 0.3. (These particular values are from Brüschweiler and Case, JACS 116: 11199 (1994).)

This program also supports pseudorotation phase angle constraints for prolines and nucleic acid sugars; each of these will generate restraints for the 5 component angles which correspond to the lb and ub values of the input pseudorotation constraint. In the torsion library, a pseudorotation definition looks like:

```
PSEUDO CYT PPA NU0 NU1 NU2 NU3 NU4
CYT NU0 C4' O4' C1' C2'
CYT NU1 O4' C1' C2' C3'
CYT NU2 C1' C2' C3' C4'
CYT NU3 C2' C3' C4' O4'
CYT NU4 C3' C4' O4' C1'
```

The first line describes that a PSEUDOrotation angle is to be defined for CYT that is called PPA and is made up of the five angles NU0-NU4. Then the definition for NU0-NU4 should also appear in the file in the same format as the example given above for LEU PSI.

PPA stands for Pseudorotation Phase Angle and is the angle that should appear in the input constraint file when using pseudorotation constraints. The program then uses the definition of that PPA angle in the library file to look for the 5 other angles (NU0-NU4 in this case) which it then generates restraints for. PPA for proline residues is included in the standard library as well as for the DNA nucleotides.

If the *-les* flag is set, the program will prepare torsion angle restraints for multiple copies (LES) simulations. In this case, the input PDB file is one *without* LES copies, i.e. with just a single copy of the molecule. The "lesfile" specified by this flag is created by the *addles* program, and contains a mapping from original atom numbers into the copy numbers used in the multiple-copies simulation.

Torsion angle constraints defined here cannot span two different copy sets, i.e., there cannot be some atoms of a particular torsion that are in one multiple copy set, and other atoms from the same torsion that are in other copy sets. It *is* OK to have some atoms with single copies, and others with multiple copies in the same torsion. The program will create as many duplicate torsions as there are copies.

A good alternative to interpreting J-coupling constants in terms of torsion angle restraints is to refine directly against the coupling constants themselves, using an appropriate Karplus relation. See the discussion of the variable RJCOEF, above.

8.7.3 Chirality restraints: makeCHIR_RST

> **Usage: makeCHIR_RST <pdb-file> <output-constraint-file>**

We also find it useful to add chirality constraints and *trans*-peptide ω constraints (where appropriate) to prevent chirality inversions or peptide bond flips during the high-temperature portions of simulated annealing runs. The program *makeCHIR_RST* will create these constraints. Note that you may have to edit the output of this program to change *trans* peptide constraints to *cis*, as appropriate.

8.7.4 Direct dipolar coupling restraints: makeDIP_RST

For simulations with residual dipolar coupling restraints, the *makeDIP_RST.protein*, *makeDIP_RST.dna* and *makeDIP_RST.diana* are simple codes to prepare the input file. Use *-help* to obtain a more detailed description of the usage. For now, this code only handles backbone NH and CαH data. The header specifying values for various parameters needs to be manually added to the output of *makeDIP_RST*.

Use of residual dipolar coupling restraints is new both for Amber and for the general NMR community. Refinement against these data should be carried out with care, and the optimal values for the force constant, penalty function, and initial guesses for the alignment tensor components are still under investigation. Here are some suggestions from the experiences so far:

1. Beware of overfitting the dipolar coupling data in the expense of Amber force field energy. These dipolar coupling data are very sensitive to tiny changes in the structure. It is often possible to drastically improve the fitting by making small distortions in the backbone angles. We recommend inclusion of explicit angle restraints to enforce ideal backbone geometry, especially for those residues that have corresponding residual dipolar coupling data.

2. The initial values for the Cartesian components of the alignment tensor can influence the final structure and alignment if the structure is not fixed (ibelly = 0). For a fixed structure (ibelly = 1), these values do not matter. Therefore, the current "best" strategy is to fit the experimental data to the fixed starting structure, and use the alignment tensor[s] obtained from this fitting as the initial guesses for further refinement.

3. Amber is capable of simultaneously fitting more than one set of alignment data. This allows the use of individually obtained datasets with different alignment tensors. However, if the different sets of data have equal directions of alignment but different magnitudes, using an overall scaling factor for these data with a single alignment tensor could greatly reduce the number of fitting parameters.

4. Because the dipolar coupling splittings depend on the square root of the order parameters ($0 \le S2 \le 1$), these order parameters describing internal motion of individual residues are often neglected (N. Tjandra and A. Bax, *Science* **278**, 1111-1113, 1997). However, the square root of a small number can still be noticeably smaller than 1, so this may introduce undesirable errors in the calculations.

8.7.5 Using NMR exchange format (NEF) files

The NMR community, in collaboration with the worldwide PDB, is developing a common format for encoding of NMR restraints, including all of the kinds discussed above. This format is not yet finalized, but we are including here a conversion script, *nef_to_RST*, that would convert these files to *sander* format. Because this format is so new, and is still subject to revisions, care should be taken in using this script: make sure that the

output files do what they should be doing. Here are the usage instructions (which you can also get by typing "nef_to_RST -help" at the command line:

```
# nef_to_RST
convert NEF restraints to Amber format
input:
   -nef <filename>: NEF file
   -pdb <filename>: PDBFILE using AMBER nomenclature and numbering
   -map <filename>: MAP file  (default:map.NEF-AMBER)
output:
   -rst <filename>:  SANDER restraint format
   -rdc <filename>:  SANDER DIP format

other options:
   -nocorr (do not correct upper bound for r**-6 averaging)
   -altdis (use alternative form for the distance restraints)
   -help   (gives you this explanation, overrides other parameters)
   -report (gives you short runtime diagnostic output)
errors come to stderr.
```

8.8 Getting summaries of NMR violations

If you specify LISTOUT=POUT when running *sander*, the output file will contain a lot of detailed information about the remaining restraint violations at the end of the run. When running a family of structures, it can be useful to process these output files with *sviol*, which takes a list of *sander* output files on the command line, and sends a summary of energies and violations to STDOUT. If you have more than 20 or so structures to analyze, the output from *sviol* becomes unwieldy. In this case you may also wish to use *sviol2*, which prints out somewhat less detailed information, but which can be used on larger families of structures. The *senergy* script gives a more detailed view of force-field energies from a series of structures. (We thank the TSRI NMR community for helping to put these scripts together, and for providing many useful suggestions.)

8.9 Time-averaged restraints

The model of the previous sections involves the "single-average-structure" idea, and tries to fit all constraints to a single model, with minimal deviations. A generalization of this model treats distance constraints arising from from NOE crosspeaks (for example) as being the average distance determined from a trajectory, rather than as the single distance derived from an average structure.

Time-averaged bonds and angles are calculated as

$$\bar{r} = (1/C) \left\{ \int_0^t e^{(t'-t)/\tau} r(t')^{-i} dt' \right\}^{-1/i} \tag{8.1}$$

where

$\bar{r}$ = time-averaged value of the internal coordinate (distance or angle)

t = the current time

τ = the exponential decay constant

$r(t')$ = the value of the internal coordinate at time t'

i = average is over internals to the inverse of i. Usually $i = 3$ or 6 for NOE distances, and -1 (linear averaging) for angles and torsions.

C = a normalization integral.

Time-averaged torsions are calculated as

$$< \varphi > = \tan^{-1}(< \sin(\phi) > / < \cos(\phi) >)$$

where ϕ is the torsion, and $< \sin(\phi) >$ and $< \cos(\phi) >$ are calculated using the equation above with $\sin(\phi(t'))$ or $\cos(\phi(t'))$ substituted for $r(t')$.

Forces for time-averaged restraints can be calculated either of two ways. This option is chosen with the DISAVI / ANGAVI / TORAVI commands. In the first (the default),

$$\partial E/\partial x = (\partial E/\partial \bar{r})(\partial \bar{r}/\partial r(t))(\partial r(t)/\partial x) \qquad (8.2)$$

(and analogously for y and z). The forces then correspond to the standard flat-bottomed well functional form, with the instantaneous value of the internal replaced by the time-averaged value. For example, when $r_3 < \bar{r} < r_4$,

$$E = k_3(\bar{r} - r_3)^2$$

and similarly for other ranges of $\bar{r}$.

When the second option for calculating forces is chosen (IINC = 1 on a DISAVI, ANGAVI or TORAVI card), forces are calculated as

$$\partial E/\partial x = (\partial E/\partial \bar{r})(\partial r(t)/\partial x) \qquad (8.3)$$

For example, when $r_3 < \bar{r} < r_4$,

$$\partial E/\partial x = 2k_3(\bar{r} - r_3)(\partial r(t)/\partial x)$$

Integration of this equation does not give Eq. 8.2, but rather a non-intuitive expression for the energy (although one that still forces the bond to the target range). The reason that it may sometimes be preferable to use this second option is that the term $\partial \bar{r}/\partial r(t)$, which occurs in the exact expression [Eq. 8.2], varies as $(\bar{r}/r(t))^{1+i}$. When i=3, this means the forces can be varying with the fourth power the distance, which can possibly lead to very large transient forces and instabilities in the molecular dynamics trajectory. [Note that this will not be the case when linear scaling is performed, i.e. when $i = -1$, as is generally the case for valence and torsion angles. Thus, for linear scaling, the default (exact) force calculation should be used].

It should be noted that forces calculated using Eq. 8.3 are not conservative forces, and would cause the system to gradually heat up, if no velocity rescaling were performed. The temperature coupling algorithm should act to maintain the average temperature near the target value. At any rate, this heating tendency should not be a problem in simulations, such as fitting NMR data, where MD is being used to sample conformational space rather than to extract thermodynamic data.

This section has described the methods of time-averaged restraints. For more discussion, the interested user is urged to consult studies where this method has been used.[205–209]

8.10 Multiple copies refinement using LES

NMR restraints can be made compatible with the multiple copies (LES) facility; see the following chapter for more information about LES. To use NMR constraints with LES, you need to do two things:

(1) Add a line like "file wnmr name=(lesnmr) wovr" to your input to *addles*. The filename (lesnmr in this example) may be whatever you wish. This will cause *addles* to output an additional file that is needed at the next step.

(2) Add "-les lesnmr" to the command line arguments to *makeDIST_RST*. This will read in the file created by *addles* containing information about the copies. All NMR restraints will then be interpreted as "ambiguous" restraints, so that if any of the copies satisfies the restraint, the penalty goes to zero.

Note that although this scheme has worked well on small peptide test cases, we have yet not used it extensively for larger problems. This should be treated as an experimental option, and users should use caution in applying or

interpreting the results.

8.11 Some sample input files

The next few pages contain excerpts from some sample NMR refinement files used at TSRI. The first example just sets up a simple (but often effective) simulated annealing run. You may have to adjust the length, temperature maximum, etc. somewhat to fit your problem, but these values work well for many "ordinary" NMR problems.

8.11.1 1. Simulated annealing NMR refinement

```
15ps simulated annealing protocol
&cntrl
  nstlim=15000, ntt=1, !(time limit, temp. control)
  ntpr=500, pencut=0.1, !(control of printout)
  ipnlty=1, nmropt=1, !(NMR penalty function options)
  vlimit=10, !(prevent bad temp. jumps)
  ntb=0, !(non-periodic simulation)
  igb=8, !(generalize Born solvent model)
/
#
# Simple simulated annealing algorithm:
#
# from steps 0 to 1000: raise target temperature 10-1200K
# from steps 1000 to 3000: leave at 1200K
# from steps 3000 to 15000: re-cool to low temperatures
#
&wt type='TEMP0', istep1=0,istep2=1000,value1=10.,
  value2=1200., /
&wt type='TEMP0', istep1=1001, istep2=3000, value1=1200.,
  value2=1200.0, /
&wt type='TEMP0', istep1=3001, istep2=15000, value1=0.,
  value2=0.0, /
#
# Strength of temperature coupling:
# steps 0 to 3000: tight coupling for heating and equilibration
# steps 3000 to 11000: slow cooling phase
# steps 11000 to 13000: somewhat faster cooling
# steps 13000 to 15000: fast cooling, like a minimization
#
&wt type='TAUTP', istep1=0,istep2=3000,value1=0.2,value2=0.2, /
&wt type='TAUTP', istep1=3001,istep2=11000,value1=4.0,value2=2.0, /
&wt type='TAUTP', istep1=11001,istep2=13000,value1=1.0,value2=1.0, /
&wt type='TAUTP', istep1=13001,istep2=14000,value1=0.5,value2=0.5, /
&wt type='TAUTP', istep1=14001,istep2=15000,value1=0.05,value2=0.05, /
#
# "Ramp up" the restraints over the first 3000 steps:
#
&wt type='REST', istep1=0,istep2=3000,value1=0.1,value2=1.0, /
&wt type='REST', istep1=3001,istep2=15000,value1=1.0,value2=1.0, /
&wt type='END' /
LISTOUT=POUT (get restraint violation list)
DISANG=RST.f (file containing NMR restraints)
```

The next example just shows some parts of the actual RST file that *sander* would read. This file would ordinarily *not* be made or edited by hand; rather, run the programs *makeDIST_RST*, *makeANG_RST* and *makeCHIR_RST*, combining the three outputs together to construct the RST file.

8.11.2 Part of the RST.f file referred to above

```
# first, some distance constraints prepared by makeDIST_RST:
 # (comment line is input to makeRST, &rst namelist is output)
 #
 #( proton 1 proton 2 upper bound)
 #---------------------------------------------
 #
 # 2 ILE HA 3 ALA HN 4.00
 #
 &rst iat= 23, 40, r3= 4.00, r4= 4.50,
 r1 = 1.3, r2 = 1.8, rk2=0.0, rk3=32.0, ir6=1, /
 #
 # 3 ALA HA 4 GLU HN 4.00
 #
 &rst iat= 42, 50, r3= 4.00, r4= 4.50, /
 #
 # 3 ALA HN 3 ALA MB 5.50
 #
 &rst iat= 40, -1, r3= 6.22, r4= 6.72,
 igr1= 0, 0, 0, 0, igr2= 44, 45, 46, 0, /
 #
 # .......etc......
 #
 # next, some dihedral angle constraints, from makeANG_RST:
 #
 &rst iat= 213, 215, 217, 233, r1=-190.0,
 r2=-160.0, r3= -80.0, r4= -50.0, /
 &rst iat= 233, 235, 237, 249, r1=-190.0,
 r2=-160.0, r3= -80.0, r4= -50.0, /
 # .......etc.......
 #
 # next, chirality and omega constraints prepared by makeCHIR_RST:
 #
 #
 # chirality for residue 1 atoms: CA CG HB2 HB3
 &rst iat= 3 , 8 , 6 , 7 ,
 r1=10., r2=60., r3=80., r4=130., rk2 = 10., rk3=10., /
 #
 # chirality for residue 1 atoms: CB SD HG2 HG3
 &rst iat= 5 , 11 , 9 , 10 , /
 #
 # chirality for residue 1 atoms: N C HA CB
 &rst iat= 1 , 18 , 4 , 5 , /
 #
 # chirality for residue 2 atoms: CA CG2 CG1 HB
 &rst iat= 22 , 26 , 30 , 25 , /
 #
 ......etc........
 # trans-omega constraint for residue 2
 &rst iat= 22 , 20 , 18 , 3 ,
 r1=155., r2=175., r3=185., r4=205., rk2 = 80., rk3=80., /
 #
```

```
    # trans-omega constraint for residue 3
    &rst iat= 41 , 39 , 37 , 22 , /
    #
    # trans-omega constraint for residue 4
    &rst iat= 51 , 49 , 47 , 41 , /
    #
    # ......etc........
    #
    The next example is an input file for volume-based NOE refinement. As with the distan
```

8.11.3 3. Sample NOESY intensity input file

```
 # A part of a NOESY intensity file:
  &noeexp
  id2o=1, (exchangeable protons removed)
  oscale=6.21e-4, (scale between exp. and calc. intensity units)
  taumet=0.04, (correlation time for methyl rotation, in ns.)
  taurot=4.2, (protein tumbling time, in ns.)
  NPEAK = 13*3, (three peaks, each with 13 mixing times)
  EMIX = 2.0E-02, 3.0E-02, 4.0E-02, 5.0E-02, 6.0E-02,
  8.0E-02, 0.1, 0.126, 0.175, 0.2, 0.25, 0.3, 0.35,
  (mixing times, in sec.)
  IHP(1,1) = 13*423, IHP(1,2) = 13*1029, IHP(1,3) = 13*421,
  (number of the first proton)
  JHP(1,1) = 78*568, JHP(1,2) = 65*1057, JHP(1,3) = 13*421,
  (number of the second proton)
  AEXP(1,1) = 5.7244, 7.6276, 7.7677, 9.3519,
  10.733, 15.348, 18.601,
  21.314, 26.999, 30.579,
  33.57, 37.23, 40.011,
  (intensities for the first cross-peak)
  AEXP(1,2) = 8.067, 11.095, 13.127, 18.316,
  22.19, 26.514, 30.748,
  39.438, 44.065, 47.336,
  54.467, 56.06, 60.113,
  AEXP(1,3) = 7.708, 13.019, 15.943, 19.374,
  25.322, 28.118, 35.118,
  40.581, 49.054, 53.083,
  56.297, 59.326, 62.174,
  /
  SUBMOL1
  RES 27 27 29 29 39 41 57 57 70 70 72 72 82 82 (residues in this submol)
 END END
```

Next, we illustrate the form of the file that holds residual dipolar coupling restraints. Again, this would generally be created from a human-readable input using the program *makeDIP_RST*.

8.11.4 Residual dipolar restraints, prepared by makeDIP_RST:

```
 &align
 ndip=91, dcut=-1.0, gigj = 37*-3.1631, 54*7.8467,
 s11=3.883, s22=53.922, s12=33.855, s13=-4.508, s23=-0.559,
 id(1)=188, jd(1)=189, dobsu(1)= 6.24, dobsl(1)= 6.24,
```

```
    id(2)=208, jd(2)=209, dobsu(2)= -10.39, dobsl(1)= -10.39,
    id(3)=243, jd(3)=244, dobsu(3)= -8.12, dobsl(1)= -8.12,
    ....
    id(91)=1393, jd(91)=1394, dobsu(91)= -19.64, dobsl(91) = -19.64,
    /
```

Finally, we show how the detailed input to *sander* could be used to generate a more complicated restraint. Here is where the user would have to understand the details of the RST file, since there are no "canned" programs to create this sort of restraint. This illustrates, though, the potential power of the program.

8.11.5 A more complicated constraint

```
# 1) Define two centers of mass. COM1 is defined by
# {C1 in residue 2; C1 in residue 3; N2 in residue 4; C1 in residue 5}.
# COM2 is defined by {C4 in residue 1; O4 in residue 1; N* in residue 1}.
# (These definitions are effected by the igr1/igr2 and grnam1/grnam2
# variables; You can use up to 200 atoms to define a center-of-mass
# group)
#
# 2) Set up a distance restraint between COM1 and COM2 which goes from a
# target value of 5.0A to 2.5A, with a force constant of 1.0, over steps 1-5000.
#
# 3) Set up a distance restraint between COM1 and COM2 which remains fixed
# at the value of 2.5A as the force slowly constant decreases from
# 1.0 to 0.01 over steps 5001-10000.
#
# 4) Sets up no distance restraint past step 10000, so that free (unrestrained)
# dynamics takes place past this step.
#
&rst iat=-1,-1, nstep1=1,nstep2=5000,
  iresid=1,irstyp=0,ifvari=1,ninc=0,imult=0,ir6=0,ifntyp=0,
  r1=0.00000E+00,r2=5.0000,r3=5.0000, r4=99.000,rk2=1.0000,rk3=1.0000,
  r1a=0.00000E+00,r2a=2.5000,r3a=2.5000, r4a=99.000,rk2a=1.0000,rk3a=1.0000,
  igr1 = 2,3,4,5,0, grnam1(1)='C1',grnam1(2)='C1',grnam1(3)='N2',
  grnam1(4)='C1', igr2 = 1,1,1,0, grnam2(1)='C4',grnam2(2)='O4',grnam2(3)='N*',
/
&rst iat=-1,-1, nstep1=5001,nstep2=10000,
  iresid=1,irstyp=0,ifvari=1,ninc=0,imult=0,ir6=0,ifntyp=0,
  r1=0.00000E+00,r2=2.5000,r3=2.5000, r4=99.000,rk2=1.0000,rk3=1.0000,
  r1a=0.00000E+00,r2a=2.5000,r3a=2.5000, r4a=99.000,rk2a=1.0000,rk3a=0.0100,
  igr1 = 2,3,4,5,0, grnam1(1)='C1',grnam1(2)='C1',grnam1(3)='N2',
  grnam1(4)='C1', igr2 = 1,1,1,0, grnam2(1)='C4',grnam2(2)='O4',grnam2(3)='N*',
/
```

9 Xray and cryoEM refinement

9.1 EMAP restraints for rigid and flexible fitting into EM maps

EMAP restrained simulation[20, 210] was developed to incorporate electron microscopy (EM) image information into macromolecular structure determination. Different from NMR and X-ray data, EM images have low resolutions (5~50Å). However, EM images of large molecular assemblies up to millions of atoms and in various biologically relevant environments are available. These low resolution images provide precious structural information that can help to determine structures of many molecular assemblies and machineries[210–220].

With EMAP restraints, Sander and PMEMD can be used to perform both rigid[210] and flexible[20] fitting of molecules into experimental maps of complexes to obtain both complex structures and conformations agreeing with experimental maps. In addition to experimental map information, homologous structural information can be used by EMAP to perform targeted conformational search (TCS) to induce simulation systems to form structures of interest.

If the restraint map or structure is very different from the starting conformation, SGLD is recommended to induce large conformational change by setting *isgld*=1. This is often used to simulate conformational transition between different states. See the Sampling and free energy search section 6.1 for details on running SGLD.

If domain motion is desired while domain structures need to be maintained, one can use an EMAP restraint generated from the initial coordinates for each domain and set *move*=1 to allow the restraint map to move with the domain, so that domains can search the conformational space without unfolding or changing shape.

Each EMAP restraint is defined by a map file and a selection of atoms, as well as related parameters. Multiple EMAP restraints can be defined. The map can be either input from an image file, or generated from a pdb structure or derived from the starting coordinates. The definition of EMAP restraints are read in from the input file as "&emap" namelists. The following are variables in each &emap namelist.

mapfile   The filename of a restraint map or structure. The restraint maps must be in "map", "ccp4", or "mrc" format. The structure must be in pdb format. The structure need not be the same as the simulation system. A resolution can be specified for the conversion to a density map. When a blank filename is specified, *mapfile*=", the input coordinates of the masked atoms will be used to generate a restraint map (default=").

atmask   The atom mask for selecting atoms to be restrained (default=':*').

fcons   The restraining constant (default=0.05 kcal/g).

move   Allow the restraint map to move when *move*>0 (default=0).

resolution The resolution used to convert an atomic structure to a map (default=2 Å).

ifit   Perform rigid fitting before simulation when *ifit*>0. One would do this when the initial coordinates don't match those of the map (default=0). When ifit=1, the map is transformed (by translation and rotation) to match the coordinates; the coordinates are not altered. EMAP allows output of the re-oriented map (*mapfit*=...) that matches the (final) simulation coordinates, *and/or* output of the coordinates (*molfit*=...) that would match the orientation of the original map. When ifit=2, the masked atoms will be transformed to fit the map and the transformed coordinates will be used for the following simulation. For periodic systems, ifit=2 may cause atoms to clash with periodic image atoms.

grids   Grid numbers in x,y,z,phi,psi,theta dimensions for grid-threading rigid fitting[210]. For example, grids=2,2,2,3,3,3 defines 2 grid points in each of x,y,z directions between the minimum and maximum coordinates, and 3 grid points in each of phi (0-360), psi(0-360), theta(0-180) angles. A

search for local minimums starts from every grid point and the global minimum is identified from all the local minimums (default=1,1,1,1,1,1).

mapfit   The filename for the final constraint map after rigid fitting and/or moving. The filename must has an extension of .map, .ccp4, or .mrc (default=″, for no map output).

molfit   The filename for the final restrained atom coordinates after rigid fitting and/or simulation. The filename must have an extension of .pdb (default=″, for no structure output).

Here is an example input file for an EMAP constrained SGLD simulation:

```
Map Constraint Self-Guided Langevin dynamics
&cntrl ntx=1, ntb=0,nstlim=100000, imin=0, maxcyc=1, ntc=2, ntf=2, cut=9.0,
ntpr=1000, ntwr=100000,ntwx=10000, ntt=3, gamma_ln=10.0,nscm=100, dt=0.001,
ntb=0,igb=0, isgld=1, tsgavg=1.0, sgft=0.5,tempsg=0,          (SGLD)
iemap=1,                       (turn on EMAP )
/
&emap         (EMAP restraint 1 )
mapfile='data/1gb1.ccp4',  (map is input from a map file)
atmask=':1-20',             (residues 1-20 are restrained)
fcons=0.1,
move=1,                     (restraint map can move)
ifit=1,                     (perform rigid fitting first)
mapfit='scratch/gb1n_1.ccp4',  (final map)
molfit='scratch/gb1n_1.pdb', / (final restrained atoms related to initial map)
&emap         (EMAP restraint 2)
mapfile='data/1gb1.pdb',  (map is generated from a pdb file)
atmask=':22-37',           (residues 22-37 are restrained)
fcons=0.1,move=0,          (restraint map is fixed)
ifit=1,                    (perform rigid fitting first)
mapfit='scratch/gb1h_1.ccp4',   (final map, same as initial)
molfit='scratch/gb1h_1.pdb', / (final restrained atoms related to initial map)
&emap         (EMAP restraint 3)
mapfile='',    (map is generated from initial coordinates)
atmask=':41-56',  (residues 41-56 are restrained)
fcons=0.1,move=1, (restraint map can move)
ifit=1,        (perform rigid fitting first)
mapfit='scratch/gb1c_1.ccp4',  (final map)
molfit='scratch/gb1c_1.pdb', / (final restrained atoms related to initial map)
```

9.2 Setting up crystal simulations

David S. Cerutti

Simulations of biomolecular crystals are in principle no different than any of the simulations that AMBER does in periodic boundary conditions. However, the setup of these systems is not trivial and probably cannot be accomplished with the LEaP software. Of principal importance are the construction of the solvent conditions (packing precise amounts of multiple solvent species into the simulation cell), and tailoring the unit cell dimensions to accommodate the inherently periodic nature of the system. The LEaP software, designed to construct simulations of molecules in solution, will overlay a pre-equilibrated solvent mask over the (biomolecular) solute, tile that mask throughout the simulation cell, and then prune solvent residues which clash with the solute. The result of this procedure is a system which will likely contract under constant pressure dynamics as the pruning process has left vacuum bubbles at the solute:solvent interface. Simulations of biomolecular crystals require that the simulation cell begin at a size corresponding to the crystallographic unit cell, and deviate very little from that size over the course of equilibration and onset of constant pressure dynamics. This demands a different strategy for placing solvent

in the simulation cell. Four programs in the *AmberTools* release are designed to accomplish this. An example of their use in given in a web-based tutorial at *https://ambermd.org/tutorials/advanced/tutorial13/XtalTutor1.html* . A recent (2018) review of crystal simulations is also worth consulting.[221]

For brevity, only basic descriptions of the programs are given in this manual. All of the programs may be run with command line input; the input options to each program may be listed by running each program with no arguments.

9.2.1 UnitCell

A macromolecular crystal contains many repeating unit cells which stack like blocks in three dimensional space just as simulation cells do in periodic boundary conditions. Each unit cell, in turn, may contain multiple symmetry-related clusters of atoms. A PDB file contains one set of coordinates for the irreducible unit of the crystal, the "asymmetric unit," and also information about the crystal space group and unit cell dimensions. The *UnitCell* program reads PDB files, seeking the SMTRY records within the REMARKs to enumerate the rotation and translation operations which may be applied to the coordinates given in the PDB file to reconstruct one complete unit cell.

Usage of the *UnitCell* program is as follows. The simple command rests on a critical assumption, that the PDB file contains an accurate CRYST1 record and that the REMARK 290 SMTRY records provide its space group symmetry operations.

```
UnitCell -p MyProtein.pdb -o UnitCell.pdb
```

9.2.2 PropPDB

Simulations in periodic boundary conditions require a minimum unit cell size: the simulation cell must be able to enclose a sphere of at least the nonbonded direct space cutoff radius plus a small buffer region for nonbonded pairlist updates. Many biomolecular crystal unit cells come in "shoebox" dimensions that may have one very short side; many unit cells are also not rectangular but triclinic, meaning that the size of the largest sphere they can enclose is further reduced. The workhorse simulation engine, pmemd.cuda, even requires that the simulation cell be at least three times as thick as the cutoff plus some buffer margin in order to run safely: for typical sum conditions this thickness is about 30Å. For these reasons, and perhaps to ensure that the rigid symmetry imposed by periodic boundary conditions does not create artifacts (crystallographic unit cells are equivalent when averaged over all time and space, but are not necessarily identical at any given moment), it may be necessary to include multiple unit cells within the simulation cell. This is the purpose of the *PropPDB* program: to propagate a unit cell in one or more directions so that the complete simulation cell meets minimum size requirements.

Drawing on the hypothetical example above, if the unit cell is too small we can extend it in the *x* and *z* dimensions:

```
PropPDB -p UnitCell -o ExpandedCell.pdb -ix 2 -iy 1 -iz 2
```

9.2.3 AddToBox

The *AddToBox* program handles placement of solvent within a crystal unit cell or supercell (as may be created by PropPDB). As described in the introduction, the basic strategy is to place solvent such that added solvent molecules do not clash with biomolecule solutes, but *may* clash with one another initially. This compromise is necessary because enough solvent must be added to the system to ensure that the correct unit cell dimensions are maintained in the long run, but it is not acceptable to place solvent within the interior of a biomolecule where it might not belong and never escape.

The *AddToBox* program takes a PDB file providing the coordinates of a complete biomolecular unit cell or supercell (argument -c), the dimensions by which that supercell repeats in space (the unit cell dimensions are taken from the CRYST1 record of this file), a PDB file describing the solvent residue to add (argument -a), and the number of copies of that solvent molecule to add (argument -na). *AddToBox* inherently assumes that the biomolecular unit cell it is initially presented may contain some amount of solvent already, and according to the AMBER convention of listing macromolecular solute atoms first and solvent last assumes that the first -P atoms in the file are the protein (or biomolecule). *AddToBox* will then color a very fine grid "black" if the grid point is

within a certain distance of a biomolecular atom (argument -RP, default 5.0Å) or other solvent atom (argument -RW, default 1.0Å); the grid is "white" otherwise (the grid is stored in binary for memory efficiency). *AddToBox* will the make a copy of the solvent residue and randomly rotate and translate it somewhere within the unit cell. If all atoms of the solvent residue land on "white" grid voxels, the solvent molecule will become part of the system and the grid around the newly added solvent will be blacked out accordingly. If the solvent molecule cannot be placed, this process will be repeated until a million consecutive failures are encountered, at which point the program will terminate. If *AddToBox* has not placed the requested number of solvent molecules by the time it terminates, the -V option can be used to order the program to recursively call itself with progressively smaller solvent buffer distances until all the requested solvent can be placed. The output of the *AddToBox* program is another PDB named by the -o option.

Successful operation of *AddToBox* may take practice. If multiple solvent species are required, as is the case with heterogeneous crystallization solutions, *AddToBox* may be called repeatedly with each input molecular cell being the previous call's output. When considering crystal solvation, the order of addition is important! It is recommended that rare species, such as trace buffer reagents, be added first, with large -RW argument to ensure that they are dispersed throughout the available crystal void zones. Large solvent species such as MPD (an isohexane diol commonly used in crystallization conditions) should be added second, and with a sufficiently large -RW argument that methyl groups and ring systems cannot become interlocked (which will likely lead to SHAKE / vlimit errors). Small and abundant species such as water should be added last, as they can go anywhere that space remains.

Below is an example of the usage for a hypothetical protein with 5431 atoms and a net charge of +6 that is to be neutralized with ammonium sulfate:

```
AddToBox -c ExpandedCell.pdb -a Sulfate.pdb -na 18 -RP 3.0 -P 5431 -o System.pdb
AddToBox -c System.pdb -a Ammonium.pdb -na 30 -RP 3.0 -P 5431 -o System.pdb
AddToBox -c System.pdb -a Water.pdb -na 1089 -RP 3.0 -P 5431 -o System.pdb
```

The use of the -V flag ensures that the desired amounts of each species are included. The protein clipping radius of 3Å is lower than the default, but safe (remember, this radius stipulates that no solvent atom, regardless of the size of the solvent molecule, come within 3Å of the protein). Note how the original protein PDB file serves as the base for system, but thereafter we work with the System.pdb to accumulate more solvent particles. Here, the ammonium sulfate serves both to neutralize the system and replicate a salty bath, perhaps from a crystallization mother liquor, hence the break from the usual 2:1 stoichiometry of ammonium sulfate ions.

It is likely that the unobservable "void" regions between biomolecules in most crystals *do not* contain solvent species in proportion to their abundance in the crystallization solution–the vast majority of these regions are within a few Ångstroms of some biomolecular surface, and different biomolecular functional groups will preferentially interact with some types of solvent over others. Also, in many crystals some solvent molecules *are* observed; in many of these, the amount of solvent observed is such that it would be impossible to pack other species into the unit cell in proportion to their abundances in the crystallization fluid. In these cases, we recommend estimating the amount of volume that must be filled with solvent *apart from solvent which has already been observed in the crystal*, and filling this void with solvent in proportion to the composition of the crystallization fluid. For example, if a crystal were grown in a 1:1 mole-to-mole water/ethanol mixture, and the crystal coordinates as deposited in the PDB contained 500 water molecules and 3 ethanol molecules, we would use *AddToBox* to add water and ethanol in a 1:1 ratio until the system contained enough solvent to maintain the correct volume during equilibrium dynamics at constant pressure.

Finally, it is difficult to estimate exactly how much solvent will be needed to maintain the correct equilibrium volume; the advisable approach is simply to make an initial guess and script the setup so that, over multiple runs and reconstructions, the correct system composition can be found. We recommend matching the equilibrium unit cell volume to within 0.3% to keep this simulation parameter within the error of most crystallographic measurements. While errors of 0.5-1% will show up quickly after constant pressure dynamics begin, a 10 to 20ns simulation may be needed to ensure that the correct equilibrium volume has been achieved.

9.2.4 ChBox

After the complex process of adding solvent, the LEaP program may be used to produce a topology and initial set of coordinates based on the PDB file produced by *AddToBox*. By using the *SetBox* command, LEaP will create a periodic system without adding any more solvent on its own. The only problem with using LEaP at this point is that the program will fail to realize that the system *does* tile in three dimensions if only the box dimensions are set properly. If visualized, the output of UnitCell / PropPDB will likely look jagged, but the output of *AddToBox*, containing lots of added water, will make it obvious how parts of biomolecules jutting out one face of the box fit neatly into open spaces on an opposite face. The topology produced by LEaP needs no editing; only the last line of the coordinates does. This can be done manually, but the *ChBox* program automates the process, taking the same coordinates supplied to AddToBox and grafting them into the input coordinates file.

The program is even unnecessary in the case of orthorhombic (rectangular) unit cells, as this the tleap command will substitute:

set [unit] box { <x> <y> <z> }

For cells that do not have only 90-degree box angles, *ChBox* will do the trick.

9.3 X-ray functionality and diffraction-based restraints

The *msander* program includes a new module dedicated to biomolecular crystallography. It is envisioned that in future Amber can be used as a platform to address various crystallography-related problems, e.g. to refine crystallographic structures of proteins and nucleic acids (similar to the existing capability in the area of biomolecular NMR). This module is intended for use with an MD simulation of the crystal unit cell or a "supercell"[222]. For information on how to set up a crystal simulation, including periodic boundary conditions to emulate crystalline lattice, see Chapter 9.2. It is expected that the crystal is solvated using an explicit (or implicit) solvent. While a number of crystallographic concepts are implemented in the new Amber module, many others have not yet been implemented. For example, an MD model of a crystal unit cell can naturally accommodate different side-chain conformations; however, the concept of alternate side-chain conformations, as employed in protein crystallography, is currently unavailable in Amber.

Although it is not a part of Amber, it is worth noting that the *phenix* crystallographic package now allows for X-ray refinement using Amber (or other) force fields[223]. This was accomplished by using the python API to *sander*, and uses locally-enhanced sampling to handle alternate conformations. It supports all of the X-ray related options in *phenix.refine*, but has limited options for molecular dynamics, and no GPU acceleration.

9.3.1 Structure factor calculations

For the crystal simulation, the program can calculate crystallographic structure factors (SFs) for individual MD frames. The calculations are conducted using direct summation formula[224]; a mask is available to define the subset of atoms included in these calculations (*atom_selection_mask*). For example, this mask could select the macromolecules, but not the solvent or the neutralizing ions present in the simulation. The B-factors used in the direct summation formula are supplied through a designated PDB file. The set of Miller indices for SF calculations is supplied as a part of the *reflection_infile*.

In principle, explicit solvent and ions can also be accounted for via the direct summation formula. However, any single individual frame does not offer an adequate statistical sampling with regard to the positioning of water molecules (if desired, such statistical sampling can be obtained by modeling of a very large supercell or otherwise by means of time averaging). As a commonly accepted alternative, Amber 22 offers two mask-based models of bulk solvent. The first one (*bulk_solvent_model* = 'simple') is a simple variant of flat mask bulk solvent model[225], which calculates the contribution from interstitial solvent into SFs using two generic parameters (*k_sol* and *b_sol*), as reported by Fokine and Urzhumtsev[226]. The implementation, including the scheme to build solvent mask, is analogous to the one in cctbx library[227]. The more advanced version (*bulk_solvent_model* = 'afonine-2013') employs the varaible k_{mask}, which replaces *k_sol* and *b_sol*; this variable is automatically optimized over the individual resolution bins[228]. The iterative optimization procedure to determinate k_{mask} also

adjusts the overall scaling coefficient that is applied to calculated SFs. The implementation follows the one in cctbx library with several minor modifications.

It is worth noting that crystal MD simulations in Amber (as described in Chap. 9.2) do not maintain a perfect space group symmetry. Therefore, strictly speaking, the calculated SFs correspond to P(1) space group with the unit cell that is identical to the simulation box. During the course of the simulation, the calculated SFs can be collected frame-by-frame at a specified interval (*ntwsf*) and stored in a form of special trajectory file (*sf_outfile*).

9.3.2 Structure-factor-based potential

The X-ray energy term E_{xray} is added to the total potential energy with the user-specified weight w_{xray} (controlled by *xray_weight_initial* / *xray_weight_final* variables):

$$E_{total} = E_{force-field} + w_{xray}E_{xray} \tag{9.1}$$

E_{xray} uses the set of target (i.e. experimentally observed) SFs, which are supplied via the input file *reflection_infile*. This file must also contain flags to divide all reflections into a "working" set and a "free" (test) set. Currently *pmemd* offers two variants of the E_{xray} term. The first one is a very simple least squares objective function (*target* = 'ls') involving the aplitudes and of calculated and observed structure factors:

$$E_{xray} = \frac{\sum_{h,k,l} (F_{calc}(h,k,l) - F_{obs}(h,k,l))^2}{\sum_{h,k,l} F_{obs}^2(h,k,l)} \tag{9.2}$$

The sum in this expression is over the working set of reflections.

The second option for E_{xray} is the Maximum Likelihood target function (*target* = 'ml')[229, 230]:

$$E_{xray} = \sum_{h,k,l} \left(-\ln\left(\frac{2F_{obs}(h,k,l)}{\varepsilon\beta}\right) + \frac{F_{obs}^2(h,k,l)}{\varepsilon\beta} + \frac{\alpha^2 F_{calc}^2(h,k,l)}{\varepsilon\beta} - \ln I_0\left(\frac{2\alpha F_{obs}(h,k,l)F_{calc}(h,k,l)}{\varepsilon\beta}\right) \right) \tag{9.3}$$

where α and β are (resolution-shell-dependent) ML likelihood distribution parameters, ε is the symmetry coefficient ($\varepsilon = 1$ for the space group P(1) at hand), $I_0(x)$ is the zeroth-order modified Bessel function of the first kind, and the summation is over the working set of reflections. For practical applications, we recommend using *target* = 'ml' along with the more advanced version of solvent, *bulk_solvent_model* = 'afonine-2013'.

The expression for E_{xray}, along with the direct-summation formula for F_{calc}, provides a basis to evaluate forces. These "restraint" forces act like those used in NMR refinement, discussed in Chap.8, and are generally used to drive minimization or MD simulations that minimize E_{total}. The value of E_{xray} is reported in the mdout file, together with R_{work} and R_{free}.

We envisage that SF-based restraints can be used for a number of purposes. For example, they can be viewed as an empirical addition to the force fields, which can potentially remedy certain existing biases[231, 232]. Another promising application is refinement of crystallographic structures. Such an Amber-based protocol has been reported by Mikhailovskii et al.[233] (the web interface is available at https://arx.bio-nmr.spbu.ru). Ultimately, the entire process of crystallographic structure determination can be incorporated into Amber. This approach may be particularly valuable for lower-quality diffraction data sets and incomplete structural models (e.g. in the case of weak or missing electron density for mobile side chains, loops or terminal regions in protein molecules). In this situation, the state-of-the-art force field provides a natural solution to model the poorly resolved or unresolved elements of the structure. This is accomplished in a highly realistic manner, by using the explicit representation of the crystal unit cell (supercell), taking into consideration the effect of solvent, crystal contacts, etc.

9.3.3 Inputs and file formats

System setup follows the general procedures outlined in Chap. 9.2. For users with access to the *phenix* package of crystallographic analysis tools, the XrayPrep tool can prepare the system: inputs are simply a PDB file (*xxxx.pdb*, where xxxx is a PDB id) and the corresponding structure factor file (*xxxx-sf.cif*).

For those who will prepare their own inputs, one needs a PDB file, expanded to the unit cell (see Chap. 9.2) that contains the B-factors. The structure factors have to be listed in the r*eflection_infile*, which is a human-readable ascii file containing the same information that can be normally found in .mtz files. The first line contains a total number of reflections followed by a zero. Subsequent lines list Miller indices *h, k* and *l*, followed by the respective SF values and their standard deviations, followed by an R-free flag (we adopt the convention that "1" indicates a member of the working set, and "0" a member of the test set). An example file is given below. Note that column spacing or number formatting is not critical, but each entry should be separated by at least one space.

```
41243 0
−19        −6        1        13.86329        9.685285        0
−19        −6        2        46.38137        3.528763        1
−19        −5        1        9.675193        21.28529        1
...
 19         6        1        13.86329        9.685285        0
 19         6        2        46.38137        3.528763        1
```

Input variables in the &xray namelist   The X-ray functionalities are activated by adding the *&xray* namelist to the mdin file. User-assigned parameters that are not used by the algorithm are silently ignored(e.g.\ *k_sol* and *b_sol* in 'afonine-2013' bulk solvent model). The keywords in *&xray* namelist include the following:

File handling:

`pdb_infile`	name of the PDB input file containing B-factors
`pdb_read_coordinates`	if true, use coordinates from the PDB file, not inpcrd, as starting coordinates
`pdb_outfile`	name of PDB file to write the final atomic coordinates from the simulation. Currently writes back the input B-factors and occupancies as read from *pdb_infile*
`reflection_infile`	name of the input file containing experimental SFs and R-flags
`fmtz_outfile`	name of the file with calculated SFs, in "formatted MTZ" format

Bulk solvent parameters:

`bulk_solvent_model`	the type of bulk solvent to use. Possible values: 'none' for disabled bulk solvent contribution, 'simple' or 'afonine-2013' (default)
`k_sol`	solvent electron density (default 0.35 e Å^{-3})
`b_sol`	determines the blurring of the boundary between the solvent region and the macromolecule (default 46 Å^2)
`solvent_mask_adjustment`	increment to be added to atomic radii of the atoms selected by *atom_selection_mask* as a part of the algorithm to build bulk solvent mask (default 1.11 Å)
`solvent_mask_probe_radius`	the radius of solvent probe to apply as a part of the algorithm to build bulk solvent mask (default 0.9 Å)
`mask_update_period`	time interval for bulk solvent grid update (expressed as a multiple of integration step, default 100 steps)

Structure-factor-based potential:

`atom_selection_mask`	ambmask-format mask to specify the atoms that contribute to F_{calc} via direct summation formula (default '!@H=')

`scale_update_period`	time interval to re-scale F_{calc} to F_{obs} (expressed as a multiple of integration step, default 100 steps)
`target`	the type of crystallographic target function. Possible values: 'ls' for Least Squares, 'ml' for Maximum Likelihood (default)
`ml_update_period`	time interval to update ML parameters α and β (expressed as a multiple of integration step, default 100 steps)
`xray_weight`	Sets the value of w_{xray} (default 1.0) This value can be variable: see Section 1.10 for more information.
`xray_weight_final`	final value that defines linear scaling of w_{xray} weight along the trajectory (if unassigned, assumed to be equal to *xray_weight_initial*)

9.4 Auxiliary scripts for X-ray refinement

This section gives a bird's-eye view of capabilities of the some useful auxiliary scripts. The hope is to get more detailed examples and documentation as time permits. The organization is based on the compuational tools required, which almost certainly not the best approach.

9.4.1 ccp4_scripts

These scripts are based on the *CCP4* and *refmac5* programs.

conf_solvent.sh Takes an electron density for the solvent (say from MD simulations or from integral equation models), plus an atomic model for the "solute" (generally a macromolecule like a protein), and refines the model with *refmac5*. As a comparison, ignores the input solvent density and uses the standard *refmac5* bulk solvent contribution, as would be done in a conventional simulation. This offers one way to see if the input density is any "better" than the standard solvent contribution.

md2diffuse.sh Takes snapshots from an MD simulation, and works through the steps to compute both the Bragg intensities and diffuse intensities. The *sfall* program is the key engine to compute scattering amplitudes. Special attention is paid to reducing disk space requirements, so that scattering amplitudes from many snapshots can be stored and analyzed. The code optionally will constuct map coefficients and an electron density map arising from the simulation.

md2map.sh

mdv2map.sh The two scripts compute the average electron density, as a CCP4 map and as map coefficients, from an input MD simulation. Unlike the **md2diffuse.sh** script, which computes the average scattering amplitudes, then uses an FFT to obtain the final map, these two scripts directly add the maps together, then uses a Fourier transform to obtain the map coefficients. Since no diffuse scattering information is needed, there is much less need to optimize disk space; still the overall amount of computation is about the same, *i.e.* that required to run *sfall* on each frame of the input trajectory. The **mdv2map.sh** script assumes that the unit cell dimensions don't change throughout the trajectory, whereas **md2map.sh** does not make this assumption.

9.4.2 phenix_scripts

XrayPrep This script currently has two parts, which can be run together, or separately. The first part uses the *phenix.AmberPrep* script to prepare an input pdb-format file for use in refinement. It usually works well, but is limited in its ability to handle unusual situations, such as post-translational modifications, etc. See the *run_alt_tleap* script below for a more flexible alternative. The second part of the script takes an *xxx-sf-cif* file from the PDB, and converts the information into files needed for amber-based refinement. This uses

phenix.refine to do conversions, reject outliers, possible convert intensities to structure factors, expand to P1 symmetry, and so on. (Going forward, I will probably remove the first part of this script.)

CryoPrep These two scripts take an atomic model (in the form of a PDB-format file), and either an electron density (as a CCP4 map) or structure factors (as an sf-cif file), and prepare all the files needed to carry out refinements that employ a molecular force field (rather than Engh-Huber like distance and angle restraints) to constrain the molecular geometry.

run_phenix.solvent This is a sample script to allow comparisons of the bulk-solvent model in *phenix* and a user-supplied solvent density. Unlike the **conf_solvent.sh** script based on *refmac5*, this only works for a single-point, and doesn't carry out refinements that include the user-supplied solvent density.

run_phenix_refine This is just an alternative way to run *phenix.refine* from the command line, with flexible ways to choose the input paramters. It's probably not for everyone.

run_fmodel This just runs *phenix.fmodel* and re-formats the output in a simple but occasionally useful way.

9.4.3 rism_scripts

run_rism A simple script to run 3D-rism calcualtions (using the *msander* program) on a single snapshot. Typical values for grid spacing, closure and solvent model are hard-wired here, but you should edit this if you wish to make changes.

run_metatwist_rho Takes the output from *run_rism* and computes an electron density map for the solvent. This can be used to replace the "flat" bulk solvent density model in programs like *msander* or *refmac5*.

9.4.4 ensemble_scripts

These are scripts that are used to run ensemble refinements, where many complete copies of the macromolecule are present, generally arranged in a supercell. These are mainly useful as part of a bigger workflow, whose documentation is not yet ready.

find_alts output a listing of alternate conformations found in an input pdb-file

select_alts this is the main script, that takes an input pdb file with alternate conformations (for example, as found in the PDB). For each chain, it randomly selects an alternate conformer for each residue, based on its input occupation. The output file sets all occupations to 1.0. This is commonly used to create a starting model for ensemble refinement.

modify_pdb is a utility perl script for making all manner of modifications to PDB files, at least that can be done on a line-by-line basis. The scripts reads an input PDB file, makes whatever changes are coded in an intermediate section, and writes out the result.

modify_frac is a variant of modify_pdb that allows modification based on fractional coordinates, useful for repacking coordinates into a single unit cell, and so on.

collapse_pdb takes an ensemble model and converts it into a more standard "alternate conformer" model

9.4.5 XtalAnalyze scripts

This is a set of scripts created by Pawel Janowski some years ago. The main current documentation is in the *README*, *XtalAnalyze.sh* and *XtalPlot.sh* files. Read these for now to see how to run things.

10 LEaP

10.1 Introduction

LEaP is the generic name given to the programs teLeap and xaLeap, which are generally run *via* the *tleap* and *xleap* shell scripts. These two programs share a common command language but the *xleap* program has been enhanced through the addition of an X-windows graphical user interface. The name LEaP is an acronym constructed from the names of the older AMBER software modules it replaces: link, edit, and parm. Thus, LEaP can be used to prepare input for the AMBER molecular mechanics programs.

LEaP is the basic tool to construct force field files (see Fig. **??**). Using *tleap*, the user can:

```
Read AMBER PREP input files
Read Amber PARM format parameter sets
Read and write Object File Format files (OFF)
Read and write PDB files
Construct new residues and molecules using simple commands
Link together residues and create nonbonded complexes of molecules
Modify internal coordinates within a molecule
Generate files that contain topology and parameters for AMBER and NAB
```

```
usage: tleap [ -I<dir> ] [ -f <file>|- ]
```

The command *tleap* is a simple shell script that calls *teLeap* with a number of standard arguments. Directories to be searched are indicated by one or more "-I" flags; standard locations are provided in the *tleap* script. The "-f" flag is used to tell tleap to take its input from a file (or from *stdin* if "-f -" is specified). If there is no "-f" flag, input is taken interactively from the terminal.

A key command for LEaP is loadPdb, which inputs sequence and structure information from Protein Data Bank Files. *Be sure to read Section **??** for information on how to "clean up" PDB files before loading them.*

10.2 Concepts

In order to effectively use LEaP it is necessary to understand the philosophy behind the program, especially the concepts of LEaP commands, variables, and objects. In addition to exploring these concepts, this section also addresses the use of external files and libraries with the program.

10.2.1 Commands

A researcher uses LEaP by entering commands that manipulate objects. An object is just a basic building block; some examples of objects are ATOMs, RESIDUEs, UNITs, and PARMSETs. The commands that are supported within LEaP are described throughout the manual and are defined in detail in the "Command Reference" section.

The heart of LEaP is a command-line interface that accepts text commands which direct the program to perform operations on objects. All LEaP commands have one of the following two forms:

```
command argument1 argument2 argument3 ...
variable = command argument1 argument2 ...
```

For example:

```
edit ALA trypsin = loadPdb trypsin.pdb
```

Each command is followed by zero or more arguments that are separated by whitespace. (Whitespace is blanks, tabs, and commas; and as of Amber version 21 carriage returns are also treated as whitespace.) Some commands return objects which are then associated with a variable using an assignment (=) statement. Each command acts upon its arguments, and some of the commands modify their arguments' contents. The commands themselves are case-insensitive. That is, in the above example, `edit` could have been entered as `Edit`, `eDiT`, or any combination of upper and lower case characters. Similarly, `loadPdb` could have been entered a number of different ways, including `loadpdb`. In this manual, we frequently use a mixed case for commands. We do this to enhance the differences between commands and as a mnemonic device. Thus, while we write `createAtom`, `createResidue`, and `createUnit` in the manual, the user can use any case when entering these commands into the program.

The arguments in the command text may be objects such as NUMBERs, STRINGs, or LISTs, or they may be variables. These two subjects are discussed next.

10.2.2 Variables

A variable is a handle for accessing an object. A variable name can be any alphanumeric string whose first character is an alphabetic character. Alphanumeric means that the characters of the name may be letters, numbers, or special symbols such as "*". The following special symbols should not be used in variable names: dollar sign, comma, period (full stop), pound sign (hash), equals sign, space, semicolon, double quote, or the curly braces { and }. LEaP commands should not be used as variable names. Unlike commands, variable names are case-sensitive: "ARG" and "arg" are different variables. Variables are associated with objects using an assignment statement not unlike that found in conventional programming languages such as Fortran or C.

```
mole = 6.02E23
MOLE = 6.02E23
myName = "Joe Smith"
listOf7Numbers = { 1.2 2.3 3.4 4.5 6 7 8 }
```

In the above examples, both mole and MOLE are variable names, whose contents are the same (6.02×10^{23}). Despite the fact that both mole and MOLE have the same contents, they are not the same variable. This is due to the fact that variable names are case-sensitive. LEaP maintains a list of variables that are currently defined. This list can be displayed using the `list` command. The contents of a variable can be printed using the `desc` command.

10.2.3 Objects

The object is the fundamental entity in LEaP. Objects range from the simple, such as NUMBERs and STRINGs, to the complex, such as UNITs, RESIDUEs and ATOMs. Complex objects have properties that can be altered using the `set` command, and some complex objects can contain other objects. For example, RESIDUEs are complex objects that can contain ATOMs and have the properties: residue name, connect atoms, and residue type.

NUMBERs

NUMBERs are simple objects holding double-precision floating point numbers. They serve the same function as "double precision" variables in Fortran and "double" variables in C.

STRINGs

STRINGs are simple objects that are identical to character arrays in C and similar to character strings in Fortran. STRINGs store sequences of characters which may be delimited by double quote characters. Example strings are:

```
"Hello there"
"String with a "" (quote) character"
"Strings contain letters and numbers:1231232"
```

LISTs

LISTs are made up of sequences of other objects delimited by LIST open and close characters. The LIST open character is an open curly bracket ({) and the LIST close character is a close curly bracket (}). LISTs can contain other LISTs and be nested arbitrarily deep. Example LISTs are:

```
{ 1 2 3 4 }
{ 1.2 "string" }
{ 1 2 3 { 1 2 } { 3 4 } }
```

LISTs are used by many commands to provide a more flexible way of passing data to the commands. The `zMatrix` command has two arguments, one of which is a LIST of LISTs where each subLIST contains between three and eight objects.

PARMSETs (Parameter Sets)

PARMSETs are objects that contain bond, angle, torsion, and non-bonding parameters for AMBER force field calculations. They are normally loaded from force field data files, such as *parm94.dat*, and frcmod files.

ATOMs

ATOMs are complex objects that do not contain any other objects. The ATOM object corresponds to the chemical concept of an atom. Thus, it is a single entity that may be bonded to other ATOMs and used as a building block for creating molecules. ATOMs have many properties that can be changed using the `set` command. These properties are defined below.

name This is a case-sensitive STRING property and it is the ATOM's name. The names for all ATOMs in a RESIDUE should be unique. The name has no relevance to molecular mechanics force field parameters; it is chosen arbitrarily as a means to identify ATOMs. Ideally, the name should correspond to the PDB standard, being 3 characters long except for hydrogens, which can have an extra digit as a 4th character.

type This is a STRING property. It defines the AMBER force field atom type. It is important that the character case match the canonical type definition used in the appropriate force field data (**.dat*) or frcmod file. For smooth operation, all atom types must have element and hybridization defined by the `addAtomTypes` command. The standard AMBER force field atom types are added by the selected leaprc file.

charge The charge property is a NUMBER that represents the ATOM's electrostatic point charge to be used in a molecular mechanics force field.

element The atomic element provides a simpler description of the atom than the type, and is used only for LEaP's internal purposes (typically when force field information is not available). The element names correspond to standard nomenclature; the character "?" is used for special cases.

position This property is a LIST of NUMBERs. The LIST must contain three values: the (X, Y, Z) Cartesian coordinates of the ATOM.

RESIDUEs

RESIDUEs are complex objects that contain ATOMs. RESIDUEs are collections of ATOMs, and are either molecules (e.g., formaldehyde) or are linked together to form molecules (e.g., amino acid monomers). RESIDUEs have several properties that can be changed using the `set` command. (Note that database RESIDUEs are each contained within a UNIT having the same name; the residue GLY is referred to as GLY.1 when setting properties. When two of these single-UNIT residues are joined, the result is a single UNIT containing the two RESIDUEs.)

One property of RESIDUEs is connection ATOMs. Connection ATOMs are ATOMs that are used to make linkages between RESIDUEs. For example, in order to create a protein, the N-terminus of one amino acid residue must be linked to the C-terminus of the next residue. This linkage can be made within LEaP by setting the N

ATOM to be a connection ATOM at the N-terminus and the C ATOM to be a connection ATOM at the C-terminus. As another example, two CYX amino acid residues may form a disulfide bridge by crosslinking a connection atom on each residue.

There are several properties of RESIDUEs that can be modified using the `set` command. The properties are described below:

connect0 This defines the first of up to three ATOMs that are used to make links to other RESIDUEs. In UNITs containing single RESIDUEs, the RESIDUE's connect0 ATOM is usually defined as the UNIT's head ATOM. (This is how the standard library UNITs are defined.) For amino acids, the convention is to make the N-terminal nitrogen the connect0 ATOM.

connect1 This defines the second of up to three ATOMs that are used to make links to other RESIDUEs. In UNITs containing single RESIDUEs, the RESIDUE's connect1 ATOM is usually defined as the UNIT's tail ATOM. (This is done in the standard library UNITs.) For amino acids, the convention is to make the C-terminal oxygen the connect1 ATOM.

connect2 This defines the third of up to three ATOMs that are used to make links to other RESIDUEs. In amino acids, the convention is that this is the ATOM to which disulfide bridges are made.

restype This property is a STRING that represents the type of the RESIDUE. Currently, it can have one of the following values: "undefined", "solvent", "protein", "nucleic", or "saccharide". Some of the LEaP commands behave in different ways depending on the type of a residue. For example, the solvate commands require that the solvent residues be of type "solvent". It is important that the proper character case be used when defining this property.

name The RESIDUE name is a STRING property. It is important that the proper character case be used when defining this property.

UNITs

UNITs are the most complex objects within LEaP, and the most important. They may contain RESIDUEs and ATOMs. UNITs, when paired with one or more PARMSETs, contain all of the information required to perform a calculation using AMBER. UNITs can be created using the `createUnit` command. RESIDUEs and ATOMs can be added or deleted from a UNIT using the `add` and `remove` commands. UNITs have the following properties, which can be changed using the `set` command:

head

tail These define the ATOMs within the UNIT that are connected when UNITs are joined together using the sequence command or when UNITs are joined together with the PDB or PREP file reading commands. The tail ATOM of one UNIT is connected to the head ATOM of the next UNIT in any sequence. (Note: a TER card in a PDB file causes a new UNIT to be started.)

box This property can either be null, a NUMBER, or a LIST. The property defines the bounding box of the UNIT. If it is defined as null then no bounding box is defined. If the value is a single NUMBER, the bounding box will be defined to be a cube with each side being *box* Å across. If the value is a LIST, it must contain three NUMBERs, the lengths of the three sides of the bounding box.

cap This property can either be null or a LIST. The property defines the solvent cap of the UNIT. If it is defined as null, no solvent cap is defined. If it is a LIST, it must contain four NUMBERs. The first three define the Cartesian coordinates (X, Y, Z) of the origin of the solvent cap in Å, while the fourth defines the radius of the solvent cap, also in Å.

Examples of setting the above properties are

```
set dipeptide head dipeptide.1.N
set dipeptide box { 5.0 10.0 15.0 }
set dipeptide cap { 15.0 10.0 5.0 8.0 }
```

The first example makes the amide nitrogen in the first RESIDUE within "dipeptide" the head ATOM. The second example places a rectangular bounding box around the origin with the (X, Y, Z) dimensions of (5.0, 10.0, 15.0) in Å. The third example defines a solvent cap centered at (15.0, 10.0, 5.0) Å with a radius of 8.0 Å. Note: the `set cap` command does not actually solvate, it just sets an attribute. See the `solvateCap` command for a more practical case.

Complex objects and accessing subobjects

UNITs and RESIDUEs are complex objects. Among other things, this means that they can contain other objects. There is a loose hierarchy of complex objects and what they are allowed to contain. The hierarchy is as follows:

- UNITs can contain RESIDUEs and ATOMs.

- RESIDUEs can contain ATOMs.

The hierarchy is loose because it does not forbid UNITs from containing ATOMs directly. However, the convention that has evolved within LEaP is to have UNITs directly contain RESIDUEs which directly contain ATOMs.

Objects that are contained within other objects can be accessed using dot "." notation. An example would be a UNIT which describes a dipeptide ALA-PHE. The UNIT contains two RESIDUEs each of which contain several ATOMs. If the UNIT is referenced (named) by the variable dipeptide, then the RESIDUE named ALA can be accessed in two ways. The user may type one of the following commands to display the contents of the RESIDUE:

```
desc dipeptide.ALA
desc dipeptide.1
```

The first command translates to "describe some RESIDUE named ALA within the UNIT named dipeptide". The second form translates as "describe the RESIDUE with sequence number 1 within the UNIT named dipeptide". The second form is more useful because every subobject within an object is guaranteed to have a unique sequence number. If the first form is used and there is more than one RESIDUE with the name ALA, then an arbitrary residue with the name ALA is returned. To access ATOMs within RESIDUEs, either of the following forms of command may be used:

```
desc dipeptide.1.CA
desc dipeptide.1.3
```

Assuming that the ATOM with the name CA has a sequence number 3 within RESIDUE 1, then both of the above commands will print a description of the alpha-carbon of RESIDUE dipeptide.ALA or dipeptide.1. The reader should keep in mind that dipeptide.1.CA is the ATOM, an object, contained within the RESIDUE named ALA within the variable dipeptide. This means that dipeptide.1.CA can be used as an argument to any command that requires an ATOM as an argument. However dipeptide.1.CA is not a variable and cannot be used on the left hand side of an assignment statement.

10.3 Running LEaP

```
tleap -h
```

will give a list of command-line arguments (which are very simple). Once you have started either program, typing "help" will display useful information about possible actions.

A file called *leaprc* is executed as a script file at the start of the LEaP session unless the user suppresses it with the *-s* command line option. Sample script files are in *$AMBERHOME/dat/leap/cmd*, and you may wish to copy one of these to become "your" default file. LEaP will look first for a *leaprc* file in the user's current directory, then in any directories included with *-I* flags.

The command line interface allows the user to specify a log file that is used to log all input and output within the command line environment. The log file is named using the *logFile* command. The file has two purposes: to

allow the user to see a complete record of operations performed by LEaP, and to help recover from (and recreate) program crashes. Output from LEaP commands is written to the log file at a verbosity level of 2 regardless of the verbosity level set by the user using the *verbosity* command. Each line in the log file that was typed in by the user begins with the two characters "> " (a greater-than sign followed by a space). This allows the user to extract the commands typed into LEaP from the log file to create a script file that can be executed using the *source* command. This provides a type of insurance against program crashes by allowing the user to regenerate their interactive sessions. An example of a command that will create a script to reenact a LEaP session is:

```
cat LOGFILE | grep "^> " | sed "s/^> //" > SOURCEFILE.x
```

10.4 Basic instructions for using LEaP to build molecules

This section gives an overview of how LEaP is most commonly used. Detailed descriptions of all the commands are given in the next section.

10.4.1 Building a Molecule For Molecular Mechanics

In order to prepare a molecule within LEaP for AMBER, three basic tasks need to be completed.

1. Any needed UNIT or PARMSET objects must be loaded;

2. The molecule must be constructed within LEaP;

3. The user must output topology and coordinate files from LEaP to use in AMBER.

The most typical command sequence is the following:

```
source leaprc.protein.ff14SB (load a force field)
x = loadPdb trypsin.pdb (load in a structure)
.... add in cross-links, solvate, etc.
saveAmberParm x prmtop prmcrd (save files)
```

There are a number of variants of this:

1. Although `loadPdb` is by far the most common way to enter a structure, one might use `loadOff`, or `loadAmberPrep`, or use the `zMatrix` command to build a molecule from a Z-matrix. For small molecules, e.g., ligand like, `loadMol2` or `loadMol3` are available. See the Commands section below for descriptions of these options. If you do not have a starting structure (in the form of a PDB file), LEaP can be used to build the molecule; you will find, however, that this is not always a straightforward process. Many experienced Amber users turn to other (commercial and non-commercial) programs to create their initial structures.

2. Be very attentive to any errors produced in the `loadPdb` step; these generally mean that LEaP has misread the file. A general rule of thumb is to keep editing your input PDB file until LEaP stops complaining. It is often convenient to use the `addPdbAtomMap` or `addPdbResMap` commands to make systematic changes from the names in your PDB files to those in the Amber topology files; see the leaprc files in *$AMBERHOME/dat/leap/cmd* for examples of this. *Be sure to read Section **??** for information on how to "clean up" PDB files before loading them.*

3. The `saveAmberParm` command cited above is appropriate for most force fields; for polarizable calculations you will need to use `saveAmberParmPol`.

10.4.2 Amino Acid Residues

For each of the amino acids found in the LEaP libraries, there has been created an N-terminal and a C-terminal analog. The N-terminal amino acid UNIT/RESIDUE names and aliases are prefaced by the letter N (e.g., NALA) and the C-terminal amino acids by the letter C (e.g., CALA). If the user models a peptide or protein within LEaP, they may choose one of three ways to represent the terminal amino acids. The user may use (1) standard amino acids, (2) protecting groups (ACE/NME), or (3) the charged C- and N-terminal amino acid UNITs/RESIDUEs. If the standard amino acids are used for the terminal residues, then these residues will have incomplete valences. These three options are illustrated below:

```
{ ALA VAL SER PHE }
{ ACE ALA VAL SER PHE NME }
{ NALA VAL SER CPHE }
```

The default for loading from PDB files is to use N- and C-terminal residues; this is established by the `addPdbResMap` command in the standard leaprc files. To force incomplete valences with the standard residues, one would have to define a sequence (" x = { ALA VAL SER PHE }") and use `loadPdbUsingSeq`, or use `clearPdbResMap` to completely remove the mapping feature.

Histidine can exist either as the protonated species or as a neutral species with a hydrogen at the δ or ε position. For this reason, the histidine UNIT/RESIDUE name is either HIP, HID, or HIE (but not HIS). The standard leaprc files assign the name HIS to HIE. Thus, if a PDB file is read that contains the residue HIS, the residue will be assigned to the HIE UNIT object. This feature can be changed within one's own leaprc file.

The AMBER force fields also differentiate between the residue cysteine (CYS) and the similar residue which participates in disulfide bridges, cystine (CYX). The user will have to explicitly define, using the `bond` command, the disulfide bond for a pair of cystines, as this information is not read from the PDB file. In addition, the user will need to load the PDB file using the `loadPdbUsingSeq` command, substituting CYX for CYS in the sequence wherever a disulfide bond will be created.

10.4.3 Nucleic Acid Residues

The "D" prefix can be used to distinguish between deoxyribose and ribose units. Residue names like "A" or "DA" can be followed by a "5" or "3" ("DA5", "DA3") for residues at the ends of chains; this is also the default established by `addPdbResMap`, even if the "5" or "3" are not added in the PDB file. The "5" and "3" residues are "capped" by a hydrogen; the plain and "3" residues include a "leading" phosphate group. Neutral residues (nucleosides) capped by hydrogens end their names with "N", as in "DAN".

10.5 Error Handling and Reporting

In Amber version 18 changes were made to LEaP's error processing. The first set of changes involve error handling. For input from a file (i.e., `tleap invoked with -f`) execution is now terminated at the first occurrence of these errors: file input/output errors, illegal command syntax, illegal command arguments, and some command parsing errors. The intent is to simplify error detection and to ease troubleshooting. For interactive input there is no change in handling: LEaP continues to be forgiving of these errors in the hope that the user can recover in real time.

The final set of changes involve error reporting. LEaP produces four kinds of messages: errors, warnings, notes, and processing messages. Messages beginning with "Fatal Error!" or "Error!" or "Error:" indicate a serious problem. Messages beginning with "Warning!" or "Warning:" indicate a potential problem that should be investigated. Messages beginning with "Note." or "Note:" provide information worth noting. Messages that are not designated by one of the above tags report processing status. Total counts of errors, warnings, and notes are outputted at the end of LEaP. The intent is to simplify error detection by emitting clear and consistent messages.

As with all computational software, LEaP's output should be carefully examined. Some error and warning messages mention likely causes or contain suggested workarounds, but all such messages provide clues. Apply common sense and the scientific method to troubleshoot. Typical first steps are to verify input files and to search the

AMBER Mail Reflector for similar reported problems. Note that LEaP normally produces a log file that contains all messages and more detailed output that can be inspected.

10.5.1 Known Issues

This is an incomplete list, started with Amber version 24, focussing on incompatibilities with standards, significant bugs, and gotchas in *LEaP*:

- LEaP does not write Mol2 files that are compliant with Sybyl bond types in the @<TRIPOS>BOND record. As of Amber version 24, single, double, and triple bond types are correctly emitted; the number 4 is used to denote aromatic bonds. In previous versions, the number 1 was always emitted.

- A workaround exists for the num lock issue in xLEaP; contact the Amber mailing list for details.

Of course other issues should be reported via the Amber mailing list.

10.6 Commands

The following is a description of the commands that can be accessed using the command line interface in *tleap*, or through the command line editor in *xleap*. Whenever an argument in a command line definition is enclosed in square brackets (e.g., [arg]), then that argument is optional. When examples are shown, the command line is prefaced by "> ", and the program output is shown without this character preface.

Some commands that are almost never used have been removed from this description to save space. You can use the "help" facility to obtain information about these commands; most only make sense if you understand what the program is doing behind the scenes.

10.6.1 add

    add a b

UNIT/RESIDUE/ATOM a,b

Add the object b to the object a. This command is used to place ATOMs within RESIDUEs, and RESIDUEs within UNITs. This command will work only if b is not contained by any other object.

The following example illustrates both the `add` command and the way the TIP3P water molecule is created for the LEaP distribution.

```
> h1 = createAtom H1 HW 0.417
> h2 = createAtom H2 HW 0.417
> o = createAtom O OW -0.834
>
> set h1 element H
> set h2 element H
> set o element O
>
> r = createResidue TIP3
> add r h1
> add r h2
> add r o
>
> bond h1 o
> bond h2 o
> bond h1 h2
>
> TIP3 = createUnit TIP3
>
> add TIP3 r
```

```
> set TIP3.1 restype solvent
> set TIP3.1 imagingAtom TIP3.1.O
>
> zMatrix TIP3 {
> { H1 O 0.9572 }
> { H2 O H1 0.9572 104.52 }
> }
>
> saveOff TIP3 water.lib
Saving TIP3.
Building topology.
Building atom parameters.
```

10.6.2 addAtomTypes

addAtomTypes { { type element hybrid } { ... } ... }

Define element and hybridization for force field atom types. This command for the standard force fields can be seen in the standard leaprc files. The STRINGs are most safely rendered using quotation marks. If atom types are not defined, confusing messages about hybridization can result when loading PDB files.

10.6.3 addC4Pairwise

addC4Pairwise unit atom1 atom2 C4Value(kcal/mol*A^4)

Adds pairwise C4 interaction between two specific atoms. C4 interaction means the non-bonded force between `atom1` and `atom2` will follow 12-6-4 pattern. Note here this 12-6-4 pattern is atom-specific, not atom-type-specific. This is achieved by generating LENNARD_JONES_DCOEF and LENNARD_JONES_DVALUE flags in the prmtop file. Under LENNARD_JONES_DCOEF flag, each row will contain the ID of `atom1`, the ID of `atom2`, and a numeric index for debugging purpose. Under LENNARD_JONES_DVALUE flag, each row will contain the C4Value. Multiple `addC4Pairwise` commands are supported in a single tleap file.

10.6.4 addC4Type

addC4Type unit type1 type2 C4Value(kcal/mol*A^4)

Similar to `add12_6_4` in `ParmEd`, this function will generate a LENNARD_JONES_CCOEF flag in the prmtop file. Under that flag, a C4 matrix will be presented with mostly zero values, except for the entries that represent non-zero C4Values between `type1` and `type2`. Multiple `addC4Type` commands are supported in a single tleap file.

10.6.5 addIons and addIons2

addIons unit ion1 numIon1 [ion2 numIon2]
addIons2 unit ion1 numIon1 [ion2 numIon2]

Adds counterions in a shell around *unit* using a Coulombic potential on a grid. If *numIon1* is 0 then the unit is neutralized. In this case, *ion1* must be opposite in charge to *unit* and *ion2* must not be specified. Otherwise, the specified numbers of *ion1* [*ion2*] are added [in alternating order]. If solvent is present, it is ignored in the charge and steric calculations, and if an ion has a steric conflict with a solvent molecule, the ion is moved to the center of that solvent molecule, and the latter is deleted. (To avoid this behavior, either solvate _after_ addions, or use `addIons2`.) Ions must be monatomic. This procedure is not guaranteed to globally minimize the electrostatic energy. When neutralizing regular-backbone nucleic acids, the first cations will generally be placed between phosphates, leaving the final two ions to be placed somewhere around the middle of the molecule. The default

grid resolution is 1 Å, extending from an inner radius of (*maxIonVdwRadius* + *maxSoluteAtomVdwRadius*) to an outer radius 4 Å beyond. A distance-dependent dielectric is used for speed. `addIons2` is the same as `addIons`, except solvent and solute are treated the same.

Algorithms for determining the number of ions to add, based on a desired salt concentration, are given in Refs. [234, 235].

10.6.6 addIonsRand

addIonsRand unit ion1 #ion1 [ion2 #ion2] [separation]

Adds counterions in a shell around *unit* by replacing random solvent molecules. If *#ion1* is 0, the unit is neutralized (*ion1* must be opposite in charge to *unit*, and *ion2* cannot be specified). Otherwise, the specified numbers of *ion1* [*ion2*] are added [in alternating order]. If *separation* is specified, ions will be guaranteed to be more than that distance apart in Angstroms.

Ions must be monoatomic. This procedure is much faster than `addIons`, as it does not calculate charges. Solvent must be present. It must be possible to position the requested number of ions with the given separation in the solvent. Algorithms for determining the number of ions to add, based on a desired salt concentration, are given in Refs. [234, 235].

10.6.7 addPath

addPath path

Add the directory in *path* to the list of directories that are searched for files specified by other commands. The following example illustrates this command.

```
> addPath /disk/howard
/disk/howard added to file search path.
```

After the above command is entered, the program will search for a file in this directory if a file is specified in a command. Thus, if a user has a library named "/disk/howard/rings.lib" and the user wants to load that library, one only needs to enter load rings.lib and not load /disk/howard/rings.lib.

10.6.8 addPdbAtomMap

addPdbAtomMap list

The atom Name Map is used to try to map atom names read from PDB files to atoms within residue UNITs when the atom name in the PDB file does not match an atom in the residue. This enables PDB files to be read in without extensive editing of atom names. Typically, this command is placed in the LEaP startup file, "leaprc", so that assignments are made at the beginning of the session. *list* should be a LIST of LISTs. Each sublist should contain two entries to add to the Name Map. Each entry has the form:

{ string string }

where the first string is the name within the PDB file, and the second string is the name in the residue UNIT.

10.6.9 addPdbResMap

addPdbResMap list

The Name Map is used to map RESIDUE names read from PDB files to variable names within LEaP. Typically, this command is placed in the LEaP startup file, "leaprc", so that assignments are made at the beginning of the session. The LIST is a LIST of LISTs. Each sublist contains two or three entries to add to the Name Map. Each entry has the form:

```
{ double string1 string2 }
```

where *double* can be 0 or 1, *string1* is the name within the PDB file, and *string2* is the variable name to which *string1* will be mapped. To illustrate, the following is part of the Name Map that exists when LEaP is started with a standard leaprc file:

```
ADE --> DADE
: :
0 ALA --> NALA
0 ARG --> NARG
: :
1 ALA --> CALA
1 ARG --> CARG
: :
1 VAL --> CVAL
```

Thus, the residue ALA will be mapped to NALA if it is the N-terminal residue and CALA if it is found at the C-terminus. The above Name Map was produced using the following (edited) command line:

```
> addPdbResMap {
> { 0 ALA NALA } { 1 ALA CALA }
> { 0 ARG NARG } { 1 ARG CARG } : :
> { 0 VAL NVAL } { 1 VAL CVAL }
> : :
> { ADE DADE } : :
> }
```

10.6.10 alias

```
alias [ string1 [ string2 ] ]
```

This command will add or remove an entry to the Alias Table or list entries in the Alias Table. If both strings are present, then *string1* becomes the alias to *string2*, the original command. If only one string is used as an argument, then that string will be removed from the Alias Table. If no arguments are given to the command, the current aliases stored in the Alias Table will be listed.

The proposed alias is first checked for conflict with the LEaP commands and rejected if a conflict is found. A proposed alias will replace an existing alias with a warning being issued. The alias can stand for more than a single word, but also as an entire string so the user can quickly repeat entire lines of input.

10.6.11 bond

```
bond atom1 atom2 [ order ]
```

Create a bond between *atom1* and *atom2*. Both of these ATOMs must be contained by the same UNIT. By default, the bond will be a single bond. By specifying "-", "=", "#", or ":" as the optional argument, order, the user can specify a single, double, triple, or aromatic bond, respectively. Example:

```
bond trx.32.SG trx.35.SG
```

10.6.12 bondByDistance

```
bondByDistance container [ maxBond ]
```

Create single bonds between all ATOMs in the UNIT *container* that are within *maxBond* Å of each other. If *maxBond* is not specified, a default distance will be used. This command is especially useful in building molecules. Example:

```
bondByDistance alkylChain
```

10.6.13 check

check unit [parms]

This command can be used to check *unit* for internal inconsistencies that could cause problems when performing calculations. This is a very useful command that should be used before a UNIT is saved with `saveAmberParm` or its variants. Currently it checks for the following possible problems:

- long bonds

- short bonds

- non-integral total charge of the UNIT

- missing force field atom types

- close contacts (< 1.5 Å) between nonbonded ATOMs

The user may collect any missing molecular mechanics parameters in a PARMSET for subsequent editing. In the following example, the alanine UNIT found in the amino acid library has been examined by the check command:

```
> check ALA
Checking 'ALA'....
Checking parameters for unit 'ALA'.
Checking for bond parameters.
Checking for angle parameters.
Unit is OK.
```

10.6.14 combine

variable = combine list

Combine the contents of the UNITs within *list* into a single UNIT. The new UNIT is placed in variable. This command is similar to the sequence command except it does not link the ATOMs of the UNITs together. In the following example, the input and output should be compared with the example given for the sequence command.

```
> tripeptide = combine { ALA GLY PRO }
Sequence: ALA
Sequence: GLY
Sequence: PRO
> desc tripeptide
UNIT name: ALA
Head atom: .R<ALA 1>.A<N 1>
Tail atom: .R<PRO 3>.A<C 13>
Contents:
R<ALA 1>
R<GLY 2>
R<PRO 3>
```

10.6.15 copy

newvariable = copy variable

In most cases, creates an exact duplicate of the object *variable*. Since *newvariable* is not pointing to the same object as *variable*, changing the contents of one object will not alter the other object. Example:

```
> tripeptide = sequence { ALA GLY PRO }
> tripeptideSol = copy tripeptide
> solvateBox tripeptideSol TIP3PBOX 8 2
```

In the above example, *tripeptide* is a separate object from *tripeptideSol* and is not solvated. Had the user instead entered

```
> tripeptide = sequence { ALA GLY PRO }
> tripeptideSol = tripeptide
> solvateBox tripeptideSol TIP3PBOX 8 2
```

then both *tripeptide* and *tripeptideSol* would be solvated since they would both refer to the same object.

Note that in a few instances, the copy command does not produce an exact copy. This is particularly relevant when making copies of oligosaccharide residues. In these, the copy command invariably inverts chirality at the anomeric carbon. The workaround for this is to use the copy command twice, where the second call inverts the chirality back.

10.6.16 createAtom

```
variable = createAtom name type charge
```

Return a new and empty ATOM with *name*, *type*, and *charge* as its atom name, atom type, and electrostatic point charge. (See the `add` command for an example of the `createAtom` command.)

10.6.17 createResidue

```
variable = createResidue name
```

Return a new and empty RESIDUE with the name *name*. (See the `add` command for an example of the `createResidue` command.)

10.6.18 createUnit

```
variable = createUnit name
```

Return a new and empty UNIT with the name *name*. (See the `add` command for an example of the `createUnit` command.)

10.6.19 deleteBond

```
deleteBond atom1 atom2
```

Delete the bond between the ATOMs *atom1* and *atom2*. If no bond exists, an error will be displayed.

10.6.20 desc

```
desc variable
```

Print a description of the object *variable*. In the following example, the alanine UNIT found in the amino acid library has been examined by the `desc` command:

```
> desc ALA
UNIT name: ALA
Head atom: .R<ALA 1>.A<N 1>
Tail atom: .R<ALA 1>.A<C 9>
Contents: R<ALA 1>
```

Now, the `desc` command is used to examine the first residue (1) of the alanine UNIT:

```
> desc ALA.1
RESIDUE name: ALA
RESIDUE sequence number: 1
Type: protein
Connection atoms:
Connect atom 0: A<N 1>
Connect atom 1: A<C 9>
Contents:
A<N 1>
A<HN 2>
A<CA 3>
A<HA 4>
A<CB 5>
A<HB1 6>
A<HB2 7>
A<HB3 8>
A<C 9>
A<O 10>
```

Next, we illustrate the `desc` command by examining the ATOM N of the first residue (1) of the alanine UNIT:

```
> desc ALA.1.N
ATOM Name: N
Type: N
Charge: -0.463
Element: N
Atom flags: 20000|posfxd- posblt- posdrn- sel- pert- notdisp- tchd-
       posknwn+ int - nmin- nbld-
Atom position: 3.325770, 1.547909, -0.000002
Atom velocity: 0.000000, 0.000000, 0.000000
Bonded to .R<ALA 1>.A<HN 2> by a single bond.
Bonded to .R<ALA 1>.A<CA 3> by a single bond.
```

Since the N ATOM is also the first atom of the ALA residue, the following command will give the same output as the previous example:

```
> desc ALA.1.1
```

10.6.21 groupSelectedAtoms

```
groupSelectedAtoms unit name
```

Create a group within *unit* with the name *name*, using all of the ATOMs within *unit* that are selected. If the group has already been defined then overwrite the old group. The `desc` command can be used to list groups. Example:

```
groupSelectedAtoms TRP sideChain
```

An expression like "TRP@sideChain" returns a LIST, so any commands that require LISTs can take advantage of this notation. After assignment, one can access groups using the "@" notation. Examples:

```
select TRP@sideChain
center TRP@sideChain
```

The latter example will calculate the center of the atoms in the "*sideChain*" group. (See the `select` command for a more detailed example.)

10.6.22 help

```
help [string]
```

This command prints a description of the command in *string*. If no argument is given, a list of help topics is provided.

10.6.23 impose

```
impose unit seqlist internals
```

The `impose` command allows the user to impose internal coordinates on *unit*. The list of RESIDUEs to impose the internal coordinates upon is in *seqlist*. The internal coordinates to impose are in *internals*, which is an object of type LIST.

The command works by looking into each RESIDUE within *unit* that is listed in *seqlist* and attempts to apply each of the internal coordinates within *internals*. The *seqlist* argument is a LIST of NUMBERS that represent sequence numbers or ranges of sequence numbers. A range of sequence numbers is represented by two element LISTs that contain the first and last sequence number in the range. The user can specify sequence number ranges that are larger than what is found in *unit*, in which case the range will stop at the beginning or end of *unit* as appropriate. For example, the range { 1 999 } will include all RESIDUEs in a 200 RESIDUE UNIT.

The internals argument is a LIST of LISTs. Each sublist contains a sequence of ATOM names which are of type STRING followed by the value of the internal coordinate. An example of the impose command would be:

```
impose peptide { 1 2 3 } { { "N" "CA" "C" "N" -40.0 } { "C" "N" "CA" "C" -60.0 } }
```

This would cause the RESIDUE with sequence numbers 1, 2, and 3 within the UNIT *peptide* to assume an α-helical conformation. The command

```
impose peptide { 1 2 { 5 10 } 12 } { { "CA" "CB" 5.0 } }
```

will impose on the residues with sequence numbers 1, 2, 5, 6, 7, 8, 9, 10, and 12 within the UNIT *peptide* a bond length of 5.0 Å between the α and β carbon atoms. RESIDUEs without an ATOM named CB, such as glycine, will be unaffected.

It is important to understand that the impose command attempts to perform the intended action on all residues in the *seqlist*, but does not necessarily limit itself to acting only upon *internals* contained within those residues. That is, the list does not limit the residues to consider. Rather, it is a list of all starting points to consider. In other words, to specify a *seqlist* of { 3 4 } tells *impose* to attempt to set two torsions, one starting in residue 3 and the other starting in residue 4. It does not specify that the torsion should only be set if the atoms are found within residues 3 and/or 4.

Because of this, one must be careful when setting torsions between two residues. It is necessary to know which atoms are contained in which residues. Consider the following trisaccharide:

$$\alpha\text{-D-Glc}p\text{-(1-6)-}\beta\text{-D-Man}p\text{-(1-6)-}\beta\text{-D-Gal}p\text{-OH}$$

To build it most simply in LEaP requires the following directive. Note that the build order in LEaP is the reverse of the standard order in which the residues are written above.

```
glycan = sequence { ROH 6LB 6MB 0GA }
```

A proper build of a 1-6 oligosaccharide linkage often requires setting three torsions. In the manner that residues are defined in the Glycam force fields, the atoms describing two of those torsions, ϕ and ψ, span two residues. However, the atoms in the third, ω, exist entirely within one residue. In fact, they exist within all three glycan residues in the example above. The following commands will set only the three torsions in the glycosidic linkage between residues 4 (0GA) and 3 (6MB).

```
impose glycan { 4 } { { "H1" "C1" "O6" "C6" -60.0 } } # O6 & C6 are in residue 3
impose glycan { 4 } { { "C1" "O6" "C6" "C5" 180.0 } } # only C1 is in residue 4
impose glycan { 3 } { { "O6" "C6" "C5" "O5" 60.0 } } # all are in residue 3
```

The common misconception that the *seqlist* sets a limit on the residues affected can cause trouble in this case. For example, this command

```
impose glycan { 4 3 } { { "H1" "C1" "O6" "C6" -60.0 } }
```

will find all sequences beginning in residue 4 and in residue 3 that contain the serially bonded atoms H1 C1 O6 and C6. Therefore, in this case, it will set the specified torsions between residues 4 and 3 as well as between 3 and 2. Similarly, this command

```
impose peptide { 4 } { { "O6" "C6" "C5" "O5" 60.0 } }
```

will not affect any inter-residue linkage, but instead will set the C5-C6 torsion in the glucopyranoside (0GA) at the non-reducing end of the oligosaccharide.

The ordering and content within the *internals* list is important as well. For these examples, consider the simple peptide sequence:

```
peptide = sequence { ALA ALA ALA ALA }
```

The ordering of the *internals* specifies the atoms to which the torsion set is applied. The *impose* command will find the first atom in the *internals* list, check for the presence of a bonded second atom, and so forth. It will then apply the action, here a torsion, to those four atoms. For example, this command:

```
impose peptide { 3 } { { "N" "CA" "C" "N" -40.0 } }  # between 3 and 4
```

will set the torsion between residues 3 and 4. However, this one:

```
impose peptide { 3 } { { "N" "C" "CA" "N" -40.0 } }  # between 3 and 2
```

will set the torsion between residues 3 and 2.

If at any point, the *impose* command does not find an atom bonded to a previous atom in an *internals* list, it will silently ignore the command. This is likely to occur in two instances. One, the atom simply might not exist in the residue:

```
impose peptide { 3 } { { "N" "CA" "CB" "HB4" 10.0 } }  # no effect, silent
```

Here, of course, there is no atom named HB4 in alanine. Similarly, improper torsions are ignored. For example, this command also has no effect:

```
impose peptide { 3 } { { "N" "HB1" "CA" "CB" 10.0 } }  # no effect, silent
```

because HB1 is not bonded to N.

Three types of conformational change are supported: Bond length changes, bond angle changes, and torsion angle changes. If the conformational change involves a torsion angle, then all dihedrals around the central pair of atoms are rotated. The entire list of internals is applied to each RESIDUE.

It is also important to note that the impose command performs its actions entirely using internal coordinates. Because of this, it is difficult to predict the resulting behavior when the coordinates are translated back to cartesian, for example when writing a PDB file.

10.6.24 list

List all of the variables currently defined. To illustrate, the following (edited) output shows the variables defined when LEaP is started with a standard leaprc file:

```
> list A ACE ALA ARG ASN : : VAL W WAT Y
```

10.6.25 loadAmberParams

```
variable = loadAmberParams filename
```

Load an AMBER format parameter set file and place it in *variable*. All interactions defined in the parameter set will be contained within *variable*. This command causes the loaded parameter set to be included in LEaP's list of parameter sets that are searched when parameters are required. General proper and improper torsion parameters are modified during the command execution with the LEaP general type "?" replacing the AMBER general type "X"

```
> parm91 = loadAmberParams parm91X.dat
> saveOff parm91 parm91.lib
```

10.6.26 loadAmberPrep

```
loadAmberPrep filename [ prefix ]
```

This command loads an AMBER PREP input file. For each residue that is loaded, a new UNIT is constructed that contains a single RESIDUE and a variable is created with the same name as the name of the residue within the PREP file. If the optional argument *prefix* (a STRING) is provided, its contents will be prefixed to each variable name; this feature is used to prefix UATOM residues, which have the same names as AATOM residues with the string "U" to distinguish them.

```
> loadAmberPrep cra.in
Loaded UNIT: CRA
```

10.6.27 loadOff

```
loadOff filename
```

This command loads the OFF library within the file named *filename*. All UNITs and PARMSETs within the library will be loaded. The objects are loaded into LEaP under the variable names the objects had when they were saved. Variables already in existence that have the same names as the objects being loaded will be overwritten. Any PARMSETs loaded using this command are included in LEaP's library of PARMSETs that is searched whenever parameters are required (the old AMBER format is used for PARMSETs rather than the OFF format in the default configuration). Example command line:

```
> loadOff parm91.lib
Loading library: parm91.lib
Loading: PARAMETERS
```

10.6.28 loadMol2

```
variable = loadMol2 filename
```

Load a Sybyl MOL2 format file into *variable*, a UNIT. This command is very much like `loadOff`, except that it only creates a single UNIT.

157

10.6.29 loadPdb

variable = loadPdb filename

Load a Protein Data Bank (PDB) format file with the file name *filename* into *variable*, a UNIT. The sequence numbers of the RESIDUEs will be determined from the order of residues within the PDB file ATOM records. This function will search the variables currently defined within LEaP for variable names that map to residue names within the ATOM records of the PDB file. If a matching variable name is found then the contents of the variable are added to the UNIT that will contain the structure being loaded from the PDB file. Adding the contents of the matching UNIT into the UNIT being constructed means that the contents of the matching UNIT are copied into the UNIT being built and that a bond is created between the connect0 ATOM of the matching UNIT and the connect1 ATOM of the UNIT being built. (This bond creation does not occur if a PDB 'TER' card separates the atoms. As of AmberTools21 a PDB TER record is also used to detect a new residue in the case of contiguous residues with identical residue sequence numbers.) The UNITs are combined in the same way UNITs are combined using the sequence command. As atoms are read from the ATOM records their coordinates are written into the correspondingly named ATOMs within the UNIT being built. If the entire residue is read and it is found that ATOM coordinates are missing, then external coordinates are built from the internal coordinates that were defined in the matching UNIT. This allows LEaP to build coordinates for hydrogens and lone-pairs which are not specified in PDB files. Note that the standard leaprc files include commands to establish automatic N- and C-termination of amino acid sequences and 5' and 3' termination of nucleic acid sequences.

> crambin = loadPdb 1crn

10.6.30 loadPdbUsingSeq

loadPdbUsingSeq filename unitlist

This command reads a PDB format file named *filename*. This command is identical to loadPdb except it does not use the residue names within the PDB file. Instead, the sequence is defined by the user in *unitlist*. For more details see loadPdb.

> peptSeq = { UALA UASN UILE UVAL UGLY }
> pept = loadPdbUsingSeq pept.pdb peptSeq

In the above example, a variable is first defined as a LIST of united atom RESIDUEs. A PDB file is then loaded, in this sequence order, from the file "pept.pdb".

10.6.31 logFile

logFile filename

This command opens the file with the file name *filename* as a log file. User input and all output is written to the log file. Output is written to the log file as if the verbosity level were set to 2. An example of this command is

> logfile /disk/howard/leapTrpSolvate.log

10.6.32 measureGeom

measureGeom atom1 atom2 [atom3 [atom4]]

Measure the distance, angle, or torsion between two, three, or four ATOMs, respectively.

In the following example, we first describe the RESIDUE ALA of the ALA UNIT in order to find the identity of the ATOMs. Next, the measureGeom command is used to determine a distance (determining simple angles and dihedral angles are straightforward extensions). As shown in the example, the ATOMs may be identified using atom names or numbers.

```
> desc ALA.ALA
RESIDUE name: ALA
RESIDUE sequence number: 1
Type: protein ....
> measureGeom ALA.ALA.3 ALA.ALA.CB
Distance: 1.52 angstroms
```

10.6.33 quit

Quit the LEaP program.

10.6.34 remove

```
remove container item
```

Remove the object *item* from the object *container*. If *container* does not contain *item*, an error message will be displayed. This command is used to remove ATOMs from RESIDUEs, and RESIDUEs from UNITs. If the object represented by *item* is not referenced by any other variable name, it will be destroyed.

```
> dipeptide = combine { ALA GLY }
Sequence: ALA
Sequence: GLY
> desc dipeptide
UNIT name: ALA
Head atom: .R<ALA 1>.A<N 1>
Tail atom: .R<GLY 2>.A<C 6>
Contents: R<ALA 1> R<GLY 2>
> remove dipeptide dipeptide.2
> desc dipeptide UNIT name: ALA
Head atom: .R<ALA 1>.A<N 1>
Tail atom: null
Contents: R<ALA 1>
```

10.6.35 saveAmberParm

```
saveAmberParm unit topologyfilename coordinatefilename
```

Save the Amber/NAB topology and coordinate files for *unit* into the files named *topologyfilename* and *coordinatefilename* respectively. This command will cause LEaP to search its list of PARMSETs for parameters defining all of the interactions between the ATOMS within *unit*. It produces topology files and coordinate files that are identical in format to those produced by Amber PARM and can be read into Amber and NAB for calculations. The output of this operation can be used for minimizations, dynamics, and thermodynamic perturbation calculations.

In the following example, the topology and coordinates from the all_amino94.lib UNIT ALA are generated:

```
> saveamberparm ALA ala.top ala.crd
```

10.6.36 saveMol2

```
saveMol2 unit filename type-flag
```

Write *unit* to the file *filename* as a Tripos mol2 format file. If *type-flag* is 0, the Tripos (Sybyl) atom types will be used; if *type-flag* is 1, the Amber atom types present in *unit* will be used. Generally, you would want to set *type-flag* to 1, unless you need the Sybyl atom types for use in some program outside Amber; Amber itself has no force fields that use Sybyl atom types.

10.6.37 saveOff

saveOff object filename

The `saveOff` command allows the user to save UNITs and PARMSETs to a file named *filename*. The file is written using the Object File Format (off) and can accommodate an unlimited number of uniquely named objects. The names by which the objects are stored are the variable names specified within the *object* argument. If the file *filename* already exists, the new objects will be added to it. If there are objects within the file with the same names as objects being saved then the old objects will be overwritten. The argument *object* can be a single UNIT, a single PARMSET, or a LIST of mixed UNITs and PARMSETs. (See the `add` command for an example of the `saveOff` command.)

10.6.38 savePdb

savePdb unit filename

Write *unit* to the file *filename* as a PDB format file. In the following example, the PDB file from the ALA unit is generated:

> savepdb ALA ala.pdb

Warning: The PDB-like file created with this command is primarily useful for reading back into *tleap*, or for other Amber-related uses. It is consistent with Amber, but not with other aspects of the PDB standard (e.g. in atom and residue names, etc.) Use the *ambpdb* program (see Section **??**) if you need a file that more fully complies with the PDB standard.

10.6.39 sequence

variable = sequence list

The `sequence` command is used to combine the contents of *list*, which should be a LIST of UNITs, into a new, single UNIT. This new UNIT is constructed by taking each UNIT in *list* in turn and copying its contents into the UNIT being constructed. As each new UNIT is copied, a bond is created between the tail ATOM of the UNIT being constructed and the head ATOM of the UNIT being copied, if both connect ATOMs are defined. If only one is defined, a warning is generated and no bond is created. If neither connection ATOM is defined then no bond is created. As each RESIDUE is copied into the UNIT being constructed it is assigned a sequence number which represents the order the RESIDUEs are added. Sequence numbers are assigned to the RESIDUEs so as to maintain the same order as was in the UNIT before it was copied into the UNIT being constructed. This command builds reasonable starting coordinates for all ATOMs within the UNIT; it does this by assigning internal coordinates to the linkages between the RESIDUEs and building the external coordinates from the internal coordinates from the linkages and the internal coordinates that were defined for the individual UNITs in the sequence.

> tripeptide = sequence { ALA GLY PRO }

10.6.40 set

This command operates in two modes. In the first, it sets default values for some parameters. In the second, it sets specific properties to containers (for example, UNITs).

Defaults can be set in LEaP for the global parameters below with this usage:

set default parameter value

For example:

set default PBRadii mbondi

OldPrmtopFormat If set to "on", the `saveAmberParm` command will write a prmtop file in the format used in Amber 6 and earlier versions; if set to "off" (the default), it will use the new format. This is discouraged for general use and is available mainly for backwards compatibility with programs that expect old-style topology files or for testing.

Dielectric If set to "distance" (the default), electrostatic calculations in LEaP will use a distance-dependent dielectric; if set to "constant", a constant dielectric will be used.

PdbWriteCharges If set to "on", atomic charges will be placed in the "B-factor" field of PDB files saved with the `savePdb` command; if set to "off" (the default), no such charges will be written.

PBRadii Used to choose various sets of atomic radii for generalized Born or Poisson-Boltzmann calculations. Options are: "bondi", which gives values from Ref. [124], which should be used with *igb* = 7; "mbondi", which is the default, and the recommended parameter set for *igb* = 1 [62]; "mbondi2", which is a second modification of the Bondi radii set [45], and should be used with *igb* = 2 or 5; "mbondi3", which is a third modification of the Bondi radii set [56] recommended for use with igb = 8; and "amber6", which is only to be used for reproducing very early calculations that used *igb* = 1 [43].

nocenter If set to "on", LEaP will not center the coordinates inside the box for a periodic simulation; it will leave them unchanged as it does for a non-periodic simulation (note that the various solvate commands can still rigidly translate a solute). If set to "off" (the default), centering of coordinates will occur (as it always has, in previous versions of LEaP). Avoiding coordinate translations can be useful to avoid changing reference (perhaps experimental) coordinates. This option may be especially helpful for crystal simulations.

reorder_residues If set to "off", residues in the output will be left in the same order they were found in the input file. The default behavior ("on") is to place non-solvent residues first, followed by solvent residues, followed by solvent cap residues (if cap exists). "off" can, for example, be useful in crystal simulations (keep residues belonging to each asymmetric unit separate), but note that turning residue ordering off is untested and may lead to unforeseen behavior. Only set to "off" if you know what you are doing!

The parameters listed below can be set for the specified *containers* within LEaP using the following syntax:

```
set container parameter object
```

Some examples:

```
set ATOM name "name"
set RESIDUE connect0 ATOM
my_system = loadPDB file.pdb
set my_system box {25 30 32}
```

For ATOMs:

name A unique STRING descriptor used to identify ATOMs.

type This is a STRING property that defines the AMBER force field atom type.

charge The charge property is a NUMBER that represents the ATOM's electrostatic point charge to be used in a molecular mechanics force field.

position This property is a LIST of NUMBERs containing three values: the (X, Y, Z) Cartesian coordinates of the ATOM.

pertName This STRING is a unique identifier for an ATOM in its final state during a Free Energy Perturbation calculation. This functionality is no longer implemented in Amber.

pertType This STRING is the AMBER force field atom type of a perturbed ATOM. This functionality is no longer implemented in Amber.

pertCharge This NUMBER represents the final electrostatic point charge on an ATOM during a Free Energy Perturbation. This function is no longer implemented in Amber.

For RESIDUEs:

connect0 This identifies the first of up to three ATOMs that will be used to make links to other RESIDUEs. In a UNIT containing a single RESIDUE, the RESIDUE's connect0 ATOM is usually defined as the UNIT's head ATOM.

connect1 This identifies the second of up to three ATOMs that will be used to make links to other RESIDUEs. In a UNIT containing a single RESIDUE, the RESIDUE's connect1 ATOM is usually defined as the UNIT's tail ATOM.

connect2 This identifies the third of up to three ATOMs that will be used to make links to other RESIDUEs. In amino acids, the convention is that this is the ATOM to which disulfide bridges are made.

restype This property is a STRING that represents the type of the RESIDUE. Currently, it can have one of the following values: "undefined", "solvent", "protein", "nucleic", or "saccharide".

name This STRING property is the RESIDUE name.

For UNITs:

head Defines the ATOM within the UNIT that is connected when UNITs are joined together: the tail ATOM of one UNIT is connected to the head ATOM of the subsequent UNIT in any sequence.

tail Defines the ATOM within the UNIT that is connected when UNITs are joined together: the tail ATOM of one UNIT is connected to the head ATOM of the subsequent UNIT in any sequence.

box This property defines the bounding box of the UNIT (*container*). If *object* is set to null then no bounding box is defined. If it is a single NUMBER, the bounding box will be defined to be a cube with each side being NUMBER Å across. If it is a LIST, it must contain three NUMBERs, the lengths (in Å) of the three sides of the bounding box. Note that this command does not allow one to set the angles for the periodic system. See the ChBox command to do that.

cap This property defines the solvent cap of the UNIT. If it is set to null then no solvent cap is defined. Otherwise, it should be a LIST of four NUMBERs; the first three NUMBERs define the Cartesian coordinates (X, Y, Z) of the origin of the solvent cap in Å, while the fourth defines the radius of the solvent cap, also in Å.

10.6.41 setBox

setBox solute enclosure [distance]

This command creates a periodic box around *solute*, which should be a UNIT. It does not add any solvent to the system. setBox creates a cuboid box. The *enclosure* parameter determines whether the box encloses entire atoms or just atom centers. The former case is specified by the STRING value "vdw" for *enclosure* and the latter case by the STRING "centers". Use "centers" if the system has been previously equilibrated as a periodic box. The minimum distance between any atom in *solute* and the edge of the periodic box is given by the *distance* parameter; see the solvateBox command for more details.

```
> mol = loadpdb my.pdb
> setBox mol "vdw"
```

10.6.42 solvateBox and solvateOct

```
solvateBox solute solvent distance [ "iso" ] [ closeness ]
solvateOct solute solvent distance [ "iso" ] [ closeness ]
```

These two commands create periodic solvent boxes around *solute*, which should be a UNIT. `solvateBox` creates a cuboid box, while `solvateOct` creates a truncated octahedron. *solute* is modified by the addition of copies of the RESIDUEs found within *solvent*, which should also be a UNIT, such that the minimum distance between any atom originally present in *solute* and the edge of the periodic box is given by the *distance* parameter. The resulting solvent box will be repeated in all three spatial directions.

If the distance parameter is a single NUMBER then the minimum distance is the same for the x, y, and z directions, unless the STRING "iso" parameter is specified to make the box or truncated octahedron isometric. For solvateBox if "iso" is used, the solute is rotated to orient the principal axes, otherwise it is just centered on the origin. For solvateOct if the "iso" option is used, the isometric truncated octahedron is rotated to an orientation used by the PME code, and the box and angle dimensions output by the saveAmberParm* commands are adjusted for PME code imaging.In solvateBox, if the distance parameter is a LIST of three NUMBERS then the NUMBERs are applied to the x, y, and z axes respectively. As the larger box is created and superimposed on the solute, solvent molecules overlapping the solute are removed.In solvateOct, when a LIST is given for the distance parameter, four numbers are given instead of three, where the fourth is the diagonal clearance. If 0.0 is given as the fourth number, the diagonal clearance resulting from the application of the x,y,z clearances is reported. If a non-0 value is given, this may require scaling up the other clearances, which is also reported. Similarly, if a single NUMBER is given, any scaleup of the x,y,z buffer to accommodate the diagonal clip is reported.

The optional *closeness* parameter can be used to control how close, in Å, solvent ATOMs may come to solute ATOMs. The default value of *closeness* is 1.0. Smaller values allow solvent ATOMs to come closer to solute ATOMs. The criterion for rejection of overlapping solvent RESIDUEs is if the distance between any solvent ATOM and its nearest solute ATOM is less than the sum of the two ATOMs' van der Waals radii multiplied by *closeness*.

```
> mol = loadpdb my.pdb
> solvateOct mol TIP3PBOX 12.0 0.75
```

10.6.43 solvateCap

```
solvateCap solute solvent position radius [ closeness ]
```

The `solvateCap` command creates a solvent cap around *solute*, which is a UNIT. *solute* is modified by the addition of copies of the RESIDUEs found within *solvent*, which should also be a UNIT. The solvent box will be repeated in all three spatial directions to create a large solvent sphere with a radius of *radius* Å.

The *position* argument defines where the center of the solvent cap is to be placed. If *position* is a UNIT, a RESIDUE, an ATOM, or a LIST of UNITs, RESIDUEs, or ATOMs, then the geometric center of the ATOM or ATOMs within the object will be used as the center of the solvent cap sphere. If *position* is a LIST containing three NUMBERs, then it will be treated as a vector describing the position of the solvent cap sphere center.

The optional *closeness* parameter can be used to control how close, in Å, solvent ATOMs may come to solute ATOMs. The default value of *closeness* is 1.0. Smaller values allow solvent ATOMs to come closer to solute ATOMs. The criterion for rejection of overlapping solvent RESIDUEs is if the distance between any solvent ATOM and its nearest solute ATOM is less than the sum of the two ATOMs' van der Waals radii multiplied by *closeness*.

This command modifies *solute* in several ways. First, the UNIT is modified by the addition of solvent RESIDUEs copied from *solvent*. Secondly, the "cap" parameter of *solute* is modified to reflect the fact that a solvent cap has been created around the solute.

```
> mol = loadpdb my.pdb
> solvateCap mol TIP3PBOX mol.2.CA 12.0 0.75
```

10.6.44 solvateShell

solvateShell solute solvent thickness [closeness]

The `solvateShell` command adds a solvent shell to *solute*, which should be a UNIT. *solute* is modified by the addition of copies of the RESIDUEs found within *solvent*, which should also be a UNIT. The resulting solute/solvent UNIT will be irregular in shape since it will reflect the contours of the original solute molecule. The solvent box will be repeated in three directions to create a large solvent box that can contain the entire solute and a shell *thickness* Å thick. Solvent RESIDUEs are then added to *solute* if they lie within the shell defined by *thickness* and do not overlap with any ATOM originally present in *solute*. The optional *closeness* parameter can be used to control how close solvent ATOMs can come to solute ATOMs. The default value of the *closeness* argument is 1.0. Please see the `solvateBox` command for more details on the closeness parameter.

```
> mol = loadpdb my.pdb
> solvateShell mol TIP3PBOX 12.0 0.8
```

10.6.45 source

source filename

This command executes the contents of the file given by *filename*, treating them as LEaP commands. To display the commands as they are read, see the `verbosity` command.

10.6.46 transform

transform atoms, matrix

Transform all of the ATOMs within *atoms* by a symmetry operation. The symmetry operation is represented as a (3×3) or (4×4) matrix, and given as nine or sixteen NUMBERs in *matrix*, a LIST of LISTs. The general matrix looks like:

r11 r12 r13 -tx r21 r22 r23 -ty r31 r32 r33 -tz 0 0 0 1

The matrix elements represent the intended symmetry operation. For example, a reflection in the (x,y) plane would be produced by the matrix:

```
1 0 0 0 1 0 0 0 -1
```

This reflection could be combined with a 6 Å translation along the x-axis by using the following matrix:

```
1 0 0 6 0 1 0 0 0 0 -1 0 0 0 0 1
```

In the following example, wrB is transformed by an inversion operation:

```
transform wrpB { { -1 0 0 } { 0 -1 0 } { 0 0 -1 } }
```

10.6.47 translate

translate atoms direction

Translate all of the ATOMs within *atoms* by the vector given by *direction*, a LIST of three NUMBERs.
Example:

```
translate wrpB { 0 0 -24.53333 }
```

10.6.48 verbosity

>   **verbosity level**

This command sets the level of output that LEaP provides the user. A value of 0 is the default, providing the minimum of messages. A value of 1 will produce more output, and a value of 2 will produce all of the output of level 1 and display the text of the script lines executed with the source command. The following line is an example of this command:

```
> verbosity 2
Verbosity level: 2
```

10.6.49 zMatrix

>   **zMatrix object zmatrix**

The `zMatrix` command is quite complicated. It is used to define the external coordinates of ATOMs within *object* using internal coordinates. The second parameter of the `zMatrix` command is a LIST of LISTs; each sub-list has several arguments:

>   **{ a1 a2 bond12 }**

This entry defines the coordinate of *a1*, an ATOM, by placing it *bond12* Å along the x-axis from ATOM *a2*. *a2* is placed at the origin if its coordinates are not defined.

>   **{ a1 a2 a3 bond12 angle123 }**

This entry defines the coordinate of *a1* by placing it *bond12* Å away from *a2* making an angle of *angle123* degrees between *a1*, *a2* and *a3*. The angle is measured in a right-hand sense and in the xy plane. ATOMs *a2* and *a3* must have coordinates defined.

>   **{ a1 a2 a3 a4 bond12 angle123 torsion1234 }**

This entry defines the coordinate of *a1* by placing it *bond12* Å away from *a2*, creating an angle of *angle123* degrees between *a1*, *a2*, and *a3*, and making a torsion angle of *torsion1234* degrees between *a1*, *a2*, *a3*, and *a4*.

>   **{ a1 a2 a3 a4 bond12 angle123 angle124 orientation }**

This entry defines the coordinate of *a1* by placing it *bond12* Å away from *a2*, and making angles *angle123* degrees between *a1*, *a2*, and *a3*, and *angle124* degrees between *a1*, *a2*, and *a4*. The argument orientation defines whether *a1* is above or below a plane defined by *a2*, *a3* and *a4*. If *orientation* is positive, *a1* will be placed so that the triple product $((a3-a2) \times (a4-a2)) \cdot (a1-a2)$ is positive. Otherwise, *a1* will be placed on the other side of the plane. This allows the coordinates of a molecule like fluoro-chloro-bromo-methane to be defined without having to resort to dummy atoms.

The first arguments within the zMatrix entries (*a1*, *a2*, *a3* and *a4*) are either ATOMs, or STRINGs containing names of ATOMs that already exist within *object*. The subsequent arguments (*bond12*, *angle123*, *torsion1234* or *angle124*, and *orientation*) are all NUMBERs. Any ATOM can be placed at the *a1* position, even one that has coordinates defined. This feature can be used to provide an endless supply of dummy atoms, if they are required. A predefined dummy atom with the name "*" (a single asterisk, no quotes) can also be used.

There is no order imposed in the sub-lists. The user can place sub-lists in arbitrary order, as long as they maintain the requirement that all ATOMs *a2*, *a3*, and *a4* must have external coordinates defined, except for entries that define the coordinate of an ATOM using only a bond length. (See the `add` command for an example of the `zMatrix` command.)

11 Antechamber and GAFF

These are a set of tools to generate files for organic molecules and for some metal centers in proteins, which can then be read into LEaP. The Antechamber suite was written by Junmei Wang, and is designed to be used in conjunction with the general AMBER force field (GAFF) (gaff.dat).[236] See Ref. [237] for an explanation of the algorithms used to classify atom and bond types, to assign charges, and to estimate force field parameters that may be missing in gaff.dat. The python Metal Site Modeling Toolbox (pyMSMT) software package was developed by Pengfei Li, and is described in Section**??**.

Like the traditional AMBER force fields, GAFF uses a simple harmonic function form for bonds and angles. Unlike the traditional AMBER force fields, atom types in GAFF are more general and cover most of the organic chemical space. In total there are 33 basic atom types and 22 special atom types. The charge methods used can be HF/6-31G* RESP, AM1-BCC,[238, 239] or ABCG2.[240, 241] The force field parametrization was performed entirely with HF/6-31G* RESP charges. (Note that in AM1-BCC, the QM electrostatic potentials that were used as fitting targets were created in a very slightly different manner and then compared to RESP charges, using different scaling factors (i.e. 0.001/0.01 [239] versus 0.0005/0.001 [242].)

To maintain force field integrity and to achieve the best performance, the following is the overall guidance on choosing force fields and charge models. Both gaff and gaff2 were developed using HF/6-31G* RESP charge, therefore, RESP charge is compatible with both general AMBER force fields. It was found that gaff/bcc combination achieves good performance in many scenarios including solvation free energy calculations. For the efficient charge models, bcc or abcg2, gaff/bcc and gaff2/abcg2 combinations are recommended, while gaff2/bcc or gaff/abcg2 are not.

The van der Waals parameters are the same as those used by the traditional AMBER force fields. The equilibrium bond lengths and bond angles came from *ab initio* calculations at the MP2/6-31G* level and statistics derived from the Cambridge Structural Database. The force constants for bonds and angles were estimated using empirical models, and the parameters in these models were trained using the force field parameters in the traditional AMBER force fields. General torsional angle parameters were extensively applied in order to reduce the huge number of torsional angle parameters to be derived. The force constants and phase angles in the torsional angle parameters were optimized using our PARMSCAN package,[243] with an aim to reproduce the rotational profiles depicted by high-level *ab initio* calculations (geometry optimizations at the MP2/6-31G* level, followed by single point calculations at MP4/6-311G(d,p)).

By design, GAFF is a complete force field (so that missing parameters rarely occur); it covers almost all the organic chemical space that is made up of C, N, O, S, P, H, F, Cl, Br and I. Moreover, GAFF is totally compatible with the AMBER macromolecular force fields. It should be noted that GAFF atom types, except metal types, are in lower case, while AMBER atom types are always in upper case. This feature makes it possible to load both AMBER protein/nucleic acid force fields and GAFF without any conflict. One can even merge the two kinds of force fields into one file. The combined force fields are capable of studying complicated systems that include both proteins/nucleic acids and organic molecules. We believe that the combination of GAFF with AMBER macromolecular force fields will provide a useful molecular mechanical tool for rational drug design, especially in binding free energy calculations and molecular docking studies. Since its introduction, GAFF has been used for a wide range of applications, including ligand docking,[244] bilayer simulations,[245, 246] and the study of pure organic liquids [247]; see also a recent overview of general force fields for small molecules.[248]

11.1 Principal programs

The *antechamber* program itself is the main program of Antechamber. If your molecule falls into any of several fairly broad categories, *antechamber* should be able to process your PDB file directly, generating output files suitable for LEaP. Otherwise, you may provide an input file with connectivity information, i.e., in a format such

as Mol2 or SDF. If there are missing parameters after *antechamber* is finished, you may want to run *parmchk2* to generate a frcmod template that will assist you in generating the needed parameters.

11.1.1 antechamber

This is the most important program in the package. It can perform many file conversions, and can also assign atomic charges and atom types. As required by the input, antechamber executes the following programs: *sqm* (or, alternatively, *mopac* or *divcon*), *atomtype*, *am1bcc*, *bondtype*, *espgen*, *respgen* and *prepgen*. It typically produces many intermediate files; these may be recognized by their names, in which all letters are upper-case. If you experience problems while running *antechamber*, you may want to run the individual programs that are described below (to facilitate this run antechamber with the option '-s 2').

Antechamber options:

```
-help print these instructions
-i      input file name
-fi     input file format
-o      output file name
-fo     output file format
-c      charge method
-cf     charge file name
-nc     net molecular charge (int)
-a      additional file name
-fa     additional file format
-ao     additional file operation
        crd   : only read in coordinate
        crg   : only read in charge
        radius: only read in radius
        name  : only read in atom name
        type  : only read in atom type
        bond  : only read in bond type
-m      multiplicity (2S+1), default is 1
-rn     residue name, overrides input file, default is MOL
-rf     residue toplogy file name in prep input file,
        default is molecule.res
-ch     check file name for gaussian, default is 'molecule'
-ek     mopac or sqm keyword, inside quotes; overwrites previous ones
-gk     gaussian job keyword, inside quotes, is ignored when both -gopt and -gsp are used
-gopt   gaussian job keyword for optimization, inside quotes
-gsp    gaussian job keyword for single point calculation, inside quotes
-gm     gaussian memory keyword, inside quotes, such as "%mem=1000MB"
-gn     gaussian number of processors keyword, inside quotes, such as "%nproc=8"
-gdsk   gaussian maximum disk usage keyword, inside quotes, such as "%maxdisk=50GB"
-gv     add keyword to generate gesp file (for Gaussian 09 only)
        1    : yes
        0    : no, the default
-ge     gaussian esp file generated by iop(6/50=1), default is g09.gesp
-tor    torsional angle list, inside a pair of quotes, such as "1-2-3-4:0,5-6-7-8"
        ':1' or ':0' indicates the torsional angle is frozen or not
-df     am1-bcc precharge flag, 2 - use sqm(default); 0 - use mopac
-at     atom type
        gaff : the default
        gaff2: for gaff2 (beta-version)
        amber: for PARM94/99/99SB
        bcc  : bcc
        abcg2: abcg2
```

```
        sybyl: sybyl
-du    fix duplicate atom names: yes(y)[default] or no(n)
-bk    component/block Id, for ccif
-an    adjust atom names: yes(y) or no(n)
       the default is 'y' for 'mol2' and 'ac' and 'n' for the other formats
-j     atom type and bond type prediction index, default is 4
       0    : no assignment
       1    : atom type
       2    : full  bond types
       3    : part  bond types
       4    : atom and full bond type
       5    : atom and part bond type
-s     status information: 0(brief), 1(default) or 2(verbose)
-eq    equalizing atomic charge, default is 1 for '-c resp' and '-c bcc' and 0 for the other charg
       0    : no use
       1    : by atomic paths
       2    : by atomic paths and structural information, i.e. E/Z configurations
-pf    remove intermediate files: yes(y) or no(n)[default]
-pl    maximum path length to determin equivalence of atomic charges for resp and bcc,
       the smaller the value, the faster the algorithm, default is -1 (use full length),
       set this parameter to 10 to 30 if your molecule is big (# atoms >= 100)
-seq   atomic sequence order changable: yes(y)[default] or no(n)
-dr    acdoctor mode: yes(y)[default] or no(n)

-i -o -fi and -fo must appear in command lines and the others are optional

Use 'antechamber -L' to list the supported file formats and charge methods
```

List of the File Formats:

```
file format type  abbre. index | file format type abbre. index
---------------------------------------------------------------
Antechamber        ac      1 | Sybyl Mol2        mol2    2
PDB                pdb     3 | Modified PDB      mpdb    4
AMBER PREP (int)   prepi   5 | AMBER PREP (car)  prepc   6
Gaussian Z-Matrix  gzmat   7 | Gaussian Cartesian gcrt    8
Mopac Internal     mopint  9 | Mopac Cartesian   mopcrt 10
Gaussian Output    gout   11 | Mopac Output      mopout 12
Alchemy            alc    13 | CSD               csd    14
MDL                mdl    15 | Hyper             hin    16
AMBER Restart      rst    17 | Jaguar Cartesian  jcrt   18
Jaguar Z-Matrix    jzmat  19 | Jaguar Output     jout   20
Divcon Input       divcrt 21 | Divcon Output     divout 22
SQM Input          sqmcrt 23 | SQM Output        sqmout 24
Charmm             charmm 25 | Gaussian ESP      gesp   26
Component cif      ccif   27 | GAMESS dat        gamess 28
Orca input         orcinp 29 | Orca output       orcout 30
pdbqt              pdbqt  31 |
---------------------------------------------------------------
```

AMBER restart file can only be read in as additional file

List of the Charge Methods:

```
charge method     abbre.  index | charge method     abbre.
```

```
------------------------------------------------------------------
RESP                resp     1  |  AM1-BCC             bcc     2
CM1                 cm1      3  |  CM2                  cm2     4
ESP (Kollman)       esp      5  |  Mulliken            mul     6
Gasteiger           gas      7  |  ABCG2               abcg2   8
Read in charge      rc       9  |  Write out charge    wc     10
Delete Charge       dc      11  |
------------------------------------------------------------------
```

Examples:

   The basic use of *antechamber* is to pick input and output files and formats (via the $-i$, $-fi$, $-o$, $-fo$ flags) , and choose various options for charge models, atom types, etc. A typical use would be:

   antechamber -i my.pdb -fi pdb -o my.mol2 -fo mol2 -c bcc -nc 1

The only "tricky" part is in generating resp charges, which requires interacting with the Gaussian program, and which varies depending on the version:

   Using Gaussian 98 files as input:
   (1) antechamber -i g98.out -fi gout -o sustiva_resp.mol2 -fo mol2 -c resp -eq 2
   (2) antechamber -i g98.out -fi gout -o sustiva_cm2.mol2 -fo mol2 -c cm2

   Using Gaussian03 files as input:
   (11)antechamber -i g03.out -fi gout -o mtx.mol2 -fo mol2 -c resp
   **   -a mtx.pdb -fa pdb -ao name**

   Using Gaussian09 (version b1 and beyond):
   (12)antechamber -i ch3I.mol2 -fi mol2 -o gcrt.com -fo gcrt -gv 1 -ge ch3I.gesp
   **   run Gaussian09 with gcrt.com as input**
   **   antechamber -i ch3I.gesp -fi gesp -o ch3I_resp.mol2 -fo mol2 -c resp -eq 2**

The following is the detailed explanations of some flags

-nc This flag specifies the net charge of the input molecule, otherwise, the net charge is read in from the input directly (such as gout, mopout, sqmout, sqmcrt, gcrt, etc.) or calculated by summing the partial charges (such as mol2, prepi, etc).

-a,-fa,-ao Sometimes, one wants to read additional information from another file other than the input, the '-ao' flag informs the program to read in which information from the additional file specified with '-a' flag. In Example (11), a mol2 file is generated from a Gaussian output file with atom names read in from a pdb file.

-ch,-gk,-gm,-gn Those flags specify the keywords and resource usage in Gaussian calculations

-ge,-gv The '-ge' flag specifies the file name of gesp file generated using iop(6/50=1) with Gaussian 09; the -gv flag specifies the Gaussian version and the default is '1' for Gaussian 09. If one wants to generate Gaussian input files (gcrt and gzmat) for older Gaussian versions, '-gv' must be set to '0'.

-rn The '-rn' line specifies the residue name to be used; thus, it must be one to three characters long.

-at This flag is used to specify whether atom types are to be created for the GAFF force field or for atom types consistent with parm94.dat and parm99.dat (i.e., the AMBER force fields). If you are using *antechamber* to create a modified residue for use with the standard AMBER parm94/parm99 force fields, you should set this flag to "amber"; if you are looking at a more arbitrary molecule, set it to "gaff", even if the molecule is intended for use as a ligand bound to a macromolecule described by the AMBER force fields.

-j This flag instructs the program how to run 'bondtype' and 'atom type'. '-j 1' assumes the bond types already exists; '-j 4' first predicts the connectivity table, then assigns bond and atom types sequentially; '-j 5' reads in connectivity table from the input and then run 'bondtype' and 'atomtype' sequentially. In most situations, '-j 4', the default option, is recommended. However, '-j 5' should be used if the input structure is not good enough and it includes the bond connectivity information (such as mol2, mdl, gzmat, etc.)

-eq This flag specifies how to do charge equilibration. With '-eq 1', atomic charge equilibration is predicted only by atom paths, in another word, if two or more atoms have exactly same sets of atom paths, they are equivalent and their charges are forced to be same. While '-eq 2' predicts charge equilibration using both atom paths and some geometrical information (E/Z configuration). With the '-eq 2' option, the charges of two hydrogen atoms bonded to the No 2 carbon of chloroethene are different as they adopt different configurations to chlorine (one is cis and the other is trans). Similarly, the two amide hydrogen atoms of acetamide do not share the same partial charge as the amide bond cannot rotate freely. To back-compatible to the older versions, the default is set to '1'

In Example (12), a gcrt file of iodine methane is generated and a gesp file named ch3I.gesp is produced when running Gaussian 09 with the default keyword. In Examples (13-15), RESP charges are generated for acetamide using different charge equilibration options. In the following table, the charges are listed for comparison purposes.

```
atom names          |      eq  =  0       |     eq  =  1     |    eq = 2
                    |no equalization      |atomic paths     | + geometry
-------------------------------------------------------------------------
methyl carbon       |-0.5190              | -0.5516         | -0.5193
methyl hydrogen     | 0.1412/0.1380/0.1396 |  0.1470        |  0.1397
carbonyl carbon     | 0.9673              |  0.9786         |  0.9673
oxygen              |-0.6468              | -0.6463         | -0.6468
nitrogen            |-1.1189              | -1.1219         | -1.1189
amide hydrogen      | 0.4556/0.4429       |  0.4501         |  0.4556/0.4429
-------------------------------------------------------------------------
```

11.1.2 parmchk2

parmchk2 reads in an ac/mol2/prepi/prepc file, an atomtype similarity index file (the default is $AMBERHOME-/dat/antechamber/PARMCHK.DAT) as well as a force field file (the default is *$AMBERHOME/dat/leap/parm/-gaff.dat*). It writes out a force field modification (frcmod) file containing any force field parameters that are needed for the molecule but not supplied by the force field (*.dat) file. Problematic parameters, if any, are indicated in the frcmod file with the note, "ATTN, need revision", and are typically given values of zero. This can cause fatal terminations of programs that later use a resulting prmtop file; for example, a zero value for the periodicity of the torsional barrier of a dihedral parameter will be fatal in many cases. For each atom type, an atom type corresponding file (ATCOR.DAT) lists its replaceable general atom types. By default, only the missing parameters are written to the frcmod file. When the "-a" switch is given the value "Y", *parmchk2* prints out all force field parameters used by the input molecule, whether they are already in the parm file or not. This file can be used to prepare the frcmod file used by thermodynamic integration calculations using sander.

Unlike *parmchk* which only checks several substitutions for a missing force field parameter, *parmchk2* enumerates all the possible substitutions and select the one with the best similarity score as the final substitute. Moreover, a penalty score, which measures the similarity between the missing force field parameter and the substitute is provided. The similarity socres are calculated using the similarity indexes defined in the atom type similarity index file (PARMCHK.DAT). A similarity index of a pair of atom types ('A/B') for a specific force field parameter type was generated by calculating the average percent absolute error of two set of force field parameters in gaff. The two set of force field parameters are identical except that one set has atom type 'A' and the other has 'B'. Each atom type pair ('A/B') has nine similarity indexes for nine different types of force field parameters, which are bond equilibrium length, bond stretching force constant, bond equilibrium angle ('A' and 'B' are central atoms), bond angle bending force constant ('A' and 'B' are central atoms), bond equilibrium angle ('A' and 'B' are non-central atoms), bond angle bending force constant ('A' and 'B' are non-central atoms),

torsional angle twisting force constant ('A' and 'B' are inner side atoms), torsional angle twisting force constant ('A' and 'B' are outter side atoms), and improper dihedral angle.

```
parmchk2 -i    input file name
         -o    frcmod file name
         -f    input file format (prepi, prepc, ac, mol2, frcmod, leaplog)
         -s    ff parm set, it is suppressed by "-p" option
               1 or gaff:   gaff (the default)
               2 or gaff2:  gaff2
               3 or parm99: parm99
               4 or parm10: parm10
               5 or lipid14: lipid14
         -frc  frcmod files to be loaded, the supported frcmods include
               ff99SB, ff14SB, ff03 for proteins , bsc1, ol15, ol3 for DNA and yil for
               eg. ff14SB+bsc1+yil, ff99SB+bsc1
         -p    parmfile, suppress '-s' flag, optional
         -pf   parmfile format
               1: for amber FF data file (the default)
               2: for additional force field parameter file
         -afrc additional frcmod file, no matter using -p or not, optional
         -c    atom type corresponding score file, default is PARMCHK.DAT
         -atc  additional atom type corresponding score file, optional
               type 'parmchk2 -l' to learn details
         -a    print out all force field parameters including those in the parmfile
               can be 'Y' (yes) or 'N' (no) default is 'N'
         -w    print out parameters that matching improper dihedral parameters
               that contain 'X' in the force field parameter file, can be 'Y' (yes)
               or 'N' (no), default is 'Y'
         -fc   option of force constant calculation for '-f frcmod' or '-f leaplog'
               1: default behavior (the default option)
               2: do empirical calculation before using corresponding atom types
         -att  for the frcmod input format, option of performing parmchk
               1: for all parameters (the default)
               2: only for those with ATTN
```

Example:

```
parmchk2 -i sustiva.prep -f prepi -o frcmod
```

This command reads in *sustiva.prep* and finds the missing force field parameters listed in *frcmod*.

11.2 A simple example for antechamber

The most common use of the antechamber program suite is to prepare input files for LEaP, starting from a three-dimensional structure, as found in a PDB file. The antechamber suite automates the process of developing a charge model and assigning atom types, and partially automates the process of developing parameters for the various combinations of atom types found in the molecule.

As with any automated procedure, the output should be carefully examined, and users should be on the lookout for any unusual or incorrect program behavior.

Suppose you have a PDB-format file for your ligand, say thiophenol, which looks like this:

```
ATOM      1  CG  TP      1      -1.959   0.102   0.795
ATOM      2  CD1 TP      1      -1.249   0.602  -0.303
ATOM      3  CD2 TP      1      -2.071   0.865   1.963
```

```
ATOM      4  CE1 TP      1      -0.646    1.863   -0.234
ATOM      5  C6  TP      1      -1.472    2.129    2.031
ATOM      6  CZ  TP      1      -0.759    2.627    0.934
ATOM      7  HE2 TP      1      -1.558    2.719    2.931
ATOM      8  S15 TP      1      -2.782    0.365    3.060
ATOM      9  H19 TP      1      -3.541    0.979    3.274
ATOM     10  H29 TP      1      -0.787   -0.043   -0.938
ATOM     11  H30 TP      1       0.373    2.045   -0.784
ATOM     12  H31 TP      1      -0.092    3.578    0.781
ATOM     13  H32 TP      1      -2.379   -0.916    0.901
```

(This file may be found at *$AMBERHOME/AmberTools/test/antechamber/tp/tp.pdb*). The basic command to create a mol2 file for LEaP is just:

```
antechamber -i tp.pdb -fi pdb -o tp.mol2 -fo mol2 -c bcc
```

The output file will look like this:

```
@<TRIPOS>MOLECULE
TP
   13    13     1     0     0
SMALL
bcc
@<TRIPOS>ATOM
      1 CG          -1.9590    0.1020    0.7950 ca      1 TP     -0.132000
      2 CD1         -1.2490    0.6020   -0.3030 ca      1 TP     -0.113000
      3 CD2         -2.0710    0.8650    1.9630 ca      1 TP      0.015900
      4 CE1         -0.6460    1.8630   -0.2340 ca      1 TP     -0.137000
      5 C6          -1.4720    2.1290    2.0310 ca      1 TP     -0.132000
      6 CZ          -0.7590    2.6270    0.9340 ca      1 TP     -0.113000
      7 HE2         -1.5580    2.7190    2.9310 ha      1 TP      0.136500
      8 S15         -2.7820    0.3650    3.0600 sh      1 TP     -0.254700
      9 H19         -3.5410    0.9790    3.2740 hs      1 TP      0.190800
     10 H29         -0.7870   -0.0430   -0.9380 ha      1 TP      0.133500
     11 H30          0.3730    2.0450   -0.7840 ha      1 TP      0.134000
     12 H31         -0.0920    3.5780    0.7810 ha      1 TP      0.133500
     13 H32         -2.3790   -0.9160    0.9010 ha      1 TP      0.136500

@<TRIPOS>BOND
     1    1     2 ar
     2    1     3 ar
     3    1    13 1
     4    2     4 ar
     5    2    10 1
     6    3     5 ar
     7    3     8 1
     8    4     6 ar
     9    4    11 1
    10    5     6 ar
    11    5     7 1
    12    6    12 1
    13    8     9 1
@<TRIPOS>SUBSTRUCTURE
     1 TP            1 TEMP              0 ****   ****     0 ROOT
```

This command says that the input format is pdb, output format is Sybyl mol2, and the BCC charge model is to be used. The output file is shown in the box titled .mol2. The format of this file is a common one understood by many programs. However, to display molecules properly in software packages other than LEaP and gleap, one needs to assign atom types using the '-at sybyl' flag rather than using the default gaff atom types.

You can now run parmchk2 to see if all of the needed force field parameters are available:

```
parmchk2 -i tp.mol2 -f mol2 -o frcmod
```

This yields the frcmod file:

```
remark goes here
MASS
BOND
ANGLE
DIHE
IMPROPER
ca-ca-ca-ha           1.1           180.0           2.0           General improper \\
                                              torsional angle (2 general atom types)
ca-ca-ca-sh           1.1           180.0           2.0           Using default value
NONBON
```

In this case, there were two missing dihedral parameters from the gaff.dat file, which were assigned a default value. (As gaff.dat continues to be developed, there should be fewer and fewer missing parameters to be estimated by parmchk2.) In rare cases, parmchk2 may be unable to make a good estimate; it will then insert a placeholder (with zeros everywhere) into the frcmod file, with the comment "ATTN: needs revision". After manually editing this to take care of the elements that "need revision", you are ready to read this residue into LEaP, either as a residue on its own, or as part of a larger system. The following LEaP input file (leap.in) will just create a system with thiophenol in it:

```
source leaprc.gaff
mods = loadAmberParams frcmod
TP = loadMol2 tp.mol2
saveAmberParm TP prmtop inpcrd
quit
```

You can read this into LEaP as follows:

```
tleap -s -f leap.in
```

This will yield a prmtop and inpcrd file. If you want to use this residue in the context of a larger system, you can insert commands after the loadAmberPrep step to construct the system you want, using standard LEaP commands.

In this respect, it is worth noting that the atom types in gaff.dat are all lower-case, whereas the atom types in the standard AMBER force fields are all upper-case. This means that you can load both gaff.dat and (say) parm99.dat into LEaP at the same time, and there won't be any conflicts. Hence, it is generally expected that you will use one of the AMBER force fields to describe your protein or nucleic acid, and the gaff.dat parameters to describe your ligand; as mentioned above, gaff.dat has been designed with this in mind, i.e., to produce molecular mechanics descriptions that are generally compatible with the AMBER macromolecular force fields.

The procedure above only works as it stands for neutral molecules. If your molecule is charged, you need to set the -nc flag in the initial antechamber run. Also note that this procedure depends heavily upon the initial 3D structure: it must have all hydrogens present, and the charges computed are those for the conformation you provide, after minimization in the AM1 Hamiltonian. In fact, this means that you must have an reasonable all-atom initial model of your molecule (so that it can be minimized with the AM1 Hamiltonian), and you may need to specify what its net charge is, especially for those molecular formats that have no net charge information, and no partial charges or the partial charges in the input are not correct. The system should really be a closed-shell molecule, since all of the atom-typing rules assume this implicitly.

Further examples of using antechamber to create force field parameters can be found in the *$AMBERHOME-/test/antechamber* directory. Here are some practical tips from Junmei Wang:

1. For the input molecules, make sure there are no open valences and the structures are reasonable. All hydrogen atoms must be present. Antechamber doesn't know what to do with metal ions (see the MCPB.py program for that), or for other non-organic elements such as Boron. Look at the *$AMBERHOME/dat/leap/parm/gaff.dat* file to see what sorts of atomic environments are supported.

2. The Antechamber package produces two kinds of messages: error messages and informative messages. Informative messages begin with "Info:" and may be safely ignored, but they may be helpful for understanding and troubleshooting antechamber. For example: "Info: Bond types are assigned for valence state 1 with penalty of 1". Messages beginning with "Fatal Error!" or "Error:" indicate a problem. Some such messages may mention likely causes or contain suggested workarounds, but all such messages provide clues. Apply common sense and the scientific method to troubleshoot. Typical first steps are to verify input files and to search the AMBER Mail Reflector for similar reported problems. Additional steps are described below.

3. Failures are most often produced when antechamber infers an incorrect connectivity. In such cases, you can revise by hand the connectivity information in "ac" or "mol2" files. Systematic errors could be corrected by revising the parameters in $AMBERHOME/dat/antechamber/CONNECT.TPL.

4. It is a good idea to check the intermediate files in case of a program failure, and you can run separate programs one by one. Use the "-s 2" flag to antechamber to see details of what it is doing.

5. *acdoctor* can diagnose many possible problems with input molecules. If you encounter failures when running antechamber programs, it is highly recommended to let *acdoctor* perform a diagnosis. Run the acdoctor program or use the acdoctor mode in program antechamber; the latter is controlled by option '-dr' and is on by default.

6. By default, the AM1 Mulliken charges that are required for the AM1-BCC procedure are computed using the *sqm* program, with the following keyword (which is placed inside the *&qmmm* namelist):

    qm_theory="AM1", grms_tol=0.0005, scfconv=1.d-10,

   For some molecules, especially if they have bad starting geometries, convergence to these tight criteria may not be obtained. If you have trouble, examine the *sqm.out* file, and try changing *scfconv* to 1.d-8 and/or increase the value of *grms_tol*. If you see failures in scf convergence that are not fixed by changing scfconv, try adding setting *ndiis_attempts*=700. You can use the −ek flag to antechamber to change these: for example

    ```
    antechamber ....  -ek "qm_theory='AM1', grms_tol=0.0005, scfconv=1.d-8, ndiis_attempts=700,"
    ....
    ```

   But be aware that there may be something "wrong" with your molecule if these problems arise; *acdoctor* may help (see the previous tip).

7. The standard procedure for obtaining AM1-BCC charges calls for a geometry optimization first. [238, 239] For some molecules (especially anions like phosphates) such a vacuum minimization may be inappropriate, since it can lead to formation of intramolecular hydrogen bonds that are not representative of the expected conformations in solution. If you trust your initial geometries, you can add *maxcyc*=0 to the −ek flag to skip the geometry minimization. You might also want to turn off geometry optimization in order try out several conformations in order to assess the sensitivity of the AM1-BCC charges to input geometry.

11.3 Programs called by antechamber

The following programs are automatically called by antechamber when needed. Generally, you should not need to run them yourself, unless problems arise and/or you want to fine-tune what antechamber does.

11.3.1 atomtype

Atomtype reads in an ac file and assigns the atom types. You may find the default definition files in $AMBERHOME/dat/antechamber: ATOMTYPE_AMBER.DEF (AMBER), ATOMTYPE_GFF.DEF (general AMBER force field). ATOMTYPE_GFF.DEF is the default definition file. It is pointed out that the usage of atomtype is not limited to assign force field atom types, it can also be used to assign atom types in other applications, such as QSAR and QSPR studies. The users can define their own atom type definition files according to certain rules described in the above mentioned files.

```
atomtype -i input file name
         -o output file name (ac)
         -f input file format(ac (the default) or mol2)
         -p atom type set, suppressed by "-d" option
            gaff  : the default
            amber : for PARM94/99/99SB
            bcc   : for AM1-BCC
            abcg2 : for ABCG2
            gas   : for Gasteiger charge
            sybyl : for atom types used in sybyl
         -d atom type definition file, optional
         -a do post atom type adjustment (it is applied with "-d" option)
            1: yes, 0: no (the default)
```

Example:

```
atomtype -i sustiva_resp.ac -o sustiva_resp_at.ac -f ac -p amber
```

This command assigns atom types for sustiva_resp.ac with amber atom type definitions. The output file name is sustiva_resp_at.ac

11.3.2 am1bcc

Am1bcc first reads in an ac or mol2 file with or without assigned AM1-BCC atom types and bond types. Then the bcc parameter file (the default, BCCPARM.DAT is in $AMBERHOME/dat/antechamber) is read in. An ac file with AM1-BCC charges [238, 239] is written out. Be sure the charges in the input ac file are AM1-Mulliken charges.

```
am1bcc -i input file name in ac format
       -o output file name
       -f output file format(pdb or ac, optional, default is ac)
       -t am1bcc type, default is 'bcc', can also be 'abcg2'
       -p bcc parm file name (optional))
       -j atom and bond type judge option, default is 0)
          0: No judgement
          1: Atom type
          2: Full bond type
          3: Partial bond type
          4: Atom and full bond type
          5: Atom and partial bond type
```

Example:

```
am1bcc -i comp1.ac -o comp1_bcc.ac -f ac -j 4
```

This command reads in comp1.ac, assigns both atom types and bond types and finally performs bond charge correction to get AM1-BCC charges. The '-j' option of 4, which is the default, means that both the atom and bond

type information in the input file is ignored and a full atom and bond type assignments are performed. The '-j' option of 3 and 5 implies that bond type information (single bond, double bond, triple bond and aromatic bond) is read in and only a bond type adjustment is performed. If the input file is in mol2 format that contains the basic bond type information, option of 5 is highly recommended. comp1_bcc.ac is an ac file with the final AM1-BCC charges.

11.3.3 bondtype

bondtype is a program to assign six bond types based upon the read in simple bond types from an ac or mol2 format with a flag of "-j part" or purely connectivity table using a flag of "-j full". The six bond types as defined in AM1-BCC [238, 239] are single bond, double bond, triple bond, aromatic single, aromatic double bonds and delocalized bond. This program takes an ac file or mol2 file as input and write out an ac file with the predicted bond types. After the continually improved algorithm and code, the current version of bondtype can correctly assign bond types for most organic molecules (>99% overall and >95% for charged molecules) in our tests.

Starting with Amber 10, bond type assignment is proceeded based upon residues. The bonds that link two residues are assumed to be single bonded. This feature allows antechamber to handle residue-based molecules, even proteins are possible. It also provides a remedy for some molecules that would otherwise fail: it can be helpful to dissect the whole molecule into residues. Some molecules have more than one way to assign bond types; for example, there are two ways to alternate single and double bonds for benzene. The assignment adopted by bondtype is purely affected by the atom sequence order. To get assignments for other resonant structures, one may freeze some bond types in an *ac* or *mol2* input file (appending 'F' or 'f' to the corresponding bond types). Those frozen bond types are ignored in the bond type assignment procedure. If the input molecules contain some unusual elements, such as metals, the involved bonds are automatically frozen. This frozen bond feature enables bondtype to handle unusual molecules in a practical way without simply producing an error message.

```
bondtype –i input file name
         –o output file name
         –f input file format (ac or mol2)
         –j judge bond type level option, default is part
            full  full judgment
            part  partial judgment, only do reassignment according
                  to known bond type information in the input file
```

Examples can be found in *$AMBERHOME/test/antechamber/bondtype* and *$AMBERHOME/test/antechamber/chemokine*.

11.3.4 prepgen

Prepgen generates the prep input file from an ac file. By default, the program generates a mainchain itself. However, you may also specify the main-chain atoms in the main chain file. From this file, you can also specify which atoms will be deleted, and whether to do charge correction or not. In order to generate the amino-acid-like residue (this kind of residue has one head atom and one tail atom to be connected to other residues), you need a main chain file. Sample main chain files are in *$AMBERHOME/dat/antechamber*.

```
prepgen –i  input file name(ac)
        –o  output file name
        –f  output file format (car or int, default: int)
        –m  mainchain file name
        –rn residue name (default: MOL)
        –rf residue file name (default: molecule.res)
            –f –m –rn –rf are optional
```

Examples:

```
prepgen -i sustiva.ac -o sustiva_int.prep -f int -rn SUS -rf SUS.res
prepgen -i sustiva.ac -o sustiva_car.prep -f car -rn SUS -rf SUS.res
prepgen -i sustiva.ac -o sustiva_int_main.prep -f int -rn SUS
        -rf SUS.res -m mainchain_sus.dat
prepgen -i ala_cm2_at.ac -o ala_cm2_int_main.prep -f int -rn ALA
        -rf ala.res -m mainchain_ala.dat
```

The above commands generate different kinds of prep input files with and without specifying a main chain file.

11.3.5 espgen

Espgen reads in a gaussian (92,94,98,03) output file and extracts the ESP information. An esp file for the resp program is generated.

```
espgen -i   input file name
       -o   output file name
       -f   input format:
            1  Gaussian log file(default)
            2  Gaussian ESP file
            3  Gamess ESP file
       -p   generate esp for pGM:
            0  no, the default)
            1  yes
       -dq  print out dipole and quadrupole moments:
            0  no, the default)
            1  yes
       -re  print out remark line
            0  no, the default)
            1  yes
```

Example:

```
(1) espgen -i sustiva_g98.out -o sustiva.esp
(2) espgen -i ch3I.gesp -o ch3I.esp
```

Command (1) reads in sustiva_g98.out and writes out sustiva.esp, which can be used by the resp program. Command (2) reads in a gesp file generated by Gaussian 09 and outputs the esp file. Note that this program replaces shell scripts formerly found on the AMBER web site that perform equivalent tasks.

11.3.6 respgen

Respgen generates the input files for two-stage resp fitting. Starting with Amber 10, the program supports a single molecule with one or multiple conformations RESP fittings. Atom equivalence is recognized automatically. Frozen charges and charge groups are read in with '-a' flag. If there are some frozen charges in the additional input data file, a RESP charge file, QIN is generated as well. Here are flags to *respgen*:

```
-i input file name(ac)
-o output file name
-l maximum path length (default is -1, i.e. the path can be any long)
-f output file format
   resp1 - first stage resp fitting
   resp2 - second stage resp fitting
   iresp1 - first stage i_resp fitting
   iresp2 - second stage i_resp fitting
```

```
        resp3 - one-stage resp fitting
        resp4 - calculating ESP from point charges
        resp5 - no-equalization
   -e equalizing atomic charge (default is 1)
        0 not use
        1 by atomic paths
        2 by atomic paths and geometry (such as E/Z configuration)
   -a additional input data (predefined charges, atom groups etc)
   -n number of conformations (default is 1)
   -w weight of charge constraint
        the default values are 0.0005 for resp1/iresp1 and 0.001 for
        resp2/iresp2
```

The following is a sample of additional respgen input file

```
//predefined charges in a format of (CHARGE partial_charge atom_ID atom_name)
CHARGE -0.417500 7 N1
CHARGE 0.271900 8 H4
CHARGE 0.597300 15 C5
CHARGE -0.567900 16 O2
//charge groups in a format of (GROUP num_atom net_charge),
//more than one group may be defined.
GROUP 10 0.00000
//atoms in the group in a format of (ATOM atom_ID atom_name)
ATOM 7 N1
ATOM 8 H4
ATOM 9 C3
ATOM 10 H5
ATOM 11 C4
ATOM 12 H6
ATOM 13 H7
ATOM 14 H8
ATOM 15 C5
ATOM 16 O2
```

Example:

```
   respgen -i sustiva.ac -o sustiva.respin1 -f resp1
   respgen -i sustiva.ac -o sustiva.respin2 -f resp2
   resp -O -i sustiva.respin1 -o sustiva.respout1 -e sustiva.esp -t qout_stage1
   resp -O -i sustiva.respin2 -o sustiva.respout2 -e sustiva.esp
           -q qout_stage1 -t qout_stage2
   antechamber -i sustiva.ac -fi ac -o sustiva_resp.ac -fo ac -c rc -cf qout_stage2
   respgen -i acetamide.ac -o acetamide.respin1 -f resp1 -e 2
   respgen -i acetamide.ac -o acetamide.respin2 -f resp2 -e 2
```

The above commands first generate the input files (sustiva.respin1 and sustiva.respin2) for resp fitting, then do two-stage resp fitting and finally use antechamber to read in the resp charges and write out an ac file, *sustiva_resp.ac*. A more complicated example has been provided in *$AMBERHOME/test/antechamber/residuegen*. The last two 'respgen' commands generate resp input files for acetamide discriminating the two amide hydrogen atoms.

11.4 Miscellaneous programs

The Antechamber suite also contains some utility programs that perform various tasks in molecular mechanical calculations. They are listed in alphabetical order.

11.4.1 acdoctor

acdoctor reads the same input file formats used by the*antechamber* program and 'diagnoses' potential issues that can cause antechamber to fail. In AmberTools version 17 the acdoctor functionality was added to program antechamber; it is controlled by option '-dr' and is on by default. The first step is to validate some commonly-used molecular formats, such as pdb, mol2, mdl (sdf), etc. Then the presence of any unusual elements (elements other than C, O, N, S, P, H, F, Cl, Br and I) is reported; in AmberTools version 19 the unusual elements check was changed from a warning to a fatal error; please contact the Amber Mail Reflector specifying the unusual element(s) to register your interest in using antechamber on those element(s). Unfilled valences are reported and additional checks are performed when atom types and/or bond types are read for file formats ac, mol2, sdf, prepi, prepc, mdl, alc and hin. The geometry is quantified by a distance matrix and atomic clashes are reported. *acdoctor* also applies a more stringent criterion than that utilized by *antechamber* to determine whether a bond is formed or not. A warning message is printed for those bonds that fail to meet the standard as well as for weird bonds. Next*acdoctor* determines whether all atoms are linked together through atomic paths. If not, an error message is printed. This kind of error typically implies that the input molecule has one or several bonds missing. Finally, *acdoctor* tries to assign bond types and atom types for the input molecule. If no error occurs during running *bondtype* and *atomtype*, presumably the input molecule should be free from problems when running the other Antechamber programs. It is recommended to diagnose your molecules with *acdoctor* when you encounter Antechamber program suite failures.

```
Usage: acdoctor -i  input file name
               -f  input file format
```

Example:

```
acdoctor -i test.mol2 -f mol2
```

The program reads test.mol2 and checks for potential problems when running the Antechamber programs. Errors and warning messages are printed. (Possible file formats are listed above in Section 11.1.1.

11.4.2 parmcal

parmcal is an interactive program to calculate the bond length and bond angle parameters, according to the rules outlined in Ref. [236].

```
Please select:
1. calculate the bond length parameter: A-B
2. calculate the bond angle parameter: A-B-C
3. exit
```

11.4.3 residuegen

It can be painful to prepare a modified amino acid or nucleotide; the complication is that a residue is not a free standing molecule, and needs to be capped with extra atoms, usually at both termini. For "simple" systems, where a single conformation can be used to estimate partial charges, the *prepgen* program described above with the "-m" flag to specify which atoms to keep in the final residue. For more complex circumstances, the *residuegen* facilitates residue topology generation. *residuegen* reads in an input file and applies a set of antechamber programs to generate residue topologies in prepi format. The program can be applied to generate amino-acid-like topologies for amino acids, nucleic acids and other polymers as well. An example is provided below and the file format of the input file is also explained.

```
Usage: residuegen input_file
```

Example:

```
residuegen ala.input
```

This command reads in ala.input and generate residue topology for alanine. The file format of ala.input is explained below.

```
#INPUT_FILE:     structure file in ac format, generated from a Gaussian output
INPUT_FILE       ala.ac
#CONF_NUM:        Number of conformations utilized
CONF_NUM         2
#ESP_FILE:        esp file generated from gaussian output with 'espgen'
#                 for multiple conformations, cat all CONF_NUM esp files onto ESP_FILE
ESP_FILE         ala.esp
#SEP_BOND:        bonds that separate residue and caps, input in a format of
#                 (Atom_Name1 Atom_Name2), where Atom_Name1 belongs to residue and
#                 Atom_Name2 belongs to a cap; must show up no more than two times
SEP_BOND         N1 C2
SEP_BOND         C5 N2
#NET_CHARGE:      net charge of the residue
NET_CHARGE       0
#ATOM_CHARGE:    predefined atom charge, input in a format of
#               (Atom_Name Partial_Charge); can show up multiple times.
ATOM_CHARGE      N1 -0.4175
ATOM_CHARGE      H4 0.2719
ATOM_CHARGE      C5 0.5973
ATOM_CHARGE      O2 -0.5679
#PREP_FILE:       prep file name
PREP_FILE:       ala.prep
#RESIDUE_FILE_NAME:     residue file name in PREP_FILE
RESIDUE_FILE_NAME:      ala.res
#RESIDUE_SYMBOL:        residue symbol in PREP_FILE
RESIDUE_SYMBOL:         ALA
```

11.4.4 match

The match program was developed to conduct least-square fittings for two molecules (one input and one reference) which are not necessarily the same in structure. Users can specify which atom or residue in the input corresponds to which in the reference in the definition file (-df). The users can also specify which atoms participating the fitting (-ds). The match matrix can be saved for translating and roating those atoms not participating the fitting procedure in separate step using '-j 2'.

```
Usage: match  -i  input file name
              -r  reference file name
              -f  format: 1-pdb (the default), 2-ac, 3-mol2, 4-sdf, 5-crd/rst
              -o  output file name
              -l  run log file name, default is "match.log"
              -s  selection mode
                  0: use all atoms (the default)
                  1: specify atom names
                  2: use atom definition file
                  3: use residue definition file - original residue IDs
                  4: use residue definition file - renumbered residue IDs
              -ds definition string if selection modes of '1' or '3' or '4'
                  e.g. 'C,N,O,CA', or 'HET' which stands for heavy atoms for '-ds 1'
              -df definition file if selection mode of '2' or '3' or '4'
                  records take a form of 'ATOM atom_id_input atom_id_reference'
                  or 'RES res_id_input res_id_reference'
              -n  number of atoms participating ls-fitting,
```

```
                           default is -1, which implies to use all the selected atoms
                    -m  matrix file, default is "match.matrix"
                    -t  job type:
                        0: calculate rms only, need -i and -r
                        1: lsfit, need -i, -r and -o the default
                        2: translation/rotation, need -i, -o and -m
```

Example:

```
    match -f pdb -r 1be9.pdb -i 3pdz.pdb -o 3pdz_aligned.pdb -s 4 -ds "CA,C,N,O" -df 3pdz_
```

The program runs least-square fitting for the non-hydrogen main chain atoms of residues defined in the 3pdz_1be9.corr. A part of the 3pdz_1be9.corr is shown below:

RES 34 35 G G
RES 35 36 I I
RES 36 37 Y F
...
RES 87 88 L I
RES 88 89 L I

11.4.5 match_atomname

One limitation of the Antechamber package is that the atom name information is lost after running Gaussian calculations. And a residue topology file in prepi or prepc or a mol2 file generated from the Gaussian output has atom names not matching those from the original file (usually a pdb file). Because of this glitch, one can not simply load the residue topology file to tleap, read in the pdb file and then to save the topolgoy. We developed match_atomname to address this problem. The match_atomname program takes an input file and a reference file in pdb, ac, prepi, prepc and mol2 format, automatically detects the corresponding atom name in the reference for each atom name in the input. An output file in the same format as that of the input is generated using the matched atom names.

```
    Usage: match_atomname -i  input file name
                          -fi input format (pdb, ac, prepi, prepc, mol2
                          -r  ref file name
                          -fr ref format (pdb, ac, prepi, prepc, mol2)
                          -o  output file name
                          -h  include hydrogen atoms or not
                              0 not, the default
                              1 yes
                          -g  geometric info (such as E/Z configuration) is considered to 
                              0 no, the default
                              1 yes
                          -l  maximum path length, default is -1 (full length)
                              if it takes very long time and/or core dump occur, a value b
```

Example:

```
    match_atomname -i SAH.prepi -fi prepi -o SAH_matched.prepi -r SAH_XRAY.pdb -fr pdb
```

The output, SAH_matched.prepi and SAH_XRAY.pdb can be loaded to tleap directly to generate a topology for minimization or MD simulations.

12 paramfit

Robin Betz

The *paramfit* program allows specific forcefield parameters to be optimized or created by fitting to quantum energy data. *Paramfit* can be used when parameters are missing in the default force fields and *antechamber* cannot find a replacement, or when existing parameters do not describe the system to the desired level of accuracy, such as for dihedral constants on protein backbones.

Paramfit attempts to make the following statement true: **With the correct AMBER parameters, calculations performed at a quantum level over many conformations of a structures should match those calculated by AMBER.**

Paramfit can calculate the energy of each conformation and/or the force on each atom, and adjust the force field parameters so that these values correspond to input quantum data.

For energies, *Paramfit* attempts to fit the AMBER energy to the quantum energy for a variety of conformations of the input structure, minimizing the equation

$$\sum_{n=1}^{N} w_i \left[\left(E_{MM}(n) - E_{QM}(n) \right)^2 + K \right] = 0$$

where K is a constant that adjusts for different origins in the QM and MM calculations so that minimization may be done to zero and N is the number of molecular conformations that are considered.

For forces, the equation that is optimized is

$$\sum_{n=1}^{N} \sum_{atom=1}^{N_{atoms}} w_i \left| F(n, atom)_{MM} - F(n, atom)_{QM} \right|^2 = 0$$

where the sum of the differences in the forces on each atom should match given the correct set of parameters. Individual structures can be assigned weights w_i to give them more or less relative importance in the fit. By default, all weights are set to 1.

The program works by altering the parameters that AMBER uses to describe the molecule, which alter the elements in the AMBER sum that is used to calculate the energy or forces. It is necessary to evaluate over many conformations of the molecule because the parameters should predict how the molecule will behave dynamically rather than statically. To get a good idea of the forces on a dihedral, for example, the energy needs to be evaluated for multiple conformations of the dihedral to see how it changes each time. *Paramfit* will fit so that the energy changes that AMBER predicts will happen when the dihedral twists match the changes predicted with quantum methods.

In order to facilitate force field development, *Paramfit* supports fitting parameters across multiple molecules (for example, fitting a single dihedral backbone term across a variety of input amino acids). Single molecule fits can also be done to generate parameters that are missing or inadequate to describe small molecules or ligands.

Paramfit provides functionality for the majority of steps in the fitting process, including writing input files for quantum packages, specifying which parameters are to be fit, determining the value of K for the system, and finally conducting the fit and saving it in a force field modification file that can be used by other programs. An external quantum program is needed to generate the energies needed for *paramfit* to conduct a fitting. Currently, the program is capable of writing input files for ADF, GAMESS, and Gaussian, although if you write your own input files instead of using *paramfit's* functionality, any quantum package will work.

Paramfit has OpenMP support for parallelization of the AMBER function evaluation over the input conformations, where each core will evaluate the energy for a subset of the conformations. Enable this by adding the *-openmp* option to configure and rebuilding *paramfit*. By default all available cores will be used. To change this, set

the `OMP_NUM_THREADS` environment variable to the number of threads to be executed. You will see a speedup directly proportional to the number of cores you are running.

Paramfit now includes several ways fitting functions to aid in parameter generation. It can fit such that the energy of each input structure matches the single-point quantum energies inputted, or can now do the same fitting only with the forces on each atom, which may produce a more accurate fit that is less sensitive to problems with the input structure, and can also fit all dihedral force constants and phases simultaneously to a small set of quantum energies using a method developed by Chad Hopkins and Adrian Roitberg. This method fits every term and requires fewer function evaluations than running the full minimization algorithm, but requires especially good sampling of each torsion angle of interest.

Fitting forces requires several additional options to specify the location of the output forces files in the job control file. The easiest way to create a job control file for any of these options is to use the wizard, which runs automatically when no job control file is specified. This will walk you through the creation of a job control file and write it for you while prompting for all necessary options for the selected fitting function.

It is highly recommended that you fit to single-point quantum energies, as fitting to forces is considerably more expensive in terms of required calculation and still somewhat experimental. The implementation of the dihedral fitting method is requires a varied set of input structures, and does not allow specifying individual dihedrals to be fit. No matter which method is used, please take care to carefully validate all parameters for reasonableness–*paramfit's* fit is dependent on the variation and quality of the input structures and the resulting parameters are not guaranteed in ill-defined areas of the input conformation set. For example, if you fit a dihedral torsion term with input structures sampling the 0-30 degree range of that dihedral, the resulting parameters cannot be expected to give a valid energy of a structure with the dihedral at 90 degrees, as the algorithm merely fits to the available data and cannot make other predictions.

12.1 Usage

Paramfit is called from the command line as follows for a single molecule fit:

```
paramfit -i Job_Control.in -p prmtop -c mdcrd -q QM_data.dat \
-v MEDIUM --random-seed seed
```

Running *paramfit* without any options will run a wizard that assists in the creation of a job control file. It is highly recommended that you use the wizard to assist you in setting run options.

The following switches apply to single molecule fits only:

-p prmtop The molecular topology file for the structure.

-c mdcrd A coordinate file containing many conformations of the input structure. These may be generated by running a short simulation in solution, or by manually specifying coordinates for each atom. It is important that there be a good representation of the solution space for any parameters that are to be optimized– for example, if you want a bond force constant it would be a good idea to have input structures with a good range of values for the length of the that bond type. See Subsection 12.2.6

-q QM_data.dat A file containing the quantum energies of the structures in the coordinate file, in order, one per line. You will have to extract the energies from the output files that the quantum package produces. An example script to do this for Gaussian formatted output files can be found in $AMBERHOME/AmberTools/src/paramfit/scripts.

To fit multiple molecules, the following switches are used:

```
paramfit -i Job_Control.in -pf prmtop_list -cf mdcrd_list -v MEDIUM --random-seed seed
```

Here is a very brief description of the command-line arguments for a multiple molecule fit. For more information on conducting these, fits, please see 12.3.

-pf prmtop_list A file containing a plain-text list of input topology files and the adjustment constant K for each file separated by a space, one per line.

-cf mdcrd_list A file containing a plain text list of input coordinate files, number of structures to read from each file, and directory containing quantum output from each file, separated by a space. These should be specified in the same order as the topologies in the prmtop_list.

The following switches apply to either type of fit:

-i Job_Control.in The job control file for the program. See Section 12.2 for a description of the options and format for this file. If no job control file is specified, a wizard will be initiated that will prompt you for options and help create the file. Use of the wizard is highly recommended when running *Paramfit* for the first time.

-v MEDIUM The verbosity level to run the program at, either LOW, MEDIUM, or HIGH.

–random-seed seed The integer seed for the random number generator. Only specify this parameter when exactly reproducible results are needed for debugging.

12.2 The Job Control File

Similarly to *sander* and other programs, *paramfit* requires a job control file that specifies individual options for each run. The options that apply to your run vary depending on the runtype and the other settings, and they are quite numerous. To aid you in creating a job control file, a wizard has been included that will prompt you about applicable settings and create the job control file for you. Using the wizard is highly recommended, especially when running a fit for the first time. To use the wizard, simply run *paramfit* without any options. **It is highly recommended that you use the wizard to create job control files,** as it prompts for all options relevant to your run and the resulting file can then be easily edited by hand.

The format consists of variable assignments, in the format variable=value, with one assignment per line. Pound signs (#) will comment out lines. See the following sections for a description of what to put in the job control file for various tasks:

12.2.1 General options

paramfit requires several options be set for every run. These variables should usually appear in your job control file.

RUNTYPE Specifies whether this run will be creating quantum input files, setting parameters, or conducting a fit.

> **= CREATE_INPUT** The structures in the coordinate file will be written out as individual input files for a quantum package. See 12.2.2.

> **= SET_PARAMS** Provides an interactive prompt allowing you to specify which parameters will be fit for this molecule. See 12.2.3.

> **= FIT** Conducts a fitting using one of the two minimization algorithms. See 12.2.4for other options that need to be specified.

NSTRUCTURES Specifies how many structures are in the input coordinate file. If this value is less than the total number of structures in the file, only the first **n** will be read. Only applies to single molecule fits! If you are fitting multiple molecules at once, the number of structures for each molecule should be specified in the mdcrd_list file as described in 12.3.

12.2.2 Creating quantum input files

Given a trajectory, *Paramfit* can write input files for a variety of quantum packages. This is necessary to generate the energy values for each input conformation that *Paramfit* will fit to. You do not necessarily need to do this step and can write your own input files if desired. Currently Gaussian, ADF, and GAMESS formats are supported.

Job files will be named sequentially with filename prefix and suffix specified in the job control file. Once all the input files are written, you must run the quantum package yourself. *Paramfit* can read Gaussian output files directly, but for other packages you must extract the energies yourself into a file with one energy per line in the same order as the input structures.

Currently *Paramfit* only supports Gaussian if you are fitting forces, and will read the output files and extract the force information for you. See 12.4 for more information on fitting these.

To enter this mode, set RUNTYPE=CREATE_INPUT and specify the following options in your job control file:

QMHEADER File that will be prepended to all created input files for the quantum program. This specifies things on a per-system basis, such as choice of basis set, amount of memory to use, etc. These parameters will vary depending on which quantum package you are using. Sample header files for all supported quantum packages are included in example_config_files in *paramfit's* source directory.

QMFILEFORMAT Specifies which quantum package the created input files should be formatted for.

> **= ADF** Use the Amsterdam Density Functional Theory package.

> **= GAMESS** Use the General Atomic and Molecular Electronic Structure System (GAMESS).

> **= GAUSSIAN** Use Gaussian.

QM_SYSTEM_CHARGE The integral charge of the system. Defaults to 0. Note that some quantum packages may require this to also be specified in your header file.

QM_SYSTEM_MULTIPLICITY The integral multiplicity of the system. Defaults to 1 (singlet).

QMFILEOUTSTART The prefix for each of the created input files. Defaults to 'Job.' The structure number and then the suffix will be appended to this value.

QMFILEOUTEND The suffix for each of the created input files. Defaults to '.in'. With both default options, the file will be named Job.**n**.in.

12.2.3 Specifying parameters

In order to facilitate batch runs as well as simplify the process of running *paramfit* on larger systems, the parameters to be fit are saved and then loaded in during actual fitting so that they do not have to be specified every time. The parameter setting runtype accomplishes this by prompting whether you would like to fit bond, angle and/or dihedral parameters and then displaying a list of the specific atom types for each so that you can pick exactly what *paramfit* should optimize. This saved file does not specify a value for any of the parameters, but simply indicates which ones are to be changed during fitting.

If you do not wish to save a parameter file, you may instead fit a default set of parameters or be prompted every time. See Subsection 12.2.4.

To enter this mode, set RUNTYPE=SET_PARAMS and the following options:

PARAMETER_FILE_NAME Specifies the name of a file in which to store the parameters. When loading these parameters in during a fitting, this line will stay the same. Do not modify this file by hand: *paramfit* numbers each bond, angle, and dihedral in a manner that is consistent but not human-readable.

12.2.4 Fitting options

The fitting function accomplishes the actual parameter modification. It does this by minimizing the least squares difference between the quantum energy and the energy calculated with the AMBER equation over all of the input conformations. For a perfect fit, this means that over all structures, $E_{MD} - E_{QM} + K = 0$.

K is the intrinsic difference between the quantum and the classical energies, which is represented as a parameter that is also fit. The value of K depends on the system, and should be fit once as the only parameter before fitting any other parameters.

To enter this mode, set `RUNTYPE=FIT` and set the following additional variables:

ALGORITHM The minimization algorithm to use. *paramfit* currently implements a genetic algorithm and a simplex algorithm for conduction minimization. Each algorithm requires several parameters and is suited to different problems. Please see 12.2.5 for descriptions of these options and a guide on choosing the appropriate algorithm.

    = GENETIC

    = SIMPLEX

    = BOTH Runs the hybrid genetic algorithm followed by the simplex algorithm to fine tune results

    = NONE No fit is performed- useful for calculating energy of each structure with the initial parameters to see their quality

FUNC_TO_FIT The fitting function to use in the calculation.

    = SUM_SQUARES_AMBER_STANDARD Standard fit to single-point energies. Recommended selection.

    = AMBER_FORCES Fit to the forces on atoms involved in fitted parameters. Currently only supports Gaussian output. See Section 12.4 for details.

    = DIHEDRAL_LEAST_SQUARES Use Chad Hopkins and Adrian Roitberg's method to fit all dihedral terms at once. This method will fit all dihedral torsion terms simultaneously with a minimal number of function evaluations, but requires very good sampling of the relevant torsion angles.

K The intrinsic difference between the quantum and classical energies. This value needs to be determined once for each system so that the algorithm can minimize to zero instead of to a constant. See Subsection 12.5.2 for an example.

PARAMETERS_TO_FIT Sets how *paramfit* determines which parameters are to be fit. *paramfit* does not fit electrostatics, but is capable of fitting every other element of the AMBER sum, which include bond harmonic force constant and equilibrium length, angle harmonic force constant and equilibrium angle, and proper and improper dihedral barrier height, phase shift, and periodicity. As a general rule, the fewer parameters there are to fit, the faster and more accurate the results will be. Avoid fitting more parameters than necessary.

    = DEFAULT Fit all bond force constants and lengths, angle force constants and sizes, and dihedral force constants. This option will usually fit a very large number of parameters, and is rarely necessary. For most cases, only a few parameters are desired, and they should be fit individually.

    = K_ONLY Do not fit any force field parameters. Only fit the value of K (the difference between quantum and classical energies for the system). This needs to be done once per system in order to determine K before any other parameters are fit, as attempting to fit it at the same time results in inaccurate results. Since small changes in K produce a great change in the overall least squares sum, the algorithm will tend to focus on changing the value of K and will neglect the parameters.

    = LOAD The list of parameters to be fit is contained in a file that was previously created with the parameter setting runtype. Set PARAMETER_FILE_NAME to the location of this file. To create this file, run *paramfit* with `RUNTYPE=SET_PARAMS`.

SCEE The value by which to scale 1-4 electrostatics for the AMBER sum. Defaults to 1.2

SCNB The value by which to scale 1-4 van der Waals for the AMBER sum. Defaults to 2.0.

QM_ENERGY_UNITS The unit of energy in the quantum data file if you are fitting to energies. This will depend on your quantum package and settings used for the single point calculations.

    = HARTREE Default

= KCALMOL

= KJMOL

QM_FORCE_UNITS The unit of force in the quantum data files if you are fitting to forces. This will depend on your quantum package and settings used for the force calculations.

= HARTREE_BOHR Default

= KCALMOL_ANGSTROM

WRITE_ENERGY Saves the final AMBER energy and the quantum data for each structure to the specified file. Plotting these data is useful in verifying the results of the fitting and identifying any problem structures. See Subsection 12.5.3 for more on how to verify the accuracy of results.

WRITE_FRCMOD When the fitting is complete, the parameters will be saved in a force field modification file at this location in addition to displaying them in standard output. This file may be used with LEaP to create a new *prmtop*. If no value is specified the file will not be created.

SCATTERPLOTS Creates graphs of the bond, angles, and dihedrals found in the input files for each parameter that is being fit. These plots can be visualized using *scripts/scatterplots.sh* found in *paramfit's* source directory. This can be helpful in assessing the quality of the input conformations. No need to specify anything after the = sign for this parameter.

SORT_MDCRDS = YES Sorts the input structures in order of increasing energy before conducting the fit. This can aid in identification of problem regions for the initial or fitted parameters, as they may be generally worse on structures in certain energy ranges.

= NO Default

COORDINATE_FORMAT The format of the input coordinate set. *Paramfit* will return an error if the file is in an unexpected format.

= TRAJECTORY Default

= RESTART

12.2.5 Algorithm options

Paramfit implements two minimization algorithms: a simplex and a hybrid simplex-genetic algorithm (GA). The current version of *paramfit* incorporates numerous refinements to the genetic algorithm that require much less input from the user– it is no longer necessary to choose between the simplex or GA. This improved algorithm means that iterative fits are no longer necessary, and the algorithm will converge very close to or at the global minimum on a single run.

The genetic algorithm starts with a randomly generated solution set, which it recombines and alters in ways similar to evolution. The GA will start with many initial randomly generated sets of parameters. It will then determine which are the best by evaluating the AMBER sum, select them for recombination to produce a new set of parameters, randomly alter a few parameters slightly to prevent premature convergence, and iterate. Once several "generations" have passed without improvement, a loosely converging simplex algorithm is run on a random subset of the population, which is then allowed to recover for several generations before further simplex iterations are conducted. This hybrid approach dramatically speeds convergence to the global minimum, while maintaining the strengths of the genetic algorithm in searching a large, complex solution space with low sampling.

The following options in the job control file will control the behavior of the genetic algorithm. In general the default values for these options is sufficient to produce good results, and alterations to them will speed convergence. Options marked *internal algorithm parameter* should not need to be altered by the vast majority of users, as they are already set to their optimum. The algorithm's results should be independent of these values if they are within reasonable ranges (run the wizard for suggestions).

OPTIMIZATIONS The integer number of possible optimizations the algorithm will use. Analogous to the population size in evolution; larger values require more function evaluations and are slower but produce better initial sampling, and smaller ones will delay convergence. Defaults to 50.

SEARCH_SPACE If positive, the algorithm will search for new parameters for everything except dihedral phases within this percentage of the original value, where 1.0 will search within $\pm 100\%$ of the value found in the input *prmtop*. Defaults to searching over the entire range of valid values and ignoring the original value in the topology file. You may wish to alter this value if you know that the original parameters are good and you wish to search in their neighborhood.

MAX_GENERATIONS The maximum number of iterations the algorithm is allowed to run before it returns the best non-converged optimization. Defaults to 50,000. If you find that you repeatedly need to increase this value compared to the default, there are likely significant problems with your system or insufficient input structures.

GENERATIONS_TO_SIMPLEX The number of iterations in a row that must pass without improvement in the best parameter set for simplex refinements to be run on a random 5% of the populations. Set to 0 for a pure genetic algorithm. Smaller values will speed convergence but may result in retrieval of local minima. Defaults to 10.

GENERATIONS_WITHOUT_SIMPLEX The number of generations that must pass between runs of simplex refinement, regardless of improvement in the best parameter set. These iterations serve as a recovery period for the population of the genetic algorithm, and allows time for the simplex results to be incorporated. If set to small or zero values, simplex refinement may run too often, resulting in convergence to a local minima and eliminating the global search properties of the genetic algorithm. Defaults to 10.

GENERATIONS_TO_CONV The number of iterations in a row that must pass without improvement in the best parameter set for the algorithm to be considered converged. Set to a larger value for a longer but potentially more accurate run. Defaults to 50, which is too large for most systems. This counter increments along with the counter to trigger simplex refinement, and at the global minimum simplex refinement will produce no improvement on the population, allowing convergence.

MUTATION_RATE *Internal algorithm parameter* The chance an allele (potential parameter) in the genetic algorithm population has to be randomly set to a new value each generation. Defaults to 0.05.

PARENT_PERCENT *Internal algorithm parameter* The percentage of each generation that is allowed to pass on alleles to the next generation. Defaults to 0.25.

The simplex algorithm is excellent at refining a good set of input parameters, but can converge on physically unreasonable values (such as negative bond force constants) if given a naive guess. For this reason, the genetic algorithm is recommended for finding the global minimum or a close approximation thereof, and the simplex algorithm may be run on the resulting parameters to confirm the results, if desired. The simplex algorithm starts at an initial set of parameters and moves "downhill" iteratively while sampling neighboring areas (much like an amoeba crawling along the function landscape), and converges when the improvement from one step to another becomes negligible. The simplex algorithm is generally faster than the GA, and excels at well-defined systems with a small number of dimensions. This algorithm requires a very well-defined sample space, and the input structures should contain a good range over all the bonds, angles, and dihedrals that are to be optimized. Otherwise, the algorithm tends to wander and will converge in badly defined areas of the sample set. In smaller, well-defined systems with only a few parameters, this algorithm will outperform the genetic algorithm.

Choose the simplex algorithm if you wish to fit only a few parameters and have a large number of input conformations. You may specify the following options to fine-tune the step sizes taken, but for the vast majority of cases the defaults should suffice:

BONDFC_dx Intrinsic length of parameter space for minimization. Used to determine the size of the steps to construct the initial simplex. Should be large enough that the steps sample a sufficiently large area but small enough to not move outside of normal parameter range. Bond force constant step size defaults to 5.0.

BONDEQ_dx Bond equilibrium length step size. Defaults to 0.02.

ANGLEFC_dx Angle force constant step size. Defaults to 1.0.

ANGLEEQ_dx Angle equilibrium step size. Defaults to 0.05.

DIHEDRALBH_dx Dihedral force constant step size. Defaults to 0.2.

DIHEDRALN_dx Dihedral periodicity step size. Defaults to 0.01.

DIHEDRALG_dx Dihedral phase step size. Defaults to 0.05.

K_dx Step size for intrinsic difference constant. Defaults to 10.0.

CONV_LIMIT Floating point number that details the convergence limit for the minimization. The smaller the number, the longer the algorithm will take to converge but the results may be more accurate. Defaults to 1.0E-15, which is very strict.

12.2.6 Bounds Checking

In order to ensure that the algorithms can return meaningful results, bounds checking routines are included in *paramfit*. The bounds checking functionality ensures that the algorithm's results are reasonable given the initial sample set, and also makes sure that the sample set is well-defined.

Since bonds and angles are approximately harmonic, the algorithm's result is reasonable if it lies within a well-defined area of the sample set. Bonds and angle values are therefore checked after the algorithm has finished running. In order to properly fit dihedrals, sample structures should span the entire range of phases for each dihedral that is to be fit. Dihedral checking is therefore accomplished before the algorithm begins to conduct the fit.

Bounds checking defaults to halting execution of the program upon reaching a failing condition. It is not recommended that this behavior be disabled, since the results of the fit are most likely inaccurate. Using the fitted parameters anyway will probably result in an inaccurate depiction of the molecule. Properly represented parameters in the input structures are crucial for a valid fit. Instead of using the parameters, fix the input structures so that data are provided in the missing ranges, which will be stated in the error message, and rerun the program twice: first in CREATE_INPUT mode to obtain quantum energies for the added structures and then in FIT mode to redo the fit.

If you **know** that your input structures describe the parameters to be fit quite well, the selectivity of the bounds checking can be altered by the specifying the following options in the job control file. Use these options with caution, and verify the generated parameters carefully.

CHECK_BOUNDS = ON The recommended and default option. This will halt execution when the bounds check fails.

 = WARN Continue upon reaching a bounds failure condition, but output a warning. Do not use the parameters generated by this fit without careful verification! Use the error message and other results to determine if they are reasonable.

BOND_LIMIT Fitting results for bond lengths that are this many Angstroms away from the closest approximation in the input structures will result in a failing condition. Defaults to 0.1.

ANGLE_LIMIT Fitting results for angles that are more than this many radians away from the closes approximation in the input structures will result in a failing condition. Defaults to 0.05π.

DIHEDRAL_SPAN The entire range of valid dihedral angles, 0 to π, for each dihedral that is to be fit should be spanned by this many input structure values, otherwise a failing condition will result. Defaults to 12, meaning that there needs to be a dihedral in every $\frac{\pi}{12}$ radian interval of the valid range.

12.3 Multiple molecule fits

Paramfit supports fitting one or more parameters across multiple molecules, and contains several features to aid in force field development. The program is invoked differently, using a prmtop list and mdcrd list that specify topology and structures for each molecule to fit. Since the value of K is also system-dependent, you will need to fit K for each molecule individually.

Input topologies are specified in a *prmtop list,* which contains the filename of each topology and the value of K for that system, separated by a space. There are no comments permitted in this file. For example:

```
molecule1.prmtop 50.0
molecule2.prmtop 100.0
```

To obtain the value of K for each topology file, conduct a single-molecule fit using all the structures corresponding to that topology and put the resulting value in this file. This enables fitting to zero over multiple molecules.

Input coordinate files are stated in the *coordinate list,* which contains the filename of each coordinate set, the number of structures contained in it, and the filename containing the energy of each structure, separated by a space. Each energy file is exactly the same as single-molecule fits, containing the energy of each structure, one per line, in the same order as the corresponding coordinate file. If there are more structures available in the coordinate file than the number N specified, the first N structures will be used in the fit. An example coordinate list would be:

```
molecule1.mdcrd 200 energy1.dat
molecule2.mdcrd 100 energy2.dat
```

Parameters to fit must be present in all of the available topologies, and the parameter specification file (PARAMETER_FILE_NAME) should be created using a single-molecule invocation of *paramfit.* Saved output files such as energy profile will be named according to the input file name, and a single frcmod will be written if specified. A multiple molecule invocation of *paramfit* uses the following command line options:

```
paramfit -i Job_Control.in -pf prmtop_list -cf mdcrd_list [-v MEDIUM] [--random-seed
```

The only alteration to the job control file necessary for multiple molecule fits is the deletion of the NSTRUCTURES parameter. NSTRUCTURES should not be specified as it is now ambiguous and will result in a program error.

12.4 Fitting Forces

Paramfit can fit to the forces on each atom within an input structure rather than to single point energies. In theory, this provides more data to the fitting algorithm and reduces noise by considering only the forces on atoms involved in a fitted parameter in the function evaluation. This section will walk you through the process of fitting forces using *paramfit.*

Currently, force fitting can only read in Gaussian output files, so input files will be created in the format accepted by that program. Specify in the QMHEADER file the "force" keyword, so Gaussian will print out the forces on each atom, and run *paramfit* in the CREATE_INPUT mode as normal. Then run Gaussian on those input files, keeping the resulting output with the same naming scheme, for example appending ".out" to the name of an input file to indicate its input. For example, in bash:

```
for i in `ls output/Job.*.gjf`; do g09 < $i > $i.out; done
```

To run a fit with forces, you must specify the following options in the job control file, or use the wizard. *Paramfit* will read in the output files from the Gaussian job using the same order and naming scheme, so alter the QM filename parameters so that they match the suffix you appended to Gaussian output files.

```
# Enable force fitting function
FUNC_TO_FIT=AMBER_FORCES
# K irrelevant for force fitting
```

```
K=0.0
# Force units used by Gaussian
QM_FORCE_UNITS=HARTREE_BOHR
# Naming scheme of gaussian output files
QMFILEOUTSTART=output/Job.
QMFILEOUTEND=.gjf.out
```

Specify parameters to fit, algorithm and output options as described previously for fits to energy.

As forces fitting is still experimental, take care to evaluate the resulting parameters.

12.5 Examples

12.5.1 Setting up to fit

The fitting process with *paramfit* follows a specific order. Example job control files for each step and a description of the step follow.

First, write a job control file to create the input structures and run *paramfit:*

```
RUNTYPE=CREATE_INPUT
# Trajectory has 50 structures
NSTRUCTURES=50
# Write in Gaussian format
QMFILEFORMAT=GAUSSIAN
# Prepend this file to QM inputs
QMHEADER=Gaussian.header
$AMBERHOME/bin/paramfit -i Job_Control.in -p prmtop -c mdcrd
```

After all 50 input files have been created, run the quantum program on them. Once it's finished, extract the quantum energies from the output files using the provided script, or write your own. Since the example used Gaussian:

```
$AMBERHOME/AmberTools/src/paramfit/scripts/process_gaussian.x \
output_directory energies.dat
```

Now, or while the quantum jobs are running, since neither the energies nor the structures are needed yet, determine which parameters are to be fit and save them.

```
RUNTYPE=SET_PARAMS
# File to be created
PARAMETER_FILE_NAME=saved_params
$AMBERHOME/bin/paramfit -i Job_Control.in -p prmtop
```

Now the quantum energies to fit have been obtained and the parameters to fit have been set, and the fitting process may begin.

12.5.2 Fitting K

The first step in fitting is determining the value of K for a system. A job control file that will only fit K follows:

```
RUNTYPE=FIT
PARAMETERS_TO_FIT=K_ONLY
# Use the simplex function
FITTING_FUNCTION=SIMPLEX
```

Then,

```
$AMBERHOME/bin/paramfit -i Job_Control.in -p prmtop -c mdcrd -q energies.dat
```

Take this value of K and put it back in the job control file when conducting the actual fit.

```
RUNTYPE=FIT
# Use the parameters specified earlier
PARAMETERS_TO_FIT=LOAD
PARAMETER_FILE_NAME=saved_params
# Genetic algorithm options
FITTING_FUNCTION=GENETIC
OPTIMIZATIONS=500
GENERATIONS_TO_CONV=10
GENERATIONS_TO_SIMPLEX=2
GENERATIONS_WITHOUT_SIMPLEX=5
# Save parameters so they can be read into leap
WRITE_FRCMOD=fitted_params.frcmod
```

And call *paramfit* just as before. This example fit will create a force field modification file that can later be read into *LEaP* to create a new *prmtop* with the modified parameters for the molecule.

12.5.3 Evaluating Results

When using *paramfit*, it is important to verify the accuracy of the fitted parameters for your input structures. The WRITE_ENERGY option in the Job Control file is useful for this. Set it to a filename and *paramfit* will write the final AMBER energy of each structure next to the quantum energy for the same structure in a file that can be easily graphed.

If you have gnuplot, a script has been provided to quickly show each structure's energies. Assuming your energy file is named energy.dat:

```
$AMBERHOME/AmberTools/src/paramfit/scripts/plot_energy.x energy.dat
```

The resulting graph makes the identification of problem structures much easier, and gives a good visualization of the fit. In general, carefully validate parameters generated by *paramfit* against other data before conducting large simulations.

The SCATTERPLOT option in the job control file can also be useful in assessing the quality of the input structures. If this option is set, *paramfit* will dump a variety of data files indicating the value for all fitted bonds, angles, and dihedrals in the input conformations. These data may be visualized if you have the program gnuplot by running the following command in the directory where *paramfit* was run:

```
$AMBERHOME/AmberTools/src/paramfit/scripts/scatterplots.sh
```

The resulting graphs feature different colored points for each bond, angle, and dihedral type that is being fit for each of the input structures. This is useful in evaluating if the results of the fit are reasonable– for example, if the algorithm converges with an equilibrium bond length that is not similar to any of the structures, that parameter may not be accurate.

Bibliography

[1] Z. Zhang; X. Liu; Z. Chen; H. Zheng; K. Yan; J. Liu. A unified thermostat scheme for efficient configurational sampling for classical/quantum canonical ensembles via molecular dynamics. *J. Chem. Phys.*, **2017**, *147*, 034109.

[2] J. Liu; D. Li; X. Liu. A simple and accurate algorithm for path integral molecular dynamics with the Langevin thermostat. *J. Chem. Phys.*, **2016**, *145*, 024103.

[3] D. Li; X. Han; Y. Chai; C. Wang; Z. Zhang; Z. Chen; J. Liu; J. Shao. Stationary state distribution and efficiency analysis of the Langevin equation via real or virtual dynamics. *J. Chem. Phys.*, **2017**, *147*, 184104.

[4] D. Li; Z. Chen; Z. Zhang; J. Liu. Understanding molecular dynamics with stochastic processes via real or virtual dynamics. *Chinese Journal of Chemical Physics*, **2017**, *30*, 735–760.

[5] Z. Zhang; K. Yan; X. Liu; J. Liu. A leap-frog algorithm-based efficient unified thermostat scheme for molecular dynamics. *Chinese Science Bulletin*, **2018**, *63*, 3467–3483.

[6] C. W. Hopkins; S. Le Grand; R. C. Walker; A. E. Roitberg. Long-Time-Step Molecular Dynamics through Hydrogen Mass Repartitioning. *J. Chem. Theory Comput.*, **2015**, *11*, 1864–1874.

[7] T. Morishita. Fluctuation formulas in molecular-dynamics simulations with the weak coupling heat bath. *J. Chem. Phys.*, **2000**, *113*, 2976.

[8] A. Mudi; C. Chakravarty. Effect of the Berendsen thermostat on the dynamical properties of water. *Mol. Phys.*, **2004**, *102*, 681–685.

[9] B. P. Uberuaga; M. Anghel; A. F. Voter. Synchronization of trajectories in canonical molecular-dynamics simulations: Observation, explanation, and exploitation. *J. Chem. Phys.*, **2004**, *120*, 6363–6374.

[10] D. J. Sindhikara; S. Kim; A. F. Voter; A. E. Roitberg. Bad seeds sprout perilous dynamics: Stochastic thermostat induced trajectory synchronization in biomolecules. *J. Chem. Theory Comput.*, **2009**, *5*, 1624–1631.

[11] B. Leimkuhler; D. T. Margul; M. E. Tuckerman. Stochastic, Resonance-Free Multiple Time-Step Algorithm for Molecular Dynamics with Very Large Time Steps. *Mol. Phys.*, **2013**, *111*, 3579–3594.

[12] R. J. Loncharich; B. R. Brooks; R. W. Pastor. Langevin dynamics of peptides: The frictional dependence of isomerization rates of N-actylananyl-N'-methylamide. *Biopolymers*, **1992**, *32*, 523–535.

[13] Y. M. Rhee; V. S. Pande. Solvent viscosity dependence of the protein folding dynamics. *J. Phys. Chem. B*, **2008**, *112*, 6221–6227. PMID: 18229911.

[14] J. A. Izaguirre; D. P. Catarello; J. M. Wozniak; R. D. Skeel. Langevin stabilization of molecular dynamics. *J. Chem. Phys.*, **2001**, *114*, 2090–2098.

[15] R. Anandakrishnan; A. Drozdetski; R. C. Walker; A. V. Onufriev. Speed of Conformational Change: Comparing Explicit and Implicit Solvent Molecular Dynamics Simulations. *Biophysical Journal*, **2015**, *108*, 1153–1164.

[16] H. C. Andersen. Molecular dynamics simulations at constant pressure and/or temperature. *J. Chem. Phys.*, **1980**, *72*, 2384–2393.

[17] Y. Zhang; S. E. Feller; B. R. Brooks; R. W. Pastor. Computer simulation of liquid/liquid interfaces. I. Theory and application to octane/water. *J. Chem. Phys.*, **1995**, *103*, 10252–10266.

[18] J.-P. Ryckaert; G. Ciccotti; H. J. C. Berendsen. Numerical integration of the cartesian equations of motion of a system with constraints: Molecular dynamics of n-alkanes. *J. Comput. Phys.*, **1977**, *23*, 327–341.

[19] S. Miyamoto; P. A. Kollman. SETTLE: An analytical version of the SHAKE and RATTLE algorithm for rigid water models. *J. Comput. Chem.*, **1992**, *13*, 952–962.

[20] X. Wu; S. Subramaniam; D. A. Case; K. Wu; B. R. Brooks. Targeted conformational search with map-restrained self-guided langevin dynamics: application to flexible fitting into electron microscopic density maps. *J. Struct. Biology*, **2013**, *183*, 429–440.

[21] P. Li; K. M. Merz, Jr. Taking into Account the Ion-Induced Dipole Interaction in the Nonbonded Model of Ions. *J. Chem. Theory Comput.*, **2014**, *10*, 289–297.

[22] T. Darden; D. York; L. Pedersen. Particle mesh Ewald–an Nlog(N) method for Ewald sums in large systems. *J. Chem. Phys.*, **1993**, *98*, 10089–10092.

[23] U. Essmann; L. Perera; M. L. Berkowitz; T. Darden; H. Lee; L. G. Pedersen. A smooth particle mesh Ewald method. *J. Chem. Phys.*, **1995**, *103*, 8577–8593.

[24] M. F. Crowley; T. A. Darden; T. E. Cheatham, III; D. W. Deerfield, II. Adventures in improving the scaling and accuracy of a parallel molecular dynamics program. *J. Supercomput.*, **1997**, *11*, 255–278.

[25] C. Sagui; T. A. Darden. in *Simulation and Theory of Electrostatic Interactions in Solution*, L. R. Pratt; G. Hummer, Eds., pp 104–113. American Institute of Physics, Melville, NY, 1999.

[26] A. Toukmaji; C. Sagui; J. Board; T. Darden. Efficient particle-mesh Ewald based approach to fixed and induced dipolar interactions. *J. Chem. Phys.*, **2000**, *113*, 10913–10927.

[27] C. Sagui; L. G. Pedersen; T. A. Darden. Towards an accurate representation of electrostatics in classical force fields: Efficient implementation of multipolar interactions in biomolecular simulations. *J. Chem. Phys.*, **2004**, *120*, 73–87.

[28] L. David; R. Luo; M. K. Gilson. Comparison of generalized born and poisson models: Energetics and dynamics of hiv protease. *J. Comput. Chem.*, **2000**, *21*, 295–309.

[29] M. Feig. Kinetics from Implicit Solvent Simulations of Biomolecules as a Function of Viscosity. *J. Chem. Theory Comput.*, **2007**, *3*, 1734–1748.

[30] R. E. Amaro; X. Cheng; I. Ivanov; D. Xu; A. J. Mccammon. Characterizing Loop Dynamics and Ligand Recognition in Human- and Avian-Type Influenza Neuraminidases via Generalized Born Molecular Dynamics and End-Point Free Energy Calculations. *J. Am. Chem. Soc.*, **2009**, *131*, 4702–4709.

[31] B. Zagrovic; V. Pande. Solvent viscosity dependence of the folding rate of a small protein: Distributed computing study. *J. Comput. Chem.*, **2003**, *24*, 1432–1436.

[32] A. V. Onufriev; D. A. Case. Generalized Born implicit solvent models for biomolecules. *Annu. Rev. Biophys.*, **2019**, *48*, 275–296.

[33] J. Weiser; P. S. Shenkin; W. C. Still. Approximate Atomic Surfaces from Linear Combinations of Pairwise Overlaps (LCPO). *J. Comput. Chem.*, **1999**, *20*, 217–230.

[34] W. C. Still; A. Tempczyk; R. C. Hawley; T. Hendrickson. Semianalytical treatment of solvation for molecular mechanics and dynamics. *J. Am. Chem. Soc.*, **1990**, *112*, 6127–6129.

[35] M. Schaefer; M. Karplus. A comprehensive analytical treatment of continuum electrostatics. *J. Phys. Chem.*, **1996**, *100*, 1578–1599.

[36] S. R. Edinger; C. Cortis; P. S. Shenkin; R. A. Friesner. Solvation free energies of peptides: Comparison of approximate continuum solvation models with accurate solution of the Poisson-Boltzmann equation. *J. Phys. Chem. B*, **1997**, *101*, 1190–1197.

[37] B. Jayaram; D. Sprous; D. L. Beveridge. Solvation free energy of biomacromolecules: Parameters for a modified generalized Born model consistent with the AMBER force field. *J. Phys. Chem. B*, **1998**, *102*, 9571–9576.

[38] C. J. Cramer; D. G. Truhlar. Implicit solvation models: Equilibria, structure, spectra, and dynamics. *Chem. Rev.*, **1999**, *99*, 2161–2200.

[39] D. Bashford; D. A. Case. Generalized Born models of macromolecular solvation effects. *Annu. Rev. Phys. Chem.*, **2000**, *51*, 129–152.

[40] A. Onufriev; D. Bashford; D. A. Case. Modification of the generalized Born model suitable for macro-molecules. *J. Phys. Chem. B*, **2000**, *104*, 3712–3720.

[41] M. S. Lee; F. R. Salsbury, Jr.; C. L. Brooks, III. Novel generalized Born methods. *J. Chem. Phys.*, **2002**, *116*, 10606–10614.

[42] B. N. Dominy; C. L. Brooks, III. Development of a generalized Born model parameterization for proteins and nucleic acids. *J. Phys. Chem. B*, **1999**, *103*, 3765–3773.

[43] V. Tsui; D. A. Case. Molecular dynamics simulations of nucleic acids using a generalized Born solvation model. *J. Am. Chem. Soc.*, **2000**, *122*, 2489–2498.

[44] N. Calimet; M. Schaefer; T. Simonson. Protein molecular dynamics with the generalized Born/ACE solvent model. *Proteins*, **2001**, *45*, 144–158.

[45] A. Onufriev; D. Bashford; D. A. Case. Exploring protein native states and large-scale conformational changes with a modified generalized Born model. *Proteins*, **2004**, *55*, 383–394.

[46] J. Srinivasan; M. W. Trevathan; P. Beroza; D. A. Case. Application of a pairwise generalized Born model to proteins and nucleic acids: inclusion of salt effects. *Theor. Chem. Acc.*, **1999**, *101*, 426–434.

[47] A. Onufriev; D. A. Case; D. Bashford. Effective Born radii in the generalized Born approximation: The importance of being perfect. *J. Comput. Chem.*, **2002**, *23*, 1297–1304.

[48] G. D. Hawkins; C. J. Cramer; D. G. Truhlar. Parametrized models of aqueous free energies of solvation based on pairwise descreening of solute atomic charges from a dielectric medium. *J. Phys. Chem.*, **1996**, *100*, 19824–19839.

[49] F. M. Richards. Areas, volumes, packing, and protein structure. *Ann. Rev. Biophys. Bioeng.*, **1977**, *6*, 151–176.

[50] M. Schaefer; C. Froemmel. A precise analytical method for calculating the electrostatic energy of macro-molecules in aqueous solution. *J. Mol. Biol.*, **1990**, *216*, 1045–1066.

[51] M. Feig; A. Onufriev; M. Lee; W. Im; D. A. Case; C. L. Brooks, III. Performance comparison of the generalized Born and Poisson methods in the calculation of the electrostatic solvation energies for protein structures. *J. Comput. Chem.*, **2004**, *25*, 265–284.

[52] R. Geney; M. Layten; R. Gomperts; C. Simmerling. Investigation of salt bridge stability in a generalized Born solvent model. *J. Chem. Theory Comput.*, **2006**, *2*, 115–127.

[53] A. Okur; L. Wickstrom; C. Simmerling. Evaluation of salt bridge structure and energetics in peptides using explicit, implicit and hybrid solvation models. *J. Chem. Theory Comput.*, **2008**, *4*, 488–498.

[54] A. Okur; L. Wickstrom; M. Layten; R. Geney; K. Song; V. Hornak; C. Simmerling. Improved efficiency of replica exchange simulations through use of a hybrid explicit/implicit solvation model. *J. Chem. Theory Comput.*, **2006**, *2*, 420–433.

[55] D. R. Roe; A. Okur; L. Wickstrom; V. Hornak; C. Simmerling. Secondary Structure Bias in Generalized Born Solvent Models: Comparison of Conformational Ensembles and Free Energy of Solvent Polarization from Explicit and Implicit Solvation. *J. Phys. Chem. B*, **2007**, *111*, 1846–1857.

[56] H. Nguyen; D. R. Roe; C. Simmerling. Improved Generalized Born Solvent Model Parameters for Protein Simulations. *J. Chem. Theory Comput.*, **2013**, *9*, 2020–2034.

[57] H. Nguyen; J. Maier; H. Huang; V. Perrone; C. Simmerling. Folding simulations for proteins with diverse topologies are accessible in days with a physics-based force field and implicit solvent. *J. Am. Chem. Soc.*, **2014**, *136*, 13959–13962. PMID: 25255057.

[58] H. Nguyen; A. Pérez; S. Bermeo; C. Simmerling. Refinement of Generalized Born Implicit Solvation Parameters for Nucleic Acids and Their Complexes with Proteins. *J. Chem. Theory Comput.*, **2015**, *11*, 3714–3728.

[59] A. Onufriev. in *Modeling Solvent Environments*, M. Feig, Ed., (Wiley, USA). pp 127–165. 2010.

[60] G. D. Hawkins; C. J. Cramer; D. G. Truhlar. Pairwise solute descreening of solute charges from a dielectric medium. *Chem. Phys. Lett.*, **1995**, *246*, 122–129.

[61] M. Schaefer; H. W. T. Van Vlijmen; M. Karplus. Electrostatic contributions to molecular free energies in solution. *Adv. Protein Chem.*, **1998**, *51*, 1–57.

[62] V. Tsui; D. A. Case. Theory and applications of the generalized Born solvation model in macromolecular simulations. *Biopolymers (Nucl. Acid. Sci.)*, **2001**, *56*, 275–291.

[63] C. P. Sosa; T. Hewitt; M. S. Lee; D. A. Case. Vectorization of the generalized Born model for molecular dynamics on shared-memory computers. *J. Mol. Struct. (Theochem)*, **2001**, *549*, 193–201.

[64] J. Mongan; C. Simmerling; J. A. McCammon; D. A. Case; A. Onufriev. Generalized Born with a simple, robust molecular volume correction. *J. Chem. Theory Comput.*, **2007**, *3*, 156–169.

[65] H. Huang; C. Simmerling. Fast Pairwise Approximation of Solvent Accessible Surface Area for Implicit Solvent Simulations of Proteins on CPUs and GPUs. *J. Chem. Theory Comput.*, **2018**, *14*, 5797–5814.

[66] D. Sitkoff; K. A. Sharp; B. Honig. Accurate calculation of hydration free energies using macroscopic solvent models. *J. Phys. Chem.*, **1994**, *98*, 1978–1988.

[67] T. Luchko; S. Gusarov; D. R. Roe; C. Simmerling; D. A. Case; J. Tuszynski; A. Kovalenko. Three-dimensional molecular theory of solvation coupled with molecular dynamics in Amber. *J. Chem. Theory Comput.*, **2010**, *6*, 607–624.

[68] D. Chandler; H. C. Andersen. Optimized cluster expansions for classical fluids. ii. theory of molecular liquids. *J. Chem. Phys.*, **1972**, *57*, 1930–1937.

[69] F. Hirata; P. J. Rossky. An extended RISM equation for molecular polar fluids. *Chem. Phys. Lett.*, **1981**, pp 329–334.

[70] F. Hirata; B. M. Pettitt; P. J. Rossky. Application of an extended rism equation to dipolar and quadrupolar fluids. *J. Chem. Phys.*, **1982**, *77*, 509–520.

[71] F. Hirata; P. J. Rossky; B. M. Pettitt. The interionic potential of mean force in a molecular polar solvent from an extended rism equation. *J. Chem. Phys.*, **1983**, *78*, 4133–4144.

[72] D. Chandler; J. McCoy; S. Singer. Density functional theory of nonuniform polyatomic systems. i. general formulation. *J. Chem. Phys.*, **1986**, *85*, 5971–5976.

[73] D. Chandler; J. McCoy; S. Singer. Density functional theory of nonuniform polyatomic systems. ii. rational closures for integral equations. *J. Chem. Phys.*, **1986**, *85*, 5977–5982.

[74] D. Beglov; B. Roux. Numerical solution of the hypernetted chain equation for a solute of arbitrary geometry in three dimensions. *J. Chem. Phys.*, **1995**, *103*, 360–364.

[75] D. Beglov; B. Roux. An integral equation to describe the solvation of polar molecules in liquid water. *J. Phys. Chem. B*, **1997**, *101*, 7821–7826.

[76] A. Kovalenko; F. Hirata. Three-dimensional density profiles of water in contact with a solute of arbitrary shape: a RISM approach. *Chem. Phys. Lett.*, **1998**, *290*, 237–244.

[77] A. Kovalenko; F. Hirata. Self-consistent description of a metal–water interface by the Kohn–Sham density functional theory and the three-dimensional reference interaction site model. *J. Chem. Phys.*, **1999**, *110*, 10095–10112.

[78] A. Kovalenko. In Hirata [639], chapter 4.

[79] A. Kovalenko; F. Hirata. Potentials of mean force of simple ions in ambient aqueous solution. i: Three-dimensional reference interaction site model approach. *J. Chem. Phys.*, **2000**, *112*, 10391–10402.

[80] A. Kovalenko; F. Hirata. Potentials of mean force of simple ions in ambient aqueous solution. ii: Solvation structure from the three-dimensional reference interaction site model approach, and comparison with simulations. *J. Chem. Phys.*, **2000**, *112*, 10403–10417.

[81] J.-P. Hansen; I. R. McDonald. *Theory of simple liquids*. Academic Press, London, 1990.

[82] F. Hirata. In *Molecular Theory of Solvation* [639], chapter 1.

[83] J. W. Kaminski; S. Gusarov; T. A. Wesolowski; A. Kovalenko. Modeling solvatochromic shifts using the orbital-free embedding potential at statistically mechanically averaged solvent density. *J. Phys. Chem. A*, **2010**, *114*, 6082–6096.

[84] M. Frigo; S. G. Johnson. FFTW: An adaptive software architecture for the FFT. in *Proc. 1998 IEEE Intl. Conf. Acoustics Speech and Signal Processing*, volume 3, pp 1381–1384. IEEE, 1998.

[85] M. Frigo. A fast Fourier transform compiler. in *Proc. 1999 ACM SIGPLAN Conf. on Programming Language Design and Implementation*, volume 34, pp 169–180. ACM, 1999.

[86] S. J. Singer; D. Chandler. Free energy functions in the extended RISM approximation. *Mol. Phys.*, **1985**, *55*, 621–625.

[87] B. M. Pettitt; P. J. Rossky. Alkali halides in water: Ion-solvent correlations and ion-ion potentials of mean force at infinite dilution. *J. Chem. Phys.*, **1986**, *15*, 5836–5844.

[88] S. M. Kast. Free energies from integral equation theories: Enforcing path independence. *Phys. Rev. E*, **2003**, *67*, 041203.

[89] G. Schmeer; A. Maurer. Development of thermodynamic properties of electrolyte solutions with the help of RISM-calculations at the Born-Oppenheimer level. *Phys. Chem. Chem. Phys.*, **2010**, *12*, 2407–2417.

[90] S. Gusarov; T. Ziegler; A. Kovalenko. Self-consistent combination of the three-dimensional RISM theory of molecular solvation with analytical gradients and the amsterdam density functional package. *J. Phys. Chem. A*, **2006**, *110*, 6083–6090.

[91] T. Miyata; F. Hirata. Combination of molecular dynamics method and 3D-RISM theory for conformational sampling of large flexible molecules in solution. *J. Comput. Chem.*, **2007**, *29*, 871–882.

[92] S. M. Kast; T. Kloss. Closed-form expressions of the chemical potential for integral equation closures with certain bridge functions. *J. Chem. Phys.*, **2008**, *129*, 236101.

[93] D. Chandler; Y. Singh; D. M. Richardson. Excess electrons in simple fluids. I. General equilibrium theory for classical hard sphere solvents. *J. Chem. Phys.*, **1984**, *81*, 1975–1982.

[94] T. Ichiye; D. Chandler. Hypernetted chain closure reference interaction site method theory of structure and thermodynamics for alkanes in water. *J. Phys. Chem.*, **1988**, *92*, 5257–5261.

[95] P. H. Lee; G. M. Maggiora. Solvation thermodynamics of polar molecules in aqueous solution by the XRISM method. *J. Phys. Chem.*, **1993**, *97*, 10175–10185.

[96] S. Genheden; T. Luchko; S. Gusarov; A. Kovalenko; U. Ryde. An MM/3D-RISM approach for ligand-binding affinities. *J. Phys. Chem.*, **2010**. Accepted.

[97] J. Johnson; D. A. Case; T. Yamazaki; S. Gusarov; A. Kovalenko; T. Luchko. Small molecule solvation energy and entropy from 3D-RISM. *J. Phys. Condens. Mat.*, **2016**.

[98] R. C. Walker; M. F. Crowley; D. A. Case. The implementation of a fast and accurate QM/MM potential method in Amber. *J. Comput. Chem.*, **2008**, *29*, 1019–1031.

[99] T. J. Giese; D. M. York. Charge-dependent model for many-body polarization, exchange, and dispersion interactions in hybrid quantum mechanical/molecular mechanical calculations. *J. Chem. Phys.*, **2007**, *127*, 194101–194111.

[100] J. J. P. Stewart. Optimization of parameters for semiempirical methods I. Method. *J. Comput. Chem.*, **1989**, *10*, 209–220.

[101] M. J. S. Dewar; E. G. Zoebisch; E. F. Healy; J. J. P. Stewart. AM1: A new general purpose quantum mechanical molecular model. *J. Am. Chem. Soc.*, **1985**, *107*, 3902–3909.

[102] G. B. Rocha; R. O. Freire; A. M. Simas; J. J. P. Stewart. RM1: A Reparameterization of AM1 for H, C, N, O, P, S, F, Cl, Br and I. *J. Comp. Chem.*, **2006**, *27*, 1101–1111.

[103] M. J. S. Dewar; W. Thiel. Ground states of molecules. 38. The MNDO method, approximations and parameters. *J. Am. Chem. Soc.*, **1977**, *99*, 4899–4907.

[104] M. P. Repasky; J. Chandrasekhar; W. L. Jorgensen. PDDG/PM3 and PDDG/MNDO: Improved semiempirical methods. *J. Comput. Chem.*, **2002**, *23*, 1601–1622.

[105] J. P. McNamara; A. M. Muslim; H. Abdel-Aal; H. Wang; M. Mohr; I. H. Hillier; R. A. Bryce. Towards a quantum mechanical force field for carbohydrates: A reparameterized semiempirical MO approach. *Chem. Phys. Lett.*, **2004**, *394*, 429–436.

[106] M. I. Bernal-Uruchurtu; M. F. Ruiz-López. Basic ideas for the correction of semiempirical methods describing H-bonded systems. *Chem. Phys. Lett.*, **2000**, *330*, 118–124.

[107] O. I. Arillo-Flores; M. F. Ruiz-López; M. I. Bernal-Uruchurtu. Can semi-empirical models describe HCl dissociation in water? *Theoret. Chem. Acc.*, **2007**, *118*, 425–435.

[108] W. Thiel; A. A. Voityuk. Extension of the MNDO formalism to d orbitals: Integral approximations and preliminary numerical results. *Theoret. Chim. Acta*, **1992**, *81*, 391–404.

[109] W. Thiel; A. A. Voityuk. Extension of the MNDO formalism to d orbitals: Integral approximations and preliminary numerical results. *Theoret. Chim. Acta*, **1996**, *93*, 315.

[110] W. Thiel; A. A. Voityuk. Erratum: Extension of MNDO to d orbitals: Parameters and results for the second-row elements and for the zinc group. *J. Phys. Chem.*, **1996**, *100*, 616–626.

[111] P. Imhof; F. Noé; S. Fischer; J. C. Smith. AM1/d Parameters for Magnesium in Metalloenzymes. *J. Chem. Theory Comput.*, **2006**, *2*, 1050–1056.

[112] K. Nam; Q. Cui; J. Gao; D. M. York. Specific Reaction Parametrization of the AM1/d Hamiltonian for Phosphoryl Transfer Reactions: H, O, and P Atoms. *J. Chem. Theory Comput.*, **2007**, *3*, 486–504.

[113] J. J. P. Stewart. Optimization of parameters for semiempirical methods V: Modification of NDDO approximations and application to 70 elements. *J. Mol. Mod.*, **2007**, *13*, 1173–1213.

[114] G. M. Seabra; R. C. Walker; M. Elstner; D. A. Case; A. E. Roitberg. Implementation of the SCC-DFTB Method for Hybrid QM/MM Simulations within the Amber Molecular Dynamics Package. *J. Phys. Chem. A.*, **2007**, *20*, 5655–5664.

[115] D. Porezag; T. Frauenheim; T. Kohler; G. Seifert; R. Kaschner. Construction of tight-binding-like potentials on the basis of density-functional-theory: Applications to carbon. *Phys. Rev. B*, **1995**, *51*, 12947.

[116] G. Seifert; D. Porezag; T. Frauenheim. Calculations of molecules, clusters and solids with a simplified LCAO-DFT-LDA scheme. *Int. J. Quantum Chem.*, **1996**, *58*, 185.

[117] M. Elstner; D. Porezag; G. Jungnickel; J. Elsner; M. Haugk; T. Frauenheim; S. Suhai; G. Seifert. Self-consistent charge density functional tight-binding method for simulation of complex material properties. *Phys. Rev. B*, **1998**, *58*, 7260.

[118] M. Gaus; Q. Cui; M. Elstner. DFTB3: Extension of the self-consistent-charge density-functional tight-binding method (SCC-DFTB). *J. Chem. Theory Comput.*, **2011**, *7*, 931–948.

[119] M. Elstner; P. Hobza; T. Frauenheim; S. Suhai; E. Kaxiras. Hydrogen bonding and stacking interactions of nucleic acid base pairs: a density-functional-theory based treatment. *J. Chem. Phys.*, **2001**, *114*, 5149.

[120] J. A. Kalinowski; B. Lesyng; J. D. Thompson; C. J. Cramer; D. G. Truhlar. Class IV charge model for the self-consistent charge density-functional tight-binding method. *J. Phys. Chem. A*, **2004**, *108*, 2545–2549.

[121] Y. Yang; H. Yu; D. M. York; Q. Cui; M. Elstner. Extension of the self-consistent charge density-functional tight-binding method: Third-order expansion of the density functional theory total energy and introduction of a modified effective Coulomb interaction. *J. Phys. Chem. A*, **2007**, *111*, 10861–10873.

[122] M. Korth. Third-generation hydrogen-bonding corrections for semiempirical qm methods and force fields. *J. Chem. Theory Comput.*, **2010**, *6*, 3808.

[123] P. Jurecka; J. Cerný; P. Hobza; D. R. Salahub. Density functional theory augmented with an empirical dispersion term. Interaction energies and geometries of 80 noncovalent complexes compared with ab initio quantum mechanics calculations. *J. Comp. Chem.*, **2007**, *28*, 555–569.

[124] A. Bondi. van der Waals volumes and radii. *J. Phys. Chem.*, **1964**, *68*, 441–451.

[125] M. Korth; M. Pitonak; J. Rezac; P. Hobza. A transferable h-bonding correction for semiempirical quantum-chemical methods. *J. Chem. Theory Comput.*, **2010**, *6*, 344–352.

[126] X. Wu; B. R. Brooks. Self-guided Langevin dynamics simulation method. *Chem. Phys. Lett.*, **2003**, *381*, 512–518.

[127] X. Wu; A. Damjanovic; B. R. Brooks. Efficient and unbiased sampling of biomolecular systems in the canonical ensemble: a review of self-guided langevin dynamics. *Adv. Chem. Phys.*, **2012**, *150*, 255–326.

[128] X. Yu; X. Wu; G. A. Bermejo; B. R. Brooks; J. W. Taraska. Accurate high-throughput structure mapping and prediction with transition metal ion fret. *Structure*, **2013**, *21*, 9–19.

[129] X. Wu; B. R. Brooks. Self-guided langevin dynamics via generalized langevin equation. *J. Comput. Chem.*, **2016**, *37*, 595–601.

[130] X. Wu; B. R. Brooks. Reformulation of the self-guided molecular simulation method. *J. Chem. Phys.*, **2020**, *153*, 094112.

[131] X. Wu; B. R. Brooks. Toward canonical ensemble distribution from self-guided Langevin dynamics simulation. *J. Chem. Phys.*, **2011**, *134*, 134108.

[132] X. Wu; B. R. Brooks. Force-momentum-based self-guided Langevin dynamics: a rapid sampling method that approaches the canonical ensemble . *J. Chem. Phys.*, **2011**, *135*, 204101.

[133] I. Kolossváry; W. C. Guida. Low mode search. An efficient, automated computational method for conformational analysis: Application to cyclic and acyclic alkanes and cyclic peptides. *J. Am. Chem. Soc.*, **1996**, *118*, 5011–5019.

[134] I. Kolossváry; W. C. Guida. Low-mode conformational search elucidated: Application to $C_{39}H_{80}$ and flexible docking of 9-deazaguanine inhibitors into PNP. *J. Comput. Chem.*, **1999**, *20*, 1671–1684.

[135] I. Kolossváry; G. M. Keserü. Hessian-free low-mode conformational search for large-scale protein loop optimization: Application to c-jun N-terminal kinase JNK3. *J. Comput. Chem.*, **2001**, *22*, 21–30.

[136] G. M. Keserü; I. Kolossváry. Fully flexible low-mode docking: Application to induced fit in HIV integrase. *J. Am. Chem. Soc.*, **2001**, *123*, 12708–12709.

[137] W. H. Press; B. P. Flannery; S. A. Teukolsky; W. T. Vetterling. *Numerical Recipes: The Art of Scientific Computing*. Cambridge University Press, New York, 1989.

[138] D. C. Liu; J. Nocedal. On the limited memory method for large scale optimization. *Math. Programming B*, **1989**, *45*, 503–528.

[139] J. Nocedal; J. L. Morales. Automatic preconditioning by limited memory quasi-Newton updating. *SIAM J. Opt.*, **2000**, *10*, 1079–1096.

[140] P. Kollman. Free energy calculations: Applications to chemical and biochemical phenomena. *Chem. Rev.*, **1993**, *93*, 2395–2417.

[141] T. Simonson. in *Computational Biochemistry and Biophysics*, O. Becker; A. D. MacKerell; B. Roux; M. Watanabe, Eds. Marcel Dekker, New York, 2001.

[142] D. Frenkel; B. Smit. *Understanding Molecular Simulation: From Algorithms to Applications. Second edition*. Academic Press, San Diego, 2002.

[143] T. Steinbrecher; D. A. Case; A. Labahn. A multistep approach to structure-based drug design: Studying ligand binding at the human neutrophil elastase. *J. Med.. Chem.*, **2006**, *49*, 1837–1844.

[144] T. Steinbrecher; A. Hrenn; K. Dormann; I. Merfort; A. Labahn. Bornyl (3,4,5-trihydroxy)-cinnamate - An optimized human neutrophil elastase inhibitor designed by free energy calculations. *Bioorg. Med. Chem.*, **2008**, *16*, 2385–2390.

[145] G. Hummer; A. Szabo. Calculation of free-energy differences from computer simulations of initial and final states. *J. Chem. Phys.*, **1996**, *105*, 2004–2010.

[146] T. Steinbrecher; D. L. Mobley; D. A. Case. Non-linear scaling schemes for Lennard-Jones interactions in free energy calculations. *J. Chem. Phys.*, **2007**, *127*, 214108.

[147] J. Kaus; L. C. T. Pierce; R. C. Walker; J. A. McCammon. PMEMD TI: Placeholder. *J. Chem. Theory Comput.*, **2013**.

[148] T. Steinbrecher; I. Joung; D. A. Case. Soft-core potentials in thermodynamic integration: Comparing one- and two-step transformations. *J. Comp. Chem.*, **2011**, *32*, 3253–3263.

[149] V. Babin; C. Roland; C. Sagui. Adaptively biased molecular dynamics for free energy calculations. *J. Chem. Phys.*, **2008**, *128*, 134101.

[150] T. Huber; A. E. Torda; W. F. van Gunsteren. Local elevation: a method for improving the searching properties of molecular dynamics simulation. *J. Comput. Aided. Mol. Des.*, **1994**, *8*, 695–708.

[151] F. Wang; D. P. Landau. Efficient, multiple-range random walk algorithm to calculate the density of states. *Phys. Rev. Lett.*, **2001**, *86*, 2050–2053.

[152] A. Laio; M. Parrinello. Escaping free-energy minima. *Proc. Natl. Acad. Sci.*, **2002**, *99*, 12562–12566.

[153] M. Iannuzzi; A. Laio; M. Parrinello. Efficient exploration of reactive potential energy surfaces using car-parrinello molecular dynamics. *Phys. Rev. Lett.*, **2003**, *90*, 238302–1.

[154] T. Lelièvre; M. Rousset; G. Stoltz. Computation of free energy profiles with parallel adaptive dynamics. *J. Chem. Phys.*, **2007**, *126*, 134111.

[155] P. Raiteri; A. Laio; F. L. Gervasio; C. Micheletti; M. Parrinello. Efficient reconstruction of complex free energy landscapes by multiple walkers metadynamics. *J. Phys. Chem.*, **2006**, *110*, 3533–3539.

[156] Y. Sugita; A. Kitao; Y. Okamoto. Multidimensional replica-exchange method for free-energy calculations. *J. Chem. Phys.*, **2000**, *113*, 6042–6051.

[157] G. Bussi; F. L. Gervasio; A. Laio; M. Parrinello. Free-energy landscape for β hairpin folding from combined parallel tempering and metadynamics. *J. Am. Chem. Soc.*, **2006**, *128*, 13435–13441.

[158] S. Piana; A. Laio. A bias-exchange approach to protein folding. *J. Phys. Chem. B*, **2007**, *111*, 4553–4559.

[159] V. Babin; C. Roland; T. A. Darden; C. Sagui. The free energy landscape of small peptides as obtained from metadynamics with umbrella sampling corrections. *J. Chem. Phys.*, **2006**, *125*, 2049096.

[160] V. Babin; V. Karpusenka; M. Moradi; C. Roland; C. Sagui. Adaptively biased molecular dynamics: an umbrella sampling method with a time dependent potential. *Inter. J. Quantum Chem.*, **2009**, *109*, 3666–3678.

[161] V. Babin; C. Sagui. Conformational free energies of methyl-alpha-l-iduronic and methyl-beta-d-glucuronic acids in water. *J. Chem. Phys.*, **2010**, *132*, 104108.

[162] M. Moradi; V. Babin; C. Roland; T. Darden; C. Sagui. Conformations and free energy landscapes of polyproline peptides. *Proc. Natl. Aca. Sci. USA*, **2009**, *106*, 20746.

[163] M. Moradi; V. Babin; C. Roland; C. Sagui. A classical molecular dynamics investigation of the free energy and structure of short polyproline conformers. *J. Chem. Phys.*, **2010**, *133*, 125104.

[164] M. Moradi; V. Babin; C. Sagui; C. Roland. in *Proline: Biosynthesis, Regulation and Health Benefits*, B. Nedjimi, Ed., pp 67–110. Nova Publishers, 2013.

[165] M. Moradi; V. Babin; C. Sagui; C. Roland. A statistical analysis of the PPII propensity of amino acid guests in proline-rich peptides. *Biophysical J.*, **2011**, *100*, 1083 – 1093.

[166] M. Moradi; V. Babin; C. Sagui; C. Roland. PPII propensity of multiple-guest amino acids in a proline-rich environment. *J. Phys. Chem. B.*, **2011**, *115*, 8645–8656.

[167] V. Babin; C. Roland; C. Sagui. The alpha-sheet: A missing-in-action secondary structure? *Proteins –Structure Function and Bioinformatics*, **2011**, *79*, 937–946.

[168] M. Moradi; V. Babin; C. Roland; C. Sagui. Are long-range structural correlations behind the aggregation phenomena of polyglutamine diseases? *PLoS Comput. Biol.*, **2012**, *8*, e1002501.

[169] M. Moradi; V. Babin; C. Roland; C. Sagui. Reaction path ensemble of the B-Z-DNA transition: a comprehensive atomistic study. *Nucleic Acids Research*, **2013**, *41*, 33–43.

[170] F. Pan; V. H. Man; C. Roland; C. Sagui. Structure and Dynamics of DNA and RNA Double Helices of CAG and GAC Trinucleotide Repeats. *Biophys. J.*, **2017**, *113*, 19–36.

[171] F. Pan; Y. Zhang; V. H. Man; C. Roland; C. Sagui. E-motif formed by extrahelical cytosine bases in DNA homoduplexes of trinucleotide and hexanucleotide repeats. *Nucl. Acids Res.*, **2018**, *46*, 942–955.

[172] F. Pan; V. H. Man; C. Roland; C. Sagui. Structure and Dynamics of DNA and RNA Double Helices Obtained From the CCG and GGC Trinucleotide Repeats. *J. Phys. Chem. B*, **2018**, *122*, 4491–4512.

[173] P. Xu; F. Pan; C. Roland; C. Sagui; K. Weninger. Dynamics of strand slippage in DNA hairpins formed by CAG repeats: roles of sequence parity and trinucleotide interrupts. *Nucl. Acids Res.*, 2020, 48, 2232–2245.

[174] M. Moradi; J.-G. Lee; V. Babin; C. Roland; C. Sagui. Free energy and structure of polyproline peptides: an ab initio and classical molecular dynamics investigation. *Int. J. Quantum Chem.*, **2010**, *110*, 2865–2879.

[175] M. Moradi; C. Sagui; C. Roland. Calculating relative transition rates with driven nonequilibrium simulations. *Chem. Phys. Lett.*, **2011**, *518*, 109.

[176] M. Moradi; C. Sagui; C. Roland. Investigating rare events with nonequilibrium work measurements: I. Nonequilibrium transition paths. *J. Chem. Phys.*, **2014**, *140*, 034114.

[177] M. Moradi; C. Sagui; C. Roland. Investigating rare events with nonequilibrium work measurements: II. Transition and reaction rates. *J. Chem. Phys.*, **2014**, *140*, 034115.

[178] M. Moradi; E. Tajkorshid. Driven Metadynamics: Reconstructing equilibrium free energies from driven adaptive-bias simulations. *J. Phys. Chem. Lett.*, **2013**, *4*, 1882.

[179] A. C. Pan; D. Sezer; B. Roux. Finding transition pathways using the string method with swarms of trajectories. *J. Phys. Chem. B*, **2008**, *112*, 3432–3440.

[180] A. Barducci and G. Bussi and M. Parrinello. Well-tempered metadynamics: a smoothly converging and tunable free energy method. *Phys. Rev. Lett.*, **2008**, *100*, 020603.

[181] K. Minoukadeh and Ch. Chipot and T. Lelievre. Potential of Mean Force Calculations: A multiple-walker adaptive biasing force technique. *J. Chem. Theor. and Comput.*, **2010**, *6*, 1008.

[182] E. A. Coutsias; C. Seok; K. A. Dill. Using quaternions to calculate RMSD. *J. Comput. Chem.*, **2004**, *25*, 1849–1857.

[183] D. K. Coutsias EA, Seok C. Using quaternions to calculate rmsd. *J Comput Chem*, **2004 Nov 30**, *25*, 1849–57.

[184] G. Fiorin; M. L. Klein; J. Hénin. Using collective variables to drive molecular dynamics simulations. *Molecular Physics*, **2013**, *111*, 3345–3362.

[185] M. Moradi; E. Tajkhorshid. Mechanistic picture for conformational transition of a membrane transporter at atomic resolution. *Proc. Natl. Acad. Sci. U.S.A.*, **2013**, *110*, 18916–18921.

[186] M. Moradi; E. Tajkhorshid. Computational Recipe for Efficient Description of Large-Scale Conformational Changes in Biomolecular Systems. *J Chem Theory Comput*, **2014**, *10*, 2866–2880.

[187] S. Park; F. Khalili-Araghi; E. Tajkhorshid; K. Schulten. Free energy calculation from steered molecular dynamics simulations using Jarzynski's equality. *J. Chem. Phys.*, **2003**, *119*, 3559–3566.

[188] M. Matsumoto; T. Nishimura. Mersenne twister: a 623-dimensionally equidistributed uniform pseudo-random number generator. *ACM Trans. Model. Comput. Simul.*, **1998**, *8*, 3–30.

[189] L. Maragliano; A. Fischer; E. Vanden-Eijnden; G. Ciccotti. String method in collective variables: Minimum free energy paths and isocommittor surfaces. *J. Chem. Phys.*, **2006**, *125*, 024106.

[190] B. M. Duggan; G. B. Legge; H. J. Dyson; P. E. Wright. SANE (Structure Assisted NOE Evaluation): An automated model-based approach for NOE assignment. *J. Biomol. NMR*, **2001**, *19*, 321–329.

[191] A. Kalk; H. J. C. Berendsen. Proton magnetic relaxation and spin diffusion in proteins. *J. Magn. Reson.*, **1976**, *24*, 343–366.

[192] E. T. Olejniczak; M. A. Weiss. Are methyl groups relaxation sinks in small proteins? *J. Magn. Reson.*, **1990**, *86*, 148–155.

[193] K. J. Cross; P. E. Wright. Calibration of ring-current models for the heme ring. *J. Magn. Reson.*, **1985**, *64*, 220–231.

[194] K. Ösapay; D. A. Case. A new analysis of proton chemical shifts in proteins. *J. Am. Chem. Soc.*, **1991**, *113*, 9436–9444.

[195] D. A. Case. Calibration of ring-current effects in proteins and nucleic acids. *J. Biomol. NMR*, **1995**, *6*, 341–346.

[196] L. Banci; I. Bertini; G. Gori-Savellini; A. Romagnoli; P. Turano; M. A. Cremonini; C. Luchinat; H. B. Gray. Pseudocontact shifts as constraints for energy minimization and molecular dynamics calculations on solution structures of paramagnetic metalloproteins. *Proteins*, **1997**, *29*, 68.

[197] C. R. Sanders, II; B. J. Hare; K. P. Howard; J. H. Prestegard. Magnetically-oriented phospholipid micelles as a tool for the study of membrane-associated molecules. *Prog. NMR Spectr.*, **1994**, *26*, 421–444.

[198] V. Tsui; L. Zhu; T. H. Huang; P. E. Wright; D. A. Case. Assessment of zinc finger orientations by residual dipolar coupling constants. *J. Biomol. NMR*, **2000**, *16*, 9–21.

[199] D. A. Case. Calculations of NMR dipolar coupling strengths in model peptides. *J. Biomol. NMR*, **1999**, *15*, 95–102.

[200] G. P. Gippert; P. F. Yip; P. E. Wright; D. A. Case. Computational methods for determining protein structures from NMR data. *Biochem. Pharm.*, **1990**, *40*, 15–22.

[201] D. A. Case; P. E. Wright. in *NMR in Proteins*, G. M. Clore; A. Gronenborn, Eds., pp 53–91. MacMillan, New York, 1993.

[202] D. A. Case; H. J. Dyson; P. E. Wright. Use of chemical shifts and coupling constants in nuclear magnetic resonance structural studies on peptides and proteins. *Meth. Enzymol.*, **1994**, *239*, 392–416.

[203] R. Brüschweiler; D. A. Case. Characterization of biomolecular structure and dynamics by NMR cross-relaxation. *Prog. NMR Spectr.*, **1994**, *26*, 27–58.

[204] D. A. Case. The use of chemical shifts and their anisotropies in biomolecular structure determination. *Curr. Opin. Struct. Biol.*, **1998**, *8*, 624–630.

[205] A. E. Torda; R. M. Scheek; W. F. VanGunsteren. Time-dependent distance restraints in molecular dynamics simulations. *Chem. Phys. Lett.*, **1989**, *157*, 289–294.

[206] D. A. Pearlman; P. A. Kollman. Are time-averaged restraints necessary for nuclear magnetic resonance refinement? A model study for DNA. *J. Mol. Biol.*, **1991**, *220*, 457–479.

[207] A. E. Torda; R. M. Brunne; T. Huber; H. Kessler; W. F. van Gunsteren. Structure refinement using time-averaged J-coupling constant restraints. *J. Biomol. NMR*, **1993**, *3*, 55–66.

[208] D. A. Pearlman. How well to time-averaged J-coupling restraints work? *J. Biomol. NMR*, **1994**, *4*, 279–299.

[209] D. A. Pearlman. How is an NMR structure best defined? An analysis of molecular dynamics distance-based approaches. *J. Biomol. NMR*, **1994**, *4*, 1–16.

[210] X. Wu; J. L. Milne; M. J. Borgnia; A. V. Rostapshov; S. Subramaniam; B. R. Brooks. A core-weighted fitting method for docking atomic structures into low-resolution maps: application to cryo-electron microscopy. *J Struct Biol*, **2003**, *141*, 63–76.

[211] J. L. Milne; X. Wu; M. J. Borgnia; J. S. Lengyel; B. R. Brooks; D. Shi; R. N. Perham; S. Subramaniam. Molecular structure of a 9-MDa icosahedral pyruvate dehydrogenase subcomplex containing the E2 and E3 enzymes using cryoelectron microscopy. *J Biol Chem*, **2006**, *281*, 4364–70.

[212] X. Wu; B. R. Brooks. Modeling of Macromolecular assemblies with map objects. *Proc. 2007 Int. Conf. Bioinform. Comput. Biol.*, **2007**, *II*, 411–417.

[213] C. M. Khursigara; X. Wu; P. Zhang; J. Lefman; S. Subramaniam. Role of HAMP domains in chemotaxis signaling by bacterial chemoreceptors. *PNAS*, **2008**, *105*, 16555–60.

[214] J. S. Lengyel; K. M. Stott; X. Wu; A. Brooks, B. R.and Balbo; P. Schuck; R. N. Perham; S. Subramaniam; J. L. Milne. Extended polypeptide linkers establish the spatial architecture of a pyruvate dehydrogenase multienzyme complex. *Structure*, **2008**, *16*, 93–103.

[215] C. M. Khursigara; X. Wu; ; S. Subramaniam. Chemoreceptors in Caulobacter crescentus: trimers of receptor dimers in a partially ordered hexagonally packed array. *J Bacteriol*, **2008**, *190*, 6805–10.

[216] J. Elegheert; A. Desfosses; A. V. Shkumatov; X. Wu; N. Bracke; K. Verstraete; K. Van Craenenbroeck; B. R. Brooks; D. I. Svergun; B. Vergauwen; I. Gutsche; S. N. Savvides. Extracellular complexes of the hematopoietic human and mouse CSF-1 receptor are driven by common assembly principles . *Structure*, **2011**, *19*, 1762–72.

[217] C. M. Khursigara; G. Lan; S. Neumann; X. Wu; S. Ravindran; M. J. Borgnia; V. Sourjik; J. Milne; Y. Tu; S. Subramaniam. Lateral density of receptor arrays in the membrane plane influences sensitivity of the E. coli chemotaxis response. *Embo J*, **2011**, *30*, 1719–29.

[218] X. Wu; B. R. Brooks. in *Microscopy: advances in scientific research and education*, A. Mendez-Vilas, Ed., pp 39–47. Formatex Research Center, Spain, 2014.

[219] X. Wu; B. R. Brooks. in *Modern electron microscopy in physical and life science*, M. Janecek, Ed., chapter 12, pp 243–262. InTech, 2016.

[220] A. Bartesaghi; A. Merk; S. Banerjee; D. Matthies; X. Wu; J. L. S. Milne; S. Subramaniam. 2.2 a resolution cryo-em structure of beta-galactosidase in complex with a cell-permeant inhibitor. *Science*, **2015**, *348*, 1147–1151.

[221] D. S. Cerutti; D. A. Case. Molecular dynamics simulations of macromolecular crystals. *Wires Comput. Mol. Sci.*, **2018**, *8*, e1402.

[222] P. A. Janowski; D. S. Cerutti; J. M. Holton; D. A. Case. Peptide crystal simulations reveal hidden dynamics. *J. Am. Chem. Soc.*, **2013**, *135*, 7938–7948.

[223] N. Moriarty; P. Janowski; J. Swails; H. Nguyen; J. Richardson; D. Case; P. Adams. Improved chemistry restraints for crystallographic refinement by integrating the Amber force field into Phenix. *Acta Cryst. D*, **2020**, *76*, 51–62.

[224] P. Afonine; A. Urzhumtsev. On a fast calculation of structure factors at a subatomic resolution. *Acta Cryst. A*, **2004**, *60*, 19–32.

[225] J. Jiang; A. Brünger. Protein hydration observed by X-ray diffraction: solvation properties of penicillopepsin and neuraminidase crystal structures. *J. Mol. Biol.*, **1994**, *243*, 100–115.

[226] A. Fokine; A. Urzhumtsev. Flat bulk-solvent model: obtaining optimal parameters. *Acta Cryst. D*, **2002**, *58*, 1387–1392.

[227] R. Grosse-Kunstleve; N. Sauter; N. Moriarty; P. Adams. The Computational Crystallography Toolbox: crystallographic algorithms in a reusable software framework. *J. Appl. Crystallogr.*, **2002**, *35*, 126–136.

[228] P. Afonine; R. Grosse-Kunstleve; P. Adams; A. Urzhumtsev. Bulk-solvent and overall scaling revisited: faster calculations, improved results. *Acta Cryst. D*, **2013**, *69*, 625–634.

[229] V. Lunin; T. Skovoroda. R-free likelihood-based estimates of errors for phases calculated from atomic models. *Acta Cryst. A*, **1995**, *51*, 880–887.

[230] P. V. Afonine; R. W. Grosse-Kunstleve; P. D. Adams. A robust bulk-solvent correction and anisotropic scaling procedure. *Acta Cryst. D*, **2005**, *61*, 850–855.

[231] Y. Xue; N. Skrynnikov. Ensemble MD simulations restrained via crystallographic data: accurate structure leads to accurate dynamics. *Prot. Sci.*, **2014**, *23*, 488–507.

[232] A. Raval; S. Piana; M. Eastwood; R. Dror; D. Shaw. Refinement of protein structure homology models via long, all-atom molecular dynamics simulations. *Proteins*, **2012**, *80*, 2071–2079.

[233] O. Mikhailovskii; Y. Xue; N. R. Skrynnikov. Modeling a unit cell: crystallographic refinement procedure using the biomolecular MD simulation platform *Amber*. *IUCrJ*, **2022**, *9*, 114–133.

[234] J. Schmit; N. Kariyawasam; V. Needham; P. Smith. SLTCAP: A Simple Method for Calculating the Number of Ions Needed for MD Simulation. *J. Chem. Theory Comput.*, **2018**, *14*, 1823–1827.

[235] M. Machado; S. Pantano. Split the Charge Difference in Two! A Rule of Thumb for Adding Proper Amounts of Ions in MD Simulations. *J. Chem. Theory Comput.*, **2020**, *16*, 1367–1372.

[236] J. Wang; R. M. Wolf; J. W. Caldwell; P. A. Kollamn; D. A. Case. Development and testing of a general Amber force field. *J. Comput. Chem.*, **2004**, *25*, 1157–1174.

[237] J. Wang; W. Wang; P. A. Kollman; D. A. Case. Automatic atom type and bond type perception in molecular mechanical. *J. Mol. Graphics Model.*, **2006**, *25*, 247–260.

[238] A. Jakalian; B. L. Bush; D. B. Jack; C. I. Bayly. Fast, efficient generation of high-quality atomic charges. AM1-BCC model: I. Method. *J. Comput. Chem.*, **2000**, *21*, 132–146.

[239] A. Jakalian; D. B. Jack; C. I. Bayly. Fast, efficient generation of high-quality atomic charges. AM1-BCC model: II. Parameterization and Validation. *J. Comput. Chem.*, **2002**, *23*, 1623–1641.

[240] X. He; V. H. Man; W. Wang; T. S. Lee; J. Wang. A fast and high-quality charge model for the next generation general AMBER force field. *J. Chem. Phys.*, **2020**, *153*, 114502.

[241] Y. Sun; X. He; T. Hou; L. Cai; V. H. Man; J. Wang. Development and test of highly accurate endpoint free energy methods. 1: Evaluation of ABCG2 charge model on solvation free energy prediction and optimization of atom radii suitable for more accurate solvationÂ freeÂ energy prediction by the PBSA method. *J Comput Chem*, **2023**, *44*, 1334–1346.

[242] C. I. Bayly; P. Cieplak; W. D. Cornell; P. A. Kollman. A well-Behaved electrostatic potential based method using charge restraints for determining atom-centered charges: The RESP model. *J. Phys. Chem.*, **1993**, *97*, 10269–10280.

[243] J. Wang; P. A. Kollman. Automatic parameterization of force field by systematic search and genetic algorithms. *J. Comput. Chem.*, **2001**, *22*, 1219–1228.

[244] A. P. Graves; D. M. Shivakumar; S. E. Boyce; M. P. Jacobson; D. A. Case; B. K. Shoichet. Rescoring docking hit lists for model cavity sites: Predictions and experimental testing. *J. Mol. Biol.*, **2008**, *377*, 914–934.

[245] B. Jojart; T. A. Martinek. Performance of the general amber force field in modeling aqueous POPC membrane bilayers. *J. Comput. Chem.*, **2007**, *28*, 2051–2058.

[246] L. Rosso; I. R. Gould. Structure and dynamics of phospholipid bilayers using recently developed general all-atom force fields. *J. Comput. Chem.*, **2008**, *29*, 24–37.

[247] J. Wang; T. Hou. Application of Molecular Dynamics Simulations in Molecular Property Prediction. 1. Density and Heat of Vaporization. *J. Chem. Theory Comput.*, **2011**, *7*, 2151–2165.

[248] X. He; B. Walker; W. H. Man; P. Ren; J. Wang. Recent progress in general force fields of small molecules. *Curr. Opin. Struc. Biol.*, **2022**, *72*, 187–193.

[249] J. I. Mendieta-Moreno; R. C. Walker; J. P. Lewis; P. Gómez-Puertas; J. Mendieta; J. Ortega. FIREBALL/AMBER: An efficient local-orbital DFT QM/MM method for biomolecular systems. *J. Chem. Theory Comput.*, **2014**, *10*, 2185–2193.

[250] J. P. Lewis; P. Jelínek; J. Ortega; A. A. Demkov; D. G. Trabada; B. Haycock; H. Wang; G. Adams; J. K. Tomfohr; E. Abad; H. Wang; D. A. Drabold. Advances and applications in the FIREBALL ab initio tight-binding molecular-dynamics formalism. *Phys. Status Solidi B*, **2011**, *248*, 1989–2007.

[251] M. Kállay; Z. Rolik; J. Csontos; I. Ladjánszki; L. Szegedy; B. Ladóczki; G. Samu; K. Petrov; M. Farkas; P. Nagy; D. Mester; B. Hegely. Mrcc, a quantum chemical program suite. www.mrcc.hu.

[252] S. N. Steinmann; R. Ferreira de Morais; A. W. Götz; P. Fleurat-Lessard; M. Iannuzzi; P. Sautet; C. Michel. *J. Chem. Theory Comput.*, **2018**.

[253] S. N. Steinmann; P. Fleurat-Lessard; A. W. Götz; C. Michel; R. Ferreira de Morais; P. Sautet. Molecular mechanics models for the image charge, a comment on "including image charge effects in the molecular dynamics simulations of molecules on metal surfaces". *J. Comput. Chem.*, **2017**, *38*, 2127–2129.

[254] Z. Rolik; L. Szegedy; I. Ladjánszki; B. Ladóczki; M. Kállay. An efficient linear-scaling CCSD(T) method based on local natural orbitals. *J. Chem. Phys.*, **2013**, *139*, 094105.

[255] B. Hégely; P. R. Nagy; G. G. Ferenczy; M. Kállay. Exact density functional and wave function embedding schemes based on orbital localization. *J. Chem. Phys.*, **2016**, *145*, 064107.

[256] Å. Skjevik; B. D. Madej; C. J. Dickson; C. Lin; K. Teigen; R. C. Walker; I. R. Gould. Simulations of lipid bilayer self-assembly using all-atom lipid force fields. *Phys. Chem. Chem. Phys.*, **2016**, *18*, 10573–10584.

[257] Å. Skjevik; B. D. Madej; C. J. Dickson; K. Teigen; R. C. Walker; I. R. Gould. All-atom lipid bilayer self-assembly with the amber and charmm lipid force fields. *Chem. Commun.*, **2015**, *51*, 4402–4405.

[258] H. T. Nguyen; S. A. Pabit; S. P. Meisburger; L. Pollack; D. A. Case. Accurate small and wide angle X-ray scattering profiles from atomic models of proteins and nucleic acids. *J. Chem. Phys.*, **2014**, *141*, 22D508.

[259] S. Park; J. P. Bardhan; B. Roux; L. Makowski. Simulated X-ray scattering of protein solutions using explicit-solvent models. *J. Chem. Phys.*, **2009**, *130*, 134114.

[260] Y. Shao; L. Fusti-Molnar; Y. Jung; J. Kussmann; C. Ochsenfeld; S. T. Brown; A. T. B. Gilbert; L. V. Slipchenko; S. V. Levchenko; D. P. O'Neill; R. A. DiStasio, Jr.; R. C. Lochan; T. Wang; G. J. O. Beran; N. A. Besley; J. M. Herbert; C. Y. Lin; T. V. Voorhis; S. H. Chien; A. Sodt; R. P. Steele; V. A. Rassolov; P. E. Maslen; P. P. Korambath; R. D. Adamson; B. Austin; J. Baker; E. F. C. Byrd; H. Daschel; R. J. Doerksen; A. Dreuw; B. D. Dunietz; A. D. Dutoi; T. R. Furlani; S. R. Gwaltney; A. Heyden; S. Hirata; C.-P. Hsu; G. Kedziora; R. Z. Khaliullin; P. Klunzinger; A. M. Lee; M. S. Lee; W. Liang; I. Lotan; N. Nair; B. Peters; E. I. Proynov; P. A. Pieniazek; Y. M. Rhee; J. Ritchie; E. Rosta; C. D. Sherrill; A. C. Simmonett; J. E. Subotnik; H. L. Woodcock, III; W. Zhang; A. T. Bell; A. K. Chakraborty; D. M. Chipman; F. J. Keil; A. Warshel; W. J. Hehre; H. F. Schaefer, III; J. Kong; A. I. Krylov; P. M. W. Gill; M. Head-Gordon. Advances in methods and algorithms in a modern quantum chemistry program package. *Phys. Chem. Chem. Phys.*, **2006**, *8*, 3172–3191.

[261] R. Assaraf; M. Caffarel; A. C. Kollias. Chaotic versus nonchaotic stochastic dynamics in monte carlo simulations: A route for accurate energy differences in n-body systems. *Phys. Rev. Lett.*, **2011**, *106*, 150601.

[262] K. Park; A. W. Götz; R. C. Walker; F. Paesani. Application of adaptive qm/mm methods to molecular dynamics simulations of aqueous systems. *J. Chem. Theory Comput.*, **2012**, *8*, 2868–2877.

[263] R. E. Bulo; C. Michel; P. Fleurat-Lessard; P. Sautet. Multiscale modeling of chemistry in water: Are we there yet? *J. Chem. Theory Comput.*, **2013**, *9*, 5567–5577.

[264] R. E. Bulo; B. Ensing; J. Sikkema; L. Visscher. Toward a practical method for adaptive qm/mm simulations. *J. Chem. Theory Comput.*, **2009**, *9*, 2212–2221.

[265] A. W. Götz; M. A. Clark; R. C. Walker. An extensible interface for QM/MM molecular dynamics simulations with AMBER. *J. Comput. Chem.*, **2014**, *35*, 95–108.

[266] B. E. Hingerty; S. Figueroa; T. L. Hayden; S. Broyde. Prediction of DNA Structure from Sequence: A Build-up Technique. *Biopolymers*, **1989**, *28*, 1195–1222.

[267] D. A. Erie; K. J. Breslauer; W. K. Olson. A Monte Carlo Method for Generating Structures of Short Single-Stranded DNA Sequences. *Biopolymers*, **1993**, *33*, 75–105.

[268] D. A. Pearlman; S.-H. Kim. Conformational Studies of Nucleic Acids I. A Rapid and Direct Method for Generating Coordinates from the Pseudorotation Angle. *J. Biomol. Struct. Dyn.*, **1985**, *3*, 85–98.

[269] D. A. Pearlman; S.-H. Kim. Conformational Studies of Nucleic Acids II. The Conformational Energetics of Commonly Occurring Nucleosides. *J. Biomol. Struct. Dyn.*, **1985**, *3*, 99–125.

[270] D. A. Pearlman; S.-H. Kim. Conformational Studies of Nucleic Acids: III. Empirical Multiple Correlation Functions for Nucleic Acid Torsion Angles. *J. Biomol. Struct. Dyn.*, **1986**, *4*, 49–67.

[271] D. A. Pearlman; S.-H. Kim. Conformational Studies of Nucleic Acids: IV. The Conformational Energetics of Oligonucleotides: d(ApApApA) and ApApApA. *J. Biomol. Struct. Dyn.*, **1986**, *4*, 69–98.

[272] D. A. Pearlman; S.-H. Kim. Conformational Studies of Nueleic Acids. V. Sequence Specificities of in the Conformational Energetics of Oligonucleotides: The Homo-Tetramers. *Biopolymers*, **1988**, *27*, 59–77.

[273] T. Schlick. A Modular Strategy for Generating Starting Conformations and Data Structures of Polynucleotide Helices for Potential Energy Calculations. *J. Comput. Chem.*, **1988**, *9*, 861–889.

[274] J. Gabarro-Arpa; J. A. H. Cognet; M. Le Bret. Object Command Language: a formalism to build molecule models and to analyze structural parameters in macromolecules, with applications to nucleic acids. *J. Mol. Graph.*, **1992**, *10*, 166–173.

[275] R. Lavery. in *Unusual DNA Structures*, R. D. Wells; S. C. Harvey, Eds. Springer-Verlag, New York, 1988.

[276] L. Shen; I. Tinoco. The Structure of an RNA Pseudoknot that Causes Efficient Frameshift in Mouse Mammary Tumor Virus. *J. Mol. Biol.*, **1995**, *247*, 963–978.

[277] J. M. Hubbard; J. E. Hearst. Predicting the Three-Dimensional Folding of Transfer RNA with a Computer Modeling Protocol. *Biochemistry*, **1991**, *30*, 5458–5465.

[278] S.-H. Chou; L. Zhu; B. R. Reid. The Unusual Structure of the Human Centromere (GGA)2 Motif. *J. Mol. Biol.*, **1994**, *244*, 259–268.

[279] M. Levitt. Detailed Molecular Model for Transfer Ribonucleic Acid. *Nature*, **1969**, *224*, 759–763.

[280] M. S. Babcock; E. P. D. Pednault; W. K. Olson. Nucleic Acid Structure Analysis. *J. Mol. Biol.*, **1994**, *237*, 125–156.

[281] J. M. Hubbard; J. E. Hearst. Computer Modeling 16S Ribosomal RNA. *J. Mol. Biol.*, **1991**, *221*, 889–907.

[282] F. Major; M. Turcotte; D. Gautheret; G. Lapalme; E. Fillon; R. Cedergren. The Combination of Symbolic and Numerical Computation for Three-Dimensional Modeling of RNA. *Science*, **1991**, *253*, 1255–1260.

[283] T. Schlick; W. K. Olson. Supercoiled DNA Energetics and Dynamics by Computer Simulation. *J. Mol. Biol.*, **1992**, *223*, 1089–1119.

[284] R. E. Dickerson. Definitions and Nomenclature of Nucleic Acid Structure Parameters. *J. Biomol. Struct. Dyn.*, **1989**, *6*, 627–634.

[285] S. R. Holbrook; J. L. Sussman; R. W. Warrant; S.-H. Kim. Crystal Structure of Yeast Phenylalanine Transfer RNA II. Structural Features and and Functional Implications. *J. Mol. Biol.*, **1978**, *123*, 631–660.

[286] B. N. Conner; C. Yoon; J. Dickerson; R. E. Dickerson. Helix Geometry and Hydration in an A-DNA Tetramer: C-C-G-G. *J. Mol. Biol.*, **1984**, *174*, 663–695.

[287] M. Le Bret; J. Gabarro-Arpa; J. C. Gilbert; C. Lemarechal. MORCAD an object-oriented molecular modeling package. *J. Chim. Phys.*, **1991**, *88*, 2489–2496.

[288] V. B. Zhurkin; Y. P. Lysov; V. I. Ivanov. Different Families of Double Stranded Conformations of DNA as Revealed by Computer Calculations. *Biopolymers*, **1978**, *17*, 277–312.

[289] A. T. Brünger. *X-PLOR: A System for Crystallography and NMR, Version 3.1*. Yale University, New Haven, CT, 1992.

[290] J. R. Wyatt; J. D. Puglisi; I. Tinoco Jr. RNA Pseudoknots. Stability and Loop Size Requirements. *J. Mol. Biol.*, **1990**, *214*, 455–470.

[291] J. D. Puglisi; J. R. Wyatt; I. Tinoco Jr. Conformation of an RNA Pseudoknot. *J. Mol. Biol.*, **1990**, *214*, 437–453.

[292] G. Kuila; J. A. Fee; J. R. Schoonover; W. H. Woodruff. Resonance Raman Spectra of the [2Fe-2S] Clusters of the Rieske Protein from Thermus and Phthalate Dioxygenase from Pseudomonas. *J. Am. Chem. Soc.*, **1987**, *109*, 1559–1561.

[293] B. Lewin. in *Genes IV*, pp 409–425. Cell Press, Cambridge, Mass., 1990.

[294] W. H. Press; S. A. Teukolsky; W. T. Vettering; B. P. Flannery. in *Numerical Recipes in C*, pp 113–117. Cambridge, New York, 1992.

[295] V. B. Zhurkin; G. Raghunathan; N. B. Ulynaov; R. D. Camerini-Otero; R. L. Jernigan. A Parallel DNA Triplex as a Model for the Intermediate in Homologous Recombination. *J. Mol. Biol.*, **1994**, *239*, 181–200.

[296] W. Saenger. in *Principles of Nucleic Acid Structure*, p 120. Springer-Verlag, New York, 1984.

[297] M. Turcotte; G. Lapalme; F. Major. Exploring the conformations of nucleic acids. *J. Funct. Program.*, **1995**, *5*, 443–460.

[298] C.-S. Tung; E. S. Carter, II. Nucleic acid modeling tool (NAMOT): an interactive graphic tool for modeling nucleic acid structures. *CABIOS*, **1994**, *10*, 427–433.

[299] E. S. Carter, II; C.-S. Tung. NAMOT2–a redesigned nucleic acid modeling tool: construction of non-canonical DNA structures. *CABIOS*, **1996**, *12*, 25–30.

[300] R. Lavery; K. Zakrzewska; H. Skelnar. JUMNA (junction minimisation of nucleic acids). *Comp. Phys. Commun.*, **1995**, *91*, 135–158.

[301] G. M. Crippen; T. F. Havel. *Distance Geometry and Molecular Conformation*. Research Studies Press, Taunton, England, 1988.

[302] D. C. Spellmeyer; A. K. Wong; M. J. Bower; J. M. Blaney. Conformational analysis using distance geometry methods. *J. Mol. Graph. Model.*, **1997**, *15*, 18–36.

[303] M. E. Hodsdon; J. W. Ponder; D. P. Cistola. The NMR solution structure of intestinal fatty acid-binding protein complexed with palmitate: Application of a novel distance geometry algorithm. *J. Mol. Biol.*, **1996**, *264*, 585–602.

[304] T. Macke; S.-M. Chen; W. J. Chazin. in *Structure and Function, Volume 1: Nucleic Acids*, R. H. Sarma; M. H. Sarma, Eds., pp 213–227. Adenine Press, Albany, 1992.

[305] B. C. M. Potts; J. Smith; M. Akke; T. J. Macke; K. Okazaki; H. Hidaka; D. A. Case; W. J. Chazin. The structure of calcyclin reveals a novel homodimeric fold S100 Ca^{2+}-binding proteins. *Nature Struct. Biol.*, **1995**, *2*, 790–796.

[306] J. J. Love; X. Li; D. A. Case; K. Giese; R. Grosschedl; P. E. Wright. DNA recognition and bending by the architectural transcription factor LEF-1: NMR structure of the HMG domain complexed with DNA. *Nature*, **1995**, *376*, 791–795.

[307] R. J. Gurbiel; P. E. Doan; G. T. Gassner; T. J. Macke; D. A. Case; T. Ohnishi; J. A. Fee; D. P. Ballou; B. M. Hoffman. Active site structure of Rieske-type proteins: Electron nuclear double resonance studies of isotopically labeled phthalate dioxygenase from *Pseudomonas cepacia and Rieske protein from Rhodobacter capsulatus* and molecular modeling studies of a Rieske center. *Biochemistry*, **1996**, *35*, 7834–7845.

[308] T. J. Macke. *NAB, a Language for Molecular Manipulation*. Ph.D. thesis, The Scripps Research Institute, 1996.

[309] D. Gautheret; F. Major; R. Cedergren. Modeling the three-dimensional structure of RNA using discrete nucleotide conformational sets. *J. Mol. Biol.*, **1993**, *229*, 1049–1064.

[310] R. Tan; S. Harvey. Molecular Mechanics Model of Supercoiled DNA. *J. Mol. Biol.*, **1989**, *205*, 573–591.

[311] T. F. Havel. An evaluation of computational strategies for use in the determination of protein structure from distance constraints obtained by nuclear magnetic resonance. *Prog. Biophys. Mol. Biol.*, **1991**, *56*, 43–78.

[312] J. Kuszewski; M. Nilges; A. T. Brünger. Sampling and efficiency of metric matrix distance geometry: A novel partial metrization algorithm. *J. Biomolec. NMR*, **1992**, *2*, 33–56.

[313] B. L. deGroot; D. M. F. van Aalten; R. M. Scheek; A. Amadei; G. Vriend; H. J. C. Berendsen. Prediction of protein conformational freedom from distance constraints. *Proteins*, **1997**, *29*, 240–251.

[314] T. F. Havel; I. D. Kuntz; G. M. Crippen. The theory and practice of distance geometry. *Bull. Math. Biol.*, **1983**, *45*, 665–720.

[315] D. K. Agrafiotis. Stochastic Proximity Embedding. *J. Comput. Chem.*, **2003**, *24*, 1215–1221.

[316] H. J. C. Berendsen; J. P. M. Postma; W. F. van Gunsteren; A. DiNola; J. R. Haak. Molecular dynamics with coupling to an external bath. *J. Chem. Phys.*, **1984**, *81*, 3684–3690.

[317] C. Brooks; A. Brünger; M. Karplus. Active site dynamics in protein molecules: A stochastic boundary molecular-dynamics approach. *Biopolymers*, **1985**, *24*, 843–865.

[318] D. T. Nguyen; D. A. Case. On finding stationary states on large-molecule potential energy surfaces. *J. Phys. Chem.*, **1985**, *89*, 4020–4026.

[319] D. A. Pearlman; D. A. Case; J. W. Caldwell; W. S. Ross; T. E. Cheatham, III; S. DeBolt; D. Ferguson; G. Seibel; P. Kollman. AMBER, a package of computer programs for applying molecular mechanics, normal mode analysis, molecular dynamics and free energy calculations to simulate the structural and energetic properties of molecules. *Comp. Phys. Commun.*, **1995**, *91*, 1–41.

[320] S. Harvey; J. A. McCammon. *Dynamics of Proteins and Nucleic Acids*. Cambridge University Press, Cambridge, 1987.

[321] M. P. Allen; D. J. Tildesley. *Computer Simulation of Liquids*. Clarendon Press, Oxford, 1987.

[322] W. F. van Gunsteren; P. K. Weiner; A. J. Wilkinson, eds. *Computer Simulations of Biomolecular Systems, Vol. 3*. ESCOM Science Publishers, Leiden, 1997.

[323] W. F. van Gunsteren; P. K. Weiner; A. J. Wilkinson, eds. *Computer Simulations of Biomolecular Systems, Vol. 2*. ESCOM Science Publishers, Leiden, 1993.

[324] L. R. Pratt; G. Hummer, eds. *Simulation and Theory of Electrostatic Interactions in Solution*. American Institute of Physics, Melville, NY, 1999.

[325] J. Wang; P. Cieplak; P. A. Kollman. How well does a restrained electrostatic potential (RESP) model perform in calculating conformational energies of organic and biological molecules? *J. Comput. Chem.*, **2000**, *21*, 1049–1074.

[326] R. W. Dixon; P. A. Kollman. Advancing beyond the atom-centered model in additive and nonadditive molecular mechanics. *J. Comput. Chem.*, **1997**, *18*, 1632–1646.

[327] W. D. Cornell; P. Cieplak; C. I. Bayly; I. R. Gould; K. M. Merz, Jr.; D. M. Ferguson; D. C. Spellmeyer; T. Fox; J. W. Caldwell; P. A. Kollman. A second generation force field for the simulation of proteins, nucleic acids, and organic molecules. *J. Am. Chem. Soc.*, **1995**, *117*, 5179–5197.

[328] M. D. Beachy; R. A. Friesner. Accurate ab intio quantum chemical determination of the relative energies of peptide conformations and assessment of empirical force fields. *J. Am. Chem. Soc.*, **1997**, *119*, 5908–5920.

[329] P. A. Kollman; R. Dixon; W. Cornell; T. Fox; C. Chipot; A. Pohorille. in *Computer Simulation of Biomolecular Systems, Vol. 3*, A. Wilkinson; P. Weiner; W. F. van Gunsteren, Eds., pp 83–96. Elsevier, 1997.

[330] J. Higo; N. Ito; M. Kuroda; S. Ono; N. Nakajima; H. Nakamura. Energy landscape of a peptide consisting of α-helix, 3_{10} helix, β-turn, β-hairpin and other disordered conformations. *Prot. Sci.*, **2001**, *10*, 1160–1171.

[331] L. Wang; Y. Duan; R. Shortle; B. Imperiali; P. A. Kollman. Study of the stability and unfolding mechanism of BBA1 by molecular dynamics simulations at different temperatures. *Prot. Sci.*, **1999**, *8*, 1292–1304.

[332] T. E. Cheatham, III; P. Cieplak; P. A. Kollman. A modified version of the Cornell et al. force field with improved sugar pucker phases and helical repeat. *J. Biomol. Struct. Dyn.*, **1999**, *16*, 845–862.

[333] S. J. Weiner; P. A. Kollman; D. A. Case; U. C. Singh; C. Ghio; G. Alagona; S. Profeta, Jr.; P. Weiner. A new force field for molecular mechanical simulation of nucleic acids and proteins. *J. Am. Chem. Soc.*, **1984**, *106*, 765–784.

[334] S. J. Weiner; P. A. Kollman; D. T. Nguyen; D. A. Case. An all-atom force field for simulations of proteins and nucleic acids. *J. Comput. Chem.*, **1986**, *7*, 230–252.

[335] J. Åqvist. Ion-water interaction potentials derived from free energy perturbation simulations. *J. Phys. Chem.*, **1990**, *94*, 8021–8024.

[336] J. Åqvist; A. Warshel. Computer simulation of the initial proton-transfer step in human carbonic anhydrase-I. *J. Mol. Biol.*, **1992**, *224*, 7–14.

[337] W. L. Jorgensen; J. Chandrasekhar; J. Madura; M. L. Klein. Comparison of simple potential functions for simulating liquid water. *J. Chem. Phys.*, **1983**, *79*, 926–935.

[338] W. L. Jorgensen; J. D. Madura. Temperature and size dependence for Monte Carlo simulations of TIP4P water. *Mol. Phys.*, **1985**, *56*, 1381–1392.

[339] M. W. Mahoney; W. L. Jorgensen. A five-site model for liquid water and the reproduction of the density anomaly by rigid, nonpolarizable potential functions. *J. Chem. Phys.*, **2000**, *112*, 8910–8922.

[340] H. J. C. Berendsen; J. R. Grigera; T. P. Straatsma. The missing term in effective pair potentials. *J. Phys. Chem.*, **1987**, *91*, 6269–6271.

[341] H. J. C. Berendsen; J. P. M. Postma; W. F. van Gunsteren; A. DiNola; J. R. Haak. Molecular dynamics with coupling to an external bath. *J. Chem. Phys.*, **1984**, *81*, 3684–3690.

[342] D. S. Wishart; D. A. Case. Use of chemical shifts in macromolecular structure determination. *Meth. Enzymol.*, **2001**, *338*, 3–34.

[343] J. W. Caldwell; P. A. Kollman. Structure and properties of neat liquids using nonadditive molecular dynamics: Water, methanol and N-methylacetamide. *J. Phys. Chem.*, **1995**, *99*, 6208–6219.

[344] B. Honig; A. Nicholls. Classical electrostatics in biology and chemistry. *Science*, **1995**, *268*, 1144–1149.

[345] J. Srinivasan; T. E. Cheatham, III; P. Cieplak; P. Kollman; D. A. Case. Continuum solvent studies of the stability of DNA, RNA, and phosphoramidate–DNA helices. *J. Am. Chem. Soc.*, **1998**, *120*, 9401–9409.

[346] L. T. Chong; Y. Duan; L. Wang; I. Massova; P. A. Kollman. Molecular dynamics and free-energy calculations applied to affinity maturation in antibody 48G7. *Proc. Natl. Acad. Sci. USA*, **1999**, *96*, 14330–14335.

[347] P. A. Kollman; I. Massova; C. Reyes; B. Kuhn; S. Huo; L. Chong; M. Lee; T. Lee; Y. Duan; W. Wang; O. Donini; P. Cieplak; J. Srinivasan; D. A. Case; T. E. Cheatham, III. Calculating structures and free energies of complex molecules: Combining molecular mechanics and continuum models. *Accts. Chem. Res.*, **2000**, *33*, 889–897.

[348] M. L. Connolly. Analytical molecular surface calculation. *J. Appl. Cryst.*, **1983**, *16*, 548–558.

[349] R. Elber; M. Karplus. Enhanced sampling in molecular dynamics. Use of the time-dependent Hartree approximation for a simulation of carbon monoxide diffusion through myoglobin. *J. Am. Chem. Soc.*, **1990**, *112*, 9161–9175.

[350] A. Roitberg; R. Elber. Modeling side chains in peptides and proteins: Application of the locally enhanced sampling and the simulated annealing methods to find minimum energy conformations. *J. Chem. Phys.*, **1991**, *95*, 9277.

[351] C. Simmerling; T. Fox; P. A. Kollman. Use of Locally Enhanced Sampling in Free Energy Calculations: Testing and Application of the alpha to beta Anomerization of Glucose. *J. Am. Chem. Soc.*, **1998**, *120*, 5771–5782.

[352] C. Simmerling; J. L. Miller; P. A. Kollman. Combined locally enhanced sampling and particle mesh Ewald as a strategy to locate the experimental structure of a nonhelical nucleic acid. *J. Am. Chem. Soc.*, **1998**, *120*, 7149–7155.

[353] C. Simmerling; M. R. Lee; A. R. Ortiz; A. Kolinski; J. Skolnick; P. A. Kollman. Combining MONSSTER and LES/PME to Predict Protein Structure from Amino Acid Sequence: Application to the Small Protein CMTI-1. *J. Am. Chem. Soc.*, **2000**, *122*, 8392–8402.

[354] C. Simmerling; R. Elber. Hydrophobic "collapse" in a cyclic hexapeptide: Computer simulations of CHDLFC and CAAAAC in water. *J. Am. Chem. Soc.*, **1994**, *116*, 2534–2547.

[355] A. Miranker; M. Karplus. Functionality maps of binding sites: A multiple copy simultaneous search method. *Proteins: Str. Funct. Gen.*, **1991**, *11*, 29–34.

[356] J. E. Straub; M. Karplus. Enery partitioning in the classical time-dependent Hartree approximation. *J. Chem. Phys.*, **1991**, *94*, 6737.

[357] A. Ulitsky; R. Elber. The thermal equilibrium aspects of the time-dependent Hartree and the locally enhanced sampling approximations: Formal properties, a correction, and computational examples for rare gas clusters. *J. Chem. Phys.*, **1993**, *98*, 3380.

[358] W. S. Ross; C. C. Hardin. Ion-induced stabilization of the G-DNA quadruplex: Free energy perturbation studies. *J. Am. Chem. Soc.*, **1994**, *116*, 6070–6080.

[359] A. Vedani; D. W. Huhta. A new force field for modeling metalloproteins. *J. Am. Chem. Soc.*, **1990**, *112*, 4759–4767.

[360] D. L. Veenstra; D. M. Ferguson; P. A. Kollman. How transferable are hydrogen parameters in molecular mechanics calculations? *J. Comput. Chem.*, **1992**, *13*, 971–978.

[361] F. H. Allen; O. Kennard; D. G. Watson; L. Brammer; A. G. Orpen; R. Taylor. *J. Chem. Soc. Perkin Trans. II*, **1987**, pp S1–S19.

[362] M. D. Harmony; R. W. Laurie; R. L. Kuczkowski; R. H. Schwendemann; D. A. Ramsay; F. J. Lovas; W. J. Lafferty; A. G. Maki. *J. Phys. Chem. Ref. Data*, **1979**, *8*, 619.

[363] A. J. Hopfinger; R. A. Pearlstein. Molecular mechanics force-field parameterization procedures. *J. Comput. Chem.*, **1985**, *5*, 486–499.

[364] J. F. Cannon. AMBER force-field parameters for guanosine triphosphate and its imido and methylene analogs. *J. Comput. Chem.*, **1993**, *14*, 995–1005.

[365] P. Cieplak; W. D. Cornell; C. Bayly; P. A. Kollman. Application of the multimolecule and multiconformational RESP methodology to biopolymers: Charge derivation for DNA, RNA and proteins. *J. Comput. Chem.*, **1995**, *16*, 1357–1377.

[366] W. D. Cornell; P. Cieplak; C. I. Bayly; P. A. Kollman. Application of RESP charges to calculate conformational energies, hydrogen bond energies and free energies of solvation. *J. Am. Chem. Soc.*, **1993**, *115*, 9620–9631.

[367] A. E. Howard; P. Cieplak; P. A. Kollman. A molecular mechanical model that reproduces the relative energies for chair and twist-boat conformations of 1,3-dioxanes. *J. Comp. Chem.*, **1995**, *16*, 243–261.

[368] A. St.-Amant; W. D. Cornell; P. A. Kollman; T. A. Halgren. Calculation of molecular geometries, relative conformational energies, dipole moments, and molecular electrostatic potential fitted charges of small organic molecules of biochemical interest by density functional theory. *J. Comput. Chem.*, **1995**, *16*, 1483–1506.

[369] T. A. Halgren. Merck Molecular Force Field (MMFF94). Part I-V. *J. Comput. Chem.*, **1996**, *17*, 490–641.

[370] J. Wang; P. Morin; W. Wang; P. A. Kollman. Use of MM-PBSA in reproducing the binding free energies to HIV-1 RT of TIBO derivatives and predicting the binding mode to HIV-1 RT of efavirenz by docking and MM-PBSA. *J. Am. Chem. Soc.*, **2001**, *123*, 5221–5230.

[371] W. Wang; P. Kollman. Free energy calculations on dimer stability of the HIV protease using molecular dynamics and a continuum solvent model. *J. Mol. Biol.*, **2000**, *303*, 567.

[372] C. Reyes; P. Kollman. Structure and thermodynamics of RNA-protein binding: Using molecular dynamics and free energy analyses to calculate the free energies of binding and conformational change. *J. Mol. Biol.*, **2000**, *297*, 1145–1158.

[373] M. R. Lee; Y. Duan; P. A. Kollman. Use of MM-PB/SA in estimating the free energies of proteins: Application to native, intermediates, and unfolded vilin headpiece. *Proteins*, **2000**, *39*, 309–316.

[374] P. Cieplak; J. Caldwell; P. Kollman. Molecular mechanical models for organic and biological systems going beyond the atom centered two body additive approximation: Aqueous solution free energies of methanol and N-methyl acetamide, nucleic acid base, and amide hydrogen bonding and chloroform/water partition coefficients of the nucleic acid bases. *J. Comput. Chem.*, **2001**, *22*, 1048–1057.

[375] E. Meng; P. Cieplak; J. W. Caldwell; P. A. Kollman. Accurate solvation free energies of acetate and methylammonium ions calculated with a polarizable water model. *J. Am. Chem. Soc.*, **1994**, *116*, 12061–12062.

[376] D. L. Beveridge; F. M. DiCapua. Free energy simulation via molecular simulations: Applications to chemical and biomolecular systems. *Annu. Rev. Biophys. Biophys. Chem.*, **1989**, *18*, 431–492.

[377] C. Chipot; P. A. Kollman; D. A. Pearlman. Alternative approaches to potential of mean force calculations: free energy perturbation versus thermodynamics integration. Case study of some representative nonpolar interactions. *J. Comput. Chem*, **1996**, *17*, 1112–1131.

[378] D. A. Pearlman; P. A. Kollman. The overlooked bond-stretching contribution in free energy perturbation calculations. *J. Chem. Phys.*, **1991**, *94*, 4532–4545.

[379] D. A. Pearlman. Determining the contributions of constraints in free energy calculations: Development, characterization, and recommendations. *J. Chem. Phys.*, **1993**, *98*, 8946–8957.

[380] D. A. Pearlman. Free energy derivatives: A new method for probing the convergence problem in free energy calculations. *J. Comput. Chem.*, **1994**, *15*, 105–123.

[381] D. A. Pearlman. A comparison of alternative approaches to free energy calculations. *J. Phys. Chem.*, **1994**, *98*, 1487–1493.

[382] D. A. Pearlman; B. G. Rao. in *Encyclopedia of Computational Chemistry*, P. von R. Schleyer; N. L. Allinger; T. Clark; J. Gasteiger; P. A. Kollman; I. H. F. Schaefer, Eds., pp 1036–1061. John Wiley, Chichester, 1998.

[383] R. J. Radmer; P. A. Kollman. Free energy calculation methods: A theoretical and empirical comparison of numerical errors and a new method for qualitative estimates of free energy changes. *J. Comput. Chem.*, **1997**, *18*, 902–919.

[384] D. A. Pearlman; P. A. Kollman. A new method for carrying out free energy perturbation calculations: dynamically modified windows. *J. Chem. PHys.*, **1989**, *90*, 2460–2470.

[385] H.-A. Yu; M. Karplus. A thermodynamic analysis of solvation. *J. Chem. Phys.*, **1988**, *89*, 2366–2379.

[386] G. Hummer. Fast-growth thermodynamic integration: Error and efficiency analysis. *J. Chem. Phys.*, **2001**, *114*, 7330–7337.

[387] S. H. Fleischman; C. L. Brooks, III. Thermodynamic calculations on biological systems: Solution properties of alcohols and alkanes. *J. Chem. Phys.*, **1988**, *87*, 221–234.

[388] J. J. Vincent; K. M. Merz, Jr. A highly portable parallel implementation of AMBER4 using the message passing interface standard. *J. Comput. Chem.*, **1995**, *16*, 1420–1427.

[389] R. Radmer; P. Kollman. The application of three approximate free energy calculations methods to structure based ligand design: Trypsin and its complex with inhibitors. *J. Comput.-Aided Mol. Design*, **1998**, *12*, 215–228.

[390] S. R. Niketic; K. Rasmussen. *The Consistent Force Field: A Documentation*. Springer-Verlag, New York, 1977.

[391] C. Cerjan; W. H. Miller. On finding transition states. *J. Chem. Phys.*, **1981**, *75*, 2800.

[392] D. T. Nguyen; D. A. Case. On finding stationary states on large-molecule potential energy surfaces. *J. Phys. Chem.*, **1985**, *89*, 4020–4026.

[393] G. Lamm; A. Szabo. Langevin modes of macromolecules. *J. Chem. Phys.*, **1986**, *85*, 7334–7348.

[394] J. Kottalam; D. A. Case. Langevin modes of macromolecules: application to crambin and DNA hexamers. *Biopolymers*, **1990**, *29*, 1409–1421.

[395] S. Huo; I. Massova; P. A. Kollman. Computational Alanine Scanning of the 1:1 Human Growth Hormone-Receptor Complex. *J. Comput. Chem.*, **2002**, *23*, 15–27.

[396] T. Darden; D. Pearlman; L. G. Pedersen. Ionic charging free energies: Spherical versus periodic boundary conditions. *J. Chem. Phys.*, **1998**, *109*, 10921–10935.

[397] R. M. Levy; M. Karplus; J. Kushick; D. Perahia. Evaluation of the configurational entropy for proteins: Application to molecular dynamics simulations of an α-helix. *Macromolecules*, **1984**, *17*, 1370–1374.

[398] E. Gallicchio; M. M. Kubo; R. M. Levy. Enthalpy-entropy and cavity decomposition of alkane hydration free energies: Numerical results and implications for theories of hydrophobic solvation. *J. Phys. Chem.*, **2000**, *104*, 6271–6285.

[399] S. Arnott; P. J. Campbell-Smith; R. Chandrasekaran. in *Handbook of Biochemistry and Molecular Biology, 3rd ed. Nucleic*, G. P. Fasman, Ed., pp 411–422. CRC Press, Cleveland, 1976.

[400] O. Becker; A. D. MacKerell; B. Roux; M. Watanabe, eds. *Computational Biochemistry and Biophysics*. Marcel Dekker, New York, 2001.

[401] A. R. Leach. *Molecular Modelling. Principles and Applications, Second Edition*. Prentice-Hall, Harlow, England, 2001.

[402] T. E. Cheatham, III; B. R. Brooks; P. A. Kollman. in *Current Protocols in Nucleic Acid Chemistry*, pp Sections 7.5, 7.8, 7.9, 7.10. Wiley, New York, 1999.

[403] G. Sigalov; P. Scheffel; A. Onufriev. Incorporating variable environments into the generalized Born model. *J. Chem. Phys.*, **2005**, *122*, 094511.

[404] G. Sigalov; A. Fenley; A. Onufriev. Analytical electrostatics for biomolecules: Beyond the generalized Born approximation . *J. Chem. Phys.*, **2006**, *124*, 124902.

[405] A. Mitsutake; Y. Sugita; Y. Okamoto. Generalized-ensemble algorithms for molecular simulations of biopolymers. *Biopolymers*, **2001**, *60*, 96–123.

[406] J. J. Prompers; R. Brüschweiler. Dynamic and structural analysis of isotropically distributed molecular ensembles. *Proteins*, **2002**, *46*, 177–189.

[407] J. J. Prompers; R. Brüschweiler. General framework for studying the dynamics of folded and nonfolded proteins by NMR relaxation spectroscopy and MD simulation. *J. Am. Chem. Soc.*, **2002**, *124*, 4522–4534.

[408] T. A. Andrea; W. C. Swope; H. C. Andersen. The role of long ranged forces in determining the structure and properties of liquid water. *J. Chem. Phys.*, **1983**, *79*, 4576–4584.

[409] R. W. Pastor; B. R. Brooks; A. Szabo. An analysis of the accuracy of Langevin and molecular dynamics algorithms. *Mol. Phys.*, **1988**, *65*, 1409–1419.

[410] J. P. Valleau; G. M. Torrie. in *Modern Theoretical Chemistry, Vol. 5: Statistical Mechanics, Part A,*, B. J. Berne, Ed. Plenum Press, New York, 1977.

[411] S. Kumar; D. Bouzida; R. H. Swendsen; P. A. Kollman; J. M. Rosenberg. The weighted histogram analysis method for free-energy calculations on biomolecules. I. The method. *J. Comput. Chem.*, **1992**, *13*, 1011–1021.

[412] S. Kumar; J. M. Rosenberg; D. Bouzida; R. H. Swendsen; P. A. Kollman. Multidimensional free-energy calculations using the weighted histogram analysis method. *J. Comput. Chem.*, **1995**, *16*, 1339–1350.

[413] J. Kottalam; D. A. Case. Dynamics of ligand escape from the heme pocket of myoglobin. *J. Am. Chem. Soc.*, **1988**, *110*, 7690–7697.

[414] B. Roux. The calculation of the potential of mean force using computer simulations. *Comput. Phys. Comm.*, **1995**, *91*, 275–282.

[415] J. W. Ponder; D. A. Case. Force fields for protein simulations. *Adv. Prot. Chem.*, **2003**, *66*, 27–85.

[416] W. H. Press; B. P. Flannery; S. A. Teukolsky; W. T. Vetterling. in *Numerical Recipes: The Art of Scientific Computing*. Cambridge University Press, New York, 1989.

[417] P. Beroza; D. A. Case. Calculations of proton-binding thermodynamics in proteins. *Meth. Enzymol.*, **1998**, *295*, 170–189.

[418] J. D. Madura; M. E. Davis; M. K. Gilson; R. C. Wade; B. A. Luty; J. A. McCammon. Biological applications of electrostatic calculations and brownian dynamics simulations. *Rev. Computat. Chem.*, **1994**, *5*, 229–267.

[419] M. K. Gilson. Theory of electrostatic interactions in macromolecules. *Curr. Opin. Struct. Biol.*, **1995**, *5*, 216–23.

[420] M. Scarsi; J. Apostolakis; A. Caflisch. Continuum electrostatic energies of macromolecules in aqueous solutions. *J. Phys. Chem. A*, **1997**, *101*, 8098–8106.

[421] R. Luo; L. David; M. K. Gilson. Accelerated Poisson-Boltzmann calculations for static and dynamic systems. *J. Comput. Chem.*, **2002**, *23*, 1244–1253.

[422] H. Wei; R. Qi; J. Wang; P. Cieplak; Y. Duan; R. Luo. Efficient Formulation of polarizable Gaussian Multipole Electrostatics for Biomolecular Simulations. *J. Chem. Phys.*, **2020**, *153*, 114116.

[423] H. Wei; A. Luo; T. Qiu; R. Luo; R. Qi. Improved Poisson-Boltzmann Methods for High-Performance Computing. *J. Chem. Theory Comput.*, **2019**, *15*, 6190.

[424] H. Wei; R. Luo; R. Qi. An Efficient Second-Order Poisson-Boltzmann Method. *J. Comput. Chem.*, **2019**, *40*, 1257.

[425] D. Greene; R. Qi; R. Nguyen; T. Qiu; R. Luo. Heterogeneous dielectric implicit membrane model for the calculation of mmpbsa binding free energies. *J. Chem. Infom. Model.*, **2019**, *59*, 3041.

[426] L. Xiao; J. Diao; D. Greene; J. Wang; R. Luo. A Continuum Poisson-Boltzmann Model for Membrane Channel Proteins. *J. Chem. Theory Comput.*, **2017**, *13*, 3398.

[427] C. Wang; P. Ren; R. Luo. Ionic solution: What goes right and wrong with continuum solvation modeling. *J. Phys. Chem. B*, **2017**, *121*, 11169.

[428] E. King; R. Qi; H. Li; R. Luo; E. Aitchison. Estimating the roles of protonation and electronic polarization in absolute binding affinity simulations. *J. Chem. Theory Comput.*, **2021**, *17*, 0000.

[429] Z. Li; I. K. *The Immersed Interface Method: Numerical Solutions of PDEs Involving Interfaces and Irregular Domains*. SIAM Frontiers in Applied Mathematics, Philadelphia, 2006.

[430] J. Wang; Q. Cai; Z. Li; H. Zhao; R. Luo. Achieving Energy Conservation in Poisson-Boltzmann Molecular Dynamics: Accuracy and Precision with Finite-difference Algorithms. *Chem. Phys. Lett.*, **2009**, *468*, 112.

[431] J. Wang; R. Luo. Assessment of Linear Finite-Difference Poisson-Boltzmann solvers. *J. Comput. Chem.*, **2010**, *31*, 1689–1698.

[432] Q. Cai; J. Wang; H. Zhao; R. Luo. On removal of charge singularity in Poisson-Boltzmann equation. *J. Chem. Phys.*, **2009**, *130*, 145101.

[433] Q. Cai; M.-J. Hsieh; J. Wang; R. Luo. Performance of Nonlinear Finite-Difference Poisson-Boltzmann Solvers. *J. Chem. Theory Comput.*, **2010**, *6*, 203.

[434] Q. Cai; X. Ye; J. Wang; R. Luo. Dielectric boundary force in numerical Poisson-Boltzmann methods: Theory and numerical strategies. *Chem. Phys. Lett.*, **2011**, *514*, 368.

[435] Q. Cai; X. Ye; J. Wang; R. Luo. On-the-Fly Numerical Surface Integration for Finite-Difference Poisson-Boltzmann Methods. *J. Chem. Theory Comput.*, **2011**, *7*, 3608–3619.

[436] Q. Cai; X. Ye; R. Luo. Dielectric Pressure in Continuum Electrostatic Solvation of Biomolecules. *Phys. Chem. Chem. Phys.*, **2012**, *14*, 15917–15925.

[437] W. M. Botello-Smith; X. Liu; Q. Cai; Z. Li; H. Zhao; R. Luo. Numerical Poisson-Boltzmann Model for Continuum Membrane Systems. *Chem. Phys. Lett.*, **2013**, *555*, 274.

[438] X. Ye; J. Wang; R. Luo. A Revised Density Function for Molecular Surface Calculation in Continuum Solvent Models. *J. Chem. Theory Comput.*, **2010**, *6*, 1157–1169.

[439] C. Wang; P. Nguyen; K. Pham; D. Huynh; T. Le; H. Wang; P. Ren; R. Luo. Calculating protein-ligand binding affinities with MMPBSA: Method and error analysis. *J. Comput. Chem.*, **2016**, *37*, 2436–2446.

[440] R. Qi; W. Botello-Smith; R. Luo. Acceleration of Linear Finite-Difference Poisson-Boltzmann Methods on Graphics Processing Units. *J. Chem. Theory Comput.*, **2017**, *13*, 3378–3387.

[441] R. Qi; R. Luo. Robustness and Efficiency of Poisson-Boltzmann Modeling on Graphics Processing Units. *J. Chem. Inf. Model.*, **2019**, *59*, 409–420.

[442] T. Simonson. Electrostatics and dynamics of proteins. *Rep. Prog. Phys.*, **2003**, *66*, 737–787.

[443] D. Bashford; M. Karplus. p'K sub a''s of ionizable groups in proteins: Atomic detail from a continuum electrostatic model. *Biochemistry*, **1990**, *29*, 10219–10225.

[444] A. Ghosh; C. S. Rapp; R. A. Friesner. Generalized Born model based on a surface integral formulation. *J. Phys. Chem. B*, **1998**, *102*, 10983–10990.

[445] Y. Duan; C. Wu; S. Chowdhury; M. C. Lee; G. Xiong; W. Zhang; R. Yang; P. Cieplak; R. Luo; T. Lee. A point-charge force field for molecular mechanics simulations of proteins based on condensed-phase quantum mechanical calculations. *J. Comput. Chem.*, **2003**, *24*, 1999–2012.

[446] J. D. Jackson. *Classical Electrodynamics*. Wiley and Sons, New York, 1975.

[447] Q. Lu; R. Luo. A Poisson-Boltzmann dynamics method with nonperiodic boundary condition. *J. Chem. Phys.*, **2003**, *119*, 11035–11047.

[448] C. H. Tan; L. J. Yang; R. Luo. How well does Poisson-Boltzmann implicit solvent agree with explicit solvent? A quantitative analysis. *J. Phys. Chem. B*, **2006**, *110*, 18680–18687.

[449] C. H. Tan; Y. H. Tan; R. Luo. Implicit nonpolar solvent models. *J. Phys. Chem. B*, **2007**, *111*, 12263–12274.

[450] M. Feig; J. Karanicolas; C. L. Brooks, III. MMTSB Tool Set: Enhanced sampling and multiscale modeling methods for application in structural biology. *J. Mol. Graphics Mod.*, **2004**, *22*, 377–395.

[451] C. Simmerling; B. Strockbine; A. E. Roitberg. All-atom structure prediction and folding simulations of a stable protein. *J. Am. Chem. Soc.*, **2002**, *124*, 11258–11259.

[452] A. E. García; K. Y. Sanbonmatsu. α-helical stabilization by side chain shielding of backbone hydrogen bonds. *Proc. Natl. Acad. Sci. USA*, **2002**, *99*, 2782–2787.

[453] K. N. Kirschner; R. J. Woods. Solvent interactions determine carbohydrate conformation. *Proc. Natl. Acad. Sci. USA*, **2001**, *98*, 10541–10545.

[454] M. Basma; S. Sundara; D. Calgan; T. Venali; R. J. Woods. Solvated ensemble averaging in the calculation of partial atomic charges. *J. Comput. Chem.*, **2001**, *22*, 1125–1137.

[455] K. N. Kirschner; R. J. Woods. Quantum mechanical study of the nonbonded forces in water-methanol complexes. *J. Phys. Chem. A*, **2001**, *105*, 4150–4155.

[456] K. A. Sharp; B. Honig. Electrostatic interactions in macromolecules: Theory and experiment. *Annu. Rev. Biophys. Biophys. Chem.*, **1990**, *19*, 301–332.

[457] M. K. Gilson; K. A. Sharp; B. H. Honig. Calculating the electrostatic potential of molecules in solution: method. *J. Comput. Chem.*, **1988**, *9*, 327–35.

[458] J. Warwicker; H. C. Watson. Calculation of the electric potential in the active site cleft due to. *J. Mol. Biol.*, **1982**, *157*, 671–679.

[459] I. Klapper; R. Hagstrom; R. Fine; K. Sharp; B. Honig. Focussing of electric fields in the active stie of Cu, Zn superoxide dismutase. *Proteins*, **1986**, *1*, 47–59.

[460] A. Nicholls; B. Honig. A rapid finite difference algorithm, utilizing successive over-relaxation to solve the Poisson-Boltzmann equation. *J. Comput. Chem.*, **1991**, *12*, 435–445.

[461] M. E. Davis; J. A. McCammon. Dielectric boundary smoothing in finite difference solutions of the Poisson equation: An approach to improve accuracy and convergence. *J. Comput. Chem.*, **1991**, *12*, 909–912.

[462] M. E. Davis; J. A. McCammon. Electrostatics in biomolecular structure and dynamics. *Chem. Rev.*, **1990**, *90*, 509–521.

[463] M. E. Davis; J. A. McCammon. Solving the finite-difference linearized Poisson-Boltzmann equation – a comparison of relaxation and conjugate gradient methods. *J. Comput. Chem.*, **1989**, *10*, 386–391.

[464] D. Bashford. An object-oriented programming suite for electrostatic effects in biological molecules. *Lect. Notes Comput. Sci.*, **1997**, *1343*, 233–240.

[465] B. A. Luty; M. E. Davis; J. A. McCammon. Electrostatic energy calculations by a finite-difference method: Rapid calculation of charge-solvent interaction energies. *J. Comput. Chem.*, **1992**, *13*, 768–771.

[466] U. C. Singh; S. J. Weiner; P. A. Kollman. Molecular dynamics simulations of d(C-G-C-G-A).d(T-C-G-C-G) with and without "hydrated" counterions. *Proc. Nat. Acad. Sci.*, **1985**, *82*, 755–759.

[467] J. Gao. Absolute free energy of solvation from Monte Carlo simulations using combined quantum and molecular mechanical potentials. *J. Phys. Chem.*, **1992**, *96*, 537–540.

[468] A. Warshel; M. Levitt. Theoretical studies of enzymic reactions: Dielectric, electrostatic and steric stabilization of the carbonium ion in the reaction of lysozyme. *J. Mol. Biol.*, **1976**, *103*, 227–249.

[469] M. J. Field; P. A. Bash; M. Karplus. A combined quantum mechanical and molecular mechanical potential for molecular dynamics simulations. *J. Comput. Chem.*, **1990**, *11*, 700–733.

[470] R. V. Stanton; D. S. Hartsough; K. M. Merz, Jr. An examination of a density functional/molecular mechanical coupled potential. *J. Comput. Chem.*, **1994**, *16*, 113–128.

[471] R. V. Stanton; L. R. Little; K. M. Merz, Jr. An examination of a Hartree-Fock/molecular mechanical coupled potential. *J. Phys. Chem.*, **1995**, *99*, 17344–17348.

[472] R. V. Stanton; D. S. Hartsough; K. M. Merz, Jr. Calculations of solvation free energies using a density functional/molecular dynamics coupled potential. *J. Phys. Chem.*, **1993**, *97*, 11868–11870.

[473] W. Yang; T.-S. Lee. A density-matrix divide-and-conquer approach for electronic structure calculations of large molecules. *J. Chem. Phys.*, **1995**, *103*, 5674–5678.

[474] S. L. Dixon; K. M. Merz, Jr. Semiempirical molecular orbital calculations with linear system size scaling. *J. Chem. Phys.*, **1996**, *104*, 6643–6649.

[475] S. L. Dixon; K. M. Merz, Jr. Fast, accurate semiempirical molecular orbital calculations for macromolecules. *J. Chem. Phys.*, **1997**, *107*, 879–893.

[476] J. Nocedal; S. J. Wright. *Numerical Optimization*. Springer-Verlag, New York, 1999.

[477] S. G. Nash. A survey of truncated-Newton methods. *J. of Computational and Applied Mathematics*, **2000**, *124*, 45–59.

[478] X. Cheng; V. Hornak; C. Simmerling. Improved conformational sampling through an efficient combination of mean-field simulation approaches. *J. Phys. Chem. B*, **2004**, *108*.

[479] M. C. Lee; Y. Duan. Distinguish protein decoys by using a scoring function based on a new Amber force field, short molecular dynamics simulations, and the generalized Born solvent model. *Proteins*, **2004**, *55*, 620–634.

[480] J. Chu; B. L. Trout; B. R. Brooks. A super-linear minimization scheme for the nudged elastic band method. *J. Chem. Phys.*, **2003**, *119*, 12708–12717.

[481] R. Elber; M. Karplus M. A method for determining reaction paths in large molecules: Application to myoglobin. *Chem. Phys. Lett.*, **1987**, *139*, 375–380.

[482] G. Henkelman; H. Jönsson. Improved tangent estimate in the nudged elastic band method for finding minimum energy paths and saddle points. *J. Chem. Phys.*, **2000**, *113*, 9978–9985.

[483] G. Henkelman; B. P. Uberuaga; H. Jönsson. A climbing image nudged elastic band method for finding saddle points and minimum energy paths. *J. Chem. Phys.*, **2000**, *113*, 9901–9904.

[484] H. Jönsson; G. Mills; K. W. Jacobsen. in *Classical and Quantum Dynamics in Condensed Phase Simulations*, B. J. Berne; G. Ciccoti; D. F. Coker, Eds., pp 385–404. World Scientific, Singapore, 1998.

[485] G. Mills; H. Jönsson. Quantum and thermal effects in H_2 dissociative adsorption: Evaluation of free energy barriers in multidimensional quantum systems. *Phys. Rev. Lett.*, **1994**, *72*, 1124–1127.

[486] J. Mongan; D. A. Case; J. A. McCammon. Constant pH molecular dynamics in generalized Born implicit solvent. *J. Comput. Chem.*, **2004**, *25*, 2038–2048.

[487] D. A. Case; T. Cheatham; T. Darden; H. Gohlke; R. Luo; K. M. Merz, Jr.; A. Onufriev; C. Simmerling; B. Wang; R. Woods. The Amber biomolecular simulation programs. *J. Computat. Chem.*, **2005**, *26*, 1668–1688.

[488] X. Wu; B. R. Brooks. Isotropic periodic sum: A method for the calculation of long-range interactions. *J. Chem. Phys.*, **2005**, *122*, 044107.

[489] X. Wu; B. R. Brooks. Using the Isotropic Periodic Sum Method to Calculate Long-Range Interactions of Heterogeneous Systems. *J. Chem. Phys.*, **2008**, *129*, 154115.

[490] X. Wu; B. R. Brooks. Isotropic periodic sum of electrostatic interactions for polar systems. *J. Chem. Phys.*, **2009**, *131*, 024107.

[491] R. M. Venable; L. E. Chen; R. W. Pastor. Comparison of the Extended Isotropic Periodic Sum and Particle Mesh Ewald Methods for Simulations of Lipid Bilayers and Monolayers. *J. Phys. Chem. B*, **2009**, *113*, 5855–5862.

[492] E. J. Sorin; V. S. Pande. Exploring the helix-coil transition via all-atom equilibrium ensemble simulations. *Biophys. J.*, **2005**, *88*, 2472–2493.

[493] T. Kruger; M. Elstner; P. Schiffels; T. Frauenheim. Validation of the density-functional based tight-binding approximation. *J. Chem. Phys.*, **2005**, *122*, 114110.

[494] P. Ren; J. W. Ponder. Temperature and pressure dependence of the AMOEBA water model. *J. Phys. Chem. B*, **2004**, *108*, 13427–13437.

[495] P. Ren; J. W. Ponder. Consistent treatment of inter- and intramolecular polarization in molecular mechanics calculations. *J. Comput. Chem.*, **2002**, *23*, 1497–1506.

[496] L. Yang; C. Tan; M.-J. Hsieh; J. Wang; Y. Duan; P. Cieplak; J. Caldwell; P. A. Kollman; R. Luo. New-generation Amber united-atom force field. *J. Phys. Chem. B*, **2006**, *110*, 13166–13176.

[497] B. Wang; K. M. Merz, Jr. A fast QM/MM (quantum mechanical/molecular mechanical) approach to calculate nuclear magnetic resonance chemical shifts for macromolecules. *J. Chem. Theory Comput.*, **2006**, *2*, 209–215.

[498] R. C. Rizzo; T. Aynechi; D. A. Case; I. D. Kuntz. Estimation of absolute free energies of hydration using continuum methods: Accuracy of partial charge models and optimization of nonpolar contributions. *J. Chem. Theory Comput.*, **2006**, *2*, 128–139.

[499] Z.-X. Wang; W. Zhang; C. Wu; H. Lei; P. Cieplak; Y. Duan. Strike a Balance: Optimization of backbone torsion parameters of AMBER polarizable force field for simulations of proteins and peptides. *J. Comput. Chem.*, **2006**, *27*, 781–790.

[500] S. C. Harvey; R. K. Tan; T. E. Cheatham, III. The flying ice cube: Velocity rescaling in molecular dynamics leads to violation of energy equipartition. *J. Comput. Chem.*, **1998**, *19*, 726–740.

[501] K. Nam; J. Gao; D. York. An efficient linear-scaling Ewald method for long-range electrostatic interactions in combined QM/MM calculations. *J. Chem. Theory Comput.*, **2005**, *1*, 2–13.

[502] E. Pellegrini; M. J. Field. A generalized-Born solvation model for macromolecular hybrid-potential calculations. *J. Phys. Chem. A*, **2002**, *106*, 1316–1326.

[503] R. P. Feynman; A. R. Hibbs. *Quantum Mechanics and Path Integrals*. McGraw-Hill, New York, 1965.

[504] R. P. Feynman. *Statistcal Mechanics*. Benjamin, Reading, MA, 1972.

[505] H. Kleinert. *Path Integrals in Quantum Mechanics, Statistics, and Polymer Physics*. World Scientific, Singapore, 1995.

[506] L. S. Schulman. *Techniques and Applications of Path Integration*. Wiley & Sons, New York, 1996.

[507] A. Messiah. *Quantum Mechanics*. Wiley & Sons, New York, 1958.

[508] D. Chandler; P. G. Wolynes. Exploiting the isomorphism between quantum theory and classical statistical mechanics of polyatomic fluids. *J. Chem. Phys.*, **1981**, *74*, 4078–4095.

[509] D. M. Ceperley. Path integrals in the theory of condensed helium. *Rev. Mod. Phys.*, **1995**, *67*, 279–355.

[510] J. Cao; B. J. Berne. On energy estimators in path integral Monte Carlo simulations: Dependence of accuracy on algorithm. *J. Chem. Phys.*, **1989**, *91*, 6359–6366.

[511] J. W. Storer; D. J. Giesen; C. J. Cramer; D. G. Truhlar. Class IV charge models: A new semiempirical approach in quantum chemistry. *J. Comput.-Aided Mol. Design*, **1995**, *9*, 87–110.

[512] J. Li; C. J. Cramer; D. G. Truhlar. New class IV charge model for extracting accurate partial charges from Wave Functions. *J. Phys. Chem. A.*, **1998**, *102*, 1820–1831.

[513] A. van der Vaart; K. M. Merz, Jr. Divide and conquer interaction energy decomposition. *J. Phys. Chem. A*, **1999**, *103*, 3321–3329.

[514] A. V. Mitin. The dynamic level shift method for improving the convergence of the SCF procedure. *J. Comput. Chem.*, **1988**, *9*, 107–110.

[515] M. D. Ermolaeva; A. van der Vaart; K. M. Merz, Jr. Implementation and testing of a frozen density matrix - divide and conquer algorithm. *J. Phys. Chem.*, **1999**, *103*, 1868–1875.

[516] B. Wang; E. N. Brothers; A. van der Vaart; K. M. Merz Jr. Fast semiempirical calculations for nuclear magnetic resonance chemical shifts: A divide-and-conquer approach. *J. Chem. Phys.*, **2004**, *120*, 11392–11400.

[517] B. Wang; K. Raha; K. M. Merz Jr. Pose scoring by NMR. *J. Am. Chem. Soc.*, **2004**, *126*, 11430–11431.

[518] K. Raha; A. van der Vaart; K. E. Riley; M. B. Peters; L. M. Westerhoff; H. Kim; K. M. Merz Jr. Pairwise decomposition of residue interaction energies using semiempirical quantum mechanical methods in studies of protein-ligand interaction. *J. Am. Chem. Soc.*, **2005**, *127*, 6583–6594.

[519] A. Luzhkov; A. Warshel. Microscopic models for quantum-mechanical calculations of chemical processes in solutions - Ld/Ampac and Scaas/Ampac calculations of solvation energies. *J. Comp. Chem.*, **1992**, *13*, 199–213.

[520] U. C. Singh; P. A. Kollman. A combined Ab initio quantum-mechanical and molecular mechanical method for carrying out simulations on complex molecular systems - Applications to the Ch3Cl + Cl- exchange-reaction and gas-phase protonation of polyethers. *J. Comp. Chem.*, **1986**, *7*, 718–730.

[521] I. B. Bersuker; M. K. Leong; J. E. Boggs; R. S. Pearlman. A method of combined quantum mechanical (QM) molecular mechanics (MM) treatment of large polyatomic systems with charge transfer between the QM and MM fragments. *Int. J. Quant. Chem.*, **1997**, *63*, 1051–1063.

[522] F. Maseras; K. Morokuma. Imomm - a new integrated ab-initio plus molecular geometry optimization scheme of equilibrium structures and transition-states. *J. Comp. Chem.*, **1995**, *16*, 1170–1179.

[523] Y. K. Zhang; T. S. Lee; W. T. Yang. A pseudobond approach to combining quantum mechanical and molecular mechanical methods. *J. Chem. Phys.*, **1999**, *110*, 46–54.

[524] J. L. Gao; P. Amara; C. Alhambra; M. J. Field. A generalized hybrid orbital (GHO) method for the treatment of boundary atoms in combined QM/MM calculations. *J Phys Chem A*, **1998**, *102*, 4714–4721.

[525] D. M. Philipp; R. A. Friesner. Mixed ab initio QM/MM modeling using frozen orbitals and tests with alanine dipeptide and tetrapeptide. *J. Comp. Chem.*, **1999**, *20*, 1468–1494.

[526] M. J. Field; M. Albe; C. Bret; F. Proust-De Martin; A. Thomas. The Dynamo library for molecular simulations using hybrid quantum mechanical and molecular mechanical potentials. *J. Comp. Chem.*, **2000**, *21*, 1088–1100.

[527] V. Hornak; R. Abel; A. Okur; B. Strockbine; A. Roitberg; C. Simmerling. Comparison of multiple Amber force fields and development of improved protein backbone parameters. *Proteins*, **2006**, *65*, 712–725.

[528] F. Floris; J. Tomasi. Evaluation of the dispersion contribution to the solvation energy. A simple computational model in the continuum approximation. *J. Comput. Chem.*, **1989**, *10*, 616–627.

[529] R. M. Levy; E. Gallicchio. Computer simulations with explicit solvent: recent progress in the thermodynamic decomposition of free energies and in modeling electrostatic effects. *Annu. Rev. Phys. Chem.*, **1999**, *49*, 531–567.

[530] H. Nymeyer; S. Gnanakaran; A. García. Atomic simulations of protein folding using the replica exchange algorithm. *Meth. Enzymol.*, **2004**, *383*, 119–149.

[531] D. H. Mathews; D. A. Case. Nudged Elastic Band calculation of minimal energy pathways for the conformational change of a GG mismatch. *J. Mol. Biol.*, **2006**, *357*, 1683–1693.

[532] X. Cheng; G. Cui; V. Hornak; C. Simmerling. Modified replica exchange simulation methods for local structure refinement. *J. Phys. Chem. B*, **2005**, *109*, 8220–8230.

[533] V. Hornak; A. Okur; R. Rizzo; C. Simmerling. HIV-1 protease flaps spontaneously open and reclose in molecular dynamics simulations. *Proc. Nat. Acad. Sci. USA*, **2006**, *103*, 915–920.

[534] V. Hornak; A. Okur; R. Rizzo; C. Simmerling. HIV-1 protease flaps spontaneously close when an inhibitor binds to the open state. *J. Am. Chem. Soc.*, **2006**, *128*, 2812–2813.

[535] C. Jarzynski. Nonequilibrium equality for free energy differences. *Phys. Rev. Lett.*, **1997**, *78*, 2690–2693.

[536] G. Hummer; A. Szabo. Free energy reconstruction from nonequilibrium single-molecule pulling experiments. *Proc. Natl. Acad. Sci. USA*, **2001**, *98*, 3658.

[537] G. Hummer; A. Szabo. Kinetics from nonequilibrium single-molecule pulling experiments. *Biophys. J.*, **2003**, *85*, 5–15.

[538] M. O. Jensen; S. Park; E. d; K. Schulten. Energetics of glycerol conduction through aquaglyceroporin GlpF. *Proc. Natl. Acad. Sci. USA*, **2002**, *99*, 6731–6736.

[539] A. Crespo; M. A. Marti; D. A. Estrin; A. E. Roitberg. Multiple-steering QM-MM calculation of the free energy profile in chorismate mutase. *J. Am. Chem. Soc.*, **2005**, *127*, 6940–6941.

[540] P. Y. Ren; J. W. Ponder. Polarizable atomic multipole water model for molecular mechanics simulation. *J. Phys. Chem. B*, **2003**, *107*, 5933–5947.

[541] P. Y. Ren; J. W. Ponder. Tinker polarizable atomic multipole force field for proteins. *to be published.*, **2006**.

[542] J. Kästner; W. Thiel. Bridging the gap between thermodynamic integration and umbrella sampling provides a novel analysis method: "Umbrella integration". *J. Chem. Phys.*, **2005**, *123*, 144104.

[543] A. M. Wollacott; K. M. Merz, Jr. Development of a parameterized force field to reproduce semiempirical geometries. *J. Chem. Theory Comput.*, **2006**, *2*, 1070–1077.

[544] A. Warshel. *Computer Modeling of Chemical Reactions in Enzymes and Solutions*. John Wiley and Sons, New York, 1991.

[545] S. R. Billeter; S. P. Webb; T. Iordanov; P. K. Agarwal; S. Hammes-Schiffer. Hybrid approach for including electronic and nuclear quantum effects in molecular dynamics simulations of hydrogen transfer reactions in enzymes. *J. Chem. Phys.*, **2001**, *114*, 6925.

[546] C. Simmerling; R. Elber. Hydrophobic "collapse" in a cyclic hexapeptide: Computer simulations of CHDLFC and CAAAAC in water. *J. Am. Chem. Soc.*, **1994**, *116*, 2534–2547.

[547] W. Kabsch; C. Sander. Dictionary of protein secondary structure: pattern recognition of hydrogen-bonded and geometrical features. *Biopolymers*, **1983**, *22*, 2577–2637.

[548] T. E. Cheatham, III; M. A. Young. Molecular dynamics simulation of nucleic acids: Successes, limitations and promise. *Biopolymers*, **2001**, *56*, 232–256.

[549] Y. Deng; B. Roux. Calculation of standard binding free energies: Aromatic molecules in the T4 lysozyme L99A mutant. *J. Chem. Theor. Comput.*, **2006**, *2*, 1255–1273.

[550] L. Marinelli; S. Cosconati; T. Steinbrecher; V. Limongelli; A. Bertamino; E. Novellino; D. A. Case. Homology Modeling of NR2B Modulatory Domain of NMDA Receptor and Analysis of Ifenprodil Binding. *ChemMedChem*, **2007**, *2*,, 1498–1510.

[551] K. N. Kirschner; A. B. Yongye; S. M. Tschampel; J. González-Outeiriño; C. R. Daniels; B. L. Foley; R. J. Woods. GLYCAM06: A generalizable biomolecular force field. Carbohydrates. *J. Comput. Chem.*, **2008**, *29*, 622–655.

[552] S. M. Tschampel; M. R. Kennerty; R. J. Woods. TIP5P-consistent treatment of electrostatics for biomolecular simulations. *J. Chem. Theory Comput.*, **2007**, *3*, 1721–1733.

[553] M. B. Tessier; M. L. DeMarco; A. B. Yongye; R. J. Woods. Extension of the GLYCAM06 biomolecular force field to lipids, lipid bilayers and glycolipids. *Mol. Simul.*, **2008**, *34*, 349–363.

[554] J. B. Klauda; X. Wu; R. W. Pastor; B. R. Brooks. Long-Range Lennard-Jones and Electrostatic Interactions in Interfaces. *J. Phys. Chem. B*, **2007**, *111*, 4393–4400.

[555] K. Takahashi; K. Yasuoka; T. Narumi. Cutoff radius effect of isotropic periodic sum method for transport. *J. Chem. Phys.*, **2007**, *127*, 114511.

[556] F. Paesani; W. Zhang; D. A. Case; T. E. Cheatham; G. A. Voth. An accurate and simple quantum model for liquid water. *J. Chem. Phys.*, **2006**, *125*, 184507.

[557] A. Okur; D. R. Roe; G. Cui; V. Hornak; C. Simmerling. Improving convergence of replica-exchange simulations through coupling to a high-temperature structure reservoir. *J. Chem. Theory comput.*, **2007**, *3*, 557–568.

[558] A. E. Roitberg; A. Okur; C. Simmerling. Coupling of replica exchange simulations to a non-Boltzmann structure reservoir. *J. Phys. Chem. B*, **2007**, *111*, 2415–2418.

[559] H. B. Schlegel; J. L. Sonnenberg. Empirical valence-bond models for reactive potential energy surfaces using distributed Gaussians. *J. Chem. Theory Comput.*, **2006**, *2*, 905.

[560] J. L. Sonnenberg; H. B. Schlegel. Empirical valence bond models for reactive potential energy surfaces. II. Intramolecular proton transfer in pyridone and the Claisen reaction of allyl vinyl ether. *Mol. Phys.*, **2007**, *105*, 2719.

[561] Y. Saad; M. H. Schultz. GMRES: A generalized minimal residual algorithm for solving nonsymmetric linear systems. *SIAM J. Sci. Stat. Comput.*, **1986**, *7*, 856.

[562] P. Pulay. Convergence acceleration of iterative sequences. The case of SCF iteration. *Chem. Phys. Lett.*, **1980**, *73*, 393.

[563] P. Pulay. Improved SCF convergence acceleration. *J. Comput. Chem.*, **1982**, *3*, 556.

[564] M. J. Frisch; G. W. Trucks; H. B. Schlegel; G. E. Scuseria; M. A. Robb; J. R. Cheeseman; G. Scalmani; V. Barone; B. Mennucci; G. A. Petersson; H. Nakatsuji; M. Caricato; X. Li; H. P. Hratchian; A. F. Izmaylov; J. Bloino; G. Zheng; J. L. Sonnenberg; M. Hada; M. Ehara; K. Toyota; R. Fukuda; J. Hasegawa; M. Ishida; T. Nakajima; Y. Honda; O. Kitao; H. Nakai; T. Vreven; J. A. Montgomery, Jr.; J. E. Peralta; F. Ogliaro; M. Bearpark; J. J. Heyd; E. Brothers; K. N. Kudin; V. N. Staroverov; R. Kobayashi; J. Normand; K. Raghavachari; A. Rendell; J. C. Burant; S. S. Iyengar; J. Tomasi; M. Cossi; N. Rega; J. M. Millam; M. Klene; J. E. Knox; J. B. Cross; V. Bakken; C. Adamo; J. Jaramillo; R. Gomperts; R. E. Stratmann; O. Yazyev; A. J. Austin; R. Cammi; C. Pomelli; J. W. Ochterski; R. L. Martin; K. Morokuma; V. G. Zakrzewski; G. A. Voth; P. Salvador; J. J. Dannenberg; S. Dapprich; A. D. Daniels; O. Farkas; J. B. Foresman; J. V. Ortiz; J. Cioslowski; D. J. Fox. Gaussian 09 Revision A.1. Gaussian Inc. Wallingford CT 2009.

[565] A. K. Rappe; C. J. Casewit; K. S. Colwell; W. A. Goddard III; W. M. Skiff. UFF, a Full Periodic Table Force Field for Molecular Mechanics and Molecular Dynamics Simulations. *J. Am. Chem. Soc.*, **1992**, *114*, 10024–10035.

[566] G. A. Voth; D. Chandler; W. H. Miller. Rigorous Formulation of Quantum Transition State Theory and Its Dynamical Corrections. *J. Chem. Phys.*, **1989**, *91*, 7749–7760.

[567] G. J. Martyna; M. L. Klein; M. Tuckerman. Nosé-Hoover chains: The canonical ensemble via continuous dynamics. *J. Chem. Phys.*, **1992**, *97*, 2635.

[568] G. J. Martyna; A. Hughes; M. E. Tuckerman. Molecular dynamics algorithms for path integrals at constant pressure. *J. Chem. Phys.*, **1999**, *110*, 3275.

[569] B. J. Berne; D. Thirumalai. On the simulation of quantum systems: path integral methods. *Annu. Rev. Phys. Chem.*, **1986**, *37*, 401.

[570] G. A. Voth. Path-integral centroid methods in quantum statistcal mechanics and dynamics. *Adv. Chem. Phys.*, **1996**, *93*, 135.

[571] I. R. Craig; D. E. Manolopoulos. Quantum statistics and classical mechnanics: Real time correlation functions from ring polymer molecular dynamics. *J. Chem. Phys.*, **2004**, *121*, 3368.

[572] T. F. Miller; D. E. Manolopoulos. Quantum diffusion in liquid water from ring polymer molecular dynamics. *J. Chem. Phys.*, **2005**, *123*, 154504.

[573] J. Cao; G. A. Voth. The formulation of quantum statistical mechanics based on the Feynman path centroid density. IV. Algorithms for centroid molecular dynamics. *J. Chem. Phys.*, **1994**, *101*, 6168.

[574] J. Vaníček; W. H. Miller; J. F. Castillo; F. J. Aoiz. Quantum-instanton evaluion of the kinetic isotope effects. *J. Chem. Phys.*, **2005**, *123*, 054108.

[575] J. Vaníček; W. H. Miller. Efficient estimators for quantum instanton evaluation of the kinetic isotope effects: application to the intramolecular hydrogen transfer in pentadiene. *J. Chem. Phys.*, **2007**, *127*, 114309.

[576] W. H. Miller; Y. Zhao; M. Ceotto; S. Yang. Quantum instanton approximation for thermal rate constants of chemical. *J. Chem. Phys.*, **2003**, *119*, 1329–1342.

[577] W. H. Miller. Semiclassical limit of quantum mechanical transition state theory for nonseparable systems. *J. Chem. Phys.*, **1975**, *62*, 1899.

[578] T. Yamamoto; W. H. Miller. On the efficient path integral evaluation of thermal rate constants with the quantum instanton approximation. *J. Chem. Phys.*, **2004**, *120*, 3086–3099.

[579] T. Yamamoto; W. H. Miller. Path integral evaluation of the quantum instanton rate constant for proton transfer in a polar solvent. *J. Chem. Phys.*, **2005**, *122*, 044106.

[580] W. H. Miller; S. D. Schwartz; J. W. Tromp. Quantum mechanical rate constants for bimolecular reactions. *J. Chem. Phys.*, **1983**, *79*, 4889–4898.

[581] A. T. Brünger; P. D. Adams; G. M. Clore; W. L. Delano; P. Gros; R. W. Grosse-Kunstleve; J.-S. Jiang; J. Kuszewski; M. Nilges; N. S. Pannu; R. J. Read; L. M. Rice; T. Simonson; G. L. Warren. Crystallography and NMR system (CNS): A new software system for macromolecular structure determination. *Acta Cryst. D*, **1998**, *54*, 905–921.

[582] N. Yu; H. P. Yennawar; K. M. Merz, Jr. Refinement of protein crystal structures using energy restraints derived from linear-scaling quantum mechanics . *Acta Cryst. D*, **2005**, *61*, 322–332.

[583] N. Yu; X. Li; G. Cui; S. Hayik; K. M. Merz, Jr. Critical assessment of quantum mechanics based energy restraints in protein crystal structure refinement. *Prot. Sci.*, **2006**, *15*, 2773–2784.

[584] H. Kopitz; A. Zivkovic; J. W. Engels; H. Gohlke. Determinants of the unexpected stability of RNA fluorobenzene self pairs. *ChemBioChem*, **2008**, *9*, 2619–2622.

[585] S. Fulle; H. Gohlke. Analyzing the flexibility of RNA structures by constraint counting. *Biophys. J.*, **2008**, *DOI:10.1529/biophysj.107.113415*.

[586] H. Gohlke; L. A. Kuhn; D. A. Case. Change in protein flexibility upon complex formation: Analysis of Ras-Raf using molecular dynamics and a molecular framework approach. *Proteins*, **2004**, *56*, 322–327.

[587] A. Ahmed; H. Gohlke. Multiscale modeling of macromolecular conformational changes combining concepts from rigidity and elastic network theory. *Proteins*, **2006**, *63*, 1038–1051.

[588] Y. Wu; H. L. Tepper; G. A. Voth. Flexible simple point-charge water model with improved liquid-state properties. *J. Chem. Phys.*, **2006**, *124*, 024503.

[589] D. J. Price; C. L. Brooks. A modified TIP3P water potential for simulation with Ewald summation. *J. Chem. Phys.*, **2004**, *121*, 10096–10103.

[590] H. W. Horn; W. C. Swope; J. W. Pitera; J. D. Madura; T. J. Dick; G. L. Hura; T. Head-Gordon. Development of an improved four-site water model for biomolecular simulations: TIP4P-Ew. *J. Chem. Phys.*, **2004**, *120*, 9665–9678.

[591] H. W. Horn; W. C. Swope; J. W. Pitera. Characterization of the TIP4P-Ew water model: Vapor pressure and boiling point. *J. Chem. Phys.*, **2005**, *123*, 194504.

[592] R. J. Woods. Derivation of net atomic charges from molecular electrostatic potentials. *J. Comput. Chem.*, **1990**, *11*, 29–310.

[593] M. L. DeMarco; R. J. Woods. Bridging computational biology and glycobiology: A game of snakes and ladders. *Glycobiology*, **2008**, *18*, 426–440.

[594] R. J. Woods. Restrained electrostatic potential charges for condensed phase simulations of carbohydrates. *J. Mol. Struct (Theochem)*, **2000**, *527*, 149–156.

[595] E. F. Pettersen; T. D. Goddard; C. C. Huang; G. S. Couch; D. M. Greenblatt; E. C. Meng; T. E. Ferrin. UCSF Chimera - A visualization system for exploratory research and analysis. *J. Comput. Chem.*, **2004**, *25*, 1605–1612.

[596] H. Sasaki; N. Ochi; A. Del; M. Fukuda. Site-specific glycosylation of human recombinant erythropoietin: Analysis of glycopeptides or peptides at each glycosylation site by fast atom bombardment mass spectrometry. *Biochemistry*, **1988**, *27*, 8618–8626.

[597] S. Dube; J. W. Fisher; J. S. Powell. Glycosylation at specific sites of erythropoietin is essential for biosynthesis, secretion, and biological function. *J. Biol. Chem.*, **1988**, *263*, 17516–17521.

[598] R. J. Darling; U. Kuchibhotla; W. Glaesner; R. Micanovic; D. R. Witcher; J. M. Beals. Glycosylation of erythropoietin effects receptor binding kinetics: Role of electrostatic interactions. *Biochemistry*, **2002**, *41*, 14524–14531.

[599] J. C. Cheetham; D. M. Smith; K. H. Aoki; J. L. Stevenson; T. J. Hoeffel; R. S. Syed; J. Egrie; T. S. Harvey. NMR structure of human erythropoietin and a comparison with its receptor bound conformation. *Nat. Struct. Biol.*, **1998**, *5*, 861–866.

[600] K. L. Dormann; R. Brueckner. Variable Synthesis of the Optically Active Thiotetronic Acid Antibiotics Thiolactomycin, Thiotetromycin, and 834-B1. *Angew. Chem. Int. Ed.*, **2007**, *46*, 1160–1163.

[601] E. Darve; A. Pohorille. Calculating free energies using average force. *J. Chem. Phys.*, **2001**, *115*, 9169–9183.

[602] A. Perez; I. Marchan; D. Svozil; J. Sponer; T. E. Cheatham; C. A. Laughton; M. Orozco. Refinement of the AMBER Force Field for Nucleic Acids: Improving the Description of alpha/gamma Conformers. *Biophys. J.*, **2007**, *92*, 3817–3829.

[603] L. Dang. Mechanism and thermodynamics of ion selectivity in aqueous solutions of 18-crown-6 ether: A molecular dynamics study. *J. Am. Chem. Soc.*, **1995**, *117*, 6954–6960.

[604] S. Joung; T. E. Cheatham, III. Determination of alkali and halide monovalent ion parameters for use in explicitly solvated biomolecular simulations. *J. Phys. Chem. B*, **2008**, *112*, 9020–9041.

[605] R. Aduri; B. T. Psciuk; P. Saro; H. Taniga; H. B. Schlegel; J. SantaLucia, Jr. AMBER force field parameters for the naturally occurring modified nucleosides in RNA. *J. Chem. Theory Comput.*, **2007**, *3*, 1465–1475.

[606] J. Shao; S. W. Tanner; N. Thompson; T. E. Cheatham, III. Clustering molecular dynamics trajectories: 1. Characterizing the performance of different clustering algorithms. *J. Chem. Theory Comput.*, **2007**, *3*, 2312–2334.

[607] P. Auffinger; T. E. Cheatham, III; A. C. Vaiana. Spontaneous formation of KCl aggregates in biomolecular simulations: a force field issue? *J. Chem. Theory Comput.*, **2007**, *3*, 1851–1859.

[608] J. Torras; G. Seabra; E. Deumens; S. B. Trickey; A. E. Roitberg. A versatile AMBER-Gaussian QM/MM interface through PUPIL. *J. Comput. Chem.*, **2008**, *29*, 1564–1573.

[609] J. Torras; Y. He; C. Cao; K. Muralidharan; E. Deumens; H. Cheng; S. Trickey. PUPIL: A systematic approach to software integration in multi-scale simulations. *Comput. Phys. Comm.*, **2007**, *177*, 265–279.

[610] P. Cieplak; F.-Y. Dupradeau; Y. Duan; J. Wang. Polarization effects in molecular mechanical force fields. *J. Phys.: Condens. Matter*, **2009**, *21*, 333102.

[611] Z. J. Shi; J. Shen. New inexact line search method for unconstrained optimization. *J. Optim. Theory Appl.*, **2005**, *127*, 425–446.

[612] A. D. MacKerell Jr.; D. Bashford; M. Bellott; R. L. Dunbrack; J. D. Evanseck; M. J. Field; S. Fischer; J. Gao; H. Guo; S. Ha; D. Joseph-McCarthy; L. Kuchnir; K. Kuczera; F. T. K. Lau; C. Mattos; S. Michnick; T. Ngo; D. T. Nguyen; B. Prodhom; W. E. Reiher; B. Roux; M. Schlenkrich; J. C. Smith; R. Stote; J. Straub; M. Watanabe; J. Wiorkiewicz-Kuczera; D. Yin; M. Karplus. All-Atom Empirical Potential for Molecular Modeling and Dynamics Studies of Proteins. *J. Phys. Chem. B*, **1998**, *102*, 3586–3616.

[613] A. D. MacKerell Jr.; N. Banavali; N. Foloppe. Development and current status of the CHARMM force field for nucleic acids. *Biopolymers*, **2000**, *56*, 257–265.

[614] B. R. Brooks; R. E. Bruccoleri; D. J. Olafson; D. J. States; S. Swaminathan; M. Karplus. CHARMM: A Program for Macromolecular Energy, Minimization, and Dynamics Calculations. *J. Computat. Chem.*, **1983**, *4*, 187–217.

[615] B. R. Brooks; C. L. Brooks; A. D. Mackerell; L. Nilsson; R. J. Petrella; B. Roux; Y. Won; G. Archontis; C. Bartels; S. Boresch; A. Caflisch; L. Caves; Q. Cui; A. R. Dinner; M. Feig; S. Fischer; J. Gao; M. Hodoscek; W. Im; K. Kuczera; T. Lazaridis; J. Ma; V. Ovchinnikov; E. Paci; R. W. Pastor; C. B. Post; J. Z. Pu; M. Schaefer; B. Tidor; R. M. Venable; H. L. Woodcock; X. Wu; W. Yang; D. M. York; M. Karplus. CHARMM: the biomolecular simulation program. *J. Comput. Chem.*, **2009**, *30*, 1545–1614.

[616] A. D. MacKerell, Jr.; M. Feig; C. L. Brooks III. Improved Treatment of the Protein Backbone in Empirical Force Fields. *J. Am. Chem. Soc.*, **2004**, *126*, 698–699.

[617] A. D. MacKerell, Jr.; M. Feig; C. L. Brooks III. Extending the treatment of backbone energetics in protein force fields: Limitations of gas-phase quantum mechanics in reproducing protein conformational distributions in molecular dynamics simulations. *J. Computat. Chem.*, **2004**, *25*, 1400–1415.

[618] M. F. Crowley; M. J. Williamson; R. C. Walker. CHAMBER: Comprehensive support for CHARMM force fields within the AMBER software. *Int. J. Quant. Chem.*, **2009**, *109*, 3767–3772.

[619] B. J. Berne; G. D. Harp. *Adv. Chem. Phys.*, **1970**, *17*, 63.

[620] R. Kubo; M. Toda; N. Hashitsume. *Statistical Physics II: Nonequilibrium Statistical Mechanics, 2nd ed.* Springer-Verlag, Heidelberg, 1991.

[621] W. H. Miller. *Adv. Chem. Phys.*, **1974**, *25*, 69.

[622] W. H. Miller. Including quantum effects in the dynamics of complex (i.e., large) molecular systems. *J. Chem. Phys.*, **2006**, *125*, 132305.

[623] H. Wang; X. Sun; W. H. Miller. Semiclassical approximations for the calculation of thermal rate constants for chemical reactions in complex molecular systems. *J. Chem. Phys.*, **1998**, *108*, 9726.

[624] X. Sun; H. Wang; W. H. Miller. Semiclassical theory of electronically nonadiabatic dynamics: Results of a linearized approximation to the initial value representation. *J. Chem. Phys.*, **1998**, *109*, 7064.

[625] J. Liu; W. H. Miller. A simple model for the treatment of imaginary frequencies in chemical reaction rates and molecular liquids. *J. Chem. Phys.*, **2009**, *131*, 074113.

[626] J. Liu; W. H. Miller; F. Paesani; W. Zhang; D. A. Case. Quantum dynamical effects in liquid water: A semiclassical study on the diffusion and the infrared absorption spectrum. *J. Chem. Phys.*, **2009**, *131*, 164509.

[627] J. Liu. Recent advances in the linearized semiclassical initial value representation/classical wigner model for the thermal correlation function. *International Journal of Quantum Chemistry*, **2015**, *115*, 657–670.

[628] J. Liu; W. H. Miller. Real time correlation function in a single phase space integral beyond the linearized semiclassical initial value representation. *J. Chem. Phys.*, **2007**, *126*, 234110.

[629] J. Liu; W. H. Miller. Test of the consistency of various linearized semiclassical initial value time correlation functions in application to inelastic neutron scattering from liquid para-hydrogen. *J. Chem. Phys.*, **2008**, *128*, 144511.

[630] J. W. Ponder; C. Wu; P. Ren; V. S. Pande; J. D. Chodera; M. J. Schieders; I. Haque; D. L. Mobley; D. S. Lambrecht; R. A. DiStasio, Jr.; M. Head-Gordon; G. N. I. Clark; M. E. Johnson; T. Head-Gordon. Current status of the AMOEBA polarizable force field. *J. Phys. Chem. B*, **2010**, *114*, 2549–2564.

[631] L. Wickstrom; A. Okur; C. Simmerling. Evaluating the performance of the ff99SB force field based on NMR scalar coupling data. *Biophys. J.*, **2009**, *97*, 853–856.

[632] Q. Shi; E. Giva. *J. Chem. Phys. A*, **2003**, *107*, 9059.

[633] M.-J. Hsieh; R. Luo. Balancing simulation accuracy and efficiency with the Amber united atom force field. *J. Phys. Chem. B*, **2010**, *114*, 2886–2893.

[634] C. Bergonzo; A. J. Campbell; R. C. Walker; C. Simmerling. A Partial Nudged Elastic Band Implementation for Use with Large or Explicitly Solvated Systems. *Int J Quantum Chem*, **2009**, *109*, 3781–3790.

[635] Q. T. Wang; R. A. Bryce. Improved hydrogen bonding at the NDDO-type semiempirical quantum mechanical/molecular mechanical interface. *J. Chem. Theory Comput.*, **2009**, *5*, 2206–2211.

[636] I. Omelyan; A. Kovalenko. MTS-MD of biomolecules steered with 3D-RISM-KH mean solvation forces accelerated with generalized solvation force extrapolation. *J. Chem. Theory Comput.*, **2015**, *11*, 1875–1895.

[637] J.-F. Truchon; B. M. Pettitt; P. Labute. A cavity corrected 3D-RISM functional for accurate solvation free energies. *J. Chem. Theory Comput.*, **2014**, *10*, 934–941.

[638] V. Sergiievskyi; G. Jeanmairet; M. Levesque; D. Borgis. Solvation free-energy pressure corrections in the three dimensional reference interaction site model. *J. Chem. Phys.*, **2015**, *143*, 184116.

[639] F. Hirata, Ed. *Molecular Theory of Solvation*. Kluwer Academic Publishers, 2003.

[640] A. Kovalenko; S. Ten-No; F. Hirata. Solution of three-dimensional reference interaction site model and hypernetted chain equations for simple point charge water by modified method of direct inversion in iterative subspace. *J. Comput. Chem*, **1999**, *20*, 928–936.

[641] M. E. Tuckerman; B. J. Berne; G. J. Martyna. Molecular dynamics algorithm for multiple time scales: Systems with long range forces. *J. Chem. Phys.*, **1991**, *94*, 6811–6815.

[642] M. Tuckerman; B. J. Berne; G. J. Martyna. Reversible multiple time scale molecular dynamics. *J. Chem. Phys.*, **1992**, *97*, 1990–2001.

[643] H. Grubmuumlller; H. Heller; A. Windemuth; K. Schulten. Generalized Verlet algorithm for efficient molecular dynamics simulations with long-range interactions. *Mol. Simulat.*, **1991**, *6*, 121–142.

[644] J. S. Perkyns; B. M. Pettitt. A site-site theory for finite concentration saline solutions. *J. Chem. Phys.*, **1992**, *97*, 7656–7666.

[645] A. W. Goetz; M. J. Williamson; D. Xu; D. Poole; S. L. Grand; R. C. Walker. Routine microsecond molecular dynamics simulations with AMBER - Part I: Generalized Born. *J. Chem. Theory Comput.*, **2012**, *8*, 1542–1555.

[646] R. Salomon-Ferrer; A. W. Goetz; D. Poole; S. L. Grand; R. C. Walker. Routine microsecond molecular dynamics simulations with AMBER - Part 2: Explicit Solvent Particle Mesh Ewald . *J. Chem. Theory Comput.*, **2012**, *in review*.

[647] T. Schlick. *Molecular modeling and simulation: an interdisciplinary guide*. Springer-Verlag New York, Inc., Secaucus, NJ, USA, 2002.

[648] M. K. Gilson; M. Davis; B. A. Luty; J. A. McCammon. Computation of electrostatic forces on solvated molecules using the Poisson-Boltzmann equation. *J Phys Chem*, **1993**, *97*, 3591–3600.

[649] D. W. Li; R. Brüschweiler. NMR-based protein potentials. *Angew. Chem. Int. Ed.*, **2010**, *49*, 6778–6780.

[650] K. Lindorff-Larsen; S. Piana; K. Palmo; P. Maragakis; J. Klepeis; R. O. Dror; D. E. Shaw. Improved side-chain torsion potentials for the Amber ff99SB protein force field. *Proteins*, **2010**, *78*, 1950–1958.

[651] P. Banáš; D. Hollas; M. Zgarbová; P. Jurecka; M. Orozco; T. E. Cheatham, III; J. Šponer; M. Otyepka. Performance of molecular mechanics force fields for RNA simulations: Stability of UUCG and GNRA hairpins. *J. Chem. Theory. Comput.*, **2010**, *6*, 3836–3849.

[652] R. Anandakrishnan; A. V. Onufriev. An N log N approximation based on the natural organization of biomolecules for speeding up the computation of long range interactions. *J. Comput. Chem.*, **2010**, *31*, 691–706.

[653] R. Anandakrishnan; M. Daga; A. V. Onufriev. An n log n Generalized Born Approximation. *J. Chem. Theory Comput.*, **2011**, *7*, 544–559.

[654] W. K. Olson; M. Bansal; S. K. Burley; R. E. Dickerson; M. Gerstein; S. C. Harvey; U. Heinemann; X.-J. Lu; S. Neidle; Z. Shakked; H. Sklenar; M. Suzuki; C.-S. Tung; E. Westhof; C. Wolberger; H. M. Berman. A standard reference frame for the description of nucleic acid base-pair geometry. *J. Mol. Biol.*, **2001**, *313*, 229–237.

[655] D. S. Cerutti; R. E. Duke; T. A. Darden; T. P. Lybrand. Staggered Mesh Ewald: An Extension of the Smooth Particle-Mesh Ewald Method Adding Great Versatility. *J. Chem. Theory Computat.*, **2009**, *5*, 2322–2338.

[656] D. S. Cerutti; D. A. Case. Multi-Level Ewald: A Hybrid Multigrid/Fast Fourier Transform Approach to the Electrostatic Particle-Mesh Problem. *J. Chem. Theory Comput.*, **2010**, *6*, 443–458.

[657] D. S. Cerutti; P. L. Freddolino; R. E. Duke, Jr.; D. A. Case. Simulations of a Protein Crystal with a High Resolution X-ray Structure: Evaluation of Force Fields and Water Models . *J. Phys. Chem. B*, **2010**, pp 12811–12824.

[658] M. B. Peters; Y. Yang; B. Wang; L. Fusti-Molnar; M. N. Weaver; K. M. Merz, Jr. Structural Survey of Zinc-Containing Proteins and Development of the Zinc AMBER Force Field (ZAFF). *J. Chem. Theor. Comput.*, **2010**, *6*, 2935–2947.

[659] M.-J. Hsieh; R. Luo. Exploring a coarse-grained distributive strategy for finite-difference poisson-boltzmann calculations. *J. Molec. Model.*, **2011**.

[660] I. Yildirim; H. A. Stern; S. D. Kennedy; J. D. Tubbs; D. H. Turner. Reparameterization of RNA chi Torsion Parameters for the AMBER Force Field and Comparison to NMR Spectra for Cytidine and Uridine . *J. Chem. Theory Comput.*, **2010**, *6*, 1520–1531.

[661] I. S. Joung; T. E. Cheatham, III. Molecular dynamics simulations of the dynamic and energetic properties of alkali and halide ions using water-model-specific ion parameters. *J. Phys. Chem. B*, **2009**, *113*, 13279–13290.

[662] I. Yildirim; H. A. Stern; J. D. Tubbs; S. D. Kennedy; D. H. Turner. Benchmarking AMBER Force Fields for RNA: Comparisons to NMR Spectra for Single-Stranded r(GACC) Are Improved by Revised chi Torsions. *J. Phys. Chem. B*, **2011**, *115*, 9261–9270.

[663] D. S. Palmer; A. I. Frolov; E. L. Ratkova; M. V. Fedorov. Towards a universal method for calculating hydration free energies: a 3D reference interaction site model with partial molar volume correction. *J. Phys.: Condens. Matter*, **2010**, *22*, 492101.

[664] M. Zgarbova; M. Otyepka; J. Sponer; A. Mladek; P. Banas; T. E. Cheatham; P. Jurecka. Refinement of the Cornell et al. Nucleic Acids Force Field Based on Reference Quantum Chemical Calculations of Glycosidic Torsion Profiles. *J. Chem. Theory Comput.*, **2011**, *7*, 2886–2902.

[665] C. Perez; F. Lohr; H. Ruterjans; J. M. Schmidt. Self-Consistent Karplus Parameterization of (3)J couplings depending on the polypeptide side-chain torsion chi(1). *J. Am. Chem. Soc.*, **2001**, *123*, 7081–7093.

[666] J. J. Chou; D. A. Case; A. Bax. Insights into the mobility of methyl-bearing side chains in proteins. *J. Am. Chem. Soc.*, **2003**, *125*, 8959–8966.

[667] H.-A. Yu; B. Roux; M. Karplus. Solvation thermodynamics: An approach from analytic temperature derivatives. *J. Chem. Phys.*, **1990**, *92*, 5020–5033.

[668] T. Yamazaki; N. Blinov; D. Wishart; A. Kovalenko. Hydration effects on the HET-s prion and amyloid-β2 fibrillous aggregates, studied with three-dimensional molecular theory of solvation. *Biophys. J.*, **2008**, *95*, 4540–4548.

[669] T. Yamazaki; A. Kovalenko; V. V. Murashov; G. N. Patey. Ion solvation in a water-urea mixture. *J. Phys. Chem. B*, **2010**, *114*, 613–619.

[670] N. Homeyer; H. Gohlke. Free energy calculations by the molecular mechanics poisson-boltzmann surface area method. *Mol. Informatics*, **2012**, *DOI: 10.1002/minf.201100135*.

[671] V. Wong; D. A. Case. Evaluating rotational diffusion from protein md simulations. *J. Phys. Chem. B*, **2008**, *112*, 6013–6024.

[672] D. Hamelberg; C. A. F. de Oliveira; J. McCammon. Sampling of slow diffusive conformational transitions with accelerated molecular dynamics. *J. Chem. Phys.*, **2007**, *127*, 155102–155109.

[673] B. J. Grant; A. A. Gorfe; J. A. McCammon. Ras conformational switching: Simulating nucleotide-dependent conformational transitions with accelerated molecular dynamics. *PLoS Computat. Biol.*, **2009**, *5*, e1000325.

[674] C. A. F. de Oliveira; B. J. Grant; M. Zhou; J. A. McCammon. Large-scale conformational changes of trypanosoma cruzi proline racemase predicted by accelerated molecular dynamics simulation. *PLoS Computat. Biol.*, **2011**, *7*, e1002178.

[675] L. C. T. Pierce; R. Salomon-Ferrer; C. A. F. de Oliveira; J. A. McCammon; R. C. Walker. Routine access to milli-second time scales with accelerated molecular dynamics. *J. Chem. Theory Comput.*, **2012**, *8*, 2997–3002.

[676] D. Hamelberg; J. Mongan; J. A. McCammon. Accelerated molecular dynamics: A promising and efficient simulation method for biomolecules. *J. Chem. Phys.*, **2004**, *120*, 11919–11929.

[677] U. Doshi; D. Hamelberg. Reoptimization of the amber forcefield for peptide bond (omega) torsions using accelerated molecular dynamics. *J. Chem. Phys. B*, **2009**, *113*, 16590–16595.

[678] X. Lu; W. Olson. 3dna: a software package for the analysis, rebuilding and visualization of three-dimensional nucleic acid structures. *NUCLEIC ACIDS RESEARCH*, **2003**, *31*, 5108–5121.

[679] C. Altona; M. Sundaralingam. Conformational analysis of the sugar ring in nucleosides and nucleotides. a new description using the concept of pseudorotation. *J Am Chem Soc*, **1972**, *94*, 8205–8212.

[680] S. Harvey; M. Prabhakaran. Ribose puckering - structure, dynamics, energetics, and the pseudorotation cycle. *J Am Chem Soc*, **1986**, *108*, 6128–6136.

[681] D. Cremer; J. Pople. A general definition of ring puckering coordinates. *J Am Chem Soc*, **1975**, *97*, 1354–1358.

[682] G. te Velde; F. M. Bickelhaupt; E. J. Baerends; C. F. Guerra; S. J. A. van Gisbergen; J. G. Snijders; T. Ziegler. Chemistry with ADF. *J. Comp. Chem.*, **2001**, *22*, 931–967.

[683] ADF2011, SCM, Theoretical Chemistry, Vrije Universiteit, Amsterdam, The Netherlands, http://www.scm.com, 2012.

[684] M. W. Schmidt; K. K. Baldridge; J. A. Boatz; S. T. Elbert; M. S. Gordon; J. H. Jensen; S. Koseki; N. Matsunaga; K. A. Nguyen; S. Su; T. L. Windus; M. Dupuis; J. A. Montgomery, Jr. General atomic and molecular electronic structure system. *J. Comp. Chem.*, **1993**, *14*, 1347–1363.

[685] M. Valiev; E. J. Bylaska; N. Govind; K. Kowalski; T. P. Straatsma; H. J. J. van Dam; D. Wang; J. Niepolcha; E. Apra; T. L. Windus; W. A. de Jong. Nwchem: a comprehensive and scalable open-source solution for large scale molecular simulations. *Comput. Phys. Commun.*, **2010**, *181*, 1477.

[686] M. S. Gordon; M. W. Schmidt. in *Theory and Applications of Computational Chemistry, the first forty years*, C. E. Dykstra; G. Frenking; K. S. Kim; G. E. Scuseria, Eds., chapter 41, pp 1167–1189. Elsevier, Asterdam, 2005.

[687] F. Neese. ORCA - an ab initio, Density Functional and Semiempirical program package, Version 2.8.0, University of Bonn, 2010.

[688] I. S. Ufimtsev; T. J. Martinez. Quantum chemistry on graphical processing units. 3. Analytical energy gradients, geometry optimization, and first principles molecular dynamics. *J. Chem. Theory Comput.*, **2009**, *5*, 2619–2628.

[689] T. Gaillard; D. A. Case. Evaluation of DNA Force Fields in Implicit Solvation. *J. Chem. Theory Comput.*, **2011**, *7*, 3181–3198.

[690] Y. Meng; A. E. Roitberg. Constant pH replica exchange molecular dynamics in biomolecules using a discrete protonation model. *J. Chem. Theory Comput.*, **2010**, *6*, 1401–1412.

[691] Y. Meng; D. Sabri Dashti; A. E. Roitberg. Computing Alchemical Free Energy Differences with Hamiltonian Replica Exchange Molecular Dynamics (H-REMD) Simulations. *J. Chem. Theory Comput.*, **2011**, *7*, 2721–2727.

[692] D. Sabri Dashti; A. E. Roitberg. Optimization of Umbrella Sampling Replica Exchange Molecular Dynamics by Replica Positioning. *J. Chem. Theory Comput.*, **2013**, *9*, 4692–4699.

[693] D. Sabri Dashti; A. E. Roitberg. Calculating the pKa Shift of Titratable Group at Position 66 of Staphylococcal Nuclease Mutant with the Replica Exchange Free Energy Perturbation method (REFEP). *In preparation*, **2012**.

[694] D. Sabri Dashti; Y. Meng; A. E. Roitberg. pH-Replica Exchange Molecular Dynamics in Proteins Using a Discrete Protonation Method. *J. Phys. Chem. B*, **2012**, *116*, 8805–8811.

[695] A. Pohorille; C. Jarzynski; C. Chipot. Good practices in Free-Energy calculations. *J. Phys. Chem. B*, **2010**, *114*, 10235–10253.

[696] M. R. Shirts; J. D. Chodera. Statistically optimal analysis of samples from multiple equilibrium states. *J. Chem. Phys.*, **2008**, *129*, 124105–124105–10.

[697] Å. Skjevik; B. D. Madej; R. C. Walker; K. Teigen. Lipid11: A modular framework for lipid simulations using amber. *J. Phys. Chem. B*, **2012**, *116*, 11124–11136.

[698] D. L. Mobley; C. I. Bayly; M. D. Cooper; M. R. Shirts; K. A. Dill. Small Molecule Hydration Free Energies in Explicit Solvent: An Extensive Test of Fixed-Charge Atomistic Simulations. *J. Chem. Theory Comput.*, **2009**, *5*, 350–358.

[699] X. Wu; B. R. Brooks. A virtual mixture approach to the study of multistate equilibrium: application to constant ph simulation in explicit water. *PLOS Computational Biology*, **2015**, *11*, e1004480.

[700] P. G. Karamertzanis; P. Raiteri; A. Galindo. The use of anisotropic potentials in modeling water and free energies of hydration. *J. Chem. Theory Comput.*, **2010**, *6*, 3153–3161.

[701] J. Wang; P. Cieplak; J. Li; T. Hou; R. Luo; Y. Duan. Development of Polarizable Models for Molecular Mechanical Calculations I: Parameterization of Atomic Polarizability. *J. Phys. Chem. B*, **2011**, *115*, 3091–3099.

[702] J. Wang; P. Cieplak; J. Li; J. Wang; Q. Cai; M. Hsieh; H. Lei; R. Luo; Y. Duan. Development of Polarizable Models for Molecular Mechanical Calculations II: Induced Dipole Models Significantly Improve Accuracy of Intermolecular Interaction Energies. *J. Phys. Chem. B*, **2011**, *115*, 3100–3111.

[703] J. Wang; P. Cieplak; J. Li; Q. Cai; M. Hsieh; R. Luo; Y. Duan. Development of Polarizable Models for Molecular Mechanical Calculations. 4. van der Waals Parametrization. *J. Phys. Chem. B*, **2012**, *116*, 7088–7101.

[704] J. Wang; P. Cieplak; Q. Cai; M. Hsieh; J. Wang; Y. Duan; R. Luo. Development of Polarizable Models for Molecular Mechanical Calculations. 3. Polarizable Water Models Conforming to Thole Polarization Screening Schemes. *J. Phys. Chem. B*, **2012**, *116*, 7999–8008.

[705] J. Wang; Q. Cai; Y. Xiang; R. Luo. Reducing Grid Dependence in Finite-Difference Poisson-Boltzmann Calculations. *J. Chem. Theory Comput.*, **2012**, *8*, 2741–2751.

[706] B. T. Thole. Molecular polarizabilities calculated with a modified dipole interaction. *Chem. Phys.*, **1981**, *59*, 341–350.

[707] R. Bosque; J. Sales. Polarizabilities of solvents from the chemical composition. *J. Chem. Inf. Comput. Sci.*, **2002**, *42*, 1154–1163.

[708] Z. X. Wang; C. Wu; H. X. Lei; Y. Duan. Accurate ab initio study on the hydrogen-bond pairs in protein secondary structures. *J. Chem. Theory Comput.*, **2007**, *3*, 1527–1537.

[709] J. Graf; P. H. Nguyen; G. Stock; H. Schwalbe. Structure and Dynamics of the Homologous Series of Alanine Peptides: A Joint Molecular Dynamics/NMR Study. *J. Am. Chem. Soc.*, **2007**, *129*, 1179–1189.

[710] T. E. Cheatham, III. Simulation and modeling of nucleic acid structure, dynamics and interactions. *Curr. Opin. Struct. Biol.*, **2004**, *14*, 360–367.

[711] I. Yildirim; S. D. Kennedy; H. A. Stern; J. M. Hart; R. Kierzek; D. H. Turner. Revision of AMBER Torsional Parameters for RNA Improves Free Energy Predictions for Tetramer Duplexes with GC and iGiC Base Pairs. *J. Chem. Theory Comput.*, **2012**, *8*, 172–181.

[712] M. Krepl; M. Zgarbova; P. Stadlbauer; M. Otyepka; P. Banas; J. Koca; T. E. Cheatham, III; J. Sponer. Reference simulations of noncanonical nucleic acids with different chi variants of the AMBER force field: Quadruplex DNA, quadruplex RNA, and Z-DNA. *J. Chem. Theory Comp.*, **2012**, *8*, 2506–2520.

[713] J. Wang; T. Hou. Application of Molecular Dynamics Simulations in Molecular Property Prediction. II. Diffusion coefficient. *J. Comput. Chem.*, **2011**, *32*, 3509–3519.

[714] C. F. Fu; S. X. Tian. A Comparative Study for Molecular Dynamics Simulations of Liquid Benzene. *J. Chem. Theory Comput.*, **2011**, *7*, 2240–2252.

[715] S. Tsuzuki; T. Uchimaru; K. Tanabe; S. Kuwajima. Refinement of Nonbonding Interaction Potential Parameters for Methane on the Basis of the Pair Potential Obtained by Mp3/6-311g(3d,3p)-Level Ab-Initio Molecular-Orbital Calculations - the Anisotropy of H/H Interaction. *J. Phys. Chem.*, **1994**, *98*, 1830–1833.

[716] G. A. Kaminski; R. A. Friesner; J. Tirado-Rives; W. L. Jorgensen. Evaluation and Reparametrization of the OPLS-AA Force Field for Proteins via Comparison with Accurate Quantum Chemical Calculations on Peptides. *J. Phys. Chem. B*, **2001**, *105*, 6474–6487.

[717] I. J. Chen; D. Yin; A. D. MacKerell. Combined Ab initio/Empirical Approach for Optimization of Lennard-Jones Parameters for Polar-Neutral Compounds. *J. Comput. Chem.*, **2002**, *23*, 199–213.

[718] M. L. DeMarco; R. J. Woods. Atomic-resolution conformational analysis of the G(M3) ganglioside in a lipid bilayer and its implications for ganglioside-protein recognition at membrane surfaces. *Glycobiology*, **2009**, *19*, 344–355.

[719] M. L. DeMarco; R. J. Woods; J. H. Prestegard; F. Tian. Presentation of Membrane-Anchored Glycosphingolipids Determined from Molecular Dynamics Simulations and NMR Paramagnetic Relaxation Rate Enhancement. *J. Am. Chem. Soc.*, **2010**, *132*, 1334–1338.

[720] R. Kadirvelraj; O. C. Grant; I. J. Goldstein; H. C. Winter; H. Tateno; E. Fadda; R. J. Woods. Structure and binding analysis of Polyporus squamosus lectin in complex with the Neu5Acα2-6Galβ1-4GlcNAc human-type influenza receptor. *Glycobiology*, **2011**, *21*, 973–984.

[721] B. L. Foley; M. B. Tessier; R. J. Woods. Carbohydrate force fields. *WIREs Comput. Mol. Sci.*, **2012**, *2*, 652–697.

[722] E. Ficko-Blean; C. P. Stuart; M. D. Suits; M. Cid; M. Tessier; R. J. Woods; A. B. Boraston. Carbohydrate Recognition by an Architecturally Complex α-N-Acetylglucosaminidase from Clostridium perfringens. *PLoS ONE*, **2012**, *7*, e33524.

[723] M. L. DeMarco; R. J. Woods. From agonist to antagonist: Structure and dynamics of innate immune glycoprotein MD-2 upon recognition of variably acylated bacterial endotoxins. *Mol. Immunol.*, **2011**, *49*, 124–133.

[724] N. Spackova; T. E. Cheatham; F. Ryjacek; F. Lankas; L. vanMeervelt; P. Hobza; J. Sponer. Molecular Dynamics Simulations and Thermodynamics Analysis of DNA-Drug Complexes. Minor Groove Binding between 4',6-Diamidino-2-phenylindole and DNA Duplexes in Solution. *J. Am. Chem. Soc.*, **2003**, *125*, 1759–1769.

[725] P. Varnai; D. Djuranovic; R. Lavery; B. Hartmann. alpha/gamma Transitions in the B-DNA backbone. *Nucl. Acids Res.*, **2002**, *30*, 5398–5406.

[726] D. Svozil; J. E. Sponer; I. Marchan; A. Perez; T. E. Cheatham; F. Forti; F. J. Luque; M. Orozco; J. Sponer. Geometrical and electronic structure variability of the sugar-phosphate backbone in nucleic acids. *J. Phys. Chem. B*, **2008**, *112*, 8188–8197.

[727] D. S. Cerutti; J. E. Rice; W. C. Swope; D. A. Case. Derivation of fixed partial charges for amino acids accommodating a specific water model and implicit polarization. *J. Phys. Chem. B*, **2103**, *117*, 2328–2338.

[728] T. Steinbrecher; J. Latzer; D. A. Case. Revised AMBER Parameters for Bioorganic Phosphates. *J. Chem. Theory Comput.*, **2012**, *8*, 4405–4412.

[729] F.-Y. Dupradeau; A. Pigache; T. Zaffran; C. Savineau; R. Lelong; N. Grivel; D. Lelong; W. Rosanskia; P. Cieplak. The R. E. D. tools: advances in RESP and ESP charge derivation and force field library building. *PhysChemChemPhys*, **2010**, *12*, 7821–7839.

[730] S. E. Feller. Molecular dynamics simulations of lipid bilayers. *Curr. Opin. Colloid Interface Sci.*, **2000**, *5*, 217–223.

[731] A. Lomize; I. Pogozheva; M. Lomize; H. Mosberg. The role of hydrophobic interactions in positioning of peripheral proteins in membranes. *BMC Struct. Biol.*, **2007**, *7*, 44.

[732] C. J. Dickson; L. Rosso; R. M. Betz; R. C. Walker; I. R. Gould. GAFFlipid: a General Amber Force Field for the accurate molecular dynamics simulation of phospholipid. *Soft Matter*, **2012**, *8*, 9617.

[733] R. M. Betz; N. A. DeBardeleben; R. C. Walker. An Investigation of the effects of hard and soft errors on graphics processing unit-accelerated molecular dynamics simulations. *Concurrency and Computation: Practice and Experience*, **2014**, *26*, 2134.

[734] D. E. Warschawski; P. F. Devaux. Order parameters of unsaturated phospholipids in membranes and the effect of cholesterol: a 1H-13C solid-state NMR study at natural abundance. *Eur. Biophys. J.*, **2005**, *34*, 987–996.

[735] L. Saiz; M. L. Klein. Computer Simulation Studies of Model Biological Membranes. *Acc. Chem. Res.*, **2002**, *35*, 482–489.

[736] J. T. Berryman; T. Schilling. Free Energies by Thermodynamic Integration Relative to an Exact Solution, Used to Find the Handedness-Switching Salt Concentration for DNA. *J. Chem. Theory Comput.*, **2013**, *9*, 679–686.

[737] J. T. Berryman; T. Schilling. Absolute Free Energies for Biomolecules in Implicit or Explicit Solvent. *Physics Procedia*, **2014**, *57*, 7–15.

[738] T. Schilling; F. Schmid. Computing absolute free energies of disordered structures by molecular simulation. *J. Chem. Phys.*, **2009**, *131*, 231102.

[739] F. Schmid; T. Schilling. A method to compute absolute free energies or enthalpies of fluids. *Physics Procedia*, **2010**, *4*, 131–143.

[740] D. Frenkel; A. J. C. Ladd. New Monte Carlo method to compute the free energy of arbitrary solids. Application to the fcc and hcp phases of hard spheres. *J. Chem. Phys.*, **1984**, *81*, 3188–3193.

[741] C. Vega; E. G. Noya. Revisiting the Frenkel-Ladd method to compute the free energy of solids: the Einstein molecule approach. *J. Chem. Phys.*, **2007**, *127*, 154113.

[742] J. M. Swails; A. E. Roitberg. Enhancing Conformation and Protonation State Sampling of Hen Egg White Lysozyme Using pH Replica Exchange Molecular Dynamics. *J. Chem. Theory Comput.*, **2012**, *8*, 4393–4404.

[743] S. G. Itoh; A. Damjanovic; B. R. Brooks. pH replica-exchange method based on discrete protonation states. *Proteins*, **2011**, *79*, 3420–3436.

[744] S. A. Showalter; R. Brüschweiler. Validation of molecular dynamics simulations of biomolecules using NMR spin relaxation as benchmarks: Application to the Amber99SB force field. *J. Chem. Theory Comput.*, **2007**, *3*, 961–975.

[745] R. B. Best; N.-V. Buchete; G. Hummer. Are Current Molecular Dynamics Force Fields too Helical? *Biophys. J.*, **2008**, *95*, L07–L09; 4494.

[746] R. B. Best; G. Hummer. Optimized Molecular Dynamics Force Fields Applied to the Helix-Coil Transition of Polypeptides. *J. Phys. Chem. B*, **2009**, *113*, 9904–9015.

[747] R. B. Best; J. Mittal. Free-energy landscape of the GB1 hairpin in all-atom explicit solvent simulations with different force fields: Similarities and differences. *Proteins*, **2011**, *79*, 1318–1328.

[748] K. K. Patapati; N. M. Glykos. Three force fields views of the 3-10 helix. *Biophys. J.*, **2011**, *101*, 1766–1771.

[749] S. Le Grand; A. W. Goetz; R. C. Walker. SPFP: Speed without compromise–A mixed precision model for GPU accelerated molecular dynamics simulations. *Comput. Phys. Commun.*, **2013**, *184*, 374–380.

[750] R. Salomon-Ferrer; D. A. Case; R. C. Walker. An overview of the Amber biomolecular simulation package. *WIREs Comput. Mol. Sci.*, **2013**, *3*, 198–210.

[751] PDB Current Holdings Breakdown. **2013**.

[752] M. L. Lundstrom, K. H.; Chiu. *G Protein-Coupled Receptors in Drug Discovery*. Taylor & Francis, London, 2005.

[753] C. Chipot; A. Pohorille, eds. *Free energy calculations. Theory and Applications in Chemistry and Biology*. Springer, Berlin, 2007.

[754] M. Griebel; S. Knapek; G. Zumbusch. *Numerical Simulation in Molecular Dynamics. Numerical Algorithms, Parallelization, Applications*. Springer-Verlag, Berlin, 2010.

[755] M. E. Tuckerman. *Statistical Mechanics: Theory and Molecular Simulation*. Oxford University Press, Oxford, 2010.

[756] M. Ester; H. Kriegel; J. Sander; X. Xu. A Density-Based Algorithm for Discovering Clusters in Large Spatial Databases with Noise. *Proc. Second Int. Conf. Knowledge Disc. Data Mining (KDD-96)*, **1996**, pp 226–231.

[757] B. R. Miller; T. D. McGee; J. M. Swails; N. Homeyer; H. Gohlke; A. E. Roitberg. MMPBSA.py: An Efficient Program for End-State Free Energy Calculations. *J. Chem. Theory Comput.*, **2012**, *8*, 3314–3321.

[758] D. R. Roe; T. E. Cheatham, III. PTRAJ and CPPTRAJ: Software for Processing and Analysis of Molecular Dynamics Trajectory Data. *J. Chem. Theory Comput.*, **2013**, *9*, 3084–3095.

[759] J. M. Swails; D. M. York; A. E. Roitberg. Constant pH replica exchange molecular dynamics in explicit solvent using discrete protonation states: implementation, testing, and validation. *J. Chem. Theory Comput.*, **2014**, *10*, 1341–1352.

[760] M. Arrar; C. A. F. de Oliveira; M. Fajer; W. Sinko; J. A. McCammon. w-REXAMD: A Hamiltonian Replica Exchange Approach to Improve Free Energy Calculations for Systems with Kinetically Trapped Conformations. *J. Chem. Theory Comput.*, **2013**, *9*, 18–23.

[761] M. Fajer; D. Hamelberg; J. A. McCammon. Replica-Exchange Accelerated Molecular Dynamics (REX-AMD) Applied to Thermodynamic Integration. *J. Chem. Theory Comput.*, **2008**, *4*, 1565–1569.

[762] P. Li; B. P. Roberts; D. K. Chakravorty; K. M. Merz, Jr. Rational Design of Particle Mesh Ewald Compatible Lennard-Jones Parameters for +2 Metal Cations in Explicit Solvent. *J. Chem. Theory Comput.*, **2013**, *9*, 2733–2748.

[763] P. Li; L. F. Song; K. M. Merz, Jr. Parameterization of Highly Charged Metal Ions Using the 12-6-4 LJ-Type Nonbonded Model in Explicit Water. *J. Phys. Chem. B*, **2015**, *119*, 883–895.

[764] P. Li; L. F. Song; K. M. Merz, Jr. Systematic Parameterization of Monovalent Ions Employing the Non-bonded Model. *J. Chem. Theory Comput.*, **2015**, *11*, 1645–1657.

[765] M. T. Panteva; G. M. Giambasu; D. M. York. Comparison of Structural, Thermodynamic, Kinetic and Mass Transport Properties of Mg2+ Models Commonly Used in Biomolecular Simulations. *J. Comput. Chem.*, **2015**, *36*, 970–982.

[766] M. T. Panteva; G. M. Giambasu; D. M. York. Force Field for Mg2+, Mn2+, Zn2+ and Cd2+ Ions That Have Balanced Interactions with Nucleic Acids. *J. Phys. Chem. B*, **2015**, *119*, 15460–15470.

[767] A. Ganguly; B. P. Weissman; T. J. Giese; N.-A. Li; S. Hoshika; S. Rao; A. A. Benner; J. A. Piccirilli; D. M. York. Confluence of theory and experiment reveals the catalytic mechanism of the Varkud satellite ribozyme. *Nat. Chem.*, **2020**, *12*, 192–201.

[768] P. Li; K. M. Merz, Jr. MCPB.py: A Python Based Metal Center Parameter Builder. *J. Chem. Inf. Model.*, **2016**, *56*, 599–604.

[769] P. Li; K. M. Merz, Jr. Metal Ion Modeling Using Classical Mechanics. *Chem. Rev.*, **2017**, *117*, 1564–1686.

[770] Z. Yu; P. Li; K. M. Merz, Jr. Extended Zinc AMBER Force Field (EZAFF). *J. Chem. Theory Comput.*, **2018**, *14*, 242–254.

[771] A. Sengupta; A. Seitz; K. M. Merz, Jr. Simulating the Chelate Effect. *J. Am. Chem. Soc.*, **2018**, *140*, 15166–15169.

[772] Z. Li; S. F. Lin; P. Li; K. M. Merz, Jr. Systematic Parametrization of Divalent Metal Ions for the OPC3, OPC, TIP3P-FB, and TIP4P-FB Water Models. *J. Chem. Theory Comput.*, **2020**, *16*, 4429–4442.

[773] S. F. Lin; A. Sengupta; K. M. Merz, Jr. Thermodynamics of Transition Metal Ion Binding to Proteins. *J. Am. Chem. Soc.*, **2020**, *142*, 6365–6374.

[774] P. Li; K. M. Merz, Jr. in *Methods Mol. Biol.*, (Humana Press, New York, NY). volume 2199. pp 257–275. 2021.

[775] A. Sengupta; Z. Li; S. F. Lin; P. Li; K. M. Merz, Jr. Parameterization of Monovalent Ions for the OPC3, OPC, TIP3P-FB, and TIP4P-FB Water Models. *J. Chem. Inf. Model.*, **2021**, *61*, 869–880.

[776] Z. Li; S. F. Lin; P. Li; K. M. Merz, Jr. Parametrization of Trivalent and Tetravalent Metal Ions for the OPC3, OPC, TIP3P-FB, and TIP4P-FB Water Models. *J. Chem. Theory Comput.*, **2021**, *17*, 2342–2354.

[777] J. M. Seminario. Calculation of Intramolecular Force Fields from Second-Derivative Tensors. *Int. J. Quantum Chem.*, **1996**, *30*, 1271–1277.

[778] P. Eastman; V. S. Pande. OpenMM: A Hardware-Independent Framework for Molecular Simulations. *Computing in Science and Engineering*, **2010**, *12*, 34–39.

[779] P. Eastman; M. S. Friedrichs; J. D. Chodera; R. J. Radmer; C. M. Bruns; J. P. Ku; K. A. Beauchamp; T. J. Lane; L. Wang; D. Shukla; T. Tye; M. Houston; T. Stich; C. Klein; M. R. Shirts; V. S. Pande. OpenMM 4: A Reusable, Extensible, Hardware Independent Library for High Performance Molecular Simulation. *J. Chem. Theory Comput.*, **2013**, *9*, 461–469.

[780] J. M. Swails. *Free Energy Simulations of Complex Biological Systems at Constant pH*. PhD thesis, University of Florida, 2013.

[781] C. N. Nguyen; T. Kurtzman Young; M. K. Gilson. Grid Inhomogeneous solvation theory: Hydration structure and thermodynamics of the miniature receptor cucurbit[7]uril. *J. Chem. Phys.*, **2012**, *137*, 044101–044118.

[782] C. Bergonzo; N. M. Henriksen; D. R. Roe; J. M. Swails; A. E. Roitberg; T. E. Cheatham III. Multidimensional Replica Exchange Molecular Dynamics Yields a Converged Ensemble of an RNA Tetranucleotide. *J. Chem. Theory Comput.*, **2013**, *10*, 492–499.

[783] A. Bakan; L. M. Meireles; I. Bahar. ProDy: Protein Dynamics Inferred from Theory and Experiments. *Bioinformatics*, **2011**, *27*, 1575–1577.

[784] X. Wu; M. Hodoscek; B. R. Brooks. Replica exchanging self-guided Langevin dynamics for efficient and accurate conformational sampling. *J. Chem. Phys.*, **2012**, *137*, 044106.

[785] N. Bernstein; C. Várnai; I. Solt; S. A. Winfield; M. C. Payne; I. Simon; M. Fuxreiter; G. Csányi. *Phys. Chem. Chem. Phys.*, **2011**, *14*, 646–656.

[786] C. Várnai; N. Bernstein; L. Mones; G. Csányi. Tests of an adaptive qm/mm calculation on free energy profiles of chemical reactions in solution. *J. Phys. Chem. B*, **2013**, *117*, 12202–12211.

[787] G. Csányi; T. Albaret; G. Moras; M. C. Payne; A. D. Vita. Multiscale hybrid simulation methods for material systems. *J. Phys. Condens. Matt.*, **2005**, *17*, R691.

[788] N. Bernstein; J. R. Kermode; G. Csányi. Hybrid atomistic simulation methods for materials systems. *Rep. Prog. Phys.*, **2009**, *72*, 026501.

[789] A. Jones; B. Leimkuhler. Adaptive stochastic methods for sampling driven molecular systems. *J. Chem. Phys.*, **2011**, *135*, 084125.

[790] T. Kerdcharoen; B. M. Rode. A QM/MM simulation method applied to the solution of Li+ in liquid ammonia. *Chem. Phys.*, **1996**, *211*, 313–323.

[791] N. Homeyer; H. Gohlke. FEW - A workflow tool for free energy calculations of ligand binding. *J. Comput. Chem.*, **2013**, *34*, 965–973.

[792] A. Metz. *Goethe University (Frankfurt am Main)*, **2006**.

[793] J. Åqvist; C. Medina; J. E. Samuelsson. A new method for predicting binding affinity in computer-aided drug design. *Protein Eng.*, **1994**, *7*, 385–391.

[794] J. Åqvist; V. B. Luzhkov; B. O. Brandsdal. Ligand binding affinities from MD simulations. *Acc. Chem. Res.*, **2002**, *35*, 358–365.

[795] H. G. Wallnoefer; K. R. Liedl; T. Fox. A challenging system: free energy prediction for factor Xa. *J. Comput. Chem.*, **2011**, *32*, 1743–1752.

[796] M. M. van Lipzig; A. M. ter Laak; A. Jongejan; N. P. Vermeulen; M. Wamelink; D. Geerke; J. H. Meerman. Prediction of ligand binding affinity and orientation of xenoestrogens to the estrogen receptor by molecular dynamics simulations and the linear interaction energy method. *J. Med. Chem.*, **2004**, *47*, 1018–1030.

[797] B. O. Brandsdal; F. Österberg; M. Almlöf; I. Feierberg; V. B. Luzhkov; Åqvist, J. Free energy calculations and ligand binding. *Adv. Protein Chem.*, **2003**, *66*, 123–158.

[798] W. Wang; J. Wang; P. A. Kollman. What determines the van der Waals coefficient beta in the LIE (linear interaction energy) method to estimate binding free energies using molecular dynamics simulations? *Proteins: Struct., Funct., Genet.*, **1999**, *34*, 395–402.

[799] D. K. Jones-Hertzog; W. L. Jorgensen. Binding affinities for sulfonamide inhibitors with human thrombin using Monte Carlo simulations with a linear response method. *J. Med. Chem.*, **1997**, *40*, 1539–1549.

[800] M. L. Lamb; J. Tirado-Rives; W. L. Jorgensen. Estimation of the binding affinities of FKBP12 inhibitors using a linear response method. *Bioorg. Med. Chem.*, **1999**, *7*, 851–860.

[801] W. Yang; R. Bitetti-Putzer; K. M. Free energy simulations: Use of reverse cumulative averaging to determine the equilibrated region and the time required for convergence. *J. Chem. Phys.*, **2004**, *120*, 2618–2628.

[802] J. B. Kruskal. On the shortest spanning subtree of a graph and the traveling salesman problem. *Proc. Amer. Math. Soc.*, **1956**, *7*, 48–50.

[803] *ROCS, OpenEye Scientific Software, Santa Fe, http://www.eyesopen.com.*

[804] P. C. D. Hawkins; A. G. Skillman; A. Nicholls. Comparison of shape-matching and docking as virtual screening tools. *J. Med. Chem.*, **2007**, *50*, 74–82.

[805] T. E. Cheatham; D. A. Case. Twenty-five years of nucleic acid simulations. *Biopolymers*, **2013**, *99*, 969–977.

[806] C. J. Cramer. *Essentials of Computational Chemistry: Theories and Models*. John Wiley & Sons, New York, 2002.

[807] T. Lazaridis. Inhomogeneous Fluid Approach to Solvation Thermodynamics. 1 Theory. *J. Phys. Chem. B*, **1998**, *102*, 3531–3541.

[808] C. N. Nguyen; T. Kurtzman Young; M. K. Gilson. Grid Inhomogeneous Solvation Theory: Hydration Structure and Thermodynamics of the Miniature Receptor cucurbit[7]uril. *J. Chem. Phys.*, **2012**, *137*, 044101.

[809] S. Chatterjee; P. G. Debenedetti; F. H. Stillinger; R. M. Lynden-Bell. A Computational Investigation of Thermodynamics, Structure, Dynamics and Solvation Behavior in Modified Water Models. *J. Chem. Phys.*, **2008**, *128*, 124511.

[810] W. Humphrey; A. Dalke; K. Schulten. VMD Visual Molecular Dynamics. *J. Molec. Graph.*, **1996**, *14*, 33–38.

[811] D. J. Sindhikara; N. Yoshida; F. Hirata. Placevent: An Algorithm for Prediction of Explicit Solvent Atom Distribution-Application to HIV-1 Protease and F-ATP Synthase. *J. Comput. Chem.*, **2012**, *33*, 1536–1543.

[812] C. J. Dickson; B. D. Madej; A. A. Skjevik; R. M. Betz; K. Teigen; I. R. Gould; R. C. Walker. Lipid14: The Amber Lipid Force Field. *J. Chem. Theory Comput.*, **2014**, *10*, 865–879.

[813] R. Konecny; N. A. Baker; J. A. McCammon. iAPBS: a programming interface to the adaptive Poisson–Boltzmann solver. *Comput. Sci. Disc.*, **2012**, *5*, 15005–15013.

[814] R. Anandakrishnan; C. Baker; S. Izadi; A. V. Onufriev. Point charges optimally placed to represent the multipole expansion of charge distributions. *PloS one*, **2013**, *8*, e67715.

[815] D. P. Fernandez; A. R. H. Goodwin; E. W. Lemmon; J. M. H. Levelt Sengers; R. C. Williams. A formulation for the static permittivity of water and steam at temperatures from 238 k to 873 k at pressures up to 1200 mpa, including derivatives and debye huckel coefficients. *J. Phys. Chem. Ref. Data*, **1997**, *26*, 1125–1166.

[816] R. Mills. Self-diffusion in normal and heavy water in the range 1-45. deg. *J. Phys. Chem.*, **1973**, *77*, 685–688.

[817] W. Wagner; A. Pruss. The iapws formulation 1995 for the thermodynamic properties of ordinary water substance for general and scientific use. *J. Phys. Chem. Ref. Data*, **2002**, *31*, 387–535.

[818] L. B. Skinner; C. Huang; D. Schlesinger; L. G. M. Pettersson; A. Nilsson; C. J. Benmore. Benchmark oxygen-oxygen pair-distribution function of ambient water from x-ray diffraction measurements with a wide q-range. *J. Chem. Phys.*, **2013**, *138*, 074506+.

[819] G. S. Kell. Precise representation of volume properties of water at one atmosphere. *J. Chem. Eng. Data*, **1967**, *12*, 66–69.

[820] S. Niu; M. L. Tan; T. Ichiye. The large quadrupole of water molecules. *J. Chem. Phys.*, **2011**, *134*, 134501+.

[821] S. Izadi; R. Anandakrishnan; A. V. Onufriev. Building Water Models: A Different Approach. *J. Phys. Chem. Lett.*, **2014**, *5*, 3863–3871.

[822] A. Mukhopadhyay; A. T. Fenley; I. S. Tolokh; A. V. Onufriev. Charge hydration asymmetry: the basic principle and how to use it to test and improve water models. *J. Phys. Chem. B*, **2012**, *116*, 9776–9783.

[823] B. Aguilar; R. Shadrach; A. V. Onufriev. Reducing the secondary structure bias in the generalized born model via r6 effective radii. *J. Chem. Theory Comput.*, **2010**, *6*, 3613–3630.

[824] B. Aguilar; A. V. Onufriev. Efficient computation of the total solvation energy of small molecules via the r6 generalized born model. *J. Chem. Theory Comput.*, **2012**, *8*, 2404–2411.

[825] A. Mukhopadhyay; B. H. Aguilar; I. S. Tolokh; A. V. Onufriev. Introducing charge hydration asymmetry into the generalized born model. *J Chem. Theory Comput.*, **2014**, *10*, 1788–1794.

[826] B. Schneider; S. Neidle; H. M. Berman. Conformations of the sugar-phosphate backbone in helical dna crystal structures. *Biopolymers*, **1997**, *42*, 113–124.

[827] B. Schneider; Z. Moravek; H. M. Berman. Rna conformational classes. *Nucleic Acids Res.*, **2004**, *32*, 1666–1677.

[828] G. Monard; M. I. Bernal-Uruchurtu; A. Van Der Vaart; K. M. Merz, Jr.; M. F. Ruiz-López. Simulation of liquid water using semiempirical Hamiltonians and the divide and conquer approach. *J. Phys. Chem. A*, **2005**, *109*, 3425–3432.

[829] A. Marion; G. Monard; M. F. Ruiz-López; F. Ingrosso. Water interactions with hydrophobic groups: assessment and recalibration of semiempirical molecular orbital methods. *J. Chem. Phys.*, **2014**, *141*, 034106.

[830] A. Marion; H. Gockan; G. Monard. SemiEmpirical Born-Oppenheimer Molecular Dynamics (SEBOMD) Within the Amber Biomolecular Package. *J. Chem. Inf. Model.*, **2019**, *59*, 206–214.

[831] E. Thiriot; G. Monard. Combining a genetic algorithm with a linear scaling semiempirical method for protein-ligand docking. *J. Mol. Struct. Theochem*, **2009**, *898*, 31–41.

[832] W. Harb; M. I. Bernal-Uruchurtu; M. F. Ruiz-López. An improved semiempirical method for hydrated systems. *Theor. Chem. Acc.*, **2004**, *112*, 204–216.

[833] M. I. Bernal-Uruchurtu; M. T. C. Martins-costa; C. Millot; M. F. Ruiz-López. Improving Description of Hydrogen Bonds at the Semiempirical Level : Water - Water Interactions as Test Case. *J. Comput. Chem.*, **2000**, *21*, 572–581.

[834] O. Ludwig; H. Schinke; W. Brandt. Reparametrisation of Force Constants in MOPAC 6.0/7.0 for Better Description of the Activation Barrier of Peptide Bond Rotations. *J. Molec. Model.*, **1996**, *2*, 341–350.

[835] M. Zgarbová; F. J. Luque; J. Šponer; T. E. C. III; M. Otyepka; P. Jurečka. Toward improved description of dna backbone: Revisiting epsilon and zeta torsion force field parameters. *J. Chem. Theory Comput.*, **2013**, *9*, 2339–2354.

[836] I. Omelyan; A. Kovalenko. Generalized canonical-isokinetic ensemble: Speeding up multiscale molecular dynamics and coupling with 3d molecular theory of solvation. *Mol. Sim.*, **2013**, *39*, 25–48.

[837] I. Omelyan; A. Kovalenko. Multiple time step molecular dynamics in the optimized isokinetic ensemble steered with the molecular theory of solvation: Accelerating with advanced extrapolation of effective solvation forces. *J. Chem. Phys.*, **2013**, *139*, 244106.

[838] D. S. Cerutti; W. C. Swope; J. E. Rice; D. A. Case. ff14ipq: A Self-Consistent Force Field for Condensed-Phase Simulations of Proteins. *J. Chem. Theory Comput.*, **2014**, *10*, 4515–4534.

[839] B. D. Madej; I. R. Gould; R. C. Walker. A Parameterization of Cholesterol for Mixed Lipid Bilayer Simulation within the Amber Lipid14 Force Field. *J Phys Chem B*, **2015**, *119*, 12424–12435.

[840] C. Vega; J. L. F. Abascal. Simulating water with rigid non-polarizable models: a general perspective. *Phys Chem Chem Phys*, **2011**, *13*, 19663–19688.

[841] P. H. Hunenberger; A. E. Mark; W. F. van Gunsteren. Fluctuation and Cross-correlation Analysis of Protein Motions Observed in Nanosecond Molecular Dynamics Simulations. *J. Mol. Biol.*, **1995**, *252*, 492–503.

[842] R. Galindo-Murillo; D. R. Roe; T. E. Cheatham, III. Convergence and reproducibility in molecular dynamics simulations of the DNA duplex d(GCACGAACGAACGAACGC). *Biochim. Biophys. Acta*, **2015**, *1850*, 1041–1058.

[843] G. M. Giambasu; T. Luchko; D. Herschlag; D. M. York; D. A. Case. Ion counting from explicit-solvent simulations and 3d-RISM. *Biophys J*, **2014**, *106*, 883–894.

[844] I. S. Joung; T. Luchko; D. A. Case. Simple electrolyte solutions: Comparison of DRISM and molecular dynamics results for alkali halide solutions. *J Chem Phys*, **2013**, *138*, 044103.

[845] J. Domanski; P. Stansfeld; M. S. P. Sansom; O. Beckstein. Lipidbook: A Public Repository for Force Field Parameters Used in Membrane Simulations. *J. Membrane Biol.*, **2010**, *236*, 255–258.

[846] S. Jo; T. Kim; W. Im. Automated builder and database of protein/membrane complexes for molecular dynamics simulations. *PLoS One*, **2007**, *2*, e880.

[847] S. Jo; T. Kim; V. G. Iyer; I. W. CHARMM-GUI: a web-based graphical user interface for CHARMM. *J. Comput. Chem.*, **2008**, *29*, 1859–1865.

[848] S. Jo; J. B. Lim; J. B. Klauda; W. Im. CHARMM-GUI Membrane Builder for mixed bilayers and its application to yeast membranes. *Biophys. J.*, **2009**, *97*, 50–58.

[849] E. L. Wu; X. Cheng; S. Jo; H. Rui; K. C. Song; E. M. Davila-Contreras; Y. Qi; J. Lee; V. Monje-Galvan; R. M. Venable; J. B. Klauda; I. W. CHARMM-GUI Membrane Builder toward realistic biological membrane simulations. *J. Comput. Chem.*, **2014**, *35*, 1997–2004.

[850] N. A. Baker; D. Sept; J. Simpson; M. J. Holst; M. J. A. Electrostatics of nanosystems: application to microtubules and the ribosome. *Proc. Natl. Acad. Sci. U. S. A.*, **2001**, *98*, 10037–10041.

[851] M. Holst; F. Saied. Multigrid solution of the Poisson-Boltzmann equation. *J. Comput. Chem.*, **1993**, *14*, 105–113.

[852] M. Holst; F. Saied. Numerical solution of the nonlinear Poisson-Boltzmann equation: Developing more robust and efficient methods. *J. Comput. Chem.*, **1995**, *16*, 337–364.

[853] M. Holst. Adaptive numerical treatment of elliptic systems on manifolds. *Adv. Comput. Math.*, **2001**, *15*, 139–191.

[854] R. Bank; M. Holst. A New Paradigm for Parallel Adaptive Meshing Algorithms. *SIAM Review*, **2003**, *45*, 291–323.

[855] K. M. Callenberg; O. P. Choudhary; G. L. de Forest; D. W. Gohara; N. A. Baker; M. Grabe. APBSmem: A graphical interface for electrostatic calculations at the membrane. *PLoS One*, **2010**, *5*, e12722.

[856] H. Nymeyer; H. X. Zhou. A method to determine dielectric constants in nonhomogeneous systems: application to biological membranes. *Biophys. J.*, **2008**, *94*, 1185–1193.

[857] H. A. Stern; S. E. Feller. Calculation of the dielectric permittivity profile for a nonuniform system: application to a lipid bilayer simulation. *J. Chem. Phys.*, **2003**, *118*, 3401–3412.

[858] N. Homeyer; H. Gohlke. Extension of the free energy workflow FEW towards implicit solvent/implicit membrane MM-PBSA calculations. *BBA - Gen. Subjects*, **2015**, *1850*, 972–982.

[859] L. Waeschenbach; C. G. W. Gertzen; V. Keitel; H. Gohlke. Dimerization energetics of the G-protein coupled bile acid receptor TGR5 from all-atom simulations. *J. Comput. Chem.*, **2019**, *41*.

[860] J. Z. Ruscio; D. Kumar; M. Shukla; M. G. Prisant; T. M. Murali; A. V. Onufriev. Atomic level computational identification of ligand migration pathways between solvent and binding site in myoglobin. *Proc. Nat. Acad. Sci. USA*, **2008**, *105*, 9204–9209.

[861] N. Homeyer; A. H. C. Horn; H. Lanig; H. Sticht. AMBER force-field parameters for phosphorylated amino acids in different protonation states: phosphoserine, phosphothreonine, phosphotyrosine, and phosphohistidine. *J. Mol. Model.*, **2006**, *12*, 281–289.

[862] M. Grabe; H. Lecar; Y. N. Jan; J. L. Y. A quantitative assessment of models for voltage-dependent gating of ion channels. *Proc. Natl. Acad. Sci. U. S. A.*, **2004**, *101*, 17640–17645.

[863] J. A. Maier; C. Martinez; K. Kasavajhala; L. Wickstrom; K. E. Hauser; C. Simmerling. ff14SB: Improving the Accuracy of Protein Side Chain and Backbone Parameters from ff99SB. *J. Chem. Theory Comput.*, **2015**, *11*, 3696–3713.

[864] K. Takemura; A. Kitao. Water Model Tuning for Improved Reproduction of Rotational Diffusion and NMR Spectral Density. *J. Phys. Chem. B*, **2012**, *116*, 6279–6287.

[865] L.-P. Wang; T. J. Martinez; V. S. Pande. Building force fields: An automatic, systematic and reproducible approach. *J. Phys. Chem. Lett.*, **2014**, *5*, 1885–1891.

[866] I. Omelyan; A. Kovalenko. MTS-MD of Biomolecules Steered with 3D-RISM-KH Mean Solvation Forces Accelerated with Generalized Solvation Force Extrapolation. *J. Chem. Theor. and Comp.*, **2014**, *11*, 1875–1895.

[867] H. Nguyen; D. R. Roe; J. M. Swails; D. A. Case. PYTRAJ: Interactive data analysis for molecular dynamics simulations. *Manuscript in preparation*, **2016**.

[868] D. L. Blood; A. M. Rosnik; B. P. Krueger. Molecular dynamics parameters for the gfp chromophore and some of its analogues. *Manuscript in preparation*, **2016**.

[869] I. Ivani; P. D. Dans; A. Noy; A. Pérez; I. Faustino; A. Hopsital; J. Walther; P. Andrió; R. Goni; A. Balaceanu; G. Portella; F. Battistini; J. L. GelpÃ; C. González; M. Vendruscolo; C. A. Laughton; S. Harris; D. A. Case; M. Orozco. Parmbsc1: A refined force field for DNA simulations. *Nature Meth.*, **2016**, *13*, 55–58.

[870] M. Zgarbová; J. Sponer; M. Otyepka; T. E. Cheatham, III; R. Galindo-Murillo; P. Jurečka. Refinement of the Sugar-Phosphate Backbone Torsion Beta for AMBER Force Fields Improves the Description of Z- and B-DNA. *J. Chem. Theor. and Comp.*, **2015**, *12*, 5723–5736.

[871] Y. Miao; V. A. Feher; J. A. McCammon. Gaussian Accelerated Molecular Dynamics: Unconstrained Enhanced Sampling and Free Energy Calculation. *J. Chem. Theory Comput.*, **2015**, *11*, 3584–3595.

[872] Y. Miao; W. Sinko; L. Pierce; D. Bucher; R. C. Walker; J. A. McCammon. Improved Reweighting of Accelerated Molecular Dynamics Simulations for Free Energy Calculation. *J. Chem. Theory Comput.*, **2014**, *10*, 2677–2689.

[873] C. Bergonzo; T. E. C. III. Improved force field parameters lead to a better description of rna structure. *J. of Chem. Theory Comput.*, **2015**, *11*, 3969–3972.

[874] K. Gao; J. Yin; N. M. Henriksen; A. T. Fenley; M. K. Gilson. Binding enthalpy calculations for a neutral host-guest pair yield widely divergent salt effects across water models. *J. of Chem. Theory Comput.*, **2015**, *11*, 4555–4564.

[875] S. Izadi; B. Aguilar; A. V. Onufriev. Protein-ligand electrostatic binding free energies from explicit and implicit solvation. *J. Chem. Theory Comput.*, **2015**, *11*, 4450–4459.

[876] C. Torrence; G. P. Compo. A practical guide to wavelet analysis. *Bull. Am. Meteorol. Soc.*, **1998**, *79*, 61–78.

[877] N. C. Benson; V. Dagget. Wavelet analysis of protein motion. *Int. J. Wavelets Multi.*, **2012**, *10*.

[878] A. Rodriguez; A. Laio. Clustering by fast search and find of density peaks. *Science*, **2014**, *344*, 1492–1496.

[879] D. R. Roe; C. Bergonzo; T. E. C. III. Evaluation of enhanced sampling provided by accelerated molecular dynamics with hamiltonian replica exchange methods. *J. Phys. Chem. B*, **2014**, *118*, 3543–3552.

[880] M. A. E. Hassan; C. R. Calladine. Two distinct modes of protein-induced bending in dna. *J. Mol. Biol.*, **1998**, *282*, 331–343.

[881] K. T. Debiec; D. S. Cerutti; L. R. Baker; A. M. Gronenborn; D. A. Case; L. T. Chong. Further along the Road Less Traveled: AMBER ff15ipq, an Original Protein Force Field Built on a Self-Consistent Physical Model. *J. Chem. Theory Comput.*, **2016**, *12*, 3926–3947.

[882] R. Galindo-Murillo; J. C. Robertson; M. Zgarbovic; J. Sponer; M. Otyepka; P. Jureska; T. E. Cheatham. Assessing the Current State of Amber Force Field Modifications for DNA. *J. Chem. Theory Comput.*, **2016**, *12*, 4114–4127.

[883] S. Izadi; A. V. Onufriev. Accuracy limit of rigid 3-point water models. *J. Chem. Phys.*, **2016**, *145*, 074501.

[884] S. Izadi; R. Anandakrishnan; A. V. Onufriev. Implicit solvent model for Million-Atom atomistic simulations: Insights into the organization of 30-nm chromatin fiber. *J. Chem. Theory Comput.*, **2016**, *12*, 5946–5959.

[885] A. H. Aytenfisu; A. Spasic; A. Grossfield; H. A. Stern; D. H. Mathews. Revised RNA Dihedral Parameters for the Amber Force Field Improve RNA Molecular Dynamics. *J. Chem. Theory Comput.*, **2017**, *13*, 900–915.

[886] T. Luchko; N. Blinov; G. C. Linon; K. P. Joyce; A. Kovalenko. SAMPL5: 3D-RISM partition coefficient calculations with partial molar volume corrections and solute conformational sampling. *J. Comput. Aided Mol. Design*, **2016**, *30*, 1115–1127.

[887] Z. Heidari; D. R. Roe; R. Galindo-Murillo; J. B. Ghasemi; T. E. Cheatham, III. Using Wavelet Analysis To Assist in Identification of Significant Events in Molecular Dynamics Simulations. *J. Chem. Inf. Model.*, **2016**, *56*, 1282–1291.

[888] G. Cui; J. M. Swails; E. S. Manas. SPAM: A Simple Approach for Profiling Bound Water Molecules. *J. Chem. Theory Comput.*, **2013**, *9*, 5539–5549.

[889] L. Wang; K. A. McKiernan; J. Gomes; K. A. Beauchamp; T. Head-Gordon; J. E. Rice; W. C. Swope; T. J. MartÃnez; V. S. Pande. Building a More Predictive Protein Force Field: A Systematic and Reproducible Route to AMBER-FB15. *J. Phys. Chem. B*, **2017**, *121*, 4023–4039.

[890] N. Forouzesh; S. Izadi; A. V. Onufriev. Grid-Based Surface Generalized Born Model for Calculation of Electrostatic Binding Free Energies. *J. Chem. Inf. Model.*, **2017**, *57*, 2505–2513.

[891] D. S. Cerutti; K. T. Debiec; D. A. Case; L. T. Chong. Links between the charge model and bonded parameter force constants in biomolecular force fields. *J. Chem. Phys.*, **2017**, *147*, 161730.

[892] V. W. D. Cruzeiro; M. S. Amaral; A. E. Roitberg. Redox Potential Replica Exchange Molecular Dynamics at constant pH in AMBER: Implementation, Validation and Application. *J. Chem. Phys.*, **2018**, *149*, 072338.

[893] V. W. D. Cruzeiro; A. E. Roitberg. Multidimensional Replica Exchange Simulations for Efficient Constant pH and Redox Potential Molecular Dynamics. *J. Chem. Theory Comput.*, **2019**.

[894] J. Khandogin; C. L. Brooks, III. Constant pH molecular dynamics with proton tautomerism. *Biophys. J.*, **2005**, *89*, 141–157.

[895] J. Khandogin; C. L. Brooks, III. Toward the accurate first-principles prediction of ionization equilibria in proteins. *Biochemistry*, **2006**, *45*, 9363–9373.

[896] J. A. Wallace; J. K. Shen. Continuous constant pH molecular dynamics in explicit solvent with pH-based replica exchange. *J. Chem. Theory Comput.*, **2011**, *7*, 2617–2629.

[897] J. A. Wallace; J. K. Shen. Charge-leveling and proper treatment of long-range electrostatics in all-atom molecular dynamics at constant pH. *J. Chem. Phys.*, **2012**, *137*, 184105.

[898] W. Chen; J. A. Wallace; Z. Yue; J. K. Shen. Introducing titratable water to all-atom molecular dynamics at constant pH. *Biophys. J.*, **2013**, *105*, L15–L17.

[899] Y. Huang; W. Chen; J. A. Wallace; J. Shen. All-Atom continuous constant pH molecular dynamics with particle mesh Ewald and titratable water. *J. Chem. Theory Comput.*, **2016**, *12*, 5411–5421.

[900] Y. Huang; R. C. Harris; J. Shen. Generalized Born based continuous constant pH molecular dynamics in Amber: implementation, benchmarking, and analysis. *J. Chem. Inform. Model.*, **2018**, *58*, 1372–1383.

[901] R. C. Harris; J. Shen. GPU-Accelerated Implementation of Continuous Constant pH Molecular Dynamics in Amber: pKa Predictions with Single-pH Simulations. *J. Chem. Inform. Model.*, **2019**, *59*, 4821–4832.

[902] O. N. Starovoytov; H. Torabifard; G. A. Cisneros. Development of amoeba force field for 1,3-dimethylimidazolium based ionic liquids. *J. Phys. Chem. B*, **2014**, *118*, 7156–7166.

[903] Y.-J. Tu; Z. Lin; M. J. Allen; G. A. Cisneros. Molecular dynamics investigation of water-exchange reactions on lanthanide ions in water/1-ethyl-3-methylimidazolium trifluoromethylsufate ([emim][otf]). *J. Chem. Phys.*, **2018**, *148*, 024503.

[904] Y.-J. Tu; M. J. Allen; G. A. Cisneros. Simulations of the water exchange dynamics of lanthanide ions in 1-ethyl-3-methylimidazolium ethyl sulfate ([emim][etso4]) and water. *Phys. Chem. Chem. Phys.*, **2016**, *18*, 30323–30333.

[905] H. Torabifard; O. N. Starovoytov; P. Ren; G. A. Cisneros. Development of an amoeba water model using gem distributed multipoles. *Theo. Chem. Acc.*, **2015**, *134*, 1–10.

[906] H. Torabifard; L. Reed; M. T. Berry; J. E. Hein; E. Menke; G. A. Cisneros. Computational and experimental characterization of a pyrrolidinium-based ionic liquid for electrolyte applications. *J. Chem. Phys.*, **2017**, *147*, 161731.

[907] G. A. Cisneros. Application of gaussian electrostatic model (gem) distributed multipoles in the amoeba force field. *J. Chem. Theo. Comput.*, **2012**, *12*, 5072–5080.

[908] G. A. Cisneros; J.-P. Piquemal; T. A. Darden. Generalization of the gaussian electrostatic model: extension to arbitrary angular momentum, distributed multipoles and computational speedup with reciprocal space methods. *J. Chem. Phys.*, **2006**, *125*, 184101.

[909] J.-P. Piquemal; G. A. Cisneros; P. Reinhardt; N. Gresh; T. A. Darden. Towards a force field based on density fitting. *J. Chem. Phys.*, **2006**, *124*, 104101.

[910] J.-P. Piquemal; G. Cisneros. in *Many-body effects and electrostatics in multi-scale computations of Biomolecules*, Q. Cui; P. Ren; M. Meuwly, Eds., pp 269–300. Pan Stanford Publishing, 2015.

[911] R. E. Duke; O. N. Starovoytov; J.-. Piquemal; G. A. Cisneros. Gem*: A molecular electronic density-based force field for molecular dynamics simulations. *J. Chem. Theo. Comput.*, **2014**, *10*, 1361–1365.

[912] Z. Zhang; X. Liu; K. Yan; M. Tuckerman; J. Liu. Unified efficient thermostat scheme for the canonical ensemble with holonomic or isokinetic constraints via molecular dynamics. *J. Phys. Chem. A*, **2019**, *123*, 6056–6079.

[913] B. Leimkuhler; C. Matthews. Rational construction of stochastic numerical methods for molecular sampling. *Appl. Math. Res. eXpress*, **2013**, *2013*, 34–56.

[914] J.-P. Ryckaert; G. Ciccotti; H. J. Berendsen. Numerical integration of the cartesian equations of motion of a system with constraints: molecular dynamics of n-alkanes. *J. of Computat. Phys.*, **1977**, *23*, 327 – 341.

[915] S. Myamoto; P. A. Kollman. Settle: An analytical version of the SHAKE and RATTLE algorithm for rigid water models. *J. Computat. Chem.*, **1992**, *13*, 952–962.

[916] H. C. Andersen. RATTLE: A "velocity" version of the shake algorithm for molecular dynamics calculations. *J. Computat. Phys.*, **1983**, *52*, 24 – 34.

[917] N. Gr"ønbech-Jensen; O. Farago. A simple and effective Verlet-type algorithm for simulating Langevin dynamics. *Mol. Phys.*, **2013**, *111*, 983–991.

[918] T. Nugent; D. T. Jones. Membrane protein orientation and refinement using a knowledge-based statistical potential. *BMC Bioinformatics*, **2013**, *14*, 276.

[919] S. Schott-Verdugo; H. Gohlke. PACKMOL-Memgen: A simple-to-use generalized workflow for membrane-protein/lipid-bilayer system building. *J. Chem. Inf. Model.*, **2019**, *59*, 2522–2528.

[920] L. Martínez; R. Andrade; E. G. Birgin; J. M. Martínez. PACKMOL: A package for building initial configurations for molecular dynamics simulations. *J. Comput. Chem.*, **2009**, *30*, 2157–2164.

[921] J. M. Martínez; L. Martínez. Packing optimization for automated generation of complex system's initial configurations for molecular dynamics and docking. *J. Computat. Chem.*, **2003**, *24*, 819–825.

[922] B. Ho. pdbremix. https://github.com/boscoh/pdbremix, 2018.

[923] X. Liu; J. Liu. Critical role of quantum dynamical effects in the Raman spectroscopy of liquid water. *Mol. Phys.*, **2018**, *116*, 755–779.

[924] H. C. Andersen. Molecular dynamics simulations at constant pressure and/or temperature. *J. Chem. Phys.*, **1980**, *72*, 2384–2393.

[925] C.-E. Chang; W. Chen; M. K. Gilson. Evaluating the Accuracy of the Quasiharmonic Approximation. *J. Chem. Theory Computat*, **2005**, *1*, 1017–1028. PMID: 26641917.

[926] D. A. McQuarrie. *Statistical Thermodynamics*. Harper and Row, New York, 1973.

[927] S. Izadi; R. C. Harris; M. O. Fenley; A. V. Onufriev. Accuracy comparison of generalized born models in the calculation of electrostatic binding free energies. *J. Chem. Theory Computat.*, **2018**, *14*, 1656–1670.

[928] H. Nguyen; D. A. Case; A. S. Rose. Nglview–interactive molecular graphics for jupyter notebooks. *Bioinformatics*, **2017**, *34*, 1241–1242.

[929] D. R. Roe; T. E. Cheatham III. Parallelization of CPPTRAJ enables large scale analysis of molecular dynamics trajectory data. *J. Computat. Chem.*, **2018**, *39*, 2110–2117.

[930] H. A. Boateng; R. Krasny. Comparison of treecodes for computing electrostatic potentials in charged particle systems with disjoint targets and sources. *J. Computat. Chem.*, **2013**, *34*, 2159–2167.

[931] Z.-H. Duan; R. Krasny. An adaptive treecode for computing nonbonded potential energy in classical molecular systems. *J. Computat. Chem.*, **2001**, *22*, 184–195.

[932] P. Li; H. Johnston; R. Krasny. A Cartesian treecode for screened Coulomb interactions. *J. Computat. Phys.*, **2009**, *228*, 3858–3868.

[933] T. Graen; M. Hoefling; H. Grubmueller. Amber-dyes: Characterization of charge fluctuations and force field parameterization of fluorescent dyes for molecular dynamics simulations. *Journal of Chemical Theory and Computation*, **2014**, *10*, 5505–5512.

[934] B. Schepers; H. Gohlke. Amber-dyes in amber: Implementation of fluorophore and linker parameters into ambertools. *Journal of Chemical Physics*, **2020**, *152*.

[935] S. Kalinin; T. Peulen; S. Sindbert; P. J. Rothwell; S. Berger; T. Restle; R. S. Goody; H. Gohlke; C. A. Seidel. A toolkit and benchmark study for fret-restrained high-precision structural modeling. *Nature Methods*, **2012**, *9*, 1218–1225.

[936] M. Dimura; T. O. Peulen; C. A. Hanke; A. Prakash; H. Gohlke; C. A. Seidel. Quantitative fret studies and integrative modeling unravel the structure and dynamics of biomolecular systems. *Curr. Opin. Struct. Biol.*, **2016**, *40*, 163–185.

[937] M. Dimura; T. O. Peulen; H. Sanabria; D. Rodnin; K. Hemmen; C. A. Seidel; H. Gohlke. Automated and optimally fret-assisted structural modeling. **2019**.

[938] R. T. McGibbon; K. A. Beauchamp; M. P. Harrigan; C. Klein; J. M. Swails; C. X. Hernandez; C. R. Schwantes; L.-P. Wang; T. J. Lane; V. S. Pande. Mdtraj: A modern open library for the analysis of molecular dynamics trajectories. *Biophys. J.*, **2015**, *109*, 1528–1532.

[939] A. Patriksson; D. van der Spoel. A temperature predictor for parallel tempering simulations. *Phys. Chem. Chem. Phys.*, **2008**, *10*, 2073–2077.

[940] P. S. Shabane; S. Izadi; A. V. Onufriev. General purpose water model can improve atomistic simulations of intrinsically disordered proteins. *Journal of Chemical Theory and Computation*, **2019**, *15*, 2620–2634.

[941] D. Pantoja-Uceda; J. L. Neira; L. M. Contreras; C. A. Manton; D. R. Welch; B. Rizzuti. The isolated C-terminal nuclear localization sequence of the breast cancer metastasis suppressor 1 is disordered. *Arch. Biochem. Biophys.*, **2019**, *664*, 95 – 101.

[942] D. Dans; D. Gallego; A. Balaceanu; L. Darre; H. Gomez; M. Orozco. Modeling, simulations, and bioinformatics at the service of rna structure. *Chem*, **2019**, *5*, 51 – 73.

[943] P. Kuhrova; V. Mlynsky; M. Zgarbova; M. Krepl; G. Bussi; R. B. Best; M. Otyepka; J. Sponer; P. Banas. Improving the performance of the Amber RNA force field by tuning the hydrogen-bonding interactions. *bioRxiv*, **2019**.

[944] A. Bochicchio; M. Krepl; F. Yang; G. Varani; J. Sponer; P. Carloni. Molecular basis for the increased affinity of an RNA recognition motif with re-engineered specificity: A molecular dynamics and enhanced sampling simulations study. *PLOS Computat. Biol.*, **2018**, *14*, 1–27.

[945] N. M. Kumbhar; J. S. Gopal. Structural significance of hypermodified nucleoside 5-carboxymethylaminomethyluridine (cmnm5U) from wobble (34th) position of mitochondrial tRNAs: Molecular modeling and Markov state model studies. *J. Molec. Graph. Model.*, **2019**, *86*, 66 – 83.

[946] F. Leonarski; M. Jasinski; J. Trylska. Thermodynamics of the fourU RNA thermal switch derived from molecular dynamics simulations and spectroscopic techniques. *Biochimie*, **2019**, *156*, 22 – 32.

[947] M. Havrila; M. Otyepka; P. Stadlbauer; J. Sponer; J. L. Mergny; P. Banas; P. Kuhrova. Structural dynamics of propeller loop: towards folding of RNA G-quadruplex. *Nucl. Acids Res.*, **2018**, *46*, 8754–8771.

[948] C. Yang; M. Kulkarni; M. Lim; Y. Pak. Insilico direct folding of thrombin-binding aptamer G-quadruplex at all-atom level. *Nucl. Acids Res.*, **2017**, *45*, 12648–12656.

[949] M. Javanainen; A. Lamberg; L. Cwiklik; I. Vattulainen; O. H. S. Ollila. Atomistic model for nearly quantitative simulations of langmuir monolayers. *Langmuir*, **2018**, *34*, 2565–2572. PMID: 28945973.

[950] O. H. S. Ollila; H. A. Heikkinen; H. IwaÃ¯. Rotational dynamics of proteins from spin relaxation times and molecular dynamics simulations. *The Journal of Physical Chemistry B*, **2018**, *122*, 6559–6569. PMID: 29812937.

[951] M. Kulkarni; C. Yang; Y. Pak. Refined alkali metal ion parameters for the opc water model. *Bulletin of the Korean Chemical Society*, **2018**, *39*, 931–935.

[952] R. G. FernÃ¡ndez; J. L. F. Abascal; C. Vega. The melting point of ice Ih for common water models calculated from direct coexistence of the solid-liquid interface. *The Journal of Chemical Physics*, **2006**, *124*, 144506.

[953] G. M. Giambasu; M. K. Gebala; M. T. Panteva; T. Luchko; D. A. Case; D. M. York. Competitive Interaction of Monovalent Cations with DNA from 3D-RISM. *Nucleic Acids Res.*, **2015**, *43*, 8405–8415.

[954] G. M. Giambasu; D. A. Case; D. M. York. Predicting Site-Binding Modes of Ions and Water to Nucleic Acids Using Molecular Solvation Theory. *J. Am. Chem. Soc.*, **2019**, *141*, 2435–2445.

[955] C. Nguyen; T. Yamazaki; A. Kovalenko; D. A. Case; M. K. Gilson; T. Kurtzman; T. Luchko. A molecular reconstruction approach to site-based 3D-RISM and comparison to GIST hydration thermodynamic maps in an enzyme active site. *PLoS One*, **2019**, *14*, e0219743.

[956] G. Bussi; D. Donadio; M. Parrinello. Canonical sampling through velocity rescaling. *The Journal of chemical physics*, **2007**, *126*, 014101.

[957] M. R. Machado; E. E. Barrera; F. Klein; M. Sonora; S. Silva; S. Pantano. The SIRAH 2.0 Force Field: Altius, Fortius, Citius. *J. Chem. Theory Comput.*, **2019**, *15*, 2719–2733. PMID: 30810317.

[958] P. D. Dans; A. Zeida; M. R. Machado; S. Pantano. A coarse grained model for atomic-detailed dna simulations with explicit electrostatics. *J. Chem. Theory Comput.*, **2010**, *6*, 1711–1725. PMID: 26615701.

[959] E. E. Barrera; M. R. Machado; S. Pantano. Fat sirah: Coarse-grained phospholipids to explore membrane-protein dynamics. *J. Chem. Theory Comput.*, **2019**, *15*, 5674–5688. PMID: 31433946.

[960] P. G. Garay; E. E. Barrera; S. Pantano. Post-translational modifications at the coarse-grained level with the sirah force field. *J. Chem. Inform. Model.*, **2020**, *60*, 964–973. PMID: 31840995.

[961] F. Klein; D. Cáceres; M. A. Carrasco; J. C. Tapia; J. Caballero; J. Alzate-Morales; S. Pantano. Coarse-Grained Parameters for Divalent Cations within the SIRAH Force Field. *J. Chem. Inf. Model.*, **2020**, *60*, 3935–3943.

[962] L. Darré; M. R. Machado; P. D. Dans; F. E. Herrera; S. Pantano. Another coarse grain model for aqueous solvation: Wat four? *J. Chem. Theory Comput.*, **2010**, *6*, 3793–3807.

[963] M. R. Machado; S. Pantano. SIRAH tools: mapping, backmapping and visualization of coarse-grained models. *Bioinformatics*, **2016**, *32*, 1568–1570.

[964] A. Zeida; M. R. Machado; P. D. Dans; S. Pantano. Breathing, bubbling, and bending: DNA flexibility from multimicrosecond simulations. *Phys. Rev. E*, **2012**, *86*, 021903.

[965] M. R. Machado; H. C. González; S. Pantano. Md simulations of viruslike particles with supra cg solvation affordable to desktop computers. *J. Chem. Theory Comput.*, **2017**, *13*, 5106–5116. PMID: 28876928.

[966] H. C. Gonzalez; L. Darré; S. Pantano. Transferable mixing of atomistic and coarse-grained water models. *J. Phys. Chem. B*, **2013**, *117*, 14438–14448. PMID: 24219057.

[967] M. R. Machado; P. D. Dans; S. Pantano. A hybrid all-atom/coarse grain model for multiscale simulations of dna. *Phys. Chem. Chem. Phys.*, **2011**, *13*, 18134–18144.

[968] M. R. Machado; S. Pantano. Exploring LacI–DNA Dynamics by Multiscale Simulations Using the SIRAH Force Field. *J. Chem. Theory Comput.*, **2015**, *11*, 5012–5023. PMID: 26574286.

[969] M. R. Machado; A. Zeida; L. Darré; S. Pantano. From quantum to subcellular scales: multi-scale simulation approaches and the sirah force field. *Interface Focus*, **2019**, *9*.

[970] R. Read; A. McCoy. A log-likelihood-gain intensity target for crystallographic phasing that accounts for experimental error. *Acta Cryst. D*, **2016**, *72*, 375–387.

[971] S. Meisburger; D. Case; N. Ando. Correlated motions in a protein crystal. *Nature Commun.*, **2020**, *11*, 1271.

[972] S. Meisburger; N. Ando. Correlated Motions from Crystallography beyond Diffraction. *Acc. Chem. Res.*, **2017**, *50*, 580–583.

[973] S. Boresch; M. Karplus. The role of bonded terms in free energy simulations. 1. theoretical analysis. *J. Phys. Chem. A*, **1999**, *103*, 103–118.

[974] S. Boresch; M. Karplus. The role of bonded terms in free energy simulations. 2. calculation of their influence on free energy differences of solvation. *J. Phys. Chem. A*, **1999**, *103*, 119–136.

[975] S. Boresch. The role of bonded energy terms in free energy simulations - insights from analytical results. *Mol. Simul.*, **2002**, *28*, 13–37.

[976] T.-S. Lee; Y. Hu; B. Sherborne; Z. Guo; D. M. York. Toward fast and accurate binding affinity prediction with pmemdgti: An efficient implementation of GPU-accelerated thermodynamic integration. *J. Chem. Theory Comput.*, **2017**, *13*, 3077–3084.

[977] T.-S. Lee; D. S. Cerutti; D. Mermelstein; C. Lin; S. LeGrand; T. J. Giese; A. Roitberg; D. A. Case; R. C. Walker; D. M. York. Gpu-accelerated molecular dynamics and free energy methods in amber18: Performance enhancements and new features. *J. Chem. Inf. Model.*, **2018**, *58*, 2043–2050.

[978] L. F. Song; T.-S. Lee; C. Zhu; D. M. York; K. M. Merz Jr. Using AMBER18 for Relative Free Energy Calculations. *J. Chem. Inf. Model.*, **2019**, *59*, 3128–3135.

[979] T. J. Giese; D. M. York. A GPU-Accelerated Parameter Interpolation Thermodynamic Integration Free Energy Method. *J. Chem. Theory Comput.*, **2018**, *14*, 1564–1582.

[980] D. Tan; S. Piana; R. Dirks; D. Shaw. RNA force field with accuracy comparable to state-of- the-art protein force fields. *Proc. Natl. Acad. Sci. USA*, **2018**, *115*, E1346–E1355.

[981] C. Tian; K. Kasavajhala; K. Belfon; L. Raguette; H. Huang; A. Migues; J. Bickel; Y. Wang; J. Pincay; Q. Wu; C. Simmerling. ff19SB: Amino-Acid-Specific Protein Backbone Parameters Trained against Quantum Mechanics Energy Surfaces in Solution. *J. Chem. Theory Comput.*, **2020**, *16*, 528–552.

[982] L. Raguette; A. Cuomo; K. Belfon; C. Tian; Q. Wu; C. Simmerling. Updated Amber force field parameters for phosphorylated amino acids for ff14SB and ff19SB. *In Prep*, **2020**.

[983] K. Belfon; C. Tian; J. Maier; L. Raguette; Q. Wu; C. Simmerling. RAGTAG: Rapid Amber Gpu Torsion pArameter Generator. . *In Prep*, **2020**.

[984] K. Belfon; L. Raguette; Q. Wu; C. Simmerling. Application of RAGTAG: modified amino acids for comparing MD simulations with FRET/EPR experiments. *In Prep*, **2020**.

[985] Y. Miao; A. Bhattarai; J. Wang. Ligand Gaussian accelerated molecular dynamics (LiGaMD): Characterization of ligand binding thermodynamics and kinetics. *bioRxiv*, **2020**.

[986] A. V. Onufriev; S. Izadi. Water models for biomolecular simulations. *WIREs Computational Molecular Science*, **2018**, *8*, e1347.

[987] V. N. Uversky; C. J. Oldfield; A. K. Dunker. Intrinsically disordered proteins in human diseases: Introducing the d2 concept. *Annual Review of Biophysics*, **2008**, *37*, 215–246.

[988] S. Piana; A. G. Donchev; P. Robustelli; D. E. Shaw. Water dispersion interactions strongly influence simulated structural properties of disordered protein states. *The Journal of Physical Chemistry B*, **2015**, *119*, 5113–5123.

[989] V. T. Duong; Z. Chen; M. T. Thapa; R. Luo. Computational studies of intrinsically disordered proteins. *The Journal of Physical Chemistry B*, **2018**, *122*, 10455–10469.

[990] D. Song; W. Wang; W. Ye; D. Ji; R. Luo; H.-F. Chen. ff14idps force field improving the conformation sampling of intrinsically disordered proteins. *Chemical Biology & Drug Design*, **2017**, *89*, 5–15.

[991] W. Ye; D. Ji; W. Wang; R. Luo; H.-F. Chen. Test and evaluation of ff99idps force field for intrinsically disordered proteins. *Journal of Chemical Information and Modeling*, **2015**, *55*, 1021–1029.

[992] J. Huang; S. Rauscher; G. Nawrocki; T. Ran; M. Feig; B. L. de Groot; H. Grubmuller; A. D. MacKerell Jr. Charmm36m: an improved force field for folded and intrinsically disordered proteins. *Nat Meth*, **2017**, *14*, 71–73.

[993] F. Meng; M. M. Bellaiche; J.-Y. Kim; G. H. Zerze; R. B. Best; H. S. Chung. Highly disordered amyloid-β monomer probes by single-molecule fret and md simulation. *Biophysical Journal*, **2018**, *114*, 870–884.

[994] E. Wang; H. Sun; J. Wang; Z. Wang; H. Liu; J. Zhang; T. Hou. End-Point Binding Free Energy Calculation with MM/PBSA and MM/GBSA: Strategies and Applications in Drug Design. *Chem. Rev.*, **2019**, *119*, 9478–9508.

[995] E. W. Weisstein. Euler angles From MathWorld—A Wolfram Web Resource.

[996] D. C. Rapaport. *The Art of Molecular Dynamics Simulation*. Cambridge University Press, 2010.

[997] C. Gebhardt; M. Lehmann; M. M. Reif; M. Zacharias; T. Cordes. Molecular and spectroscopic characterization of green and red cyanine fluorophores from the alexa fluor and af series. *bioRxiv*, **2020**.

[998] M. E. O'Neill. PCG: A Family of Simple Fast Space-Efficient Statistically Good Algorithms for Random Number Generation. Technical Report HMC-CS-2014-0905, Harvey Mudd College, Claremont, CA, 2014.

[999] S. Vigna. Further scramblings of Marsaglia's xorshift generators. *J. Comput. Appl. Math.*, **2017**, *315*, 175–181.

[1000] D. R. Roe; B. R. Brooks. A protocol for preparing explicitly solvated systems for stable molecular dynamics simulations. *J. Chem. Phys.*, **2020**, *153*, 054123.

[1001] D. R. Roe; B. R. Brooks. Improving the Speed of Volumetric Density Map Generation via Cubic Spline Interpolation. *J. Mol. Graphics Model.*, **2021**, *104*, 107832.

[1002] V. W. D. Cruzeiro; G. T. Feliciano; A. E. Roitberg. Exploring Coupled Redox and pH Processes with a Force-Field-Based Approach: Applications to Five Different Systems. *J. Am. Chem. Soc.*, **2020**, *142*, 3823–3835.

[1003] V. W. D. Cruzeiro; M. Manathunga; J. Merz, Kenneth M.; A. W. Götz. Open-Source Multi-GPU-Accelerated QM/MM Simulations with AMBER and QUICK. *ChemRxiv*, **2021**. https://doi.org/10.26434/chemrxiv.13984028.v1.

[1004] M. Manathunga; C. Jin; V. W. D. Cruzeiro; J. Smith; K. Keipert; D. Pekurovsky; D. Mu; Y. Miao; X. He; K. Ayers; E. Brothers; A. W. Goetz; K. M. Merz. QUICK, version 21.03. University of California San Diego, CA and Michigan State University, East Lansing, MI. 2021.

[1005] Y. Miao; K. M. Merz. Acceleration of Electron Repulsion Integral Evaluation on Graphics Processing Units via Use of Recurrence Relations. *J. Chem. Theory Comput.*, **2013**, *9*, 965–976.

[1006] Y. Miao; K. M. Merz. Acceleration of High Angular Momentum Electron Repulsion Integrals and Integral Derivatives on Graphics Processing Units. *J. Chem. Theory Comput.*, **2015**, *11*, 1449–1462.

[1007] M. Manathunga; Y. Miao; D. Mu; A. W. Götz; K. M. Merz. Parallel Implementation of Density Functional Theory Methods in the Quantum Interaction Computational Kernel Program. *J. Chem. Theory Comput.*, **2020**, *16*, 4315–4326.

[1008] M. Manathunga; C. Jin; V. W. D. Cruzeiro; Y. Miao; D. Mu; K. Arumugam; K. Keipert; H. M. Aktulga; J. Merz, Kenneth M.; A. W. Götz. Harnessing the Power of Multi-GPU Acceleration into the Quantum Interaction Computational Kernel Program. *ChemRxiv*, **2021**. https://doi.org/10.26434/chemrxiv.13769209.v1.

[1009] H. M. Aktulga; J. C. Fogarty; S. A. Pandit; A. Y. Grama. Parallel reactive molecular dynamics: Numerical methods and algorithmic techniques. *Parallel Computing*, **2012**, *38*, 245–259.

[1010] S. B. Kylasa; H. M. Aktulga; A. Y. Grama. Puremd-gpu: A reactive molecular dynamics simulation package for gpus. *Journal of Computational Physics*, **2014**, *272*, 343–359.

[1011] A. C. Van Duin; S. Dasgupta; F. Lorant; W. A. Goddard. Reaxff: a reactive force field for hydrocarbons. *The Journal of Physical Chemistry A*, **2001**, *105*, 9396–9409.

[1012] A. K. Rappe; W. A. Goddard III. Charge equilibration for molecular dynamics simulations. *The Journal of Physical Chemistry*, **1991**, *95*, 3358–3363.

[1013] W. J. Mortier; S. K. Ghosh; S. Shankar. Electronegativity-equalization method for the calculation of atomic charges in molecules. *Journal of the American Chemical Society*, **1986**, *108*, 4315–4320.

[1014] M. Samieegohar; F. Sha; A. Z. Clayborne; T. Wei. Reaxff md simulations of peptide-grafted gold nanoparticles. *Langmuir*, **2019**, *35*, 5029–5036.

[1015] S. Yang; T. Zhao; L. Zou; X. Wang; Y. Zhang. Reaxff-based molecular dynamics simulation of dna molecules destruction in cancer cells by plasma ros. *Physics of Plasmas*, **2019**, *26*, 083504.

[1016] P. O. Hubin; D. Jacquemin; L. Leherte; D. P. Vercauteren. Parameterization of the reaxff reactive force field for a proline-catalyzed aldol reaction. *Journal of computational chemistry*, **2016**, *37*, 2564–2572.

[1017] S. Monti; J. Jose; A. Sahajan; N. Kalarikkal; S. Thomas. Structure and dynamics of gold nanoparticles decorated with chitosan–gentamicin conjugates: Reaxff molecular dynamics simulations to disclose drug delivery. *Physical Chemistry Chemical Physics*, **2019**, *21*, 13099–13108.

[1018] T. Trnka; I. Tvaroska; J. Koca. Automated training of reaxff reactive force fields for energetics of enzymatic reactions. *Journal of chemical theory and computation*, **2018**, *14*, 291–302.

[1019] A. Rahnamoun; A. Van Duin. Reactive molecular dynamics simulation on the disintegration of kapton, poss polyimide, amorphous silica, and teflon during atomic oxygen impact using the reaxff reactive force-field method. *The Journal of Physical Chemistry A*, **2014**, *118*, 2780–2787.

[1020] D. Raymand; A. C. van Duin; M. Baudin; K. Hermansson. A reactive force field (reaxff) for zinc oxide. *Surface science*, **2008**, *602*, 1020–1031.

[1021] K. Chenoweth; S. Cheung; A. C. Van Duin; W. A. Goddard; E. M. Kober. Simulations on the thermal decomposition of a poly (dimethylsiloxane) polymer using the reaxff reactive force field. *Journal Of The American Chemical Society*, **2005**, *127*, 7192–7202.

[1022] M. F. Russo Jr; R. Li; M. Mench; A. C. Van Duin. Molecular dynamic simulation of aluminum–water reactions using the reaxff reactive force field. *International Journal of Hydrogen Energy*, **2011**, *36*, 5828–5835.

[1023] J. Ludwig; D. G. Vlachos; A. C. Van Duin; W. A. Goddard. Dynamics of the dissociation of hydrogen on stepped platinum surfaces using the reaxff reactive force field. *The Journal of Physical Chemistry B*, **2006**, *110*, 4274–4282.

[1024] K. Yoon; A. Rahnamoun; J. L. Swett; V. Iberi; D. A. Cullen; I. V. Vlassiouk; A. Belianinov; S. Jesse; X. Sang; O. S. Ovchinnikova et al. Atomistic-scale simulations of defect formation in graphene under noble gas ion irradiation. *ACS nano*, **2016**, *10*, 8376–8384.

[1025] A. Rahnamoun; A. Van Duin. Study of thermal conductivity of ice clusters after impact deposition on the silica surfaces using the reaxff reactive force field. *Physical Chemistry Chemical Physics*, **2016**, *18*, 1587–1594.

[1026] C. Zou; A. Van Duin. Investigation of complex iron surface catalytic chemistry using the reaxff reactive force field method. *Jom*, **2012**, *64*, 1426–1437.

[1027] Y. K. Shin; H. Kwak; A. V. Vasenkov; D. Sengupta; A. C. van Duin. Development of a reaxff reactive force field for fe/cr/o/s and application to oxidation of butane over a pyrite-covered cr2o3 catalyst. *Acs Catalysis*, **2015**, *5*, 7226–7236.

[1028] T. P. Senftle; S. Hong; M. M. Islam; S. B. Kylasa; Y. Zheng; Y. K. Shin; C. Junkermeier; R. Engel-Herbert; M. J. Janik; H. M. Aktulga et al. The reaxff reactive force-field: development, applications and future directions. *npj Computational Materials*, **2016**, *2*, 1–14.

[1029] L. Chen; A. Cruz; D. R. Roe; A. C. Simmonett; L. Wickstrom; N. Deng; T. Kurtzman. Thermodynamic Decomposition of Solvation Free Energies with Particle Mesh Ewald and Long-Range Lennard-Jones Interactions in Grid Inhomogeneous Solvation Theory. *J. Chem. Theory Comput.*, **2021**, *17*, 2714–2724.

Index